Intramolecular Stabilization of 2,6-Diarylphenylsilylium Ions by π-Arene and Lone Pair–Halogen Coordination

Dissertation zur Erlangung
der naturwissenschaftlichen Doktorwürde
(Dr. sc. nat.)

vorgelegt der
Mathematisch-naturwissenschaftlichen Fakultät
der Universität Zürich
von
Paola Romanato
aus Italien

Promotionskomitee
Prof. Dr. Jay S. Siegel (Vorsitz)
Prof. Dr. Kim K. Baldridge
Prof. Dr. Cristina Nevado
Prof. Dr. Yitzhak Apeloig

Zürich, 2011

Die vorliegende Arbeit wurde von

der Mathematisch-naturwissenschaftlichen Facultät

der Universität Zürich im Januar 2011

als Dissertation angenommen.

Promotionskomitee:

Jay S. Siegel, Vorsitz

Kim K. Baldridge

Cristina Nevado

Universität Zürich

Zürich, Switzerland 2011

To My Family

Acknowledgement

I would like to open my thesis with thanking all the people that made possible for me to reach this day. First of all, many thanks to my thesis advisor, Professor Jay Siegel, for allowing me to join his group and kindly guide me into the world of physical organic chemistry. His support, enthusiasm, and confidence in my skills always went beyond my expectations and motivated me during this time and at the moment of taking fundamental decisions about my future.

I am extremely grateful to two people that shared this project with me: Prof. Kim Baldridge and Dr. Anthony Linden. The calculations carried out by Kim helped me many times to choose the target molecules for my synthesis and gave a much more rational approach to this project. But more important, she has been always a kind, helpful and supportive presence during these years. The X-ray analyses performed by Tony and his coworker Sasha, added to this thesis informations that I could have not achieved by any other means. I really appreciated their constant efforts in trying to resolve the structure of my crystals.

My sincere thanks go to Dr. Simon Duttwyler for supervising me during my first months in the lab and afterwards for becoming an invaluable colleague in the silicon cations project. It has been a special privilege and a great pleasure to work with him.

I would like to express my gratitude to Dr. Nathaniel Finney for being always helpful in the lab and during the toughest moments in group meetings, and to Prof. Peter Ruedi, Prof. Cristina Nevado and Prof. Stefan Bienz for initiating me into the art of teaching chemistry to young students.

I would like to thank Simon Jurt, Nadia Bross and the MS-Team for all the great analytical work performed. My sincere gratitude goes also to Dr. Thomas Fox for his help with my most difficult NMR measurements and for showing me an infinite passion for his job.

I would like to thank my master thesis advisor, Professor Franco Cozzi, for the unlimited support he offered me since the first day I joined his lab in Italy. I will never forget the fun we, students, always had every time he was back in lab to set up his own reactions. He taught me that chemistry is passion, commitment and, most of all, a lot of fun.

And it is with infinite gratitude that I would like to mention in this thesis all my lab–mates, past and present: Fitore, Daphne, Nelly, Derik, Martin, Silvia, Ashley, Oliver, Simon, Swen, Michael, Benno, Lee, Davide, Ela, Fabienne, Eoin, Raul, Caroline, Karla, Amit, Roman, Marek, Anna, Mireille, Fabian, Yazmin, Ylenia, because during my toughest days in lab, they gave me a reason to smile and laugh. Special thanks go to Derik Frantz, who patiently and kindly took the time to proofread my thesis, and to Oliver Allemann, for the great collaboration we have established in the silicon cation project.

Moving to Zurich represented for me the beginning of a new life far from my family and my childhood friends. I met in Zurich an amazing group of people that made me feel at home: thanks to all of them. A special thanks goes to Davide, Simon, Silvia and Marek for their support and encouragement over these years and for being now terrific friends.

For his patience, love and support during every single day of this PhD, and for being able to make me smile in almost any situation, I would like to thank a very special person, Michele.

Finally, a deep, affectionate thanks goes to my mum, Gabriella, my dad, Selvino, and my brother, Mauro, for their unlimited love. In particular, I owe to my mum a special thank because she though me the value of sacrifice and commitment in life. I would not be the person I am today without her guidance.

ABSTRACT OF THE DISSERTATION

Intramolecular Stabilization of 2,6-Diarylphenylsilylium Ions
by π-Arene and Lone Pair–Halogen Coordination

by
Paola Romanato
University of Zurich, 2011
Prof. Dr. Jay S. Siegel, Chair

Silylium ions are group 14 analogs of carbocation of the general structure R_3Si^+. Their most striking feature is their extreme electrophilicity. The generation of long-lived silyl cationic species has therefore necessitated the development of novel synthetic approaches and weakly nucleophilic conditions. It was only in 2002 that the first crystal structure of a triarylsilylium ion dispelled any doubt about the existence of tricoordinated silyl cations in the condensed phase. In the recent years, several research groups have succeeded in applying silylium ion chemistry to the preparation of other reactive intermediates and to the field of Lewis acid catalysis.

The aim of this thesis is to expand the family of terphenylsilylium ions previously developed in the Siegel group. The terphenyl skeleton provides steric shielding of the positively charged cavity as well as an overall thermodynamic stabilization by internal π-coordination. A systematic study was performed in order to tune the Lewis acidity at silicon by reducing the electron density of the flanking rings. At first, halogen atoms were introduced at the *ortho* positions of the flanking rings with the effect of quenching π-arene coordination in favor of lone pair–halogen coordination to silicon. This coordination mode was confirmed *via* NMR, X-ray and computational studies.

A second generation of terphenylsilylium ions, featuring halogen atoms in the *para* position of the flanking rings, was synthesized with the aim of avoiding both lateral ring and halogen coordination, in favor of a very deshielded silylium ion. As a result, the intramolecular coordination of the positively charged cavity by the flanking

rings was effectively reduced but the intermolecular coordination by the counterion became competitive, as shown by X-ray crystallography.

We became interested in probing the energetic details of π-arene coordination compared to lone pair–halogen coordination to silicon, and therefore a series of cations bearing 2,6-difluoro- and 2,6-dimethyl-substituted rings were synthesized. Remarkably, a competition, rather than a cooperation, is established between the two modes of stabilization: with methylated rings of lower basicity the preferred interaction is F→Si, while with duryl and pentamethylphenyl substituents π-coordination is favored.

In the search of silylium ions as active as the truly tricoordinated triarylsilylium ion, but sterically more accessible, a new family of phenylsilylium ions featuring aliphatic chains in place of the flanking aromatic rings was synthesized and studied. These compounds exhibited very low field-shifted resonances in ^{29}Si NMR spectroscopy, sign of a very deshielded cationic center. At first, the stability of these "naked" silylium ions, which did not display significant solvent or anion coordination, was attributed to agostic interactions with the nearby aliphatic groups. Recently, a new hypothesis has been formulated regarding a rearrangement of the initial cations into more stable triarylsilyl cationic structures, which are responsible for the low field-shifted resonances. Further investigations are now ongoing to elucidate the mechanism of this rearrangement.

ZUSAMMENFASSUNG

Intramolecular Stabilization of 2,6-Diarylphenylsilylium Ions
by π-Arene and Lone Pair–Halogen Coordination

von
Paola Romanato
Universität Zürich, 2011
Prof. Dr. Jay S. Siegel, Chair

Silyliumionen sind höhere Analoge von Carbokationen der Struktur R_3Si+. Was sie vor allem auszeichnet, ist ihre enorme Elektrophilie. Die Erzeugung langlebiger silylkationen hat deshalb die Entwicklung neuartiger synthetischer Wege und schwach nucleophile Reaktionsbedingungen bedingt. Erst 2002 wurden mit der Kristallstruktur eines Triarylsilyliumions letzte Zweifel an der Existenz dreifach koordinierter Siliziumkationen ausgeräumt. In den vergangenen Jahren haben verschiedene Forschungsgruppen Silyliumionen erfolgreich zur Erzeugung reaktiver Zwischenstufen und in der Lewissäure-Katalyse angewandt.

Das Ziel dieser Arbeit ist die Erweiterung der Familie dieser Terphenylsilyiumionen, die in der Siegel Gruppe bereits entwickelt wurden. Die Terphenylgrundstruktur bietet sterische Abschirmung von der positiven Ladun des Siliciumkerns sowie eine komplette thermodynamsiche Stabilisierung durch die pie-Koordination. Um die Lewis-Acidität zu regeln, wurde die Elektronendichte der benachbarten Ringe reduziert. Zuerst wurden Halogenatome an der *ortho*-Position dieser benachbarten Ringe eingeführt Diese mindern die Koordination der pie-Arene, so dass eine bevorzugte Koordination zwischen dem Halogen und dem Silicium stattfinden.

Diese Konformation wurde durch NMR, X-Ray und Berechnungsmethoden bestätigt.

Eine zweite Generation von Terphenylsilyliumionen wurde synthetisiert, mit Halogenatome in *para*-Position zu der benachbarten Ringen. Somit sollte eine Koordination am lateralen Ring und an den Halogenatomen vermieden werden wodurch das Silyiumion entschirmt wird. Durch Verwendung von X-Ray-Kristallographie wurde gezeigt, dass die intramolekulare Koordination des positiv

geladenen Kerns mit den benachbarten Ringen tatsächlich reduziert wurde und dass die intermolekulare Koordination mit dem Gegenion konkurriert.

Durch ein grosses Interesse die Energetik der π-Arene-Koordinationen detailliert zu erforschen, wurden eine Reihe von Kationen aus 2,6-Difluoro- und 2,6-Dimethyl-substitutierte Ringe synthetisiert. Somit wurde die Koordination zwischen den abgeschiedenen Halogenpaar zu Silicium verglichen.

Dabei wurde bedeutsamerweise eine Konkurrenz anstatt einer Kooperation zwischen den beiden Stabilisierungsmethoden erkannt. Eine Interaktion von F→Si wird durch methylierte Ringe mit niedrigere Basizität, wohingegen eine π-Koordination mit duryl- und pentamethylphenyl-Substituenten bevorzugt wird.

In dieser Arbeit wurde erfolgreich eine neue Art der Phenylsilyiumionen, die sterisch zugänglichere trikoordinierte Triarylsilyliumionen widerspiegeln, synthetisiert und untersucht. Diese Strukturen weisen niedrige Resonanzverschiebung in ^{29}Si-NMR Spektroskopie auf, was ein klares Zeichen von abgeschirmten kationischen Zentren darstellt. Die Stabilität dieser nackten Silyliumionen ist auf die agostische Wechselwirkung mit den benachbarten aliphatischen Gruppen zurückzuführen. Eine erst kürzlich aufgesetzte Hypothese befasst sich mit Kationen, die in eine stabilere Triarylsilylkation-Struktur neu geordnet werden. Diese sind verantwortlich für eine niedrige chemische Resonanzverschiebung.

Weitere Untersuchungen werden nun folgen, um die Mechanismen dieser Neuanordnung aufzuklären.

Contents

List of Figures

List of Schemes

List of Tables

1 What Is a Silylium Ion and What Makes It so Reactive?

1.1 Nomenclature

According to the IUPAC conventions,[1] a *silyl cation* is any positively charged species in which silicon possesses a formal charge, without specification of the coordination number. Tricoordinate ions R_3Si^+ are called *silylium ions*, and the term *silanium ions* refers to pentacoordinate species R_5Si^+.

1.2 Criteria for the Definition of a Silylium Ion

Crystallographic evidence for a free silylium ion was first reported in 2002 with the structure of $[Mes_3Si][HCB_{11}Me_5Br_6]$.[2] The criteria that the authors adopt to define this silylium ion as a "free" cation are the following:

- the downfield shifted resonance in the ^{29}Si NMR spectrum, close to 220 ppm;
- the planarity at silicon, indicated by the summation of the three C–Si–C angles to 360° (Σ C–Si–C), as expected for an sp^2 silylium ion center (Figure 1.1);
- the distances between Si^+ and the closest molecules of solvent, counterion, or substituents, larger than the sum of their respective van der Waals radii (the van der Waals radius of cationic Si is unknown but the positive charge should shrink it substantially from that of neutral Si, 2.1 Å). In this thesis all three parameters will be taken into account in the description of new silylium ions; in the absence of X-ray analysis, we will refer only to the ^{29}Si NMR shift as a measure of the residual electron density on the silicon center.

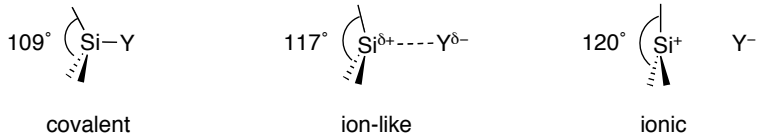

Figure 1.1 C–Si–C angle for covalent silane, ion-like silicon species,[3] and ionic silylium ion species

To date, ^{29}Si shifts as high as 115,[3] 226[2] and 316[4] ppm have been observed for R_3Si^+ with R = alkyl, aryl, silyl, respectively. However, most examples of silyl cations show an NMR shift in the range of 20–100 ppm because of the interaction of the Si center with sources of electron density. For classical carbenium ions, there is a clear demarcation between ionic/planar and covalent/tetrahedral species. In a work published by Reed and coworkers on the ionization of $Me_3Si–Cl$ to Me_3Si^+ and Cl^-,[3] the authors support the idea that silicon is quite different on this regard. Their calculations show a continuum of increasing ionicity as the anion becomes less coordinating and the C–Si–C angle approches 120˚C, typical value of an sp^2-hybridized center (Figure 1.2). This result creates difficulties in defining precisely what properly constitutes a silylium ion in condensed media because it is always going to be a matter of degree.

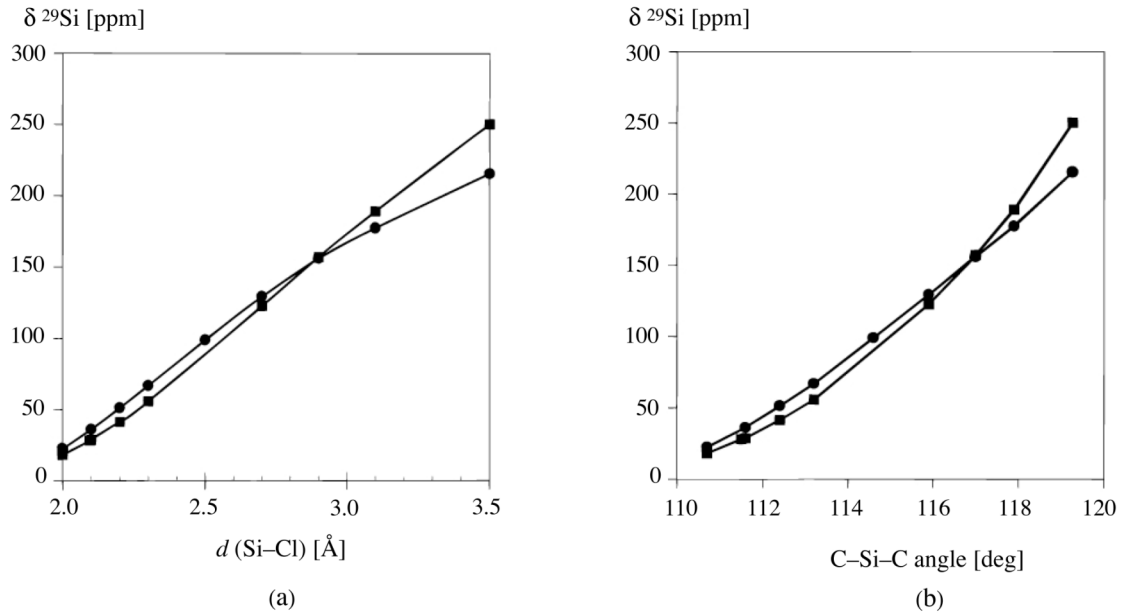

Figure 1.2 Calculated ^{29}Si NMR shifts for the Me_3SiCl molecule as a function of (a) (Si–Cl) distance and (b) C-Si-C angle. The ● and ■ lines refer to the SOS-DEPT and GIAO methods, respectively.[3]

1.3 Silicon versus Carbon

Although silylium ions are thermodynamically more stable than their carbon analogues, because silicon, larger and more electropositive than carbon, is expected to accommodate better a positive charge, they are kinetically extremely unstable. This instability is a consequence of the electronegativity and the size of silicon, especially when it is substituted with second period elements. Electronegativity differences are important since they cause electron deficiency on silicon by inductive effects. Carbon has a Pauling electronegativity of 2.5, silicon has 1.8.[5] The greater electropositivity of silicon confers an inductive C(δ–)–Si(δ+) bond polarization in silanes (R_4Si, R = alkyl, aryl) as well as in R_3Si^+ ions and localizes the positive charge at silicon.

The location of silicon in the third row of the periodic table means that its size is significantly larger than that of carbon. The covalent radii of Si, 1.17 Å, and C, 0.77 Å, lead to Si–C and C–C bond lengths of 1.94 Å and 1.54 Å, respectively.[5] Thus, a typical Si–C bond is ca. 26% longer than an analogous C–C bond and this automatically reduces the overlap with substituents and allows attack by nucleophiles. Carbocations R_3C^+ are often stabilized by interactions of filled π, n or σ orbitals of R with the empty 2p C orbital. When the substituent R is a second period element, the interaction between R and C^+ becomes more favorable because of the similarity in size, energy and orientation of the orbitals. As an example, we can study the case of a C–H substituent interacting with an empty 2p C and 3p Si orbital (Figure 1.3). A filled C–H σ orbital can donate electron density into an empty 2p C orbital, a phenomenon called hyperconjugation. Such an overlap can be tracked experimentally: in the crystal structure of the *tert*-butyl cation for example, the C–C^+ bond lengths lie in the range of 1.43–1.46 Å, indicating partial double bond character due to σ-p interations.[6] In the case of R_3Si^+, the empty orbital is a 3p orbital, which has diminished overlap with filled R orbitals. The orbital energies are less well matched and the σ–p interaction is weakened (Figure 1.3). This situation is reflected in the general tendency of silicon to form single bonds rather than double bonds.

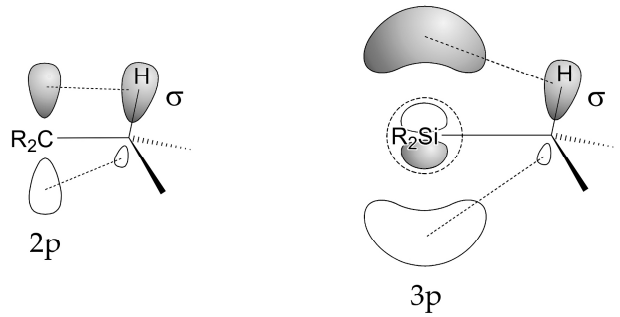

Figure 1.3 Overlap of a filled σ C–H orbital with an empty 2p C orbital in a carbenium ion (left) and overlap of a filled σ C–H orbital with an empty 3p Si orbital in a silylium ion (right). The dashed circle represents a spherical node of the 3p orbital.

In silylium ions, the combination of bond polarization and reduced overlap among orbitals of the substituents and 3p Si orbital is what creates the extraordinary avidity for electron density at the silicon center.

Of fundamental importance is also the difference in bond strengths of silicon and carbon to certain main group elements. In Table 1.1, typical dissociation energies of C–X and Si–X bonds are compared. C–H and C–C bonds are stronger than Si–H and Si–C bonds. Silicon shows a high affinity for O and halogen: Si–X (X = O, halogen) are uniformly stronger bonds than the analogous C–X bonds.

Table 1.1 Average C–X and Si–X bond energies in kJ mol^{-1}.[5]

Bond	C	Si
H	411	318
C	346	318
O	358	452
F	485	565
Cl	327	381
Br	285	310
I	213	234

1.4 History of Investigations into Silylium Ions

While carbocations, R_3C^+, have been known for more than 100 years,[7] the quest for stable trivalent silyium ions has been one of the most difficult challenges that organo-silicon chemists have faced in the last five decades. The so-called "silylium ion problem" refers to the possibility of isolating R_3Si^+ species, unfettered by interactions with the solvent, the counterion and neighbouring groups. The extremely high electrophilicity of silylium ions, renders them prone to react with a variety of π- and σ-electron-donating compounds, including solvents and counterions, forming positively charged species with valencies of four or higher. A historical overview of the strategies applied to overcome the high kinetic lability of these species, towards the synthesis of a "free" silylium ion, has been reported.

1.4.1 Synthetic Routes to Silylium Ions: Hydride Abstraction and "Allyl Leaving Group Approach".

Carbenium ions are traditionally obtained from the departure of a leaving group in S_N1 or $E1$ reactions. Leaving groups in carbon chemistry include halides, carboxylic esters, and sulfonic esters. When attached to silicon, these groups are bound extremely strongly, because of the high dissociation energies of Si–halogen and Si–O bonds. Electrophilic abstraction of X from four-coordinated R_3SiX is the typical approach to the synthesis of a silylium ion. A few attempts were originally conducted having as X a halogen atom, but these reactions were strongly limited by thermodynamic factors. For example, while precipitation of silver bromide drives the reaction toward the products in Eq. 1.1, simply switching to a silver salt with the less-coordinating carborane anion leads to no reaction in Eq. 1.2.[8]

$$R_3SiBr + AgClO_4 \xrightarrow{\text{toluene}} R_3Si(OClO_3) + AgBr\downarrow \qquad \textbf{Eq. 1.1}$$

$$R_3SiBr + Ag(CB_{11}H_6Br) \xrightarrow{\text{toluene}} \text{no reaction} \qquad \textbf{Eq. 1.2}$$

This results shows that a large part of the driving force in Eq. 1.1 is the formation of the Si–O bond to perchlorate, which behaves as a strong donor toward the silyl cation.

Whereas bonds from silicon to electronegative elements (halogen, O, N) are uniformly stronger than the analogous bonds to carbon, the Si–H bond is weaker than the C–H bond. In 1975, this consideration inspired Corey and West to develop a new approach for the generation of silylium ions: the hydride transfer from a silane to a carbocation (Eq. 1.3).[9]

$$Ph_3C^+ + R_3SiH \longrightarrow Ph_3CH + R_3Si^+ \qquad \textbf{Eq. 1.3}$$

This reaction can be envisioned as an analogous to the Bartlett–Condon–Schneider reaction,[10] which uses a carbocation to produce a second, more stable, carbocation starting from its neutral hydrogen-containing precursor (Eq. 1.4).

$$R_3C^+ + R'_3CH \longrightarrow R_3CH + R'_3C^+ \qquad \textbf{Eq. 1.4}$$

The use of hydride as a leaving group represented a landmark achievement in silyl cation chemistry. This reaction can be followed by ^{1}H NMR spectroscopy, from loss of the Si–H resonance, appearance of the C–H resonance in the product, or loss of the H–Si–C–H coupling for methyl substituted cases. The carbocation of choice in the Corey–West reaction is usually a trityl salt (Ph_3C^+); the large size of this cation, which has to approach the silane, sometimes represents a kinetic barrier. An example is the lack of reaction between trityl-[$B(C_6F_5)_4$] and trimesitylsilane (mesityl = 2,4,6-trimethylphenyl, Eq. 1.5).

$$Mes_3SiH + [Ph_3C][B(C_6F_5)_4] \xrightarrow{\text{toluene}} \text{no reaction} \qquad \textbf{Eq. 1.5}$$

This problem reappeared in 1995 when chemists were trying to synthesize silylium ions with substituents larger than alkyl groups. Reed found that *tert*-butyl substituents at Si were insufficient to remove the coordination to the anion, but

substituents larger than *tert*-butyl rendered the Corey–West reaction impossible.[11] Zhao and Lambert reasoned that, since it was not possible to bring the electrophile to the hydride in case of large substituents at Si, it was worth to try to bring the hydride (intended as leaving group) closer to the electrophile. Other groups that might fulfill the role of a hydride should possess a suitable dimension and geometry, in order to be reached by the abstracting agent beyond the steric shield created by the substituents at silicon, necessary to inhibit complexation of the cation with solvent and anion. Allyl abstraction offers a viable alternative to the use of hydride as leaving groups. Uhlig[12] observed that some allylsilanes loose their allyl group when treated with triflic acid; Shade and Mayr[13] found that the reaction of allyltrimethylsilane with trytil tetrachloroborate leads to abstraction of allyl to give allyltriphenylmethane and chlorotrimethylsilane (Scheme 1.1).

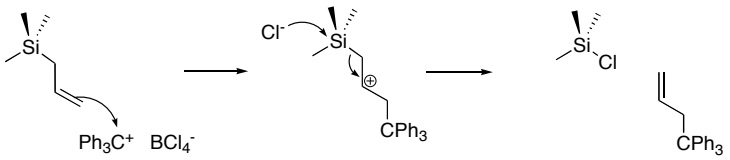

Scheme 1.1 Reaction of allyltrimethylsilane with trityl tetrachloroborate.

Inspired by this experiment, Lambert and Zhao in 1997 extended the scope of the allyl abstraction reaction to the silylium ion synthesis.[14] They prepared allyltrimesitylsilane and tried the allyl group abstraction with $[Ph_3C][B(C_6F_5)_4]$ ($[B(C_6F_5)_4]$ is also known as TPFPB = tetrakis pentafluorophenylborate): only a sluggish reaction occurred, with low conversion (Scheme 1.2 a). Since the trityl TPFPB proved to be relatively unreactive, they tried to use $[Et_3Si(benzene)]^+$ as electrophile, with the idea that the thermodinamically more stable silylium ion would be obtained as product of the reaction. The reaction occurred, but resulted in considerably decomposition (Scheme 1.2 b). The next option was to try an electrophile of intermediate reactivity: the β-silyl cation $Et_3SiCH_2C^+Ph_2$ had been prepared one year earlier by the same authors[15] (Scheme 1.3), and turned out to be the electrophile of choice for the allyl abstraction from the sterically hindered allyltrimesitylsilane (Scheme 1.2 c).

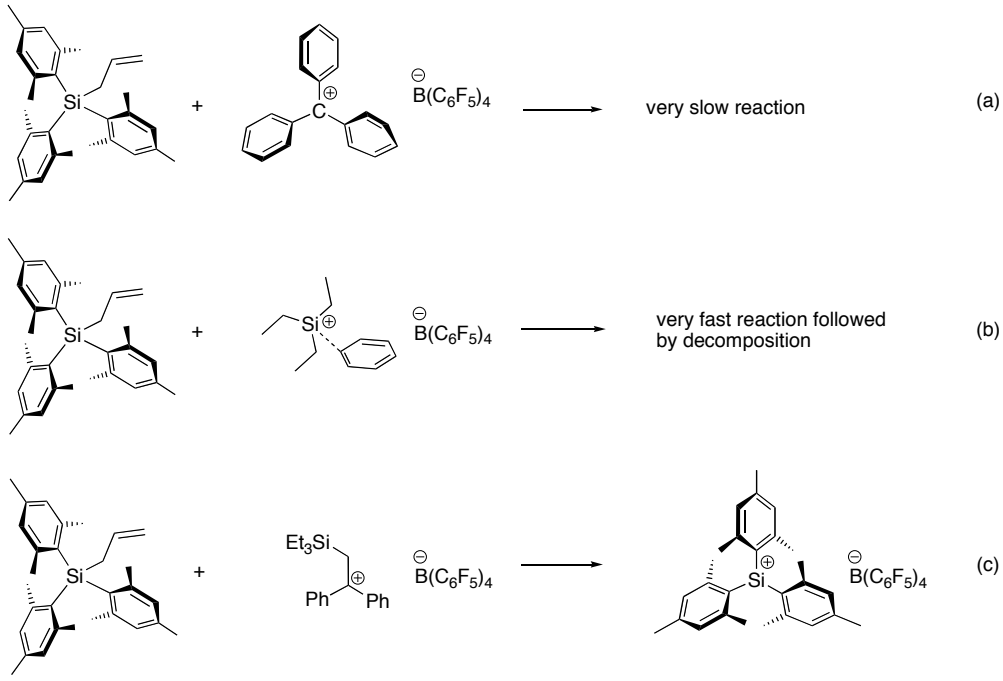

Scheme 1.2 Allyl abstraction from allyltrimesitylsilane with different electrophiles.

Over a period of 20 years, two useful strategies for the synthesis of silylium ions starting from their neutral precursors have been developed: the Corey–West hydride abstraction and the allyl abstraction of Lambert and Zhao. In this thesis, we will make use of the Corey–West reaction as a synthetic route to silylium ions because the substituents at silicon are designed to allow access of reagents of different sizes, including the trityl TPFPB.

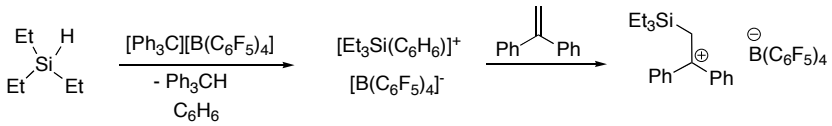

Scheme 1.3 Preparation of the diphenyl[(triethylsilyl)methyl]methylium ion.

1.4.2 Optimization of Solvents and Anions

At an early stage of the work in the silylium ion field, the problem of having a non-nucleophilic solvent was masked by the fact that the anion (*e.g.*, perchlorate anion

ClO_4^-) was always closely interacting with the silicon center.[16, 17] Solvents like acetonitrile, dichloromethane, sulpholane were used, but as soon as new, less nucleophilic anions appeared, it was clear that those solvents would replace the counterion in the coordination to silicon. In 1993 Boudjouk[18] and Sakurai[19] demonstrated that, in the presence of acetonitrile, an initially formed silylium ion produces a silylnitrilium ion (Scheme 1.4). The ^{29}Si NMR resonances of such species are in the range of 20–40 ppm for different alkyl and aryl substituents at silicon, values that are far from those expected for a free silylium ion.

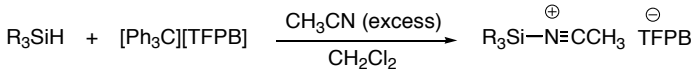

Scheme 1.4 Preparation of a silylnitrilium ion. TFPB: tetrakis[3,5-bis(trifluoromethyl) phenyl]borate.

Dichloromethane presents an additional problem with respect to the coordinating solvents: at temperature higher than –20˚C, decomposition of a silylium ion by chloride abstraction from CH_2Cl_2 is likely to happen, as described by Oestreich[20] in his report on a ferrocene-substituted silylium ion (Scheme 1.5). Aliphatic solvents of lower nucleophilicity than dichloromethane and 1,2-dichloroethane are hydrocarbons like hexane. Unfortunately the ionic products of the Corey–West reaction are not soluble in these solvents. Instead, non-polar aromatics, such as benzene and toluene,

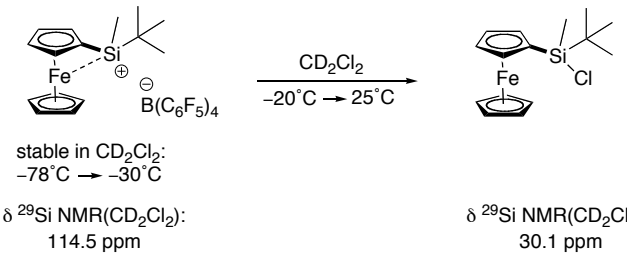

Scheme 1.5 Decomposition of a silylium ion by chloride abstraction from CH_2Cl_2.

possess considerable polarizability and have been known to offer appreciable solubility for ions, as demonstrated at first in 1992 by the study of Kuhlmann on a tricoordiante tin cation in solution.[21] From that moment on, most of the studies of silylium ions have used aromatic solvents. Interestingly, it was observed that the Corey–West method with non-polar aromatic solvents always leads to the formation of two layers. The solvent is the same in both layers, but the ionic product oils out in the bottom layer, while the upper layer is a dilute solution of the solvent containing the hyrocarbon byproducts, e.g. triphenylmethane. The formation of two layers provides a straightforward separation of the product: the upper layer, containing an excess of starting material and neutral byproducts, can be syringed off and discarded, leaving the ionic species uncontaminated in the oily phase. Aromatics of slightly higher polarity, such as fluorobenzene, chlorobenzene, *ortho*-dichlorobenzene, are also suitable for silylium ions synthesis; in these cases, clear solutions are formed instead of two layers. Typically, aromatic solvents avoid coordination to the cationic center; nevertheless, cases where even with the least nucleophilic solvent and counterion available coordination to the silylium ion take place (see 1.4.3), will be discussed later in this thesis. Only a juxtaposition of optimized conditions, including solvent, counterion and substituents at silicon, can lead to a free silylium ion.

Along with the work on non-coordinating solvent, there have been considerable efforts in the last decades towards a non-coordinating anion. Chemists have reached the consensus that there is no such thing as a non-nucleophilic anion, and that it would be more meaningful and precise to use the relative term *weakly coordinating anion* (as well as *weakly coordinating solvent*). The original members of this category included perchlorate (ClO_4^-), triflate ($CF_3SO_3^-$), hexachloro- and hexafluoroantimonate ($SbCl_6^-$, SbF_6^-), tetrafluoroborate (BF_4^-). These all contain available oxygen or halogen atoms, which would complex or, in some cases, even be abstracted by the strongly electrophilic silicon center. For example, treatment of $(i\text{-}Pr_3S)_3SiH$ with trityl tetrafluoroborate leads to the fluorinated compound $(i\text{-}Pr_3S)_3SiF$.[22] Another weakly nucleophilic anion taken into consideration was tetraphenylborate (BPh_4^-), but it was quickly observed that a positively charged

silicon species abstracts a phenyl group from it, leading to decomposition. The 3,5-bis(trifluoromethyl)tetraphenylborate ion (TFPB, Figure 1.4 a) is also labile with respect to fluoride ion abstraction and boron–phenyl bond cleavage.[23] In attempts to circumvent this drawback, the phenyl rings of BPh_4^- were functionalized with fluorine atoms. The total electronic effect of fluorine is a balance of induction and resonance, so it was reasonable to imagine that inductive withdrawal by fluorine might reduce the nucleophilicity of the phenyl rings and resonance donation ($C{=}F^+$) might decrease the nucleophilicity of the fluorine atoms. The incorporation of electron withdrawing substituents should also reduce the tendency for B–Ar cleavage, by decreasing the amount of negative charge at the *ipso* carbon atom. This strategy turned out to be extremely successful when tetrakis(pentafluophenyl)borate (TPFPB, Figure 1.4 b) was used with a variety of silanes to afford the corresponding cationic species.[24]

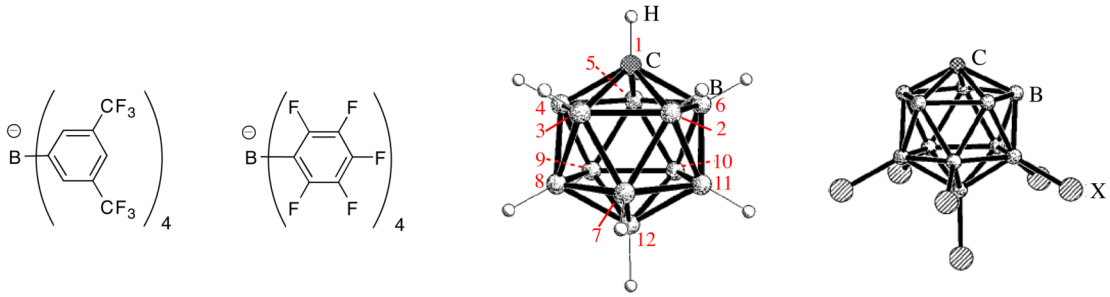

Figure 1.4 Weakly nucleophilic anions: (a) TFPB, (b) TPFPB, (c) parent carborane $CB_{11}H_{12}^-$ (in red numbering of the vertex), (d) hexahalocarborane $CB_{11}H_6X_6^-$.

The TPFPB anions have been widely and succesfully used in silylium ion chemistry, but they have two limitations: they have the tendency to form liquid clathrates rather then crystallize and, in presence of potent, hard electrophiles, they might still undergo phenyl abstraction. For example, TPFPB anions sustain the acidity of protonated pentamethylbenzenium ($C_6Me_5H_2^+$), tetramethylbenzenium ($C_6Me_4H_3^+$), and mesitylenium ions ($C_6Me_3H_4^+$), but they decompose in the presence of protonated xylenium ($C_6Me_2H_5^+$), toluenium ($C_6MeH_6^+$), and benzenium ions ($C_6Me_2H_5^+$).[25] Analogous to the toluenium ion, the solvated complex $[Et_3Si(toluene)]^+$ decomposes

in a few days, both in solution and in the solid state, because of the acidity of the protons in coordinated toluene molecules, that can be released and cleave the B–C_{aryl} bond of the TBFPB anion.[26]

In 1996, Reed published the crystal structure of *i*-$Pr_3Si(Cl_6\text{-}CB_{11}H_6)$;[3] he used a hexachlorocarborane (Figure 1.4 d) as a low nucleophilic counterion. Carboranes [27, 28] are not only weakly nucleophilic anions, but they have extraordinary chemical and electrochemical stability. Having tangentially delocalized σ bonding (*i.e.*, σ aromaticity), and σ bonds being the strongest in chemistry, the HOMO–LUMO gap in $CB_{11}H_{12}^-$ is enormous; therefore, very high energy is required to disrupt the cluster framework of these anions. The protruding B–H bonds of carboranes are amenable to electrophilic substitution, in a manner reminiscent of benzene. For example, strong electrophiles such as dihalogens lead to the very useful hexahalo derivatives $CB_{11}H_6X_6$.[29] The CB_{11} cage is polarized such that substitution occurs preferentially at the boron end of the cluster. Position 12 (Figure 1.4 c) is usually substituted first, followed by the lower pentagonal belt (position 7–11). While the B–H bonds undergo electrophilic substitution, the C–H bond can be lithiated with butyllithium, and subsequently alkylated upon treatment of the lithio species with alkyl halides, to afford 1-R–$CB_{11}H_{11}^-$ derivatives.[30] Typically, the parent carborane, $CHB_{11}H_{11}^-$, has to be at least hexa-halogenated at boron (positions 7–12) to achieve the required level of inertness for fierce electrophiles such as silylium ions. Inertness increases with the extent of halogenation, presumably because halide substituents screen the negative charge and create an impervious layer that protect the CB_{11} core from chemical attack. Anion basicity decreases in the order I > Br > Cl > F, which can be ascribed to decreasing polarizability of the halide.[3] The fluorinated carboranes,[31] expected to be the least coordinating members of the family, are only available to those willing to work with F_2. The easiest carboranes to prepare are the hexachloro and hexabromo anions (undecahalogenation requires harsher conditions): their inertness, low nucleophilicity, and good crystallizing ability have designed them as the counterions of choice for the crystallographic studies performed in this thesis.

1.4.3 Optimization of Substituents

Traditional attempts to stabilize silylium ions have utilized p_π–p_π donation (C→Si^+), strategies that proved to be successful in carbocation chemistry. There are two drawbacks to this approach. First, carbon is more electronegative than silicon, so that a carbon substituent automatically destabilizes a silylium ion inductively. Second, the p_π–p_π overlap between carbon and silicon is considerably poorer than between carbon and carbon because of the differences in orbital dimensions (see 1.3). Based on these considerations, the Lambert group, in 1983, developed a sulfur substituted silyl cation (Figure 1.5 a).[32] Sulfur is higly polarizable, possesses 3p lone pairs that can overlap with the empty 3p on Si, and has an electronegativity similar to that of silicon, so that inductive effects should no be unfavorable.

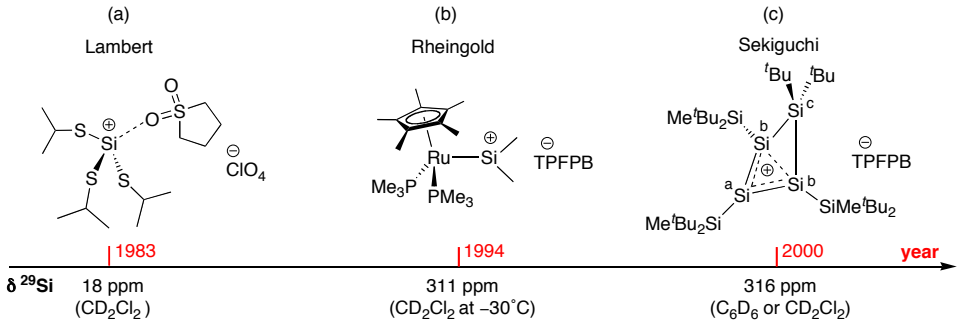

Figure 1.5 Examples of non-carbon-substituted silyl cations in literature.

Cryoscopy (investigation of freezing point depression) indicated that the new sulfur–containing species consisted of separated ions, but this method did not distinguish between a free cation $[(i\mathrm{Pr_3S})_3\mathrm{Si}]^+$ and a cation interacting with the solvent sulfolane $[(i\mathrm{Pr_3S})_3\mathrm{Si}\text{–solvent}]^+$; the relatively highfield shift of the ^{29}Si NMR resonance suggested that solvent coordination had taken place. In the late 1980s, and early 1990s, transition metal-containing compounds of the formula $[(\mathrm{L_nM})\mathrm{SiR_2}]^+$ were developed. One example is $[(\mathrm{Cp(PMe_3)_2RuSiMe_2}][\mathrm{TPFPB}]$ (Figure 1.5 b).[33] The downfield NMR resonance of $\delta(^{29}\mathrm{Si})$ = 311 ppm indicated high electron deficiency at the silicon atom. In the crystal structure, the silicon center was tricoordinated with a sum of angles around Si of 359˚. The relatively short Si–Ru bond (2.24 Å) was

consistent with the presence of significant double bond character, potentially due to $\sigma_{Si\rightarrow Ru}$ bonding, as well as π back donation from the ruthenium center into the empty 3p Si orbital. The definition of this species is not trivial and it is probably between a "dimethylruthenylsilylium ion" and a "ruthenium silylene complex". In 2000, Sekiguchi's group prepared an unusual silyl cation with the positive charge delocalized over a trisilacycle and with $^{t}Bu_2MeSi$ groups as substituents at silicon (Figure 1.5 c).[4] The cation in the crystal structure was free from coordination by anion or solvent molecules. The chemical shifts were $\delta(^{29}Si^{a})$ = 316 ppm, $\delta(^{29}Si^{b})$ = 77 ppm, and $\delta(^{29}Si^{c})$ = 16 ppm, independent of the solvent (dichloromethane, benzene, toluene). Thus, this species represents a silyl cation with a strongly deshielded silicon atom but a relatively low reactivity; all attempts to synthesize an analogous cation with less bulky substituents than $^{t}Bu_2MeSi$ groups failed.

Despite the interesting results obtained with the non carbon-containing silicon species, most of the research in this field has contemplated the synthesis of a free silylium ion with carbon substituents at silicon. The first efforts in this direction where done in the 1970s and 1980s, especially by the Lambert group. At that time, the knowledge about low coordinating solvents and counterions was still at an early stage and most of the cations synthesized were strongly coordinated to the nucleophiles present in solution.[34, 35] Therefore, the historical overview on carbon-substituted silyl cations is going to focus on the developments of the last two decades, when non polar aromatic solvents and counterions such as TPFPB and carboranes were used, guaranteeing the best environment for strongly electrophilic species. In 1993, Lambert and coworkers published the crystal structure of a "*silyl cation with no coordination to anion and distant coordination to solvent*".[36] $[Et_3Si(tolune)]$ [TPFPB] (Figure 1.6 a) presents a ^{29}Si chemical shift of 92.3 ppm in C_6D_6, 81.8 ppm in toluene-d_8 and of 87.1 ppm in a benzene/toluene (3/1) mixture. The observation of a single peak in the mixed solvent means that binding and dissociation between solvent and silylium ion are fast on the NMR timescale. In the crystal structure, the silicon center presents coordination with the carbon in *para* position of a toluene molecule (solvent): the Si–C_{para} distance of 2.18 Å is about 0.3 Å longer than a typical Si–C σ bond. If we apply

the Pauling bond order equation, we find that this value corresponds to a bond order of 0.35.[37, 38] The C–Si–C angle sum is 314° and the angle between Si–C and the ring plane is 104° (Figure 1.7 b). All these data opened a discussion on the definition of this new species: is the Et_3Si^+ forming a σ- or a π- complex with toluene? In a η^1

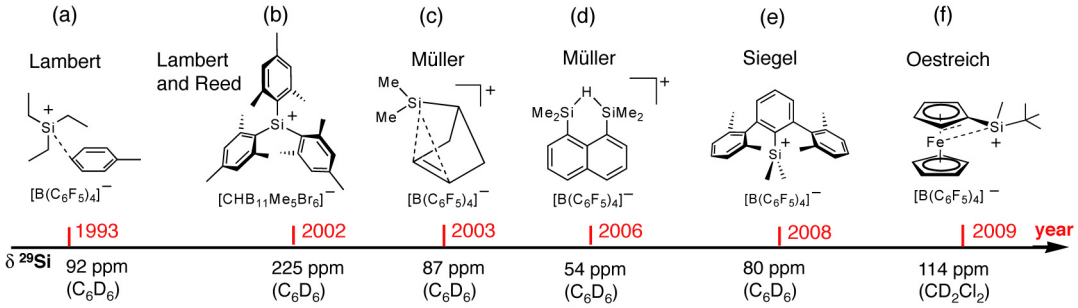

Figure 1.6 Significant examples of carbon-substituted silyl cations in literature.

π-coordination, e.g. the silver complex to benzene (Figure 1.7 a) found in 1985,[39] the silver atom is positioned directly above one carbon atom of the benzene ring, with an angle of 93° between Ag–C and the ring plane, and the positive charge mostly on the silver atom. A σ-complex, such as $Me_7H_6^+$ (Figure 1.7 c),[40] has an sp^3 carbon at the point of attachment of the electrophile, positive charge predominantly on the arene, and a marked alternation of C–C bond lengths indicating substantial loss of aromaticity. The properties of $Et_3Si(toluene)^+$ support a hybrid structure somewhere between an idealized π-complexed silyl cation and σ-bonded arenium ions.

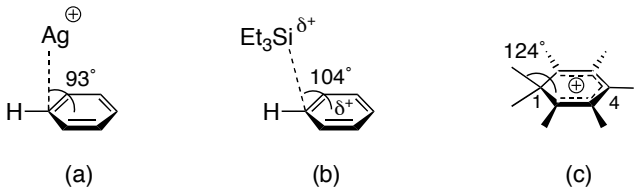

Figure 1.7 Examples of π– (a) and σ– (c) coordination modes compared to $[Et_3Si(toluene)]^+$ (b).

In 1995, the Reed group reported the solvent free X-ray crystal structures of four trialkylsilylium carborane compounds: $[Et_3Si][Br_6–CB_{11}H_6]$, $[iPr_3Si][Br_6–CB_{11}H_6]$, $[tBu_3Si][Br_6–CB_{11}H_6]$, and $[tBu_2MeSi][Br_6–CB_{11}H_6]$.[41] In these cases,

interactions with solvent and counterion were not found (Figure 1.8). The Si–Br bonds are in the range of 2.44–2.48 Å. The B–Br bonds of boron to coordinating bromine atoms are only 2–5% longer than the other B–Br bonds, showing little perturbation of the carborane structures.

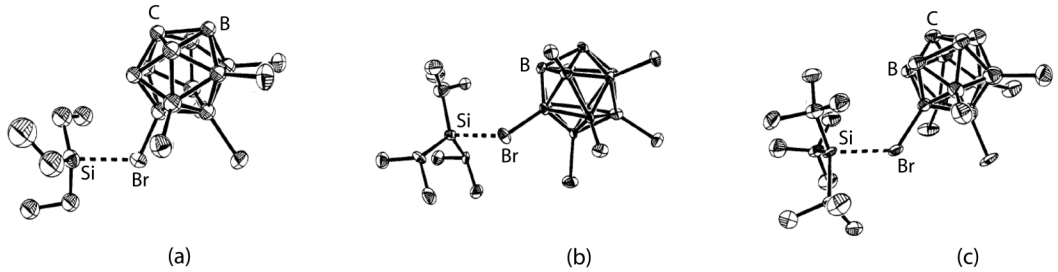

Figure 1.8 X-ray crystal structures of (a) $[Et_3Si][Br_6–CB_{11}H_6]$, (b) $[iPr_3Si][Br_6–CB_{11}H_6]$, (c) $[tBu_3Si][Br_6–CB_{11}H_6]$.

A question arises from these new results: are carboranes more coordinating anions than TPFPB? If we look at the ^{29}Si NMR of species such as *i*Pr_3Si–Y (Table 1.2), and use the chemical shift as a measure of the coordinating power of the anions, we see that hexachloro and hexabromocarborane are less coordinating than TPFPB. It looks then counterintuitive that the more coordinating counterion, TPFPB, does not interact with the silicon center, while hexabromo- and hexachlorocarborane do. It is important to consider that the equilibrium constant for solvent/anion coordination is a composite of intrinsic bond strength and solvation energy. Apparently the free TPFPB ion is better solvated in toluene than the hexabromocarborane to such an extent that the strongest silicon–anion bond is more easily dissociated.

$$[R_3Si][B(C_6F_5)_4] + \text{toluene} \rightleftharpoons R_3Si(\text{toluene})^+ B(C_6F_5)_4^- \qquad \textbf{Eq. 1.6}$$

The equilibrium in Eq. 1.6 is going to be less pronounced to the right-hand side when the anion is hexabromo- or haxachlorocarborane.

Table 1.2 ^{29}Si chemical shifts of iPr_3SiY species. [a] These data were collected in the solid state to remove any ambiguity about the coordination of the anion.

Compd	$\delta(^{29}Si)$ ppm
iPr$_3$SiH	12
iPr$_3$Si(OSO$_2$CF$_3$)	40
iPr$_3$Si(toluene)$^+$	94
iPr$_3$Si[B(C$_6$F$_5$)$_4$][a]	107
iPr$_3$Si(CB$_{11}$H$_6$Br$_6$) [a]	110
iPr$_3$Si(CB$_{11}$H$_6$Cl$_6$) [a]	115

Another important consideration that can be done on Reed's work concerns the effect of the alkyl substituents on Si. The compounds [Et$_3$Si][Br$_6$–CB$_{11}$H$_6$], [iPr$_3$Si][Br$_6$–CB$_{11}$H$_6$], [tBu$_2$MeSi][Br$_6$–CB$_{11}$H$_6$] resonate at $\delta(^{29}Si)$ = 112, 110, 113 ppm in the solid state, respectively. No solid state ^{29}Si NMR signal could be obtained for [tBu$_3$Si][Br$_6$–CB$_{11}$H$_6$], which was attributed to the lack of hydrogen nuclei on α-carbons to Si. Considering the steric and inductive effects of the substituents, one could have expected the *tert*-butyl groups to better expel the large anion and stabilize the positive charge at silicon. However, the presence of hydrogens on α-carbons leads to σ_{C-H}–3p interactions (hyperconjugation), as the relatively short bond length of one of the Si–C$_{i\text{Pr}}$ shows. The stabilization of alkyl groups on silyl cations is resulting from steric, inductive, and hyperconjugative effects.

Even the use of carboranes in aromatic solvents did not allow trigonality at silicon to be reached. Rather than considering solvent and anion complexation as an intractable problem, Reed and Lambert groups tried to take advantage of the steric effects, with the hope that larger substituents at silicon would decrease or eliminate these interactions. If the *tert*-butyl group had proved to be insufficient in order to avoid the halocarborane anion coordination, alkyl groups bigger than that rendered the Corey–West equation impossible. The real breakthrough happened in 1997, when Lambert and Zhao prepared the trimesitylsilylium ion (Figure 1.6 b).[14] The new compound showed the same ^{29}Si NMR shift of 225 ppm in three solvent systems

C_6D_6, C_6D_6/toluene-d_8 (3:1), C6D6/*p*-xylene-d_{10} (1:1). The spectroscopic data indicated the formation of a silyl cationic species with large downfield NMR shifts and no significant cation–solvent coordination. The structure of the product was elucidated in 2002, thanks to the collaboration of the Lambert and the Reed groups.[2] The use of the hexabromocarborane $[CB_{11}H_6Br_6]^-$ was fundamental to get crystals suitable for X-ray analysis. The crystal structure revealed a planar silylium ion with Σ(C–Si–C) = 360˚, a propeller-like arrangement of the three mesityl substituents, and no interaction of Si to atoms other than C_{ipso}. This achievement represented the solution to the *silylium ion problem*: the first tricoordinated, planar silylium ion had been synthesized, thanks to the efforts of that part of the chemical community that had worked for the development of new synthetic routes, anions and substituents.

The next challenge that chemists faced after the synthesis of the first free silylium ion, was the generation of cationic species with controlled stability and reactivity, in order to explore the limitation of silicon cation chemistry, and its possible application in organic synthesis. Over the past 10 years, the Müller group has developed a series of group 14 cations that were stabilized intramolecularly (Figure 1.6 c, d). Compound a in Figure 1.9 is an example of a silanorbornyl cation;[42] the π bond donates electron density to the silicon atom, which causes the positive charge to be distributed among silicon and carbon atoms. The ^{29}Si NMR shift is 87 ppm in benzene and shows only a small change of $\Delta\delta$ = +0.3 ppm when measured in toluene. NMR experiments and calculations at several level of theory consistently support a symmetrical cationic structure (Figure 1.9 a).

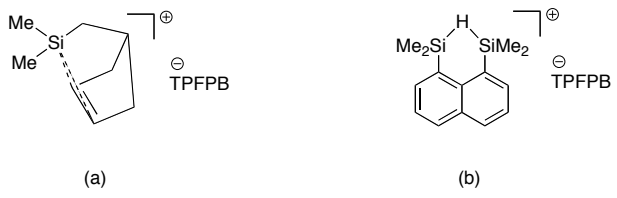

(a) (b)

Figure 1.9 Intramolecularly stabilized silicon species developed by the Müller group.

Another interesting system prepared by Müller is a hydrogen–bridged disilyl cation (Figure 1.9 b). Even though the ^{29}Si NMR of 54 ppm in benzene does not indicate an extremely high silylium ion character, the 1,8-naphthalenediyl backbone confers to this cation high stability, as demonstrated by the fact that it does not decompose upon heating at 90ºC in toluene for 3 days. The solid-state structure reveals that the cation is well separated from the anion and the solvent; the Σ(C–Si–C) = 345.5˚ and 346.7˚ for the silicon atoms indicates consistent deviation towards planarity, when compared to the values for ideal tetrahedral environment Σ(C–Si–C) = 328˚ and for trigonal planar coordination Σ(C–Si–C) = 360˚.

(a) (b)

Figure 1.10 Intramolecularly stabilized silylium ions developed by Siegel (a) and Oestreich (b).

To conclude this historical overview on the development of silicon substituents, two recent examples are discussed (Figure 1.6 e, f, Figure 1.10). In 2008, the Siegel group published a new class of silylium ions substituted with a terphenyl moiety.[43] The idea is that the terphenyl scaffold would offer steric protection to the Si center, as well as thermodynamic stabilization of the entire cation by π_{arene}–$3p_{Si}$ interaction. The flanking rings, which have restricted rotation about the biaryl bonds, prevent anions and solvent molecules from interacting with the positively charged cavity, while donation of electron density from the lateral π systems into the empty 3p(Si) orbital leads to a pacified silicon center. In accordance with this hypothesis, it was found that the ^{29}Si NMR shifts of these silylium ions reflect the electron donation ability of the lateral rings: for xylyl, it is 80 ppm; for mesityl, 79 ppm; for tetramethyl, 61 ppm, and for pentamethyl, 59 ppm. The solid state structures of the tetramethyl and pentamethyl substituted cations reveals that there is a specific interaction between

the silicon and the carbon β of the flanking rings (Figure 1.11). The same interaction exists in solution, as proven by the analysis of the ^{13}C NMR resonances of the flanking rings. The Cα, Cγ, Cδ are deshielded relative to their neutral precuror, while the Cβ is shielded. This pattern resembles the behaviour of a Wheland intermediate, where the tetracoordinate atom in the ^{13}C NMR is upfield shifted, while the other carbons are lowfield shifted, compared to the free arene. The authors define these structures as η^1 π coordinated cations, not having full silylium ion character.

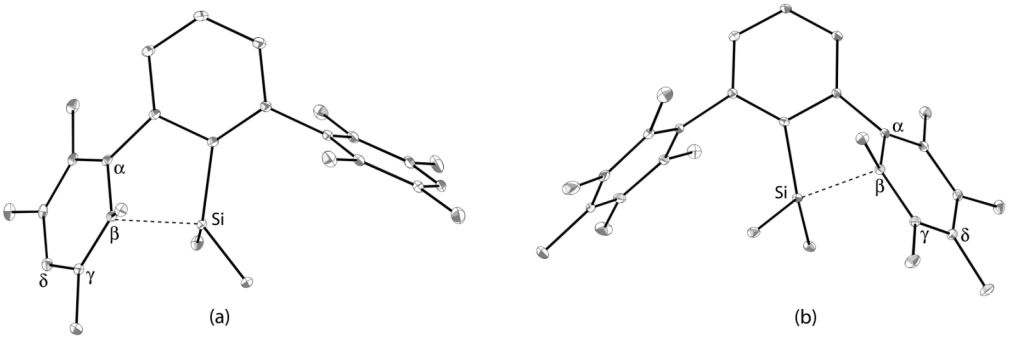

Figure 1.11 X-ray crystal structures of silylium ions with tetramethyl- (a) and pentamethyl- (b) substituted flanking rings.[43] Dashed lines: closest Si–C interaction.

We can interpret these systems as an evolution of Lambert's $Et_3Si(toluene)^+$ cation, where solvent coordination has been replaced by an intramolecular coordination to the flanking rings. The advantages of such a system are related to the long-term stability of the cations, in solution and in the solid-state, and to the tunability of the scaffold.

In 2009, Oestreich published a ferrocene-based silylium ion, in which the trivalent silicon center was intramolecularly stabilized by an electron-rich Ir atom (Figure 1.6 f, Figure 1.10 b).[20] The significantly downfield shifted ^{29}Si resonance of 114 ppm, if compared with other values reported in Figure 1.6, indicates that this iron-stabilized silylium ion is not "quenched" by a solvent molecule and is therefore still a reasonably strong Lewis acid. In the design of the substituents the authors were looking for a good balance of inherent Lewis acidity and steric accessibility to silicon,

to secure reversible coordination of Lewis basic functional groups essential for a catalytic turnover.

1.5 Application of Silyl Cations in Synthetic Chemistry

After many efforts aimed at synthesizing and isolating silylium ions, attention has recently been turned to the feasibility of their use in synthetic chemistry. The sensitivity of silylium ions towards oxygen and moisture undoubtedly preclude their use as bench reagents; nevertheless, the ability to control and direct their high electrophilicity can lead to the exploration of new reactivities. In particular, the affinity of silicon to electronegative elements, *i. e.* halogen atoms, can be exploited as a mean to perform leaving group abstraction.

Reed and coworkers obtained exceptionally strong Brønstead acids and methylating reagents by the reaction of triethylsilyl carborane with hydrogen chloride and methyl triflate (Scheme 1.6). Carborane acids (H^+–carborane$^-$) are currently the strongest isolable acids, capable of quantitative protonation of alkanes and arenes.[25, 29,44-46] The strong Lewis acidity of silylium ion species can be converted into strong Brønstead acidity by treatment with anhydrous HCl. The greater bond strength of Si–Cl (ca. 113 kcal mol^{-1}) versus H–Cl (103 kcal mol^{-1}) provides the driving force for this reaction. The electrophilicity of methyl carboranes, generated from silylium carborane, exceeds that of methyl triflate and has allowed the methylation of a number of weakly basic molecules that are inert to methyl triflate (*e.g.* benzene, tetramethylhydrazine).[45-47]

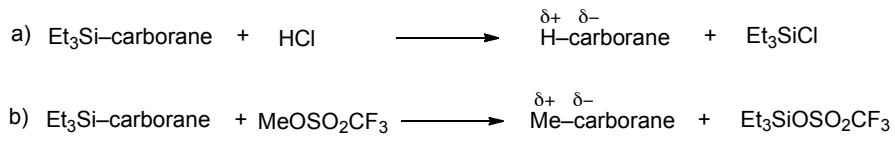

Scheme 1.6 Preparation of a) carborane acids and b) methyl carborane reagents.

Lewis acid catalysts are of great importance in cationic polymerization. The utility of silylium ions in this field has been demonstrated by a recent work in the Reed group. It was discovered that silyl carboranes such as $Et_3Si–CHB_{11}H_5Br_6$ catalyze the ring–opening polymerization of the cyclic chlorophosphazene trimer $(NPCl_2)_3$ to give linear $(N=PCl_2)_n$ (Scheme 1.7).[48] This inorganic polymer posses high

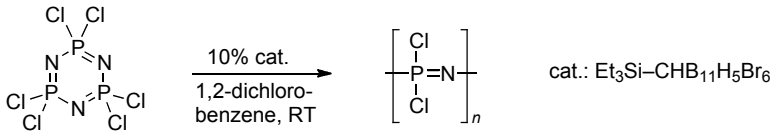

Scheme 1.7 Silyl carborane-promoted polymerization of $(NPCl_2)_3$.

tunability because of the possible substitutions of chlorine atoms by oxygen and nitrogen nucleophiles, and provide, therefore, a versatile scaffold for widespread material applications. Thermal ring opening polymerization of the cyclic phosphazene trimer can occur in a melt at ca. 250º; if Lewis acids such as BCl_3 and $AlCl_3$ are employed, the reduction in the process temperature is modest (to ca. 200º). It is generally accepted that the initiation step in this process involves thermal-induced or Lewis acid-assisted chloride abstraction from a cyclophosphatriazene; the resulting cation $(N_3P_3Cl_5)^+$ undergoes nucleophilic attack from another molecule of phosphazene and propagates the chain. Considering that, the use of silyl cations as chloride abstractors represented a valid alternative to the Lewis acids previously employed. In the presence of 10 mol % of $Et_3Si–CHB_{11}H_5Br_6$, the polymerization occurs readily at room temperature.

In organometallic chemistry, halogen abstraction from transition metal complexes is a useful methodology that is applied to obtain electronically and coordinatively unsaturated intermediates. Silyl cation $[Et_3Si][B(C_6F_5)_4]$ proved to be a suitable reagent for this transformation; it combines a highly electrophilic silicon center capable of halide abstraction, with a weakly coordinating anion. The Heinekey group performed chloride abstraction under H_2 atmosphere on a series of chloride metal complexes of rhenium, rhodium, iridium and osmium, and obtained the

corresponding cationic dihydrogen complexes (Scheme 1.8).[49-51] The dihydrogen bound to these complexes is significantly activated and is often in equilibrium with a dihydride form.

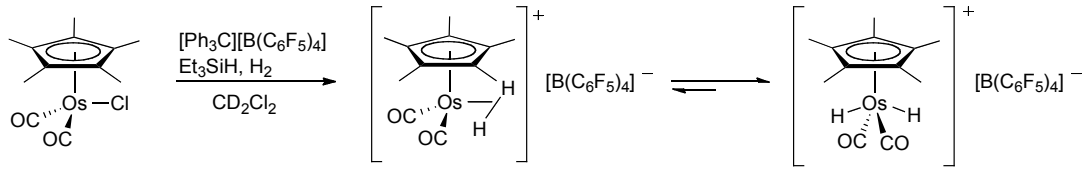

Scheme 1.8 Chloride abstraction from an organometallic complex by *in situ* generated Et_3Si^+.

Of extreme interest is also the activation of carbon–halogen bonds by silylium ions. Müller and Ozerov took the first steps in this direction, performing activation of $C(sp^3)$–halogen bonds.[52-55] Experiments with alkyl halides demonstrated the distinct preference for hydrodehalogenation of lighter halides, with the propensity for fluorine abstraction over chlorine being greater than that for chlorine over bromine.[56] If the halide abstraction is considered as the rate-liming step, this selectivity can be rationalize on the basis of the hard silylium acid exhibiting preference for the harder base. In particular, carbon–fluorine bond activation still represents a challenging topic in catalysis research. The extremely high affinity of silicon for fluorine was indeed seen as the way to activate one of the most passive functionalities in chemistry. This activation, which formally affords a carbocation, can be coupled to a subsequent reaction with a hydrosilane, leading to a reduced starting material and a fluorosilane (Scheme 1.9). Comparison of the bond strength for the bonds created and disrupted in the reaction $R_3C–F + Et_3SiH \rightarrow R_3C–H + Et_3Si–F$, *i.e.* C–F < Si–F and C–H > Si–H, indicates that this metathesis is thermodynamically favored. Various saturated and benzylic substrates undergo hydrodefluorination at room temperature in aromatic solvents or in neat silanes.

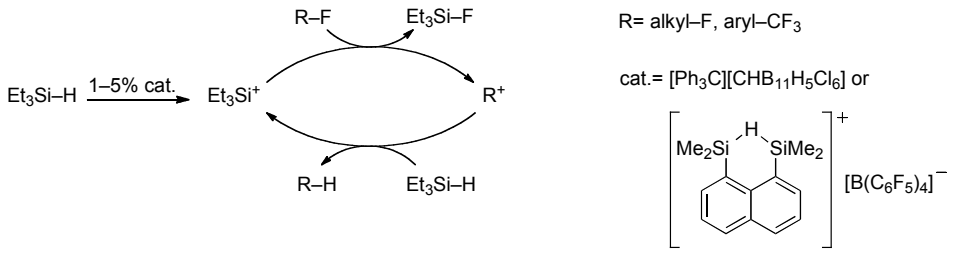

Scheme 1.9 Hydrodefluorination using Et_3SiH and a cationic initiator.

Further studies in the Müller group focused on turning the hydrodefluorination process, which in essence is a defunctionalization, into a synthetically preferable C–C coupling process.[57] This idea followed the observation that when primary and secondary alkyl fluorides were used as substrates of hydrodefluorination reactions in the presence of aromatic solvents, simple alkakes (R–H) were not formed, instead alkylated arenes were found to be the main products. The catalytic cycle proposed by Müller involves a silylium ion initiator abstracting a fluoride from the fluoroalkane R–F (Scheme 1.10); the carbocation R^+ reacts preferentially with trimethyl(phenyl)silane forming an arenium ion which delivers the alkylated arene and silyl cation Me_3Si^+. This cation abstracts a fluoride from the fluorodisilane, restoring the starting silylium ion catalyst. The $SiMe_3$ group on benzene is employed to *ipso*-direct the alkylation; nevertheless, the activating effect of the alkyl group facilitate further Friedel–Crafts-like alkylation reactions, leading to multiple substitution products.

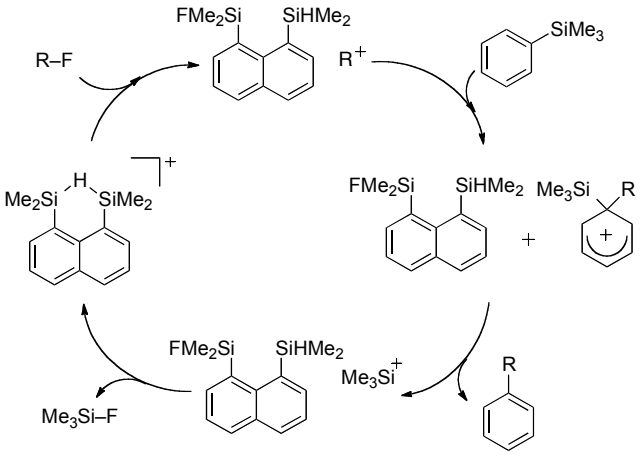

Scheme 1.10 Proposed catalytic cycle for C(sp^3)–F activation followed by C–C coupling.

Recently, the Siegel group successfully extended the reactivity just described for fluoroalkanes to fluoroarenes. The silicon–fluorine bond exceeds even the C(aryl)–F bond by about 120 kJ mol^{-1} and makes the fluoride abstraction from fluoroarenes by silylium ions a thermodynamically favored process.[58] Heating a solution of $[Et_3Si][CHB_{11}Cl_{11}]$ in fluorobenzene at 80ºC for several hours afforded two Ph-$CHB_{11}Cl_{11}$ isomers (Scheme 1.11).[59] The C–F activation hinges upon the use of the extremely weakly coordinating $CHB_{11}Cl_{11}^-$ counterion. Silylium ion-like species Et_3Si–Y with more nucleophilic carboranes (Y = $CHB_{11}H_5Cl_6^-$ and

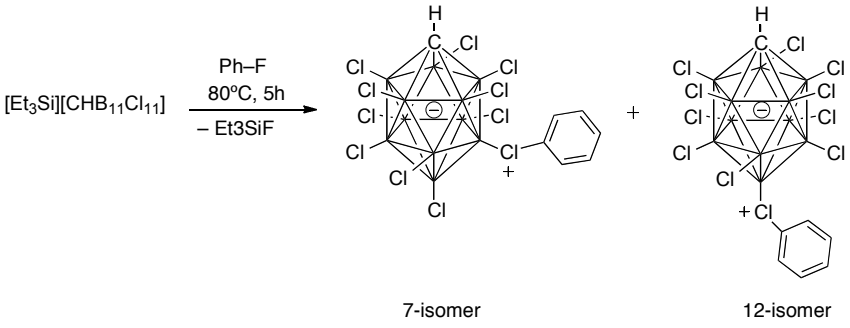

Scheme 1.11 C(sp^2)–F activation by $[Et_3Si][CHB_{11}Cl_{11}]$ affording phenyl carboranes.

$CHB_{11}H_5Br_6^-$) did not abstract fluoride from fluorobenzene under the conditions given in Scheme 1.11. Ph-$CHB_{11}Cl_{11}$ isomers are inert in solution, but can act as

phenylating agents towards nucleophiles: upon heating at 50ºC for 1h in the presence of nucleophiles, such as pyridine, Et_3N or PPh_3, $[Nu\text{-}Ph]^+$ and free $CHB_{11}Cl_{11}^-$ are formed. The use of a more fluorophilic silylium ion allowed the activation of fluorobenzene to occur at room temperature within hours (Scheme 1.12). The activation of fluoroarenes under mild reaction conditions opens the way for the development of a phenylating procedure using $Ph\text{-}CHB_{11}Cl_{11}$ and a novel Friedel–Crafts arylation method.

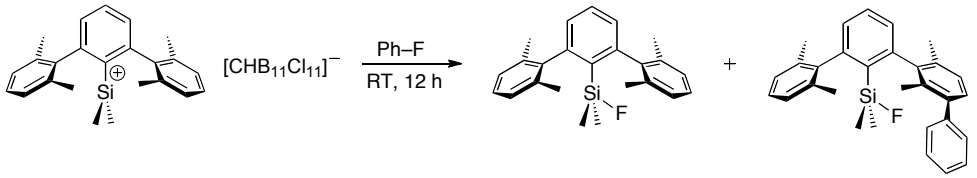

Scheme 1.12 C(sp^2)–F activation of fluorobenezene to give fluorosilanes.

Silyl cations are strong Lewis acids and therefore they represent a potential alternative to metal based Lewis acid catalysts. An early report on the use of silylnitrilium catalyst was provided by Helmchen and Jørgensen in 1998.[60] A chiral silylnitrilium ion anchored to a binaphtyl backbone promoted the Diels Alder reaction between 1,3-cyclohexadiene and acryloyl oxazolidinone under mild conditions. Regardless the low enantiomeric excess obtained, this study demonstrated that silyl Lewis acids were capable of effectively activating carbonyl groups and the excess of oxygen donor atoms with respect to the silyl cation catalyst did not suppressed their activity.

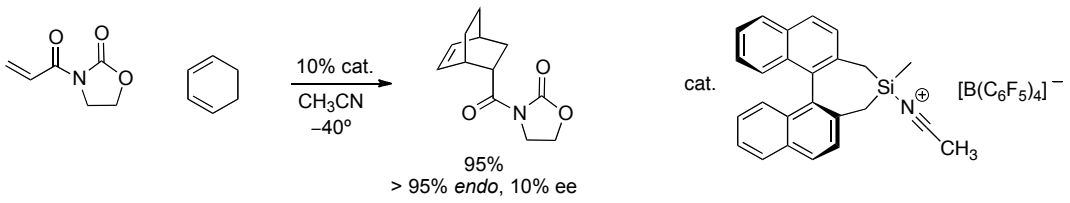

Scheme 1.13 Silylnitrilium ion-mediated Diels–Alder reaction.

If the ^{29}Si NMR shift is considered as a measure of Lewis acidity, $[Et_3Si(toluene)][B(C_6F_5)_4]$ should have an increased reactivity compared to silylnitrilium ion complexes. Sawamura decribed the high catalytic activity of this toluene-coordinated silyl borate in Diels Alder and Mukaiyama aldol reactions.[61] The performance of $[Et_3Si(toluene)][B(C_6F_5)_4]$ was first tested in Mukaiyama aldol reactions of ketones, for which only a limited number of effective catalysts have been reported to date. Reaction of acetophenone with 1-phenylvinyl trimethylsilyl ether was carried out at −78ºC and was completed in one hour to afford, after hydrolytic workup, the corresponding aldol product in a quantitative yield (Scheme 1.14). In contrast, low conversion was observed using Me_3SiNTf_2 and Et_3SiNTf_2, and no reactivity at all using Me_3SiOTf. The catalytic performance of $[Et_3Si(toluene)][B(C_6F_5)_4]$ was evaluated also for Diels–Alder reactions between 1,3-cyclohexadiene

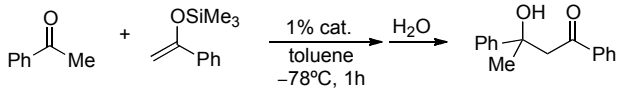

cat.	yield
Me_3SiOTf	0%
Me_3SiNTf_2	12%
Et_3SiNTf_2	8%
$[Et_3Si(toluene)][B(C_6F_5)_4]$	97%

Scheme 1.14 Mukaiyama aldol reaction catalyzed by silyl Lewis acids of different reactivity.

and methyl acrylate: analogously to the previous screening this catalyst demonstrated significantly higher activity than Me_3SiOTf, Me_3SiNTf_2 and Et_3SiNTf_2 (Scheme 1.15).

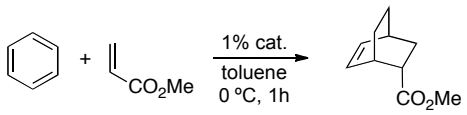

cat.	yield
Me_3SiOTf	0%
Me_3SiNTf_2	6%
Et_3SiNTf_2	13%
$[Et_3Si(toluene)][B(C_6F_5)_4]$	97%

Scheme 1.15 Diels–Alder reaction catalyzed by silyl Lewis acids of different reactivity.

Oestreich and coworkers in 2009 employed a new ferrocene-based silylium ion as catalyst for low temperature Diels–Alder reactions (Table 1.3).[20] In this cation, the interaction between silicon and the electron-rich late transition metal attenuates the Lewis acidity, while methyl and *tert*-buthyl substituents secure steric accessibility

to the silicon center. These parameters bring about the conditions for reversible coordination of Lewis basic functional groups essential for catalytic turnover. To test the potential of this ferrocene-based silyl cation, Diels–Alder reactions between cyclohexadiene (ca. 500 times less reactive than cyclopentadiene) and dienophiles of gradually decreasing reactivity were investigated. The cycloadditions were performed with high *endo* selectivity at −78ºC within hours in the case of dienophiles such as acroleine, 3-buten-2-one and methylacrilate. Cyclic α,β unsaturated ketones, such as cyclopentenone, as well as the reaction with the markedly deactivated chloroprene, required slightly elevated reaction temperatures and longer reaction times.

Table 1.3 Scope of the Diels–Alder catalyzed by a ferrocene stabilized silylium ion.

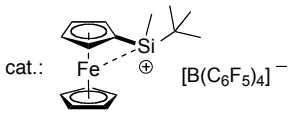

Entry	Diene	Dienophile	T[ºC]	*t* [h]	Product	Yield [%]	*endo/exo*
1			−78	1	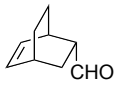	94	97:3
2			−78	3	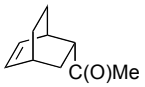	93	99:1
3			−78	3	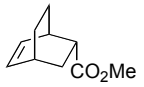	95	> 99:1
4			−40	12	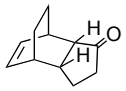	85	96:4
5			−30	24	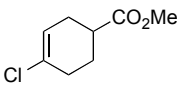	68	> 99:1 *para/meta*

The results obtained with Diels–Alder and Mukaiyama reactions have proved that it is possible to achieve a reversible coordination of a Lewis base to a silylium ion of moderate acidity. The next predictable step in this field, most likely, will involve

the use of a chiral silylium ion catalyst to control the stereochemical outcome of these reactions.

1.6 Thesis Objectives

The aim of this thesis is to expand the family of terphenyl silylium ions, previously developed in the Siegel group (Figure 1.10 a),[43] and to study their properties and their possible applications in organic synthesis. The tunability of these systems has been already tested: by varying the number of methyl substituents on the flanking rings, the degree of shielding at Si changes. We thought it would be interesting to introduce electron-withdrawing groups, compatible with silyl cations acidity, to reduce the degree of $\pi_{arene} \rightarrow 3p_{Si}$ donation (arene = aromatic flanking ring). For this purpose, halogen atoms have been chosen as first candidates, and the β-position of the lateral rings, where the closest Si–C interaction takes place in the methylated analogs, as the first one to be functionalized.

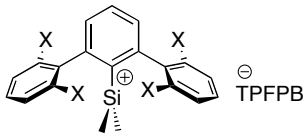

X = halogen

Besides the desire of tuning the electronic and steric features of terphenyl silyl cations, our efforts have been further directed towards the design and synthesis of a new family of silylium ions as active as the trimesitylsilylium ion, but sterically less hindered. The steric accessibility to the silicon center is fundamental when we think about a possible application of silylium ions in organic synthesis, *i.e.* in Lewis acid catalyzed reactions.

Furthemore, other molecules, more distant from the design of the first target, were developed in light of the results obtained along the way, as will be illustrated in the next chapters.

1.7 References

1. Powell, W. H., *Pure Appl. Chem.* **1993**, *65*, 1357.
2. Kim, K. C.; Reed, C. A.; Elliott, D. W.; Mueller, L. J.; Tham, F.; Lin, L. J.; Lambert, J. B., *Science* **2002**, *297*, 825.
3. Xie, Z. W.; Manning, J.; Reed, R. W.; Mathur, R.; Boyd, P. D. W.; Benesi, A.; Reed, C. A., *J. Am. Chem. Soc.* **1996**, *118*, 2922.
4. Sekiguchi, A.; Matsuno, T.; Ichinohe, M., *J. Am. Chem. Soc.* **2000**, *122*, 11250.
5. Huheey, J. K., E.; Keiter R., *Anorganische Chemie. Prinzipien von Struktur und Reaktivität*. Walter de Gruyter: Berlin, New York, 1995; p 1160-1165.
6. Kato, T.; Reed, C. A., *Angew. Chem. Int. Ed.* **2004**, *43*, 2908.
7. Olah, G. A., *J. Org. Chem.* **2001**, *66*, 5943.
8. Reed, C. A., *Acc. Chem. Res.* **1998**, *31*, 325.
9. Corey, J. Y.; West, R., *J. Am. Chem. Soc.* **1963**, *85*, 2430.
10. Barlett, P. D.; Condon, F. E.; Schneider, A., *J. Am. Chem. Soc.* **1944**, *66*, 1531.
11. Lambert, J. B.; Zhao, Y.; Zhang, S. M., *J. Phys. Org. Chem.* **2001**, *14*, 370.
12. Auner, N. W., J.; Uhlig, W., *Organosilicon Chemistry*. VCH: Weinheim, 1994; p 21-26.
13. Shade, L. M., H., *Makromol. Chem. Rapid. Commun.* **1988**, *9*, 477.
14. Lambert, J. B.; Zhao, Y., *Angew. Chem. Int. Ed.* **1997**, *36*, 400.
15. Lambert, J. B.; Zhao, Y., *J. Am. Chem. Soc.* **1996**, *118*, 7867.
16. Lambert, J. B.; Sun, H., *J. Am. Chem. Soc.* **1976**, *98*, 5611.
17. Prakash, G. K. S.; Keyaniyan, S.; Aniszfeld, R.; Heiliger, L.; Olah, G. A.; Stevens, R. C.; Choi, H. K.; Bau, R., *J. Am. Chem. Soc.* **1987**, *109*, 5123.
18. Bahr, S. R.; Boudjouk, P., *J. Am. Chem. Soc.* **1993**, *115*, 4514.
19. Kira, M.; Hino, T.; Sakurai, H., *Chem. Lett.* **1993**, 153.
20. Klare, H. F. T.; Bergander, K.; Oestreich, M., *Angew. Chem. Int. Ed.* **2009**, *48*, 9077.

21. Lambert, J. B.; Kuhlmann, B., *J. Chem. Soc. Chem. Commun.* **1992**, 931.
22. Lambert, J. B.; Schulz, W. J.; McConnell, J. A.; Schilf, W., *J. Am. Chem. Soc.* **1988**, *110*, 2201.
23. Kira, M.; Hino, T.; Sakurai, H., *J. Am. Chem. Soc.* **1992**, *114*, 6697.
24. Lambert, J. B.; Zhang, S. H., *J. Chem. Soc. Chem. Commun.* **1993**, 383.
25. Reed, C. A.; Kim, K. C.; Stoyanov, E. S.; Stasko, D.; Tham, F. S.; Mueller, L. J.; Boyd, P. D. W., *J. Am. Chem. Soc.* **2003**, *125*, 1796.
26. Lambert, J. B.; Zhang, S. Z.; Ciro, S. M., *Organometallics* **1994**, *13*, 2430.
27. Reed, C. A., *Acc. Chem. Res.* **1998**, *31*, 133.
28. Körbe, S.; Schreiber, P. J.; Michl, J., *Chem. Rev.* **2006**, *106*, 5208.
29. Reed, C. A., *Acc. Chem. Res.* **2010**, *43*, 121.
30. Jelinek, T.; Baldwin, P.; Scheidt, W. R.; Reed, C. A., *Inorg. Chem.* **1993**, *32*, 1982.
31. Ivanov, S. V.; Rockwell, J. J.; Polyakov, O. G.; Gaudinski, C. M.; Anderson, O. P.; Solntsev, K. A.; Strauss, S. H., *J. Am. Chem. Soc.* **1998**, *120*, 4224.
32. Lambert, J. B.; Schulz, W. J., *J. Am. Chem. Soc.* **1983**, *105*, 1671.
33. Grumbine, S. K.; Tilley, T. D.; Arnold, F. P.; Rheingold, A. L., *J. Am. Chem. Soc.* **1994**, *116*, 5495.
34. Lambert, J. B.; McConnell, J. A.; Schulz, W. J., *J. Am. Chem. Soc.* **1986**, *108*, 2482.
35. Lambert, J. B.; McConnell, J. A.; Schilf, W.; Schulz, W. J., *J. Chem. Soc. Chem. Commun.* **1988**, 455.
36. Lambert, J. B.; Zhang, S. H.; Stern, C. L.; Huffman, J. C., *Science* **1993**, *260*, 1917.
37. Pauling, L., *Science* **1994**, *263*, 983.
38. Pauling, L., *J. Am. Chem. Soc.* **1947**, *69*, 542.
39. Shelly, K.; Finster, D. C.; Lee, Y. J.; Scheidt, W. R.; Reed, C. A., *J. Am. Chem. Soc.* **1985**, *107*, 5955.
40. Baenzige.Nc; Nelson, A. D., *J. Am. Chem. Soc.* **1968**, *90* (24), 6602-&.
41. Xie, Z. W.; Bau, R.; Benesi, A.; Reed, C. A., *Organometallics* **1995**, *14*, 3933.

42. Müller, T.; Bauch, C.; Ostermeier, M.; Bolte, M.; Auner, N., *J. Am. Chem. Soc.* **2003**, *125*, 2158.
43. Duttwyler, S.; Do, Q. Q.; Linden, A.; Baldridge, K. K.; Siegel, J. S., *Angew. Chem. Int. Ed.* **2008**, *47*, 1719.
44. Juhasz, M.; Hoffmann, S.; Stoyanov, E.; Kim, K. C.; Reed, C. A., *Angew. Chem. Int. Ed.* **2004**, *43*, 5352.
45. Kato, T.; Stoyanov, E.; Geier, J.; Grutzmacher, H.; Reed, C. A., *J. Am. Chem. Soc.* **2004**, *126*, 12451.
46. Stasko, D.; Reed, C. A., *J. Am. Chem. Soc.* **2002**, *124*, 1148.
47. Zhang, Y.; Reed, C. A., *Dalton Trans.* **2008**, 4392.
48. Zhang, Y.; Huynh, K.; Manners, I.; Reed, C. A., *Chem. Commun.* **2008**, (4), 494-496.
49. Gelabert, R.; Moreno, M.; Lluch, J. M.; Lledos, A.; Pons, V.; Heinekey, D. M., *J. Am. Chem. Soc.* **2004**, *126*, 8813.
50. Matthews, S. L.; Pons, V.; Heinekey, D. M., *J. Am. Chem. Soc.* **2005**, *127*, 850.
51. Egbert, J. D.; Bullock, R. M.; Heinekey, D. M., *Organometallics* **2007**, *26*, 2291.
52. Scott, V. J.; Celenligil-Cetin, R.; Ozerov, O. V., *J. Am. Chem. Soc.* **2005**, *127* , 2852.
53. Panisch, R.; Bolte, M.; Muller, T., *J. Am. Chem. Soc.* **2006**, *128*, 9676.
54. Douvris, C.; Ozerov, O. V., *Science* **2008**, *321*, 1188.
55. Meier, G.; Braun, T., *Angew. Chem. Int. Ed.* **2009**, *48*, 1546.
56. Douvris, C.; Nagaraja, C. M.; Chen, C. H.; Foxman, B. M.; Ozerov, O. V., *J. Am. Chem. Soc.* **2010**, *132*, 4946.
57. Luhmann, N.; Panisch, R.; Muller, T., *Appl. Organomet. Chem.* **2010**, *24*, 533.
58. Blanksby, S. J.; Ellison, G. B., *Acc. Chem. Res.* **2003**, *36*, 255.
59. Duttwyler, S. D., C.; Fackler, N. L. P.; Tham, F. S.; Reed, C. A.; Baldridge, K. K.; Siegel, J. S., *Angew. Chem. Int. Ed.* **2010**, *49*, 7519.

60. Johannsen, M.; Jorgensen, K. A.; Helmchen, G., *J. Am. Chem. Soc.* **1998**, *120*, 7637.

61. Hara, K.; Akiyama, R.; Sawamura, M., *Org. Lett.* **2005**, *7*, 5621.

2 Through-Space Interactions in Enshrouded *meta*-Terphenylsilanes[†]

2.1 Introduction

Steric shrouds are an integral part of molecular systems designed to isolate and observe "reactive intermediates". In the field of silicon-based reactive intermediates, several unsaturated silicon compounds,[1-3] charged reactive silyl intermediates, [4] and transition metal complexes bearing silicon ligands exemplify the success of this design.[5, 6] Besides shielding the reactive functionality from the ambient environment, the shroud mediates the local environment. Tuning the symmetry, geometry and electronic character of the shroud provides a vehicle to control the reactivity of the silyl core for the development of new reagents.

meta-Terphenylsilanes are tunable, sterically-demanding substituents,[7-18] which can be employed to stabilize cationic and unsaturated species,[19-22] and which are facile to synthesize in various derivatives.[23] The conical shielding created by the three rings limits the number of energetically feasible trajectories for intermolecular reactions.[24, 25] Several terphenylsilanes of type **I** have appeared and form an empirical basis upon which to begin a structure/property relationship.[22, 26-30] Correlation of structural changes of the shroud with the resultant properties at silicon will define the prospects for this class of silyl reagent design.

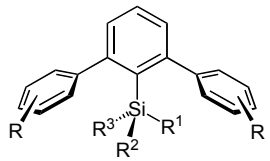

I

Our analysis carefully follows the conformation and conformational dynamics of the derivatives compared to reference compound **1**. *meta*-Terphenylsilanes can exhibit varying degrees of symmetry, depending on the nature of the substituents at silicon

[†] This work has been done in collaboration with Simon Duttwyler, University of Zurich.

and the nature of the distal rings. High dynamic symmetry is obtained with identical lateral rings and three identical groups attached to silicon. Desymmetrization results by substitution of one ligand at silicon, of one ring in a flanking position, or both. The molecular geometry of such systems can be described by the conformation of the silyl group with respect to the central ring (torsion angle α) and the relative orientation of the least-squares planes through the aromatic rings (dihedral angles β and γ) (Figure 2.1). In *meta*-terphenylsilanes, β and γ are usually between 60 and 90°, whereas the value of α depends on the nature of the substituents at silicon.[28-30] This relationship, between the substituent at silicon and the energy profile of α, gives important insight into the shroud/core interaction.

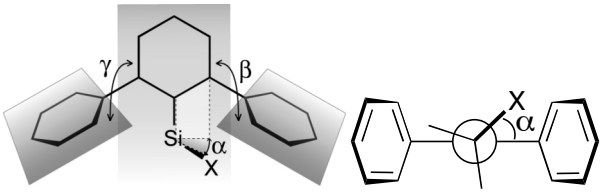

Figure 2.1 Definition of torsion angles: α (torsion about C(ar)–Si bond); β and γ (dihedral angles between the least-squares planes of flanking and core rings).

2.2 Structure and Dynamics of Molecule 1

Our study of the interactions between the steric shroud and silane core starts with evaluation of the symmetric bis[2,6-(2,4,6-trimethylphenyl)]phenyltrimethylsilane **1** as a reference molecule; the flanking mesityl rings serve as the shroud and trimethyl-

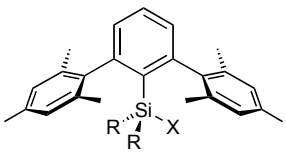

	R	X
1	Me	Me
2	Me	H
3	Me	$CH_2CH{=}CH_2$
4	*i*Pr	H
5	Me	OH
6	Me	F

silane as the core. From there, the evaluation of lower symmetry derivatives, **2**–**6**, in which exchange of one of the methyl groups at silicon by a substituent varying in size and/or electronic properties, creates a context for teasing out substituent effects. The relatively bulky mesityl rings were expected to minimize interactions of the silyl group with solvent molecules in solution or other molecules in the solid state, thus highlighting the SiR_3–π interactions.

Bromo- and iodoterphenyls are obtained in two or three steps from commercially available starting materials and can be functionalized by lithiation and subsequent treatment with an electrophile of choice.[31-33] Compound **1** was prepared from the corresponding iodoterphenyl $Mes_2C_6H_3I$ by lithiation with *n*-butyllithium and subsequent treatment with chlorotrimethylsilane, similarly to a reported procedure.[19]

The structure and dynamic behavior of **1** was examined by NMR spectroscopy and X-ray crystallography. The ^{29}Si NMR resonance at –6.2 ppm in C_6D_6 lies in the typical range for neutral, tetracoordinate silanes (Table 2.1).[34] ^{1}H and ^{13}C NMR spectra in various solvents at room temperature showed time-averaged signals for the methyl groups at silicon and the mesityl rings, *i.e.*, one for $Si(Me)_3$, one for CH_3-C_{ortho}, and one for CH_3-C_{para}, the result of a fast rotation of the silyl group about the Si–C_{ring} bond. Although in any given conformation at least two of the methyl groups at silicon are diastereotopic, rapid site exchange on the NMR timescale gives rise to averaged peaks, corresponding to dynamic [C_3xC_2xC_s] symmetry of the molecule.

Table 2.1 ^{29}Si NMR shifts and selected distances (Å) and angles (°) for silanes **1**–**6**.

	δ^{29}Si exp[a]	δ^{29}Si calc[b]	Si–X	Si–C1	Si–C2	Si–C_{ring}	α	β	γ
1[c]	–6.2	–5.7	1.865(2)	1.871(2)	1.866(2)	1.917(2)	13.2(2)	88.55(9)	84.17(9)
2	–23.0	–19.2	1.41(2)	1.859(2)	1.860(2)	1.901(2)	42.0(8)	93.93(9)	87.22(8)
3	–7.0	–	1.892(3)	1.863(2)	1.859(2)	1.921(1)	54.9(2)	80.04(7)	76.00(7)
4	3.7	–	1.36(2)	1.885(2)	1.900(2)	1.912(2)	20(1)	89.76(9)	88.06(9)
5	5.7	1.5	1.647(1)	1.852(2)	1.853(2)	1.910(2)	19.9(2)	91.1(1)	86.2(1)
6	19.4	16.9	1.605(1)	1.848(2)	1.848(2)	1.891(2)	47.2(1)	93.04(9)	85.45(8)

a ppm in C_6D_6 vs $SiMe_4$. *b* M06-l/DZ+(2df,pd)//M06-2X/DZ(2df,pd). *c* There are two symmetry-independent molecules in the asymmetric unit and these molecules have almost identical conformations. The r.m.s. fit of the corresponding atoms of the two molecules is 0.14 Å.

Low-temperature NMR measurements of **1** show no splitting of signal degeneracy in solution or in the solid state, which supports a low barrier to rotation about the C(ar)–Si bond. Deuterated dichlorofluoromethane $CDCl_2F$ was used for low-temperature NMR studies, in order to achieve near liquid nitrogen temperatures while retaining good solvent characteristics.[35] ^{1}H NMR spectra of **1** were recorded over the range of 0 °C to –130 °C; however, neither decoalescence nor peak broadening were observed. By the Gutowsky–Holm approximation, this finding indicates a barrier smaller than 29 kJ mol^{-1} for the rotation of the silyl group about the Si–C_{ring} bond. [36] Solid-state ^{13}C NMR measurements of **1** in the range of +50 °C to –110 °C also afforded only time-averaged spectra, consistent with virtually unhindered rotation of the silyl group even in the solid state. A rationale for the observed behavior comes from an X-ray crystallographic analysis of **1**.

Solvent-free crystals of **1** suitable for X-ray crystallography were obtained from an isopropanol–methanol solution at room temperature. Two symmetry-independent molecules of near identical conformation were found in the asymmetric unit at 160 K (Figure 2.2, Table 2.1). The well-separated molecules are packed in

such a way that there is no restriction to rotation of the $SiMe_3$ group. The absence of an interlocking motif accounts for the result of the solid-state NMR study. The preferred conformation of the silyl group appears to be a manifestation of repulsion between the methyl groups and the lateral rings. One of the methyl groups at silicon shows an almost eclipsed orientation to one of the mesityl systems (α = 13.2(2) °), while the other two occupy positions with larger distances to ring atoms. Indicative of strain even in the preferred solid-state structure is the Si–C_{ring} distance of 1.917(2) Å, which is longer than typical Si–(sp^2)C bonds found in comparable silanes with less steric crowding, having lengths of 1.85–1.88 Å.[28, 30]

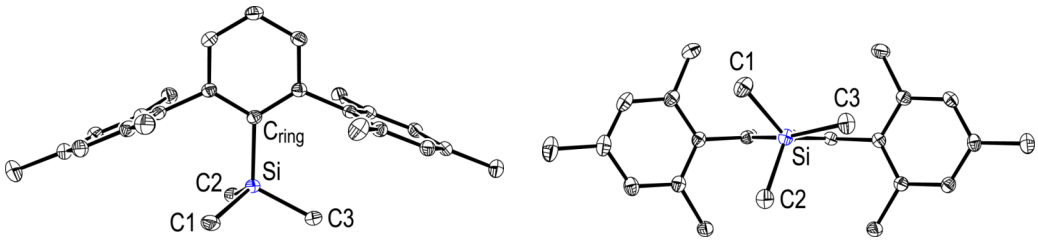

Figure 2.2 ORTEP representation of one of the two symmetry-independent molecules in the crystal structure of **1** (H atoms omitted for clarity; displacement ellipsoids drawn at the 30% level).

Exchange processes can be evaluated by NMR and diffraction methods. At –130 °C, exchange processes with activation barriers up to about 30 kJ mol^{-1} will manifest only time-averaged NMR signals. On the other hand, the electron density map derived from the diffraction pattern reflects a large number of fast snapshots and gives a weighted average of the atomic positions in the crystal.[37, 38] A positional preference of 1000:1 renders a very localized atomic position. A second determination of the crystal structure of **1** shows slightly larger thermal displacement parameters of the refined atoms compared to those derived from the 160 K structure. Thus, in the case of silane **1**, there is a conformational preference for the silyl group, such that the methyl groups spend most of their time in this conformation but still exchange their sites rapidly. This situation, reflected by the two spectroscopic methods, is consistent with an exchange process in the crystal of between 15–30 kJ mol^{-1}.

2.3 Conformational Analysis of Derivatives 2–6

Replacing the trimethylsilyl group by a group of lower symmetry, SiR_2X, results in a conformational bias, the magnitude of which reflects a difference in size and electronic character between R and X. Extreme conformations include $\alpha = 0°$ (eclipsed), where the X substituent eclipses the central-ring plane and points directly into the face of a flanking ring, and $\alpha = 90°$ (staggered), where the X substituent points perpendicular to the central-ring plane and avoids contact with either flanking ring. Intermediate conformations are also possible and will be discussed in context.

On the basis of classical steric arguments and considerations of polar-π effects, one expects larger and more negatively charged substituents to disfavor the eclipsed conformation when 2,4,6-trimethylphenyl is the flanking ring. Small substituents bearing a partial positive charge should favor the eclipsed conformer. However, the total energy of interaction also includes a van der Waals (dispersive) term, which depends strongly on the contact surface area, unlike the Coulombic terms, that depend on the relative charge distribution. Therefore, looking at a series of substituents of varying electronic effects can provide a more accurate picture of the range of structure and properties in such a scaffold. Empirical aspects of physical organic substituent constants give a crude assessment of the ranking of size and polarity in the variable substitutents of **1**–**6** (Table 2.2).

Table 2.2 Substituent character (5 most; 1 least)

	Cl	CH_3	$OH_{(anti)}$	$OH_{(syn)}$	F	H
Size	5	4	3	3	2	1
vdW	5	4	3	3	2	1
δq	δ^- (5)	* (1)	δ^- (4)	δ^+	δ^- (3)	δ^- (2)

The series **2–6** was synthesized in a similar manner to that of **1** and showed no unusual spectroscopic features (Table 2.1).[39] X-ray crystallographic studies of **2–6** suggest an unsymmetrical ground state conformation, in which the methyl groups of the silane would be diastereotopic. For all molecules, NMR spectra, obtained in $CDCl_3$ and C_6D_6 at room temperature, revealed only a single methyl resonance, implying a dynamic exchange process that renders the signals equivalent. In the range of 0 °C to –130 °C in $CDCl_2F$, no signal broadening or decoalescence was observed, supporting a low activation barrier processes. Calculations performed on **1**, **2**, **5**, **6**, at the dispersion-enabled density functional level of theory were also carried out, and in general, are in good agreement with the experimental results.

The crystallographic conformation of **2** shows a methyl group eclipsed to one mesityl ring and one methyl group resting between the lateral rings (Figure 2.3). The hydrogen atom at silicon can be assumed to be relatively small; therefore, the observed structure is attributed to minimized repulsion between the methyl groups and the mesityl systems.

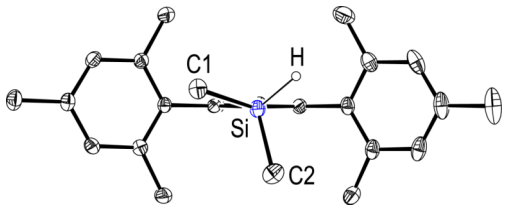

Figure 2.3 ORTEP representation of **2** (H atoms omitted for clarity, except for H–Si; displacement ellipsoids drawn at the 30% level).

The hypothesis that larger substituents dictate the preferred conformation is supported by the crystal structures of **3** and **4**. In silane **3**, the allyl group, the sterically most demanding substituent at silicon, dominates the picture and occupies a position with $\alpha > 60°$ and leads to a distorted terphenyl scaffold (Figure 2.4). When viewed along the $Si–C_{ring}$ axis, the molecule shows a bent structure, and reduced dihedral angles β and γ reflect enhanced repulsion between the allyl group and the mesityl systems. On the other hand, in **4**, comprising one small hydrogen and two markedly bigger isopropyl groups at silicon, the hydrogen is forced into the face of a lateral ring (Figure 2.5).

The isopropyl groups minimize interaction with the mesityl rings, which adopt an almost perfect orthogonal conformation with respect to the central ring.

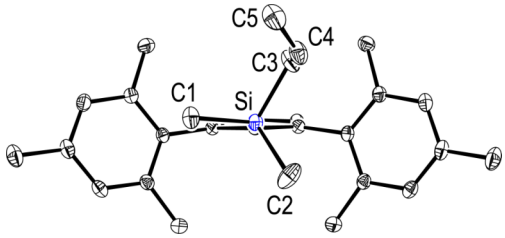

Figure 2.4 ORTEP representation of **3** (H atoms omitted for clarity; displacement ellipsoids drawn at the 30% level; only one conformation of the disordered allyl group is shown).

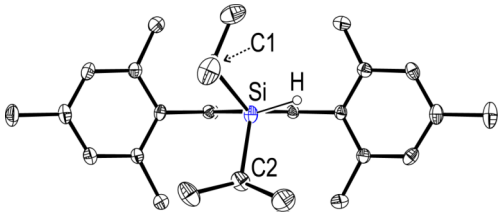

Figure 2.5 ORTEP representation of **4** (H atoms omitted for clarity, except for H–Si; displacement ellipsoids drawn at the 30% level).

The conformation of the silyl group, in the crystal structure of silanol **5**, supports a model involving more than steric effects. The OH group exhibits a near eclipsed orientation to one of the mesityl rings (Figure 2.6). The proximity of the OH hydrogen atom to the centroid of the mesityl ring is 2.42(3) Å, the perpendicular distance from the H atom to the least-squares plane through the ring atoms is 2.30 Å and the O–H···centroid angle is 160(3)°. A similar O–H···π geometry has been found in the terphenylsilanetriol congener of **5**.[40-43] Coulombic interactions between the π electrons and hydrogen of ROH would favor this conformation.[26]

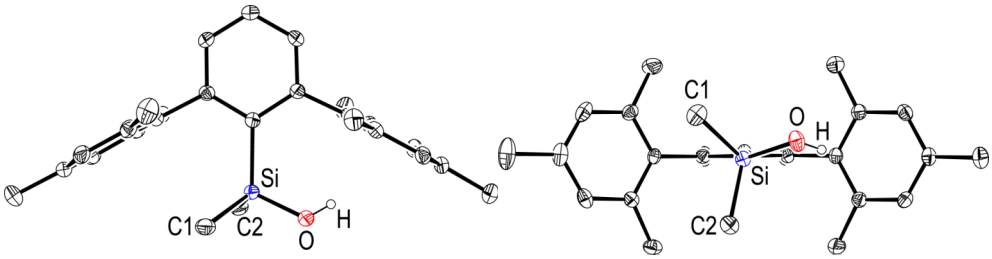

Figure 2.6 ORTEP representation of **5** (H atoms omitted for clarity, except for H–O; displacement ellipsoids drawn at the 30% level).

When OH is replaced by fluorine, as in **6**, a geometry resembling that of **2** is found in the crystal (Figure 2.7). While a fluorine substituent is similar in size and electronegativity to oxygen, a fluorine substituent carries a partially negative terminal charge that make its proximity to an electron-rich π system unfavorable.[44, 45] As in the case of **2**–**4**, the structure of **6** is a result of a delicate balance of *de*stabilizing effects. However, the contribution of F···π repulsion to the observed conformation is difficult to assess in view of the structural similarities of **2** and **6**.

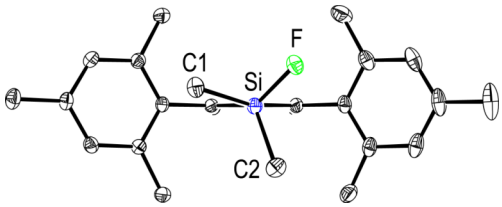

Figure 2.7 ORTEP representation of **6** (H atoms omitted for clarity, displacement ellipsoids drawn at the 30% level).

M06-2X/DZ(2df,pd) geometry optimization and vibrational analysis was carried out on **1**, **2**, **5**, **6**. Conformations associated with eclipsed, staggered, and intermediate geometries were investigated in each case. For X = H or Me, the energy between all three positions is less than 1 kcal mol^{-1}, indicating essentially no preference (Table 2.3). In contrast, when X = F, **6**, the staggered conformation is predicted to be the more stable, with a gradual increase in energy as the fluorine moves towards the eclipsed conformation, illustrating the increase in repulsive interaction between fluorine and the π-density of the flanking ring. Similar behavior

is found with X = Cl, except that the repulsive interaction is much stronger than with fluorine (3.3 kcal vs 1.3, respectively). When X = OH, **5**, the minimum energy structure is found to be eclipsed. As in the experimental structure, the hydrogen atom of the OH group points into the aryl ring with the distance from H to the centroid of the ring being 2.46 Å, from the H atom to the least-squares plane of the ring 2.28 Å, and the O–H···centroid angle 149.5°.

The energy difference between any conformation along the α trajectory in all cases is less than ~3 kcal mol^{-1} (Table 2.3), indicative of a very soft potential. The calculated small barriers to rotation and the lowest-energy structures of these compounds are consistent with the experimental findings. Theoretical values and the upper limits for all rotational barriers inferred from NMR spectroscopy can be interpreted as a high-energy ground state phenomenon. The three substituents on the central benzene ring repel each other regardless of the conformation of the SiR_2X group. In the transition state of rotation, steric interactions are only slightly increased with respect to the ground state. In other words, even in the most favored conformation, little activation energy is needed to reach another minimum.

Table 2.3 M06-2X/DZ(2df,pd) calculated structure and energetic properties of **1**, **2**, **5**, **6**, and **6**-Cl.

Compd.	**α (°)**	**Rel. E (incl. ZPE) kcal mol^{-1}**
1	0–90	< 1 kcal/mol
2	0–90	< 1 kcal/mol
5	0	0.0
	90	2.2
6	0	1.3
	90	0.0
6-Cl	0	3.3
	90	0.0

In order to detect the possible presence of different rotamers in the crystals of **2**, **5**, and **6**, electron density difference maps were used. The data for these three compounds, both at 160 K and at room temperature, were taken, and the occupancy of the Si-methyl groups and the X atoms were set to zero. Then in each case a difference map was constructed in the plane of X-Si-C, C being the carbon atom of the methyl groups. The difference maps are shown in Figure 2.8, Figure 2.9, and Figure 2.10. In case of **2**, X has just one electron. If there were rotamers present with swapped H/Me sites, there should be a noticeable increase in electron density near the H atom site. There is no indication of that, which is in agreement with the presence of only one rotamer. For compound **5**, an analysis based on the bond lengths of Si–O and Si–C was carried out. As the Si–O and Si–C bond lengths differ by about 0.20 Å, one would expect some distortion in the electron density along the bonds if there was any significant amount of rotamers in the structure. However, the electron density of the plot looks fairly uniformly circular, or at least not elongated or shortened along the bonds (either towards or away from Si). Thus the plots do not seem to suggest any significant amount of rotamers present. In the case of **6**, the bond lengths Si–F and Si–C differ a little bit more, by about 0.25 Å. An analogous analysis for **6** and **5** did not indicate the presence of different rotamers.

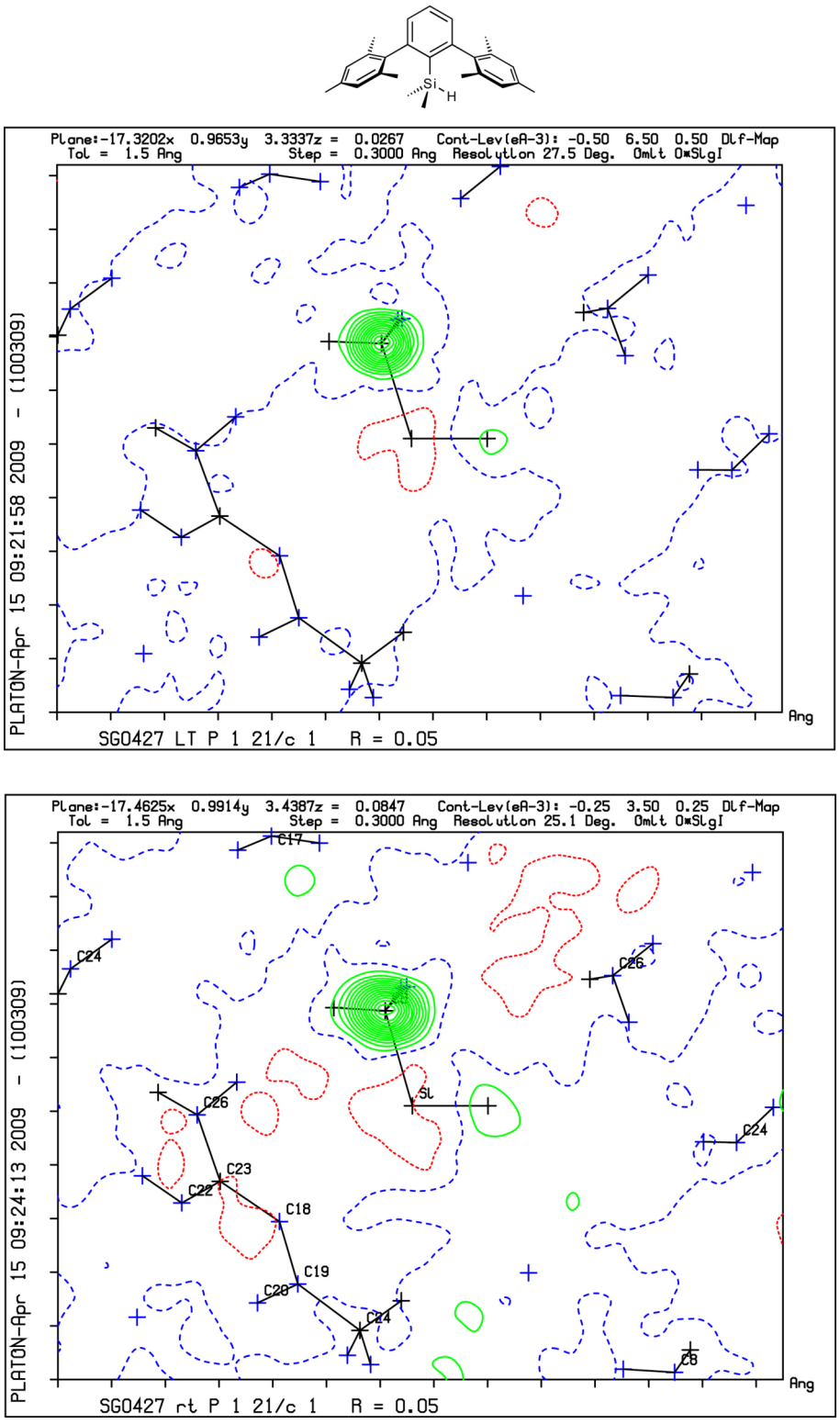

Figure 2.8 Electron density difference map of $Mes_2C_6H_3SiMe_2H$ (**2**) at 160 K (top) and RT (bottom).

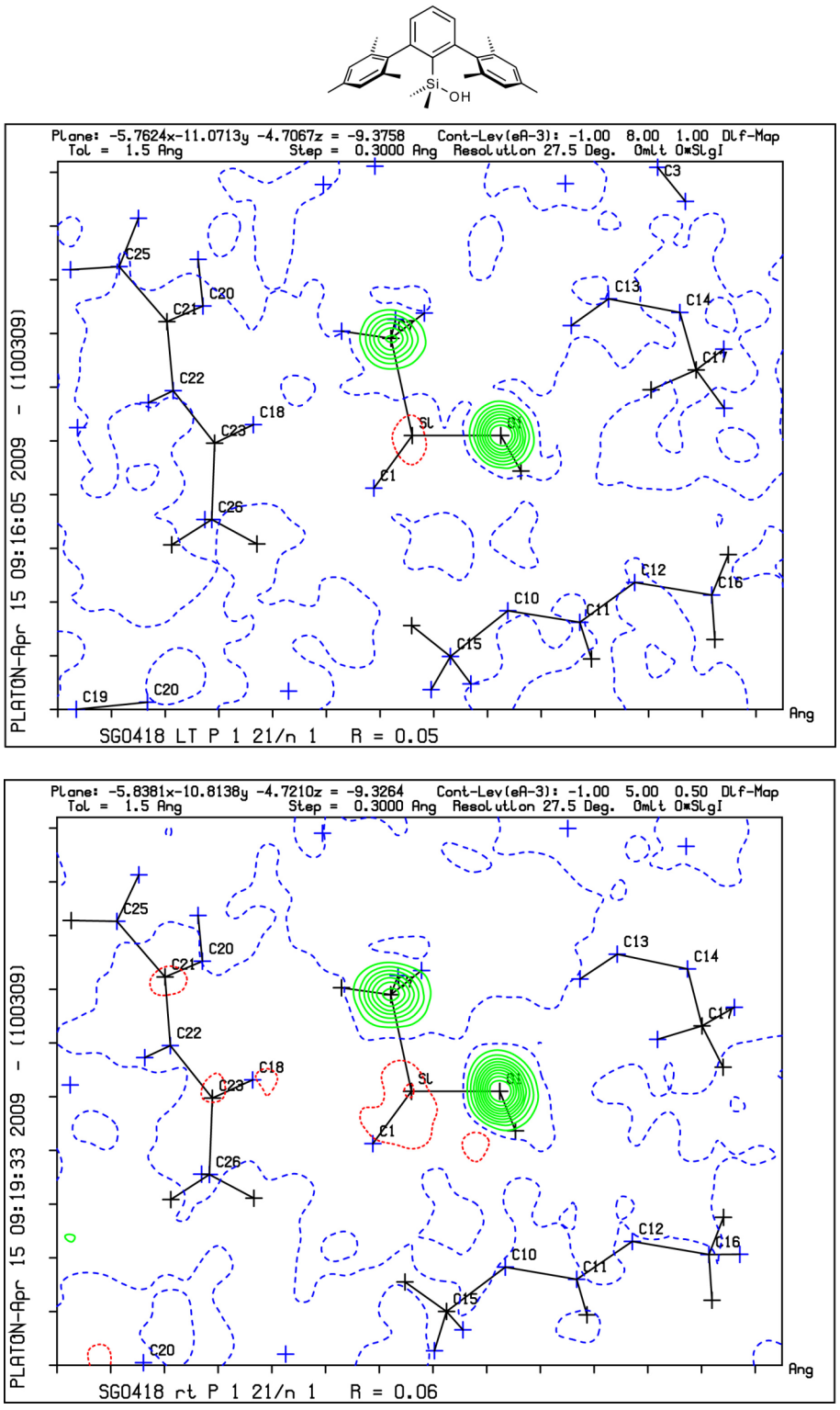

Figure 2.9 Electron density difference map of $Mes_2C_6H_3SiMe_2OH$ (**5**) at 160 K (top) and RT (bottom).

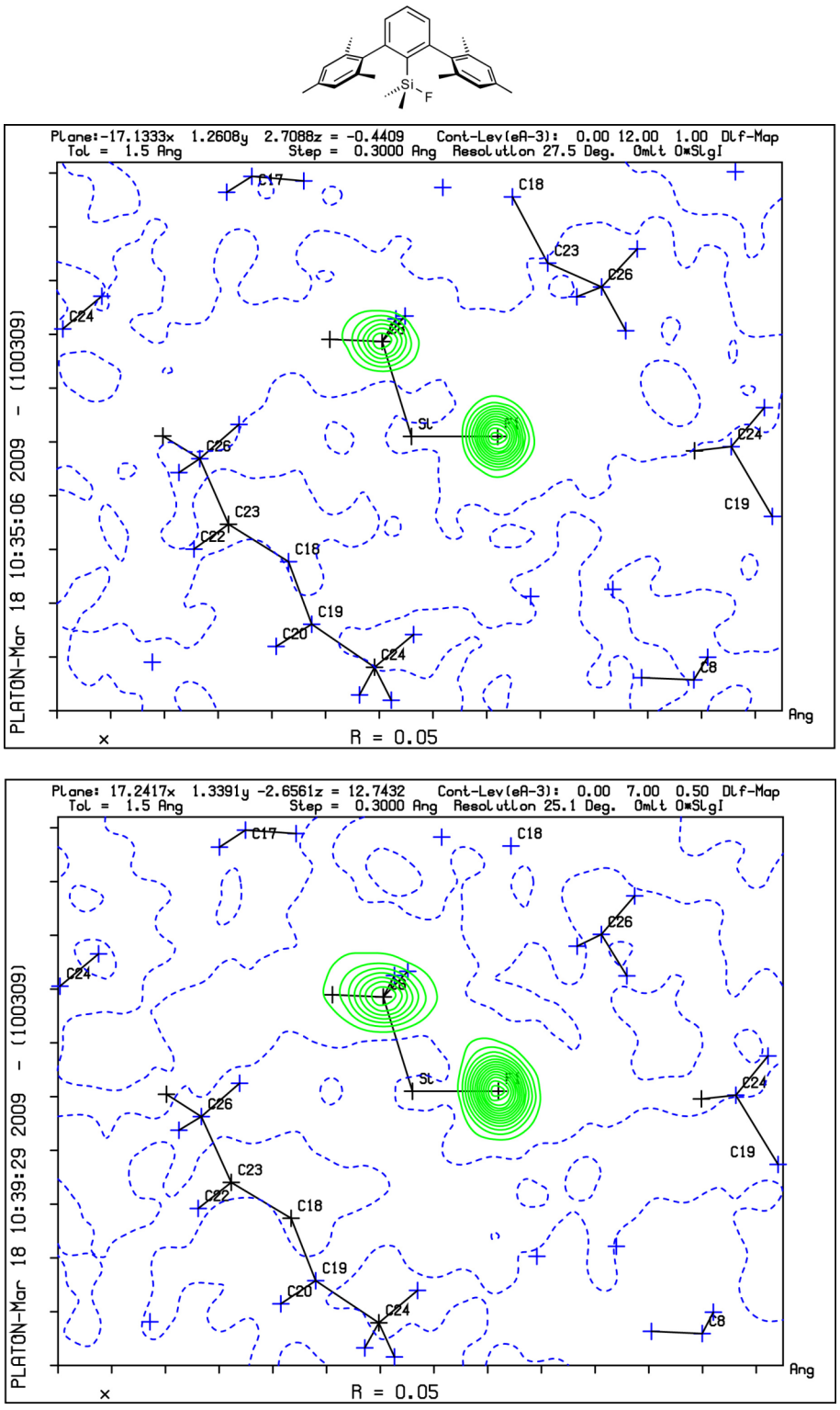

Figure 2.10 Electron density difference map of $Mes_2C_6H_3SiMe_2F$ (**6**) at 160 K (top) and RT (bottom).

2.4 Conformational Analysis of 7–13.

Modification of the flanking rings and further desymmetrization by breaking the equivalance of the flanking ring substitutions refine the shroud/core interaction model. Ring substituents of different size and electronic properties enable the tunability of the terphenyl systems by varying the steric demand and π basicity of the lateral rings. Previously, such a model was used to explain the pK_a values of a series of terphenyl carboxylic acids as due to through-space effects.[23] A related investigation of properties within a series of silanes, **7**–**13**, with varying methylated and halogenated aryl rings was undertaken here.

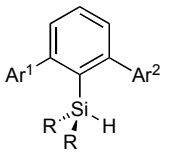

	R	Ar^1	Ar^2
7	Me		
8	Me		
9	Me		
10	Me		
11	Me		
12	*i*Pr		
13	Me		

Synthesis of silanes **7**–**9** is parallel to that of **2**.[19] The first target of a halogenated series was a silane having 2,6-dichlorophenyl as flanking substituents (**10**). The iodoterphenyl precursor was synthesized according to a procedure of Saednja and Hart.[32] Lithiation of the iodoterphenyl followed by reaction with dimethylchlorosilane lead to the chlorinated *m*-terphenyl **10**. Preparation of **11** involved a Negishi double cross-coupling reaction of 1-(2,6-dibromophenylazo)pyrrolidine[46] with the zincate of 1,3-difluorobenzene to form 1-[2,6-bis(2,6-difluorophenyl)phenylazo]pyrrolidine, which was converted to the iodoterphenyl.[47] Lithiation of the iodoterphenyl and treatment with dimethylchlorosilane afforded silane **11** (Scheme 2.1).[48]

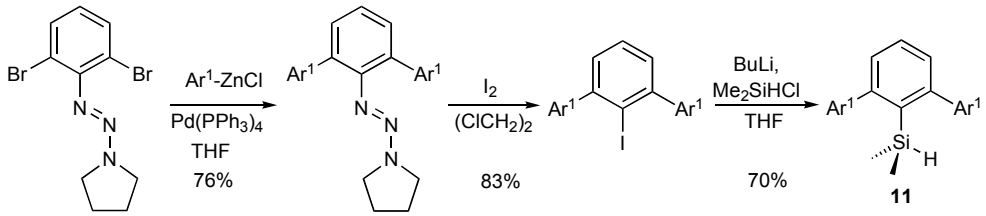

Scheme 2.1 Synthesis of **11**; $Ar^1 = 2,6\text{-}F_2C_6H_3$.

Increasing the number of methyl groups on an arene has been observed to enhance the π electron density and basicity.[19] In silanes **7**–**9**, the properties of these silanes are not significantly different from those of **2** (Table 2.4, Figure 2.11).

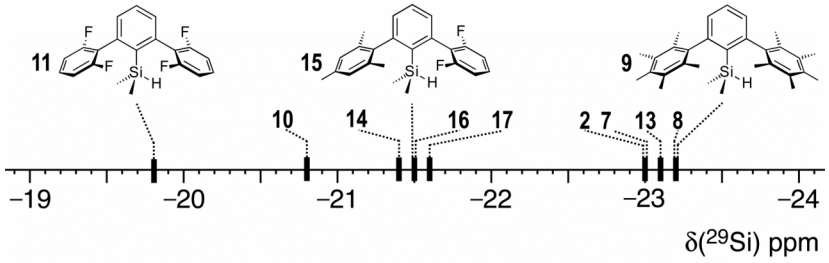

Figure 2.11 ^{29}Si NMR shifts of the terphenylsilanes $TerSiMe_2H$ (C_6D_6, ppm *vs* $SiMe_4$).

The ^{29}Si NMR signal of **10** is noticeably shifted downfield with respect to the signals for methylated analog **7** (cf. Figure 2.11). The solid-state structure of **10** shows a twisting of the flanking rings (β and γ values of 83.2(1)° and 80.5(1)°) such that the Si···Cl1 and Si···Cl3 distances (3.886(1) Å, 4.006(1) Å) are shorter than the Si···Cl2 and Si···–Cl4 distances (4.373(1) Å, 4.451(1) Å) (Figure 2.12).

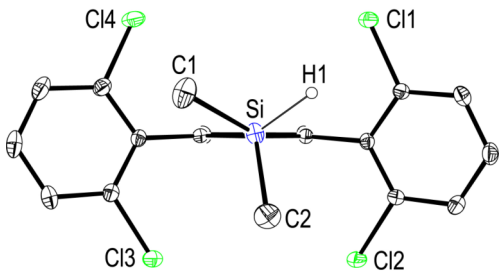

Figure 2.12 ORTEP representation of **14** (H atoms omitted for clarity, except for H-Si; displacement ellipsoids drawn at 30% level).

The silane bearing 2,6-difluorophenyl rings (**11**) has higher electronegative substituents compared to chlorine and the NMR activity of the ^{19}F nucleus provides another way to probe interactions with silicon. The ^{29}Si nucleus signal of **11** is observed to be more deshieded than in the chlorinated analog **10** (Figure 2.11), as anticipated due to the higher electronegativity of fluorine. The ^{29}Si signal is sharp, which indicates no through-space magnetic coupling between ^{29}Si and ^{19}F. In contrast, the ^{1}H NMR spectra support through-space fluorine to hydrogen interactions. A closer look at the ^{1}H NMR spectra of **10** and **11** revealed that, whereas the H–Si signal of the chlorinated terphenylsilane **10** is a septuplet, that of **11** appears as a pentet of septuplets. In addition to the larger hydrogen–hydrogen coupling, the resonance in **11** exhibits a second splitting with a smaller coupling constant (Figure 2.13 a and Figure 2.13 b). This phenomenon correlates to a through-space interaction between the silyl group and the fluorine atoms of the lateral rings. The ^{19}F spectrum was not sharp enough to resolve less than a 1.5 Hz coupling, so an investigation of reciprocal coupling was not feasible. Nonetheless, the phenomenon was consistent across the series of fluorinated silanes.

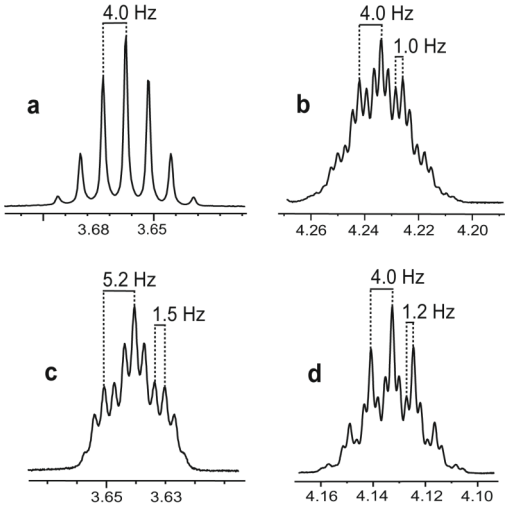

Figure 2.13 ^{1}H NMR signals of Si–H of compounds **10** (a), **11** (b), **12** (c), **15** (d). Solvent C_6D_6, spectra measured at 300 MHz (a), 400 MHz (c, d) or 500 MHz (b) and referenced against solvent residual peak (C_6HD_5 = 7.16 ppm).

Table 2.4 ^{29}Si NMR shifts and selected distances (Å) and angles (°) for silanes **7**–**13**.

	δ^{29}Si exp[a]	δ^{29}Si calc[b]	Si–X	Si–C1	Si–C2	Si–C_{ring}	α	β	γ
7	–23.0	–	–	–	–	–	–	–	–
8	–23.2	–	–	–	–	–	–	–	–
9	–23.2	–19.4	–	–	–	–	–	–	–
10	–20.8	–	1.49(3)	1.856(3)	1.859(3)	1.898(2)	35(1)	83.2(1)	80.5(1)
11[c]	–19.8	–15.9	1.42(2)	1.858(3)	1.861(3)	1.898(2)	32(1)	87.5(1)	79.3(1)
11'			1.37(3)	1.852(3)	1.857(4)	1.904(3)	19(1)	67.9(2)	73.8(1)
11',			1.39(3)	1.856(3)	1.836(3)	1.899(2)	11(1)	67.0(1)	68.9(1)
12[d]	6.4	–	1.45(3)	1.885(3)	1.865(2)	1.912(2)	15(1)	102.0(1)	72.9(1)
13[e]	–23.1	–	1.47(2)	1.850(4)	1.860(4)	1.916(3)	61(1)	88.3(1)	83.9(1)
13'			1.41(2)	1.857(4)	1.866(3)	1.903(3)	11(1)	98.9(1)	91.2(1)

[a] ppm in C_6D_6 vs $SiMe_4$. [b] M06-l/DZ+(2df,pd)//M06-2X/DZ(2df,pd). [c] There are three molecules in the asymmetric unit. [d] The substituents on the Si atom are disordered about a pseudo-mirror that is perpendicular to the Si–H bond and parallel to the Si–C_{ring} bond; only the values for the major conformation with 87% site occupation are given. [e] There are two molecules in the asymmetric unit.

The solid-state structure of **11** was determined by X-ray crystallography (Figure 2.14). In the asymmetric unit there are three molecules with conformations differing in α, β, and γ. An interesting feature that two of these structures have in common is a deviation in β and γ from the ideal 90° angle. A similar analysis for **10** shows little deviation (within 10°), while in **11** the distortion is more pronounced, as high as 23°. For the most distorted molecule, this deviation allows two of the fluorine atoms (F2 and F3 in Figure 11) to approach within 3.551(2) and 3.672(2) Å of the silicon atom, respectively, which is significantly smaller than the distances Si···F1

(4.406(2) Å) and Si···F4 (4.385(2) Å). On the other hand, we can notice that the hydrogen atom of this molecule is pointing towards one of the flanking rings (α = 11(1)°) and as a consequence F1 and F2 are much closer to the hydrogen than F3 and F4. It is tempting to infer an attractive through-space Si···F interaction in the distorted geometry of this molecule; however, the smaller size of fluorine compared to CH_3 results in a smaller barrier to rotation about the biaryl bonds in **11** than in **2**, and the observed distortions could also be the result of packing effects.

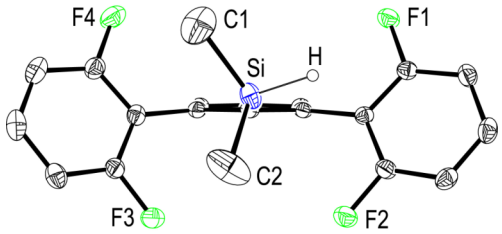

Figure 2.14 ORTEP representation of the most distorted of the three symmetry-independent molecules of **11** in the crystal (H atoms omitted for clarity, except for H–Si; displacement ellipsoids drawn at 30% level).

Of the two readily envisioned mechanisms to account for the particular ^{1}H NMR pattern of **11**, fluorine–hydrogen coupling mediated through silicon seems less likely than a direct hydrogen atom interaction with proximal fluorine atoms. The absence of coupling between silicon and fluorine in the ^{29}Si NMR of **11** supports the hypothesis of a direct hydrogen-fluorine interaction. Variable-temperature ^{1}H and ^{29}Si NMR studies in $CDCl_2F$, in a range of 0 °C to –110 °C, were performed, however, no signal broadening or decoalescence was observed. Furthermore, attempted silicate formation by addition of an excess of KF/18-C-6 crown ether to **11** and **6** did not lead to any change in the respective NMR spectra (Scheme 2.2).[49] Penta-coordination of the silicon center in these molecules would have resulted in a significant shift of the signals and change in coupling patterns.

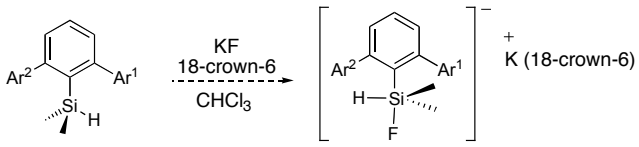

Scheme 2.2 Attempted synthesis of a pentacoordinated silicate

To understand better the nature of the through-space H···F interaction suggested from the NMR data of **11**, we synthesized analogs of **11**. Initially, the methyl substituents at silicon were exchanged with diisopropyl groups (**12**). In this case, the hydrogen atom attached to silicon appears as a pentet of triplets in the ^{1}H NMR spectrum, indicating similar secondary splitting, as in **11** (Figure 10c). This finding also supports an H···F interaction considering the bulkiness of the isopropyl groups that make a Si···F interaction less favorable (for crystal structrure, see Figure 2.15).

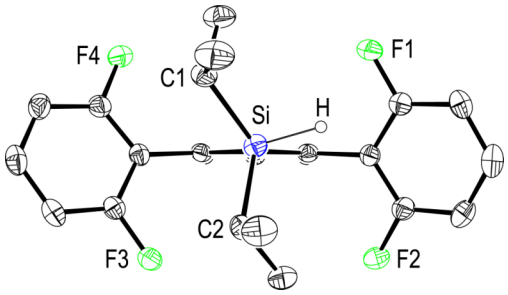

Figure 2.15 ORTEP representation of **12** (H atoms omitted for clarity, except for H–Si; displacement ellipsoids drawn at 30% level; only one of the disordered conformations of the substituents at the Si atom, that with 87% occupancy, is shown).

Moving the fluorine substituents from the *ortho* to the *para* position in the flanking rings (**13**) results in no such splitting of the Si–H ^{1}H NMR signal. This strongly suggests that the hydrogen–fluorine interaction proposed for the *ortho* system, is a purely intramolecular phenomenon. Silane **13** crystallized with two molecules in the asymmetric unit. The two molecules differ primarily in their values for the angle α (61(1)° and 11(1)°). The presence of two rotamers is in agreement with low energy

differences among different conformations of the silyl group as concluded from previous data.

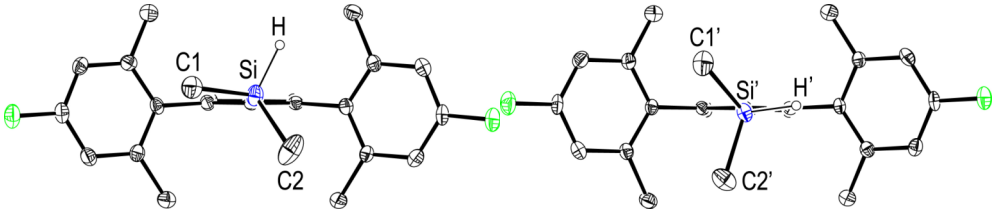

Figure 2.16 ORTEP representation of the two symmetry-independent molecules of **13** in the crystal (H atoms omitted for clarity, except for H–Si; displacement ellipsoids drawn at 30% level).

2.5 Conformational Analysis of 14–17.

To complete the present study, a series of silanes with reduced symmetry at silicon as well as in the terphenyl moiety was investigated. In these molecules, one of the flanking rings is methylated, whereas the other is fluorinated.

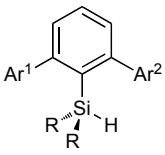

	R	Ar^1	Ar^2
14	Me		
15	Me		
16	Me		
17	Me		

Synthesis of compounds **14–17** was carried out starting from 1-(2,6-dibromophenylazo)pyrrolidine (Scheme 2.3). The first ring was introduced via Negishi coupling, followed by iodination of the azopyrrolidine compound.[47] The methylated ring was then inserted by a Hart-type coupling.[32]

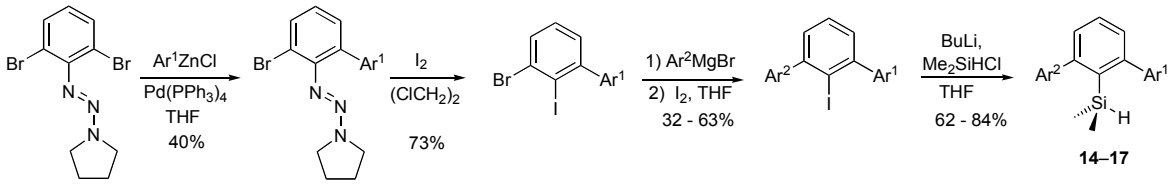

Scheme 2.3 Synthesis of **14**, **15**, **16**, **17**; $Ar^1 = 2,6\text{-}F_2C_6H_3$, $Ar^2 = 2,6\text{-}Me_2C_6H_3$, $2,4,6\text{-}Me_3C_6H_2$, $2,3,5,6\text{-}Me_4C_6H$, C_6Me_5.

The ^{29}Si NMR resonances of these silanes lie between those of the purely halogenated systems **10/11** and those of the purely methylated compounds **2/7–9** (Figure 2.11, Table 2.5). The ^{1}H NMR spectra of **14–17** show splittings of the H–Si resonances comparable to those of compounds **11** and **12**, but now clearly as a triplet (Figure 2.13 d). The coupling patterns observed for **11**, **12** and **14–17** support the idea that the fluorine atoms of the flanking rings interact directly with the Si–H hydrogen atoms.

Table 2.5 ^{29}Si NMR shifts for silanes **14–17**.

Cmpd	$\delta^{29}Si_{exp}$ [a]	$\delta^{29}Si_{calc}$ [b]	Cmpd	$\delta^{29}Si_{exp}$ [a]	$\delta^{29}Si_{calc}$ [b]
14	–21.4	–	**16**	–21.5	–
15	–21.5	–16.7	**17**	–21.6	–

[a] ppm in C_6D_6 vs $SiMe_4$. [b] M06-l/DZ+(2df,pd)//M06-2X/DZ(2df,pd).

In conclusion, a series of new *m*-terphenylsilanes has been synthesized. The variation of substituents attached to silicon reveals a certain trend in the solid-state structures. However, while in no case rotational barriers were determined, upper limits of 29 kJ mol^{-1} could be inferred from NMR experiments. The calculations performed on closely related compounds suggested small energy differences among rotamers and were in agreement with the data obtained experimentally. Changes in the substitution at the lateral rings modulate the electron density within the terphenyl cavity, as illustrated by increasing ^{29}Si NMR shifts with less electron-rich π systems. Furthermore, where fluorine atoms are present in the *ortho* positions of the flanking

rings, a through-space coupling with the Si–H hydrogen atom can be detected by NMR spectroscopy. This finding is best explained by a direct H···F interaction.

2.6 References

1. Haaf, M.; Schmedake, T. A.; West, R. *Acc. Chem. Res.* **2000**, *33*, 704.
2. Ottosson, H.; Eklöf, A. M. *Coordination Chemistry Review* **2007**, *252*, 1287.
3. Sekiguchi, A.; Kinjo, R.; Ichinohe, M. *Science* **2004**, *305*, 1755.
4. Lee, E. C.; Kim, D.; Jurecka, P.; Tarakeshwar, P.; Hobza, P.; Kim, K. S. *J. Phys. Chem. A* **2007**, *111*, 3446.
5. Simons, R. S.; Gallucci, J. C.; Tessier, C. A.; Youngs, W. J. *J. Organomet. Chem.* **2002**, *654*, 224.
6. Waterman, R.; Hayes, P. G.; Tilley, T. D. *Acc. Chem. Res.* **2007**, *40*, 712.
7. Clyburne, J. A. C.; N., M. *Coord. Chem. Rev.* **2000**, *210*, 73.
8. Crittendon, R. C.; Li, X. W.; Su, J. R.; Robinson, G. H., *Organometallics* **1997**, *16*, 2443.
9. Goto, K.; Holler, M.; Okazaki, R., *J. Am. Chem. Soc.* **1997**, *119*, 1460.
10. Goto, K.; Kawashima, T. *J. Synth. Org. Chem. Jpn.* **2005**, 101.
11. Grigsby, W. J.; Power, P. P. *J. Am. Chem. Soc.* **1996**, *118*, 7981.
12. Haubrich, S. T.; Power, P. P., *J. Am. Chem. Soc.* **1998**, *120*, 2202.
13. Li, X. W.; Su, J. R.; Robinson, G. H. *Chem. Commun.* **1998**, 1281.
14. Niemeyer, M.; Power, P. P. *Angew. Chem. Int. Ed.* **1998**, *37*, 1277.
15. Shimada, K.; Goto, K.; Kawashima, T.; Takagi, N.; Choe, Y. K.; Nagase, S. *J. Am. Chem. Soc.* **2004**, *126*, 13238.
16. Simons, R. S.; Pu, L. H.; Olmstead, M. M.; Power, P. P. *Organometallics* **1997**, *16*, 1920.
17. Twamley, B.; Sofield, C. D.; Olmstead, M. M.; Power, P. P. *J. Am. Chem. Soc.* **1999**, *121*, 3357.
18. Urnézius, E.; Protasiewicz, J. D., *Main Group Chem.* **1996**, *1*, 369.

19. Duttwyler, S.; Do, Q. Q.; Linden, A.; Baldridge, K. K.; Siegel, J. S., *Angew. Chem. Int. Ed.* **2008**, *47*, 1719.
20. Niemeyer, M. *Organometallics* **1998**, *17*, 4649.
21. Niemeyer, M.; Power, P. P. *Organometallics* **1997**, *16* , 3258.
22. Ruhlandtsenge, K.; Bartlett, R. A.; Olmstead, M. M.; Power, P. P., *Angew. Chem. Int. Ed.* **1993**, *32*, 425.
23. Chen, C. T.; Siegel, J. S. *J. Am. Chem. Soc.* **1994**, *116*, 5959.
24. Chen, C. T.; Chadha, R.; Siegel, J. S.; Hardcastle, K. *Tetrahedron Lett.* **1995**, *36*, 8403.
25. Luning, U.; Baumstark, R.; Wangnick, C.; Muller, M.; Schyja, W.; Gerst, M.; Gelbert, M. *Pure Appl. Chem.* **1993**, *65*, 527.
26. Pietschnig, R.; Belaj, F.; Tirree, A. J. *Organometallics* **2004**, *23*, 4897.
27. Pietschnig, R.; Schäfer, S. *Silicon Chem.* **2003**, *2*, 131.
28. Pietschnig, R.; West, R.; Powell, D. R. *Organometallics* **2000**, *19*, 2724.
29. Simons, R. S.; Haubrich, S. T.; Mork, B. V.; Niemeyer, M. *Main Group Chem.* **1998**, *2*, 275.
30. Weidemann, N.; Schnakenburg, G.; Filippou, Z. *Anorg. Allg. Chem.* **2009**, *635*, 253.
31. Du, C. J. F.; Hart, H.; Ng, K. K. D. *J. Org. Chem.* **1986**, *51*, 3162.
32. Saednya, A.; Hart, H. *Synthesis* **1996**, 1455.
33. Shah, S.; Burdette, S. C.; Swavey, S.; Urbach, F. L.; Protasiewicz, J. D. *Organometallics* **1997**, *16*, 3395.
34. Diehl, P.; Fluck, E.; Kosfeld, R. *NMR, Basic Principles and Progress*. Springer: Berlin, 1981.
35. Siegel, J. S.; Anet, F. A. L. *J. Org. Chem.* **1988**, *53*, 2629.
36. Gutowsky, H. S.; Holm, C. H. *J. Chem. Phys.* **1956**, *25*, 1228.
37. Bott, A. W.; Johnson, B. F. G. *Transition Met. Chem.* **1989**, *14* , 79.
38. Mutterties, E. L. *Inorg. Chem.* **1965**, *4*, 769.

39. For detailed synthetic procedures and analytical data for compounds 2-6, see: Duttwyler, S. '2,6-Diarylphenyl Silylium Ions: Synthesis and Study of a New Class of Silyl Cations', University of Zurich, Switzerland 2010.
40. Allen, F. H.; Howard, J. A. K.; Hoy, V. J.; Desiraju, G. R.; Reddy, D. S.; Wilson, C. C. *J. Am. Chem. Soc.* **1996**, *118*, 4081.
41. Khelashvili, L. *Chemistry*. Univeristät Duisburg-Essen, Essen, 2004.
42. Ma, J. C.; Dougherty, D. A., *Chem. Rev.* **1997**, *97*, 1303.
43. Tamres, M. *J. Am. Chem. Soc.* **1952**, *74*, 3375.
44. Millevolte, A. J.; vandenWinkel, Y.; Powell, D. R.; West, R. *Organometallics* **1997**, *16*, 5375.
45. Schottel, B. L.; Chifotides, H. T.; Dunbar, K. R. *Chem. Soc. Rev.* **2008**, *37*, 68.
46. Liu, C. Y.; Knochel, P. *Org. Lett.* **2005**, *7*, 2543.
47. Wu, Z. Y.; Moore, J. S. *Tetrahedron Lett.* **1994**, *35*, 5539.
48. Romanato, P.; Duttwyler, S.; Linden, A.; Baldridge, K. K.; Siegel, J. S. *J. Am. Chem. Soc.* **2010**, *132*, 7828.
49. Setaka, W.; Nirengi, T.; Kabuto, C.; Kira, M. *J. Am. Chem. Soc.* **2008**, *130*, 15762.

3 Intramolecular Halogen Stabilization of Silylium Ions

3.1 Introduction

Silicon cations are highly reactive Lewis acids; even relatively weak Lewis bases, such as the π-basic solvent toluene, form tetrahedral complexes with silylium ions (see 1.4.3).[1] In order to avoid intermolecular interactions of silylium ions with solvent or other nucleophilic species present in the reaction media, a sterically demanding substitutent, such as the conical, shielding terphenyl group, is envisioned as an integral part of our target design. The flanking rings, which have restricted rotation about the biaryl bonds in the 2- and 6- positions, should prevent anion and solvent molecules from interacting with the positively charged cavity. At the same time, donation of π(aryl) electron density into the empty 3p(Si) orbital leads to a reduced amount of positive charge on the silicon and decreses Lewis acidity. Such intramolecular π-coordination with the flanking rings distorts the ideal C_{2v}-symmetric geometry of a purely tricoordinated terphenyl silylium ion in favor of the C_1-symmetric geometry of a Wheland-like complex (Figure 3.1).[2]

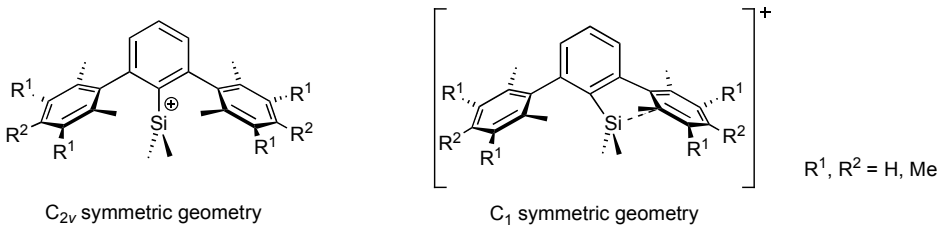

Figure 3.1 Ideal C_{2v} (left) and C_1 (right) geometry in terphenyl silylum ions with methylated flanking rings.

An analysis of the NMR signals of the lateral aryl carbon atoms reveals, in the case of methylated flanking rings, the presence of a dominant interaction between Si^+ and Cβ (Figure 3.2). The Cα, Cγ and Cδ in **B** are deshielded relative to those in precursor **A** and the shift effects are greater than 10 ppm for Cα and Cγ; in contrast, the Cβ atom is shielded by 6–9 ppm. Analogous behavior is detected in Wheland complexes that display an upfield shift of the ^{13}C signal of the tetracoordinate atom relative to those of free arenes, whereas the other carbon atoms are more deshielded.[3, 4]

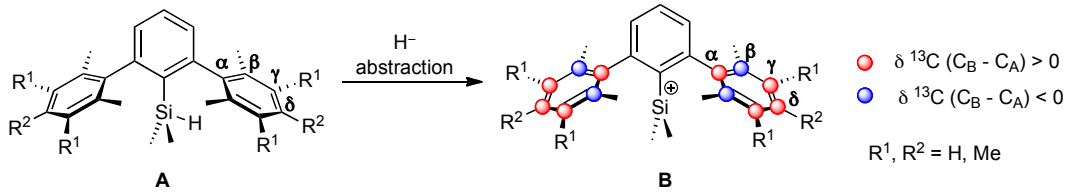

Figure 3.2 ^{13}C NMR analysis of the chemical shift of the lateral ring nuclei in a silylium ion **B** compared to the silane precursor **A**. Solvent: C_6D_6; counterion: $B(C_6F_5)_4^-$.

Furthermore, varying the number of electron-donating methyl groups on the flanking rings of **B** allows a tuning of the silicon Lewis acidity, *i.e.* the less substituted the flanking ring, the more deshielded the silylium ion (Figure 3.3). These cations, though they experience a significant buildup of positive charge at silicon on going from the silane to the silylium ion ($\delta\Delta$ ^{29}Si ≈ 80–100 ppm), are significantly shielded with respect to the trimesitylsilylium ion, the first example of free silylium ion with a ^{29}Si NMR shift of 225 ppm.[5]

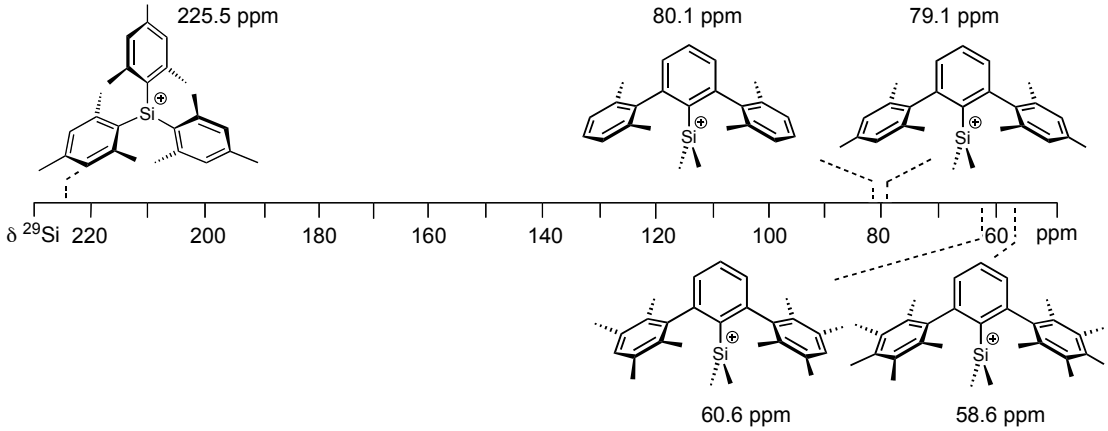

Figure 3.3 ^{29}Si NMR shift of terphenyl silylium ions with methylated flanking rings compared to trimesityl silylium ion. Solvent: C_6D_6; counterion: $B(C_6F_5)_4^-$.

In light of these results, we decided to attempt the synthesis of terphenyl silylium ions with lateral rings of basicity lower than benzene, in order to reduce the degree of π(arene)→Si donation and therefore increase the amount of positive charge at silicon. Such cations, where the silicon center is still very deshielded but sterically more accessible than in the trimesityl analog, are optimal candidates to study the reactivity of silylium ions when they are involved in chemical reactions. Substituents of choice to reduce π basicity of the lateral rings are halogen atoms. Contrary to

$C_{aliphatic}$–halogen bonds, some C_{aryl}–halogen bonds proved to be stable in presence of reactive silylium ions; this is the case for C–F bond in the tetrakispentafluorophenylborate anion and for C–Cl bond in chlorobenzene (see 1.4.2). In particular, we envisioned that halogen substitution in the *ortho* position of the flanking rings should be the most effective; an electronegative element on the Cβ should disfavor, in fact, the π(arene)→Si coordination described for methylated lateral rings.

3.2 Lone Pair-Halogen Stabilization in Silylium Ions

3.2.1 Preliminary Calculations

A set of target molecules containing electron-deficient flanking rings was identified in [2,6-Bis(2,6-difluorophenyl)phenyl]dimethylsilylium ion **18**, [2,6-Bis(2,4,6-trifluorophenyl)phenyl]dimethylsilylium ion **19**, [2,6-Bis(2,3-tetrafluorophenyl) phenyl]dimethylsilylium ion **20**, and [2,6-Bis(2,3,4-pentafluorophenyl)phenyl] dimethylsilylium ion **21**.

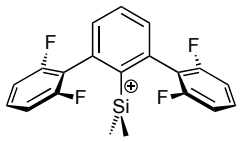

18

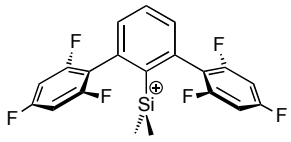

19

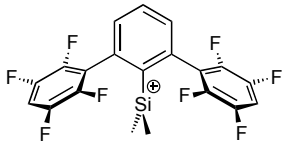

20

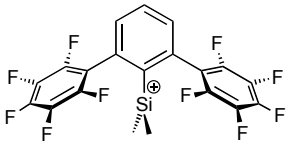

21

A series of calculations was performed with the aim of determining the best candidate for our purposes, before embarking in their syntheses. The parameters that have been investigated are the ^{29}Si NMR shifts, and the relative energy of four possible conformations that these cations can assume (Figure 3.4). Along with structural parameters obtained by X-ray analysis, the ^{29}Si NMR shift is the most widely accepted criterion for determining silylium ion character: the higher the resonance of the silicon nucleus, the stronger the silylium ion character and less pronounced any

possible intra- or intermolecular coordination to the cation center. Calculations revealed a strong correlation between ^{29}Si NMR shift and conformation of the cation (Table 3.1). C_1 and C_2 conformations in **18**–**21** are the lowest in energy and do not significantly differ from each other. The respective calculated ^{29}Si NMR values fall in the region of 75-94 ppm, resembling the values for the internally coordinated cations with methylated flanking rings (Figure 3.3). If the molecule assumes a C_s or C_{2v} conformation, its silylium ion character would greatly increase, as demonstrated by

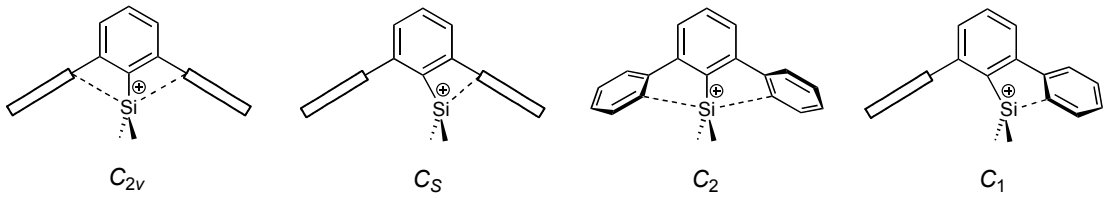

Figure 3.4 Schematic representation of the C_{2v}, C_s, C_2, C_1 conformations of a terphenyl silylium ion displaying π(arene)→Si interaction (substituents on flanking rings omitted for clarity).

the ^{29}Si shifts in the region of 150–280 ppm. The differences in energy between the C_1/C_2 and C_s/C_{2v} conformations is quite similar in the series **18**-**21**, and it is in the order of 14–17 kcal/mol. Varying the number of fluorine substitutes on the lateral rings is predicted to not have a significant effect on the conformational preference of the corresponding silylium ions; therefore, we decided to synthesize and study only one member of this family, cation **18**, as representative of the behavior of this class of compounds.

Table 3.1 Calculated ^{29}Si NMR and relative energies for the C_1, C_2, C_s, C_{2v} symmetrical geometries of silylium ions **18-21**.

Cmpd	Symmetry	Calcd ^{29}Si NMR[a]	Rel E + ZPE[b]
18	C_1	75.8	0.00
18	C_2	75.7	0.01
18	C_s	173.7	16.25
18	C_{2v}	268.8	17.81
19	C_1	85.2	0.00
19	C_2	85.3	0.01
19	C_s	149.1	14.25
19	C_{2v}	266.7	16.22
20	C_1	86.0	0.00
20	C_2	86.0	0.00
20	C_s	220.9	17.20
20	C_{2v}	281.0	17.50
21	C_1	94.0	0.00
21	C_2	94.0	0.01
21	C_s	192.2	14.69
21	C_{2v}	277.8	16.09

[a]B3LYP/DZ(2df,pd) GIAO NMR, anisotropic values referenced against Me_4Si;
[b]MP2/DZ(2d,p)//B3LYP/DZ(2df,pd) units = kcal/mol.

3.2.2 2,6-Difluorophenyl Lateral Rings

Our synthesis of cation **18** commenced from commercially available 2,6-dibromoaniline that underwent protection at the amino group in the form of triazene (Scheme 3.1).[6] Double Negishi coupling on triazene **22** led to diarylphenyltriazene **23**, which gave the corresponding iodoterphenyl **24** when treated with iodine.[7] Lithiation of **24**, followed by treatment with chlorodimethylsilane, afforded silane **11**. Hydride abstraction was performed by $[Ph_3C][B(C_6F_5)_4]$ to give silylium ion [**18**][$B(C_6F_5)_4$].

The ^{29}Si NMR resonance of **18** (88.6 ppm) is downfield-shifted relative to its neutral precursor **11** (–19.8 ppm), an indication that a species with partial positive charge on silicon is formed (Figure 3.5). While this value is still far from that of a free silylium ion (R_3Si^+),[5] it indicates deshielding in comparison with classical silanium ions (R_5Si^+).[8-12] ^{1}H and ^{29}Si NMR spectra of **18** reveal magnetic coupling to the

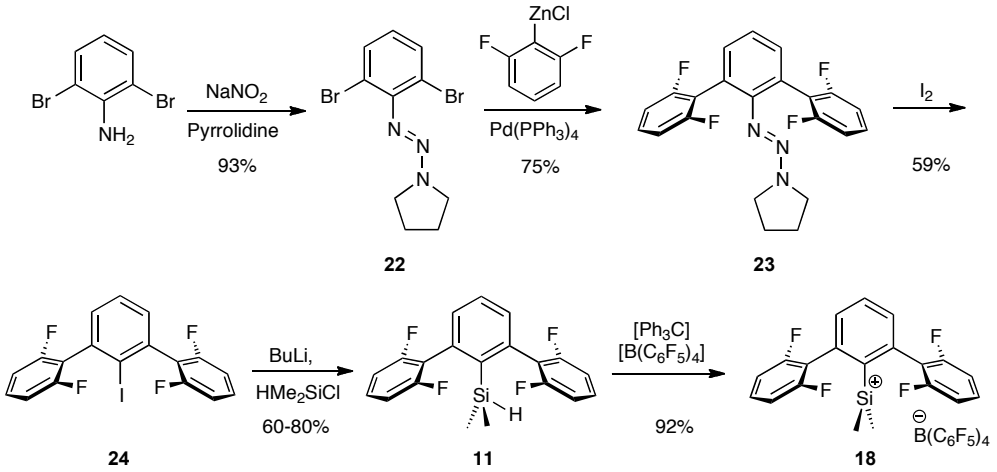

Scheme 3.1 Synthesis of [**18**][$B(C_6F_5)_4$].

fluorine substituents (Figure 3.5). The ^{1}H NMR signal of the methyl groups attached to silicon in **18** appears as a quintet, and the same multiplicity is maintained upon cooling to 223 K.[1] The ^{13}C NMR signal for these methyl groups also appears as a quintet, with a coupling constant of 5.8 Hz (^{13}C NMR reveals a splitting of methyl group resonance already in silane **11**; the coupling constant of 0.9 Hz is indicative of a very weak interaction, probably due to a through-space interaction between the hydrogen at silicon and the two fluorine atoms closer in space (see 2.4)). Finally, the silicon signal, which appears as a broad resonance at room temperature, is resolved into a quintet at lower temperature.[13] Fluorine–silicon coordination can explain the multiplicity and the coupling constant of the ^{1}H, ^{13}C and ^{29}Si signals for the Me_2Si moiety in cation **18**; the lone pairs of the fluorine atoms can coordinate the positively charged silicon center and the effect of this interaction reaches the methyl groups covalently bond to silicon. ^{19}F NMR spectroscopy revealed signal isochrony for the fluorine substituents over the temperature range 293–223K (see 5.3.1).

1 As NMR solvent a 1:1 mixture of toluene-d_8 and chlorobenzene was used in order to obtain a solution of silylium ion instead of the oily clathrate that forms when only toluene is employed. At low temperature, the ^{1}H NMR signals for cation **18** in toluene are very broad and no splitting can be detected.

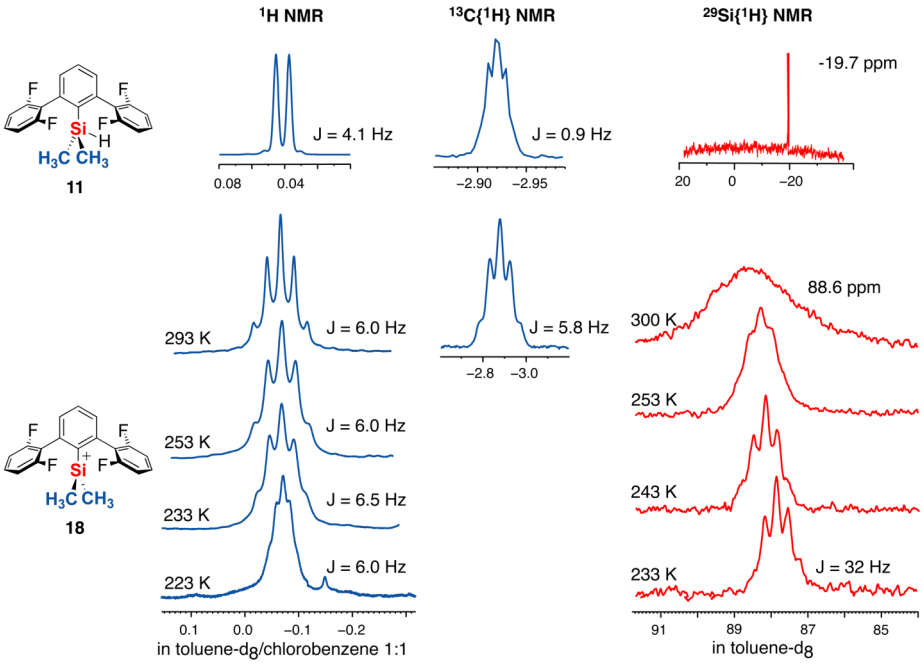

Figure 3.5 ^{1}H and ^{13}C NMR analysis of Me groups at silicon (blue colored) and ^{29}Si NMR analysis (red colored) for silane **11** and silylium ion **18**. Counterion: $B(C_6F_5)_4^-$. Solvent, if not specified, C_6D_6.

A comparison of the nuclei chemical shift between the cation and its neutral precursor is a good indication of the electron density redistribution that takes place when the silylium ion forms. Being particularly interested in the role that lateral rings play in the stabilization of silylum ion **18**, we performed an analysis of the ^{13}C NMR shift of the relative nuclei (Figure 3.6). The chemical shift assignments were determined by ^{1}H/^{13}C HSQC and ^{1}H/^{13}C HMBC spectroscopy. The chemical shift comparison for cation **18** reinforces the idea that a coordination mode different than the one described for methylated flanking rings takes place (see 3.1). Cα is significantly shielded compared to the silane (–6.4 ppm), and Cγ is only slightly deshielded (+2.5 ppm). This resonance pattern is not typical of a Wheland intermediate and does not account for a π (arene)→Si coordination via Cβ (for comparison see Figure 3.2).

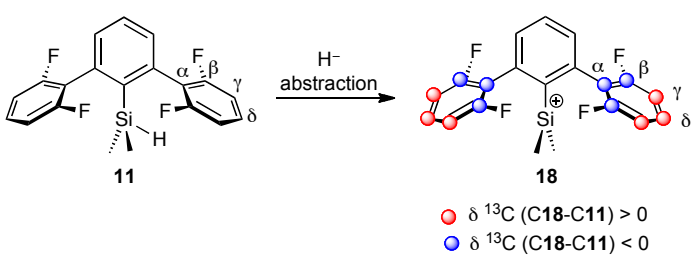

Δ (δ^{13}C) [ppm]	
C atom	**18** - **11**
α	– 6.4
β	– 0.7
γ	+ 2.5
δ	+ 2.2

Figure 3.6 ^{13}C NMR analysis of the chemical shift of the lateral rings nuclei in silylium ion **18** compared to silane **11**. Solvent: C_6D_6; counterion: $B(C_6F_5)_4^-$.

Convinced of the presence of a dominant F→Si interaction, we tried to identify the reason for the magnetic equivalence of the fluorine substituents: is this equivalence originating from a dynamic exchange of lower symmetry conformations or is it due to a static conformer having C_{2v} symmetry? Computational analysis proposes that a dynamic exchange of lower symmetry conformations is energetically favored. Density functional theory calculations favored a C_2 ground state (B1-C_2) for **18**, in which the silicon interacts with one fluorine atom from each of the opposing flanking rings (the C_1 starting geometry converged to the C_2 structure); the experimental ^{29}Si NMR value matches the computed value for the B1-C_2 conformer (Table 3.2). Eight conformations of **18** can be arranged into a bipartite graph; each conformer is connected to the next one, depending whether it undergoes a conrotatory or disrotatory pathway for the exchange of the fluorine atoms coordinating to silicon (Figure 3.7).[14] Computations further predict that cation **18** should undergo fluorine exchange at silicon *via* a disrotatory gearing of the lateral aryl rings (Figure 3.7, Figure 3.8); the circuit B_1-A_2-B_1 was predicted to require only 4.5 kcal mol^{-1}, therefore it is expected to be the preferred one.

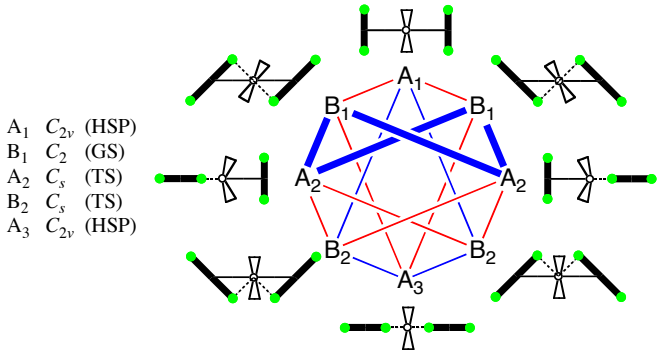

Figure 3.7 Bipartite conformational graph of **18**, view along Si–C_{aryl} axis. Blue paths – disrotary, red paths – conrotary, bold path – gearing circuit. GS – ground state, TS – transition state, HSP – higher order stationary point. Bold black lines – lateral aryl rings (green dots = F), wedges – methyl groups at silicon.

Table 3.2 B98/DZ(2df,pd)-Calculated relative gas-phase energies (kcal mol^{-1}) and B98/DZ+(2df,pd) ^{29}Si NMR shifts for **18**.[a]

Conform.	Rel. *E.*	^{29}Si NMR	
		Calcd	Exptl
A_1-C_{2v}	13.2	272.2	-
A_2-C_s	4.5	160.3	-
A_3-C_{2v}	22.0	33.6	-
B_1-C_2	0.0	87.6[b]	88.6
B_2-C_s	9.6	69.2	-

[a] NMR shift data calibrated relative to Me_4Si. [b] B98/DZ+(2df,pd) calibrated ^{29}Si NMR shift in toluene for B1-C_2 conformer: 87.2 ppm.

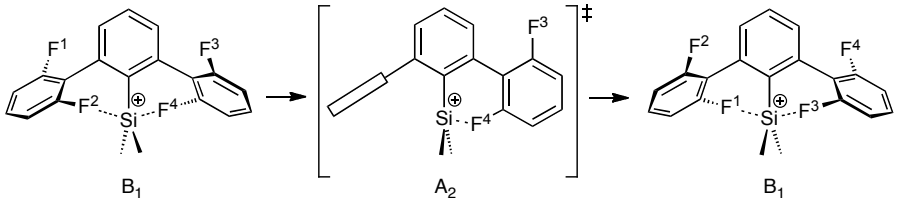

Figure 3.8 Proposed conformational gearing circuit for cation **18**.

The behavior of cation **18** has also been analyzed in the solid state. Crystals of composition [**18**][$CB_{11}H_6Cl_6$] were obtained from a C_6H_5Cl/C_6H_{14} mixture using carborane $CB_{11}H_6Cl_6^-$ as the counterion.[15] X-ray crystallographic analysis revealed the cation structure to be essentially the C_2 trigonal-bipyramidal B_1-C_2 form predicted computationally (Figure 3.9).

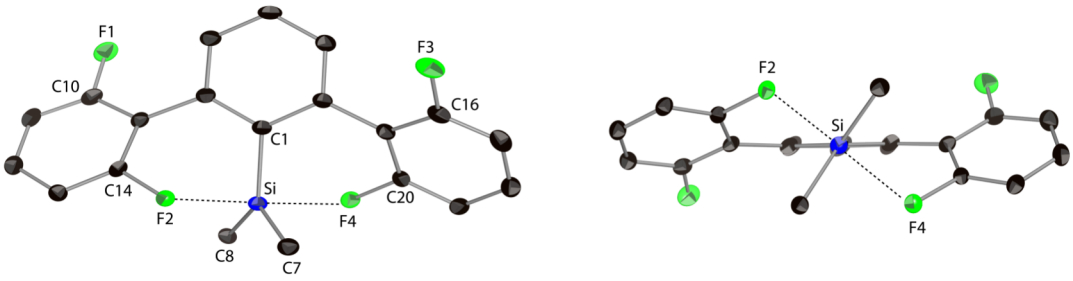

Figure 3.9 X-ray structures of [**18**][$CB_{11}H_6Cl_6$] with 30% probability ellipsoids. Front view, left; view through Si–C_{aryl} bond, right. Anion and hydrogen atoms omitted for clarity. Dashed lines show the Si–F interactions.

Coordination to solvent or counterion is not detected; instead two significant F2–Si and F4–Si interactions are revealed (Table 3.3). Even though F2–Si and F4–Si distances are longer than a typical F–Si bond by 0.55 Å and 0.46 Å respectively (as reference: Me_3SiF = 1.600 Å),[16] their values are lower than the sum of the van der

Waals radii of silicon and fluorine (2.00 Å for Si, 1.35 Å for F). The sum of C–Si–C angles is 359.9 (1)˚ and the F2–Si–F4 angle is 174.20 (6)˚; these values indicate that F2 and F4 fluorine atoms occupy the apical position of a trigonal bipyramid, C1, C7 and C8 occupy the equatorial positions, and the silicon atom sits in the center.

Table 3.3 Selected bond lengths (Å) and dihedral angles (deg) for the calculated C_2 conformer and the single X-ray structure of **18**.

Parameter	**Expt.**	**Calculated C_2**	
		gas phase[a]	toluene[b]
F2→Si	2.151(2)	2.118 [2.126]	2.133
F4→Si	2.065(2)	2.118 [2.126]	2.133
C14–F2	1.410(3)	1.397 [1.397]	1.394
C20–F4	1.421(3)	1.397 [1.397]	1.394
C10–F1	1.352(3)	1.331 [1.332]	1.336
C16–F3	1.351(3)	1.331 [1.332]	1.336
Dihedral angle[c]	35.14	36.25	38.28 (13)[d]
	35.14	36.25	31.14 (13)[e]
dfp-Si[f]	0.0	0.0	0.0184 (7)

[a] B98/DZ(2df,pd) [B98/DZ+(2df,pd)]. [b] B98/DZ+(2df,pd) in toluene. [c]Angle between least square planes of flanking rings and central ring. [d] Between ring containing F2 and central ring. [e] Between ring containing F4 and central ring. [f] Deviation from planarity: distance between the Si atom and the plane defined by the three C atoms bound to Si.

Unexpectedly, an earlier attempt to crystallize **18** using $B(C_6F_5)_4^-$ as counterion showed that traces of THF and Et_2O had coordinated to the silicon center. Cocrystals [**25**][$B(C_6F_5)_4$] and [**26**][$B(C_6F_5)_4$] were obtained and X-ray analysis displayed a distorted tetrahedral arrangement around silicon (Figure 3.10). This crystal structure is most likely the results of vapors of THF and Et_2O present in the glove box atmosphere that coordinate to the silicon center. The sum of the C–Si–C angles in compound **25** and **26** is in the order of 346˚–347˚, while in silylium ion **18** is 360˚ (Table 3.4); the distance of silicon from the plane defined by the three carbon atoms attached to it in **25** and **26** is in the range of 0.39–0.40 Å, while in **18** it is 0.01 Å

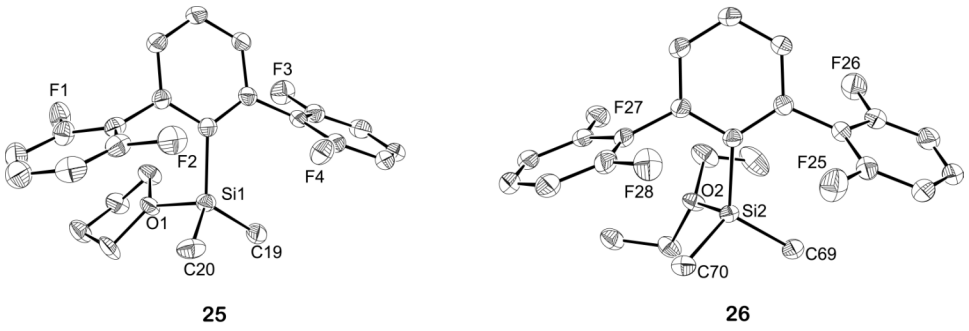

Figure 3.10 ORTEP plot of [**25**][$B(C_6F_5)_4$] and [**26**][$B(C_6F_5)_4$] with 30% probability ellipsoids. Anion and hydrogen atoms omitted for clarity.

Table 3.4 Selected distances [Å] and dihedral angles [deg] for the X-ray structure of [**25**][$B(C_6F_5)_4$] and [**26**][$B(C_6F_5)_4$].

Cation 25		**Cation 26**	
Parameter	**Expt.**	**Parameter**	**Expt.**
F1–Si1	4.2630(18)	F27–Si2	4.1277(19)
F2–Si1	3.7223(19)	F28–Si2	3.8517(18)
F3–Si1	4.669(2)	F26–Si2	4.6641(18)
F4–Si1	3.3259(18)	F25–Si2	3.4004(19)
Σ C–Si–C[a]	346.92(23)	Σ C–Si–C[a]	346.26(21)
dihedral angle[b]	72.82(14)[c]	dihedral angle[b]	77.78(13)[c]
	59.17(13)[d]		59.70(13)[d]
dfp-Si[e]	0.3910(7)	dfp-Si[e]	0.4012(7)

[a] Sum of the C–Si–C angles around silicon. [b] Angles between least square planes of the flanking rings and central ring. [c] Between left and central ring. [d] Between right and central ring. [e] Deviation from planarity: distance between the Si atom and the plane defined by the three C atom bound to Si.

(ideal values of deviation from planarity: in trigonal or trigonal-bipyramidal structures, 0 Å; in tetrahedral structures, 0.6 Å).[12] These results show that an intermolecular coordination by an ether molecule, either THF or diethyl ether, is preferable over the intramolecular coordination of two fluorine atoms in cation **18**.

The labilility of this F→Si coordination represents the novelty of this system. It accounts for the fast ligand exchange at silicon and allows the signal isochrony of the fluorine atoms in a range of 300–223 K (measurement at temperature lower than 223 K were not possible because of freezing of the solvent mixture). The originality of the coordination mode in compound **18** stands out against other literature examples of trigonal bipiramidal silanium ions (Figure 3.11).[8-12] In the systems developed by Corriu and Jutzi, intramolecular coordination by N, O, S, or P stabilize the positive

silicon center and leads to trigonal bipyramidal silanium ions **27**. Their ^{29}Si NMR resonances are in the negative region of the spectrum (from −51 to −104 ppm) and indicative of a pentacoordinate geometry. In contrast, the downfield-shifted resonance for cation **18** is an unusual value for pentacoordinate species, and we therefore name it silylium ion.

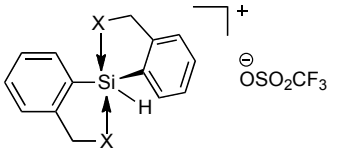

27

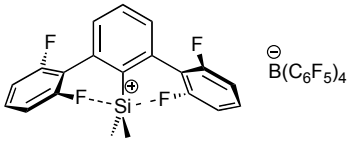

18

27	**a**	**b**	**c**	**d**
X	NMe_2	OMe	SMe	PMe_2
δ ^{29}Si	−51.6	−47.2	−47.9	−104.3

δ ^{29}Si = 88.6 ppm

Figure 3.11 ^{29}Si NMR shift comparison of silanium ions **27a**–**d** and silylium ion **18**.

3.2.3 2,6-Dichlorophenyl Lateral Rings

Motivated by the discovery of a new mechanism of weak intramolecular coordination in silylium ions, we decided to investigate whether this phenomenon could be extended to halogen atoms other than fluorine. From a synthetic point of view, [2,6-bis(2,6-dichloro)phenyl]dimethylsilylium ion **28** represented an appealing target. The synthesis commenced from 1,3-dichloro-2-iodobenzene, which underwent Hart-type couplings to afford iodoterphenyl **29** (Scheme 3.2).[17] Lithiation of **29**, followed by treatment with dimethylchlorosilane, furnished silane **30**. Cation **28** was prepared by hydride abstraction using $[Ph_3C][B(C_6F_5)_4]$.

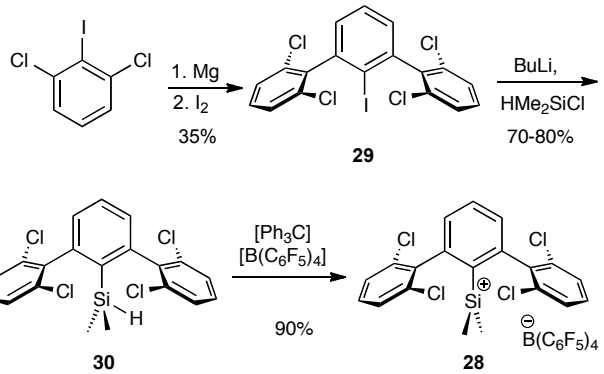

Scheme 3.2 Synthesis of [**28**][$B(C_6F_5)_4$].

The ^{29}Si NMR shift of silylium ion **28** is 90.5 ppm. The ^{29}Si signal for the silicon nucleus and the ^{1}H and ^{13}C signals for the methyl groups appear as singlets. Because coupling to ^{35}Cl and ^{37}Cl can generally not be observed and ^{35}Cl NMR spectroscopy would have led to extremely broad signals, the silicon–chlorine interaction could not be deduced directly from the experimental data.[18, 19] However, a comparison of the ^{13}C NMR shifts of the flanking rings in cations **28** and **18** suggests a similar coordination mode for both (Figure 3.12; for comparison with compound **18**, see Figure 3.6).

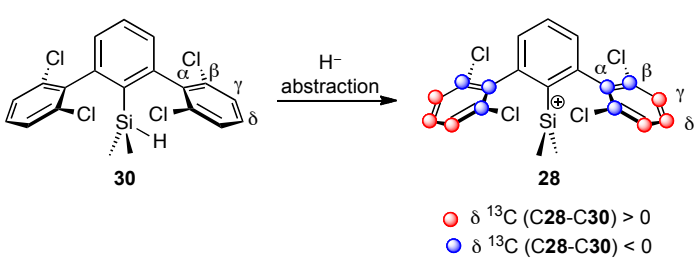

Δ (δ^{13}C) [ppm]	
C atom	**28** – **30**
α	– 6.6
β	– 2.9
γ	+ 2.5
δ	+ 2.2

Figure 3.12 ^{13}C NMR analysis of the chemical shift of the lateral rings nuclei in silylium ion **28** compared to silane **30**. Solvent: C_6D_6; counterion: $B(C_6F_5)_4^-$.

Calculations at the density functional theory level also favor a C_2 ground state for cation **28**, in which the silicon interacts with one chlorine atom from each of the opposing flanking rings (Figure 3.13, Table 3.5). The Cl–Si distance for the coordinating chlorine atoms is predicted to be 2.661 Å, about 0.61 Å longer than in a typical Si–Cl bond (the Si–Cl bond length in Me_3SiCl, 2.055(2) Å, is taken as reference)[20] but within the sum of van der Waals radii of silicon and chlorine (2.00 Å for silicon, 1.75 Å for chlorine). The dihedral angle between the flanking rings and the central ring is calculated to be 52.1 Å, a smaller deviation from the ideal 90° compared to cation **18**. The calculated ^{29}Si NMR for the C_2 conformation is very close to the experimental value ($\Delta\ \delta^{29}$Si ≈ 2 ppm). The next conformer, closer in energy to the C_2 ground state, is a C_{2v} structure in which the flanking rings are perpendicular to the central ring.

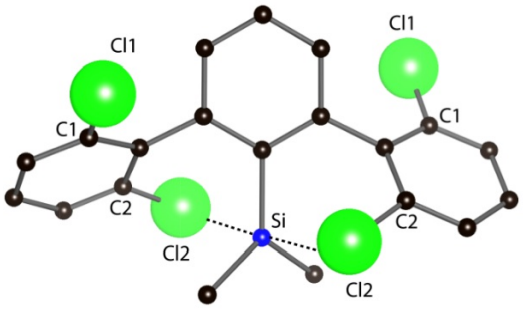

Figure 3.13 Ball and stick representation of the calcuated C_2 ground state of **28**. Significant distances[Å] and angles[deg] – Si–Cl1: 5.195; Si–Cl2: 2.661Å; C1–Cl1:1.738; C2–Cl2: 1.771; dihedral angle between lateral and central ring: 52.08.

Table 3.5 B98/DZ(2df,pd)-Calculated relative gas-phase energies (kcal•mol^{-1}) and B98/DZ+(2df,pd) ^{29}Si NMR shifts for **28**.[a]

Conform.	**Rel. *E.***	**^{29}Si NMR**	
		Calcd	Exptl
A_1-C_{2v}	9.3	208.3	-
A_2-C_s	16.6	195.5	-
A_3-C_{2v}	79.8	13.6	-
B_1-C_2	0.0	93.8[b]	90.5
B_2-C_s	21.4	66.3	-

[a] NMR shift data calibrated relative to Me_4Si. [b] B98/DZ+(2df,pd) calibrated ^{29}Si NMR shift in toluene for B1-C_2 conformer: 87.2 ppm.

Looking at the conformational graph already used to describe the fluorine exchange in cation **18**, we can now highlight a different path for ligand exchange in silylium ion **28** (Figure 3.14). Chlorine exchange at silicon takes place *via* a conrotatory B_1-A_1-B_1 path, which is predicted to require 9.3 kcal mol^{-1} (Figure 3.15). As mentioned earlier, there is not a direct proof of the magnetic equivalence of the chlorine atoms, but the hypothesis of a fast exchange of the coordinating chlorine atoms is supported by the magnetic equivalence of the carbon atoms of the flanking rings in positions β. For example, in the case that B_1 does not interchange to B_1' (Figure 3.15), we would expect the Cβ bounded to the coordinating chlorine atom to resonate at a different frequency compared to the Cβ bounded to the free chlorine atoms.

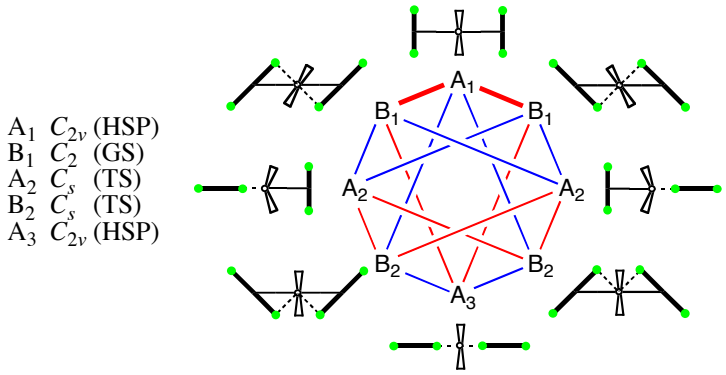

Figure 3.14 Bipartite conformational graph of **28**, view along Si–C_{aryl} axis. Blue paths – disrotary, red paths – conrotary, bold red – preferred path for coordinating chlorine exchange at silicon. GS – ground state, TS – transition state, HSP – higher order stationary point. Bold black lines – lateral aryl rings (green dots = Cl), wedges – methyl groups at silicon.

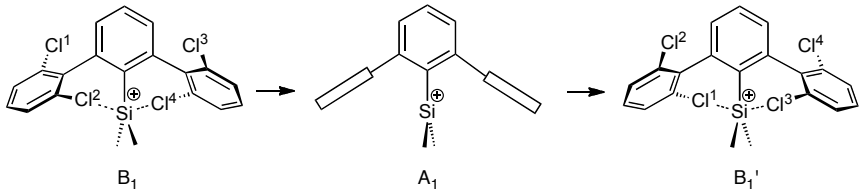

Figure 3.15 Proposed conformational circuit for the exchange of coordinating chlorine in cation **28**.

Compounds **18** and **28** belong to a new class of silylium ions that display dynamic C(Ar)–X halogen binding to R_3Si^+. The energy of this interaction is comparable to that of analogous cations with xylene or mesitylene as flanking rings (Figure 3.16). The initial goal of reducing π basicity of the lateral rings allowed the disclosure of a new mode of stabilization of reactive intermediates. Nevertheless, the aim of obtaining a truly tricoordinate R_3Si^+ cation, with resonances in the range of the trimesitylsilylium ion, remains an open challenge.

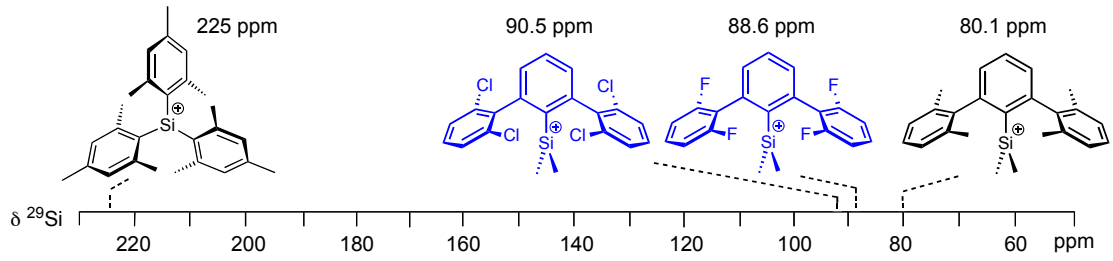

Figure 3.16 ^{29}Si NMR shift comparison of cations **18** and **28** with trimesityl silylium ion and one of the cations with methyalted flanking rings. Blue – cations displaying halogen→Si interaction. Solvent: C_6D_6; counterion: $B(C_6F_5)_4^-$.

3.2.4 Moving the Halogen Atom in the *para* Position of the Flanking Rings

Our next approach to the synthesis of terphenyl silylium ions featuring reduced interactions with the lateral rings utilized the introduction of electron withdrawing fluorine atoms in the *meta* and *para* positions of the flanking rings. In cations **31**–**33** the *ortho* carbon atoms of the lateral rings should be deactivated in terms of π–coordination ability and a direct silicon–fluorine interaction is highly improbable. A series of preliminary calculations, analogous to those performed on **18**–**21**, revealed that for cations **31**–**33** there is no more degeneracy between C_1 and C_2 conformations.

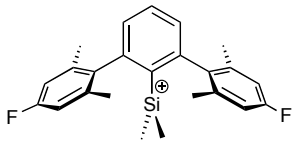

31

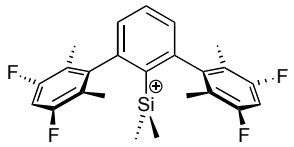

32

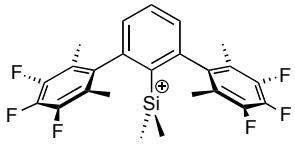

33

Furthermore, the difference in energy between the ground state C_1 and the C_{2v} geometries is now reduced to values between 9–12 kcal mol^{-1} (Table 3.6). Very low field-shifted ^{29}Si resonances are predicted to be obtained in presence of a C_{2v}-symmetric silylium ion; therefore, we chose cation **31** as our synthetic target because it presents the lowest energy for a C_{2v} symmetric conformation.

Table 3.6 Calculated ^{29}Si NMR and relative energies for the C_1, C_2, C_s, C_{2v} symmetrical geometries of compounds **31**-**33**.

Cmpd	Symmetry	Calcd ^{29}Si NMR[a]	Rel E + ZPE[b]
31	C_1	89.1	0.00
31	C_2	204.9	4.31
31	C_s	120.1	5.68
31	C_{2v}	243.9	9.08
32	C_1	51.7	0.00
32	C_2	179.9	4.86
32	C_s	177.8	9.46
32	C_{2v}	258.8	12.36
33	C_1	65.5	0.00
33	C_2	196.8	5.23
33	C_s	153.9	8.12
33	C_{2v}	255.0	11.27

[a] B3LYP/DZ(2df,pd) GIAO NMR, anisotropic values referenced against Me_4Si; [b]MP2/DZ(2d,p)//B3LYP/DZ(2df,pd) units = kcal/mol.

We attempted the synthesis of cation **31** starting from 4-bromo-3,5-dimethylbenzylamine (**34**), which can be obtained by selective bromination of commercially available 3,5-dimethylaniline (Scheme 3.3).[21] A modification of the Balz–Schiemann procedure was employed to obtain 2-bromo-5-fluoro-1,3-dimethylbenzene (**35**).[22] Hart-type coupling on **35** afforded the terphenyliodo derivative **36**;[17] subsequent lithiation and silylation furnished silane **37**. At this point the usual hydride abstraction with $[Ph_3C][B(C_6F_5)_4]$ was attempted, but decomposition occurred and a mixture of unknown compounds, which could not be separated by column chromatography, was obtained. The first sign suggesting that decomposition had taken place was the presence of a single dark brown phase in the reaction vial. The reaction mixture is usually clearly separated into a dark oily phase containing the ionic species at the bottom of the vial and a clear and almost colorless upper phase containing the neutral species.

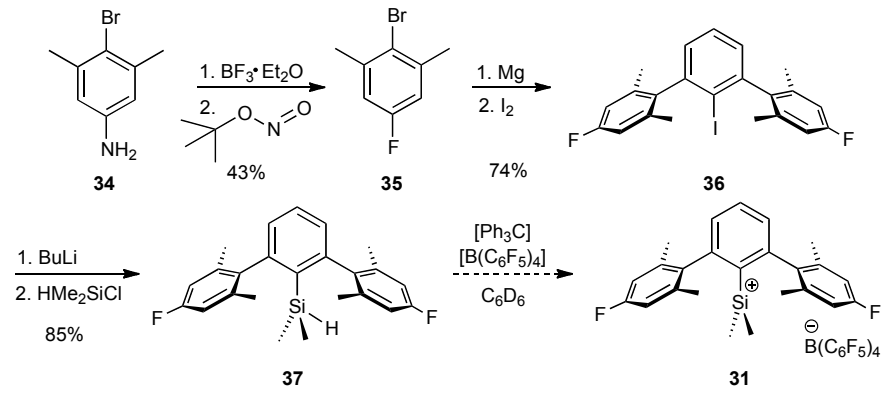

Scheme 3.3 Attempted synthesis of silylium ion **31**.

We decided to investigate the feasibility of the hydride abstraction step on silane **37** by performing this reaction in presence of few drops of acetonitrile-d_3. Hydride abstraction in presence of acetonitrile has been reported to furnish silylnitrilium ions that feature a ^{29}Si NMR shift in the range of 20–40 ppm. It is not completely understood whether acetonitrile coordinates the silylium ion as soon as this one is formed, or weather it first coordinates to the silane, assists in the hydride abstraction, and finally remains coordinated to the cation. Regardless of the exact mechanism of this reaction, it is recognized that silylnitrilium ions are more stable that the corresponding silylium ions because the positive silicon center is partially pacified by the lone pair of the nitrogen atom.[23, 24] Silylnitrilium ion **38** was readily synthesized from silane **37** and presents a ^{29}Si NMR resonance of 17 ppm; this experiment determined that the hydride abstraction is not the limiting step in our synthetic strategy towards cation **31**, but an unexpected decomposition pathway likely takes place as soon as compound **31** forms.

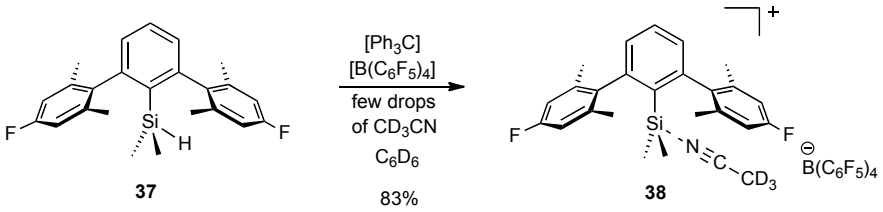

Scheme 3.4 Synthesis of silylnitrilium ion **38**.

Hydride abstraction on silane **37** was attempted again with undecachloro-carborane as counterion. It is known, in fact, that carborane anions are more stable than tetrakis(pentafluorophenyl)borate anions, particularly in the presence of strong acids. Reed and coworkers, during their studies on the isolation of benzenium ion

salts, discovered that the boron–phenyl bonds in $B(C_6F_5)_4^-$ are subject to acid cleavage if acids stronger than mesitylenium ion are present (Figure 3.17).[25] In the presence of a proton source, under the reaction conditions presented in Scheme 3.3, a benzenium salt forms, leading to decomposition of the $B(C_6F_5)_4^-$ anion. When the reaction was performed with a carborane anion (the use of dichlorobenzene as solvent is due to the scarce solubility of undecachlorocarborane in other aromatic solvents), the ^{29}Si NMR analysis of the reaction mixture presented a doublet at 15.2 ppm, with a $^1J_{C–F}$ coupling constant of 280 Hz. Compound **39** could not be isolated from other byproducts formed during the reaction, but ^{29}Si NMR and GC-MS analyses confirm its formation. Compound **39** is proposed to derive from fluoride abstraction by the transiently formed silylium ion **31** on another molecule of silane or silylium ion (Scheme 3.5). Computational and experimental studies on C_{aryl}–F activation in our group indicate that, under these reaction conditions, fluoride abstraction is likely to occur.[26]

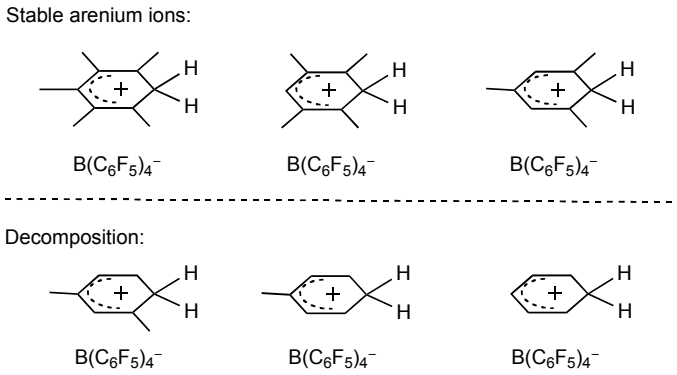

Figure 3.17 Stability of B–Ph bond of tetrakis(pentafluorophenyl)borate in the presence of strong acids.

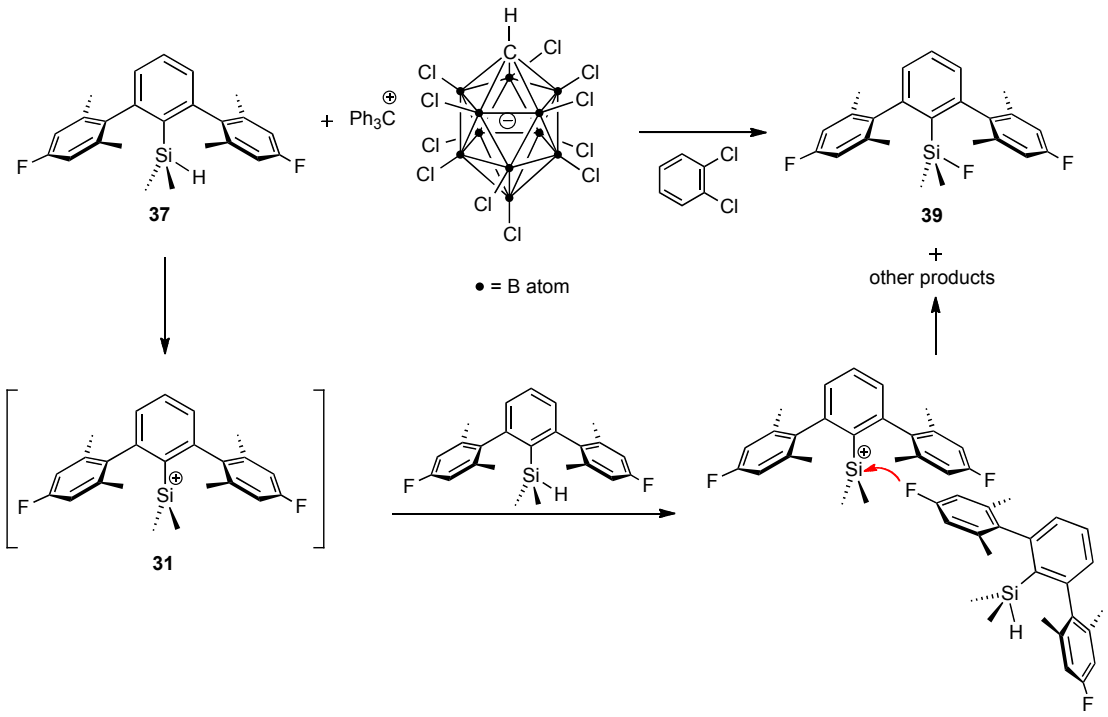

Scheme 3.5 Attempted synthesis of cation **31** using the $CHB_{11}Cl_{11}^-$ anion.

In light of these results, one last possibility remained to be explored in order to synthesize a silylium ion with 3,5-dimethylfluorophenyl flanking rings. Since the decomposition of cation **31** occurs because of intermolecular fluoride abstraction at the silicon center, increasing the steric hindrance with isopropyl substituents at these positions could preserve intact the positive center once the hydride abstraction has occurred. Silane **40** was synthesized following the same strategy adopted for silane **37** (Scheme 3.3): iodoterphenyl **36** underwent lithiation followed by quenching with diisopropylchlorosilane. Hydride abstraction did not occur in silane **40**: after one week, the ^{29}Si NMR of the reaction mixure showed only one signal corresponding to the starting material (Scheme 3.6). Indeed, the steric hindrance at silicon also prevented the hydride abstraction step. A similar obstacle was faced in the synthesis of the trimesitylsilylium ion (see Scheme 1.2); in this case, as an alternative to the use of hydride as leaving group, Lambert and Zhao performed allyl abstraction with diphenyl[(triethylsilyl)methyl]methylium ion.[27] As an outlook, we consider this approach a feasible strategy for the synthesis of silylium ion **41**.

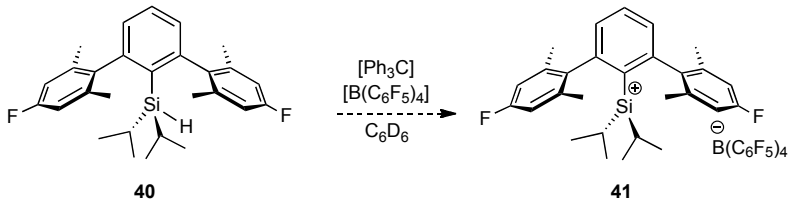

40 41

Scheme 3.6 Attempted synthesis of silylium ion **41**.

The instability of silyium ion **31** can be taken as sign of increased reactivity of this cationic species, compared to the ones previously synthesized, due to the absence of interactions with the flanking rings. Alternatively, the presence of fluorine substituents able to approach the cationic cavity could be the factor determing the instability of cation **31**. In this regard, it is interesting to compare the behavior of an analogous cation bearing chlorine instead of fluorine susbstituents in the *para* position of the lateral rings. The extraordinarily high strength of a silicon–fluorine bond (bond dissociation energy of $Me_3Si–F$ = 158 kcal mol^{-1})[28, 29] is a good indication of the affinity of these two nuclei and of the thermodynamic feasibility of the fluoride abstraction performed by silylium ion **31**. The affinity of silicon for halogen atoms decreases along the group and the silicon–chlorine bond energy is already significantly diminished (bond dissociation energy of $Me_3Si–Cl$ = 117 kcal mol^{-1});[28, 29] this set for us the conditions to attempt the synthesis of compound **42**.

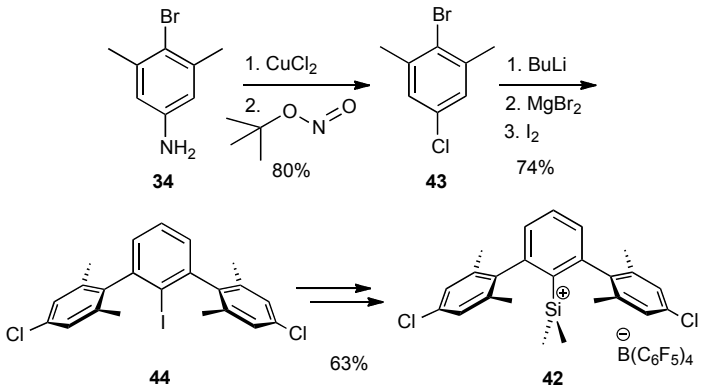

34 43 44 42

Scheme 3.7 Synthesis of silylium ion **42**.

The synthesis started from 4-bromo-3,5-dimethylbenzylamine (**34**), which could be obtained by selective bromination of commercially available 3,5-dimethylaniline (Scheme 3.7).[21] A Sandmeyer reaction afforded compound **43**, which underwent Hart-type coupling to furnish the iodoterphenyl **44**. The Hart coupling

requires the formation of a Grignard reagent; in the case of compound **43**, direct magnesium–halogen exchange was unsuccessful; lithium–bromine exchange could instead be performed, followed by Mg–Li transmetallation. The final steps of the synthesis involved lithiation and silylation of iodoterphenyl **44**, followed by hydride abstraction on the corresponding silane.

Silylium ion **42** was generated cleanly and was fully characterized; its ^{29}Si NMR shift at 95.4 ppm (in C_6D_6) indicates that the silicon center is slightly more deshielded compared to cations **18** and **28**, but far from the region of a free silylium ion (Figure 3.18). Analysis of the ^{13}C NMR shifts of the flanking rings for silylim ion **42** and silane **45** reveals a resonance pattern typical of a Wheland intermediate with coordination of the silicon center to the Cβ (Figure 3.19). This Cβ→Si π coordination is comparable in strength to those of **18** and **28**, although they differ in δ(^{29}Si) by ~ 6 ppm.

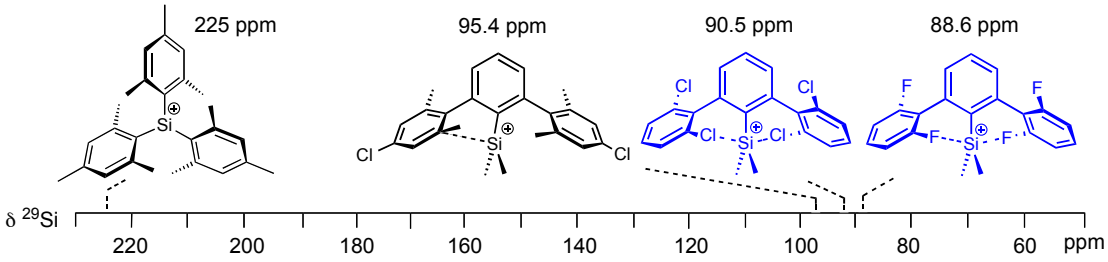

Figure 3.18 ^{29}Si NMR shift comparison of cations **18**, **28**, **42** and trimesityl silylium ion. Blue– cations displaying halogen→Si interaction. Solvent: C_6D_6; counterion: $B(C_6F_5)_4^-$.

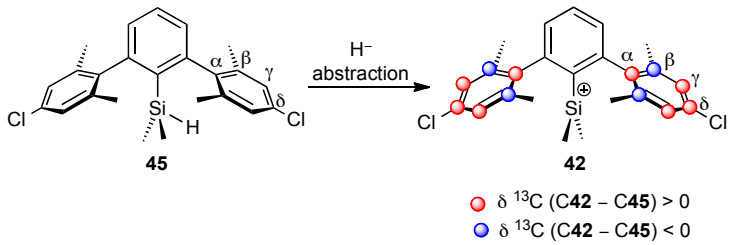

Δ (δ^{13}C) [ppm]	
C atom	**42** – **45**
α	+ 8.6
β	– 5.3
γ	+ 10.0
δ	+ 4.3

Figure 3.19 ^{13}C NMR analysis of the chemical shift of the lateral rings nuclei in silylium ion **42** compared to silane **45**. Solvent: C_6D_6; counterion: $B(C_6F_5)_4^-$.

Calculations at the density functional theory level suggest that the ground state conformation for cation **42** is C_1 symmetric (Table 3.7). The calculated ^{29}Si NMR shift is in accordance with the calculated value for the C_1 geometry (Δ (δ ^{29}Si) ≈ 4

ppm). Conformations other than C_1 are between 4 and 11 kcal mol^{-1} higher in energy and their ^{29}Si NMR shifts are significantly more deshielded than the experimental values obtained for compound **42**. The magnetic equivalence of the *ortho* positions of the flanking rings (^{1}H and ^{13}C NMR) can be explained by the fast exchange of the Cβ atom coordinating to silicon.

Table 3.7 Calculated ^{29}Si NMR and relative energies for the C_1, C_2, C_s, C_{2v} symmetrical geometries of compound **42**.

Cmpd	Symmetry	Calcd ^{29}Si NMR[a]	Rel E + ZPE[b]
42	C_1	91.9	0.00
42	C_2	201.3	3.55
42	C_s	132.5	5.92
42	C_{2v}	254.5	9.95

[a] SOGGA/DZ+(2df,pd)//B98/DZ(2df,pd) CSGT Si NMR, anisotropic values referenced against Me_4Si; [b] B98/DZ(2df,pd), units = kcal mol^{-1}.

Crystals of compund **42** were obtained in combination with the carborane anion $CB_{11}H_6Cl_6^-$ from a mixture of C_6H_5Cl/C_6H_{14}. Surprisingly, the X-ray analysis revealed an interaction between a lower belt chlorine atom of the carborane and silicon (Figure 3.20). The Si1–Cl1 distance is 2.3130(5) Å, almost identical to that in $iPr_3Si–CB_{11}H_6Cl_6$, a precedent example reported by Reed and coworkers on the carborane–silylium ion interaction.[30, 31] Coordination of **42** by the anion causes a pyramidalization of the silicon center, as shown by the sum of angles around silicon (Σ C–Si–C = 351.40(12)˚) and by the corresponding out of plane distance (dfp-Si = 0.3154(4)Å, Table 3.8). Furthermore, the dihedral angles between the flanking rings and the central ring are in the range of 80–84˚, values close to a perpendicular geometry and that do not account for π(aryl)→Si interaction. While the data for [**42**][$B(C_6F_5)_4$] in solution of C_6D_6 account for C_{ortho}–Si coordination, the X-ray structure of **42**–$CB_{11}H_6Cl_6$ presents a new structural feature for the class of terphenylsilylium ions.

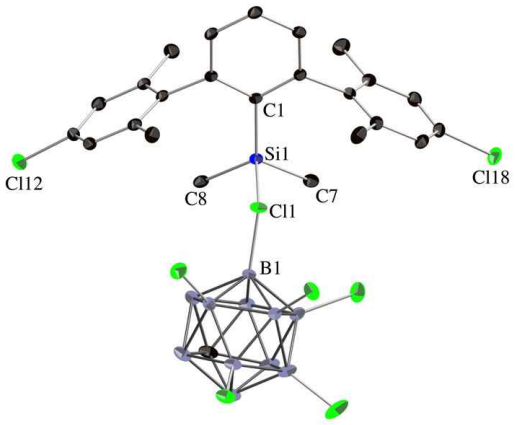

Figure 3.20 X-ray structure of **42**–$CB_{11}H_6Cl_6$ with 35% probability ellipsoids; hydrogen atoms omitted for clarity.

Table 3.8 Selected distances [Å] and dihedral angles [deg] for the X-ray structure of **42**–$CB_{11}H_6Cl_6$.

Parameter	**Expt.**
Cl1–Si1	2.3130(5)
B1–Cl1	1.8550(17)
B–Cl $_{\text{non coord}}$	1.7820-1.7927(45)
Σ C–Si–C[a]	351.40(12)
dihedral angle[b]	80,83(7)[c] 84.13(8)[d]
dfp-Si[e]	0.3154(4)

[a] Sum of the C–Si–C angles around silicon. [b] Angles between least square planes of the flanking rings and central ring. [c] Between ring containing Cl12 and central ring. [d] Between ring containing Cl18 and central ring. [e] Deviation from planarity: distance between the Si atom and the plane defined by the three C atom bound to Si.

How can the discrepancy between solution and solid phase data be explained? As discussed already in 1.4.3, it looks counterintuitive that the less coordinating carborane anion $CB_{11}H_6Cl_6^-$ complex the silicon center, while $B(C_6F_5)_4^-$ does not interact with it. Apparently, $B(C_6F_5)_4^-$ is solvated in benzene to such an extent that the silicon anion bond is dissociated, and the silicon center, seeking electron density, interacts with the flanking rings. On the contrary, $CB_{11}H_6Cl_6^-$ is not well solvated in chlorobenzene, the ion pair is not well separated, and the anion, in proximity to silicon, becomes the favorable coordination partner for silylium ion **42**.

These results led us to the conclusion that terphenyl substituents are an optimal vehicle to tune the Lewis acidity at the silicon center but not the solution to

obtain a free silylium ion, sterically more accessible than the trimesitylsilylum ion. Reducing the electron density at the lateral rings, in order to deactivate π(aryl)→Si coordination, induces, in fact, a switch to anion→Si coordination, as shown by the solid state structure of **42**–$CB_{11}H_6Cl_6$.

3.3 Competition between π-Arene and Lone Pair-Halogen Stabilization in Silylium Ions

A 2,6-diarylphenyl scaffolds exhibits η^1 π coordination to the silicon center if the lateral rings are substituted with methyl groups (see 3.1), while halogen→Si interactions dominates when fluorine and chlorine are in the *ortho* positions of the flanking rings (see 3.3). We became interested in probing the energetic details of these two mechanisms and, therefore, a series of cations **46**–**49** bearing 2,6-difluoro- and 2,6-dimethyl-substituted rings were synthesized.

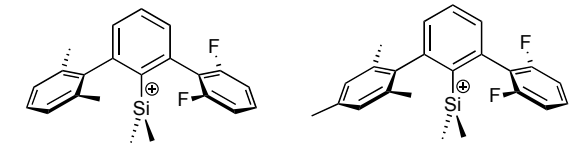

46 **47**

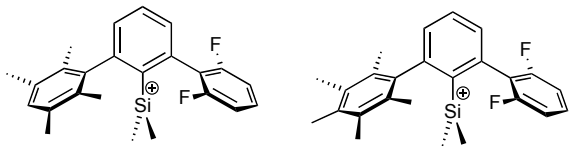

48 **49**

Our synthesis of cations **46**–**49** commenced from commercially available 2,6-dibromoaniline that underwent protection at the amino group in the form of triazene (Scheme 3.8).[6] A single Negishi coupling on triazene **22**, followed by treatment of the corresponding product **50** with iodine, afforded biphenyl **51**. Hart-type coupling[17] of **51**, and subsequent lithiation and silylation, furnished silane **53**. Cations **46**–**49** were prepared by hydride abstraction using $[Ph_3C][B(C_6F_5)_4]$.

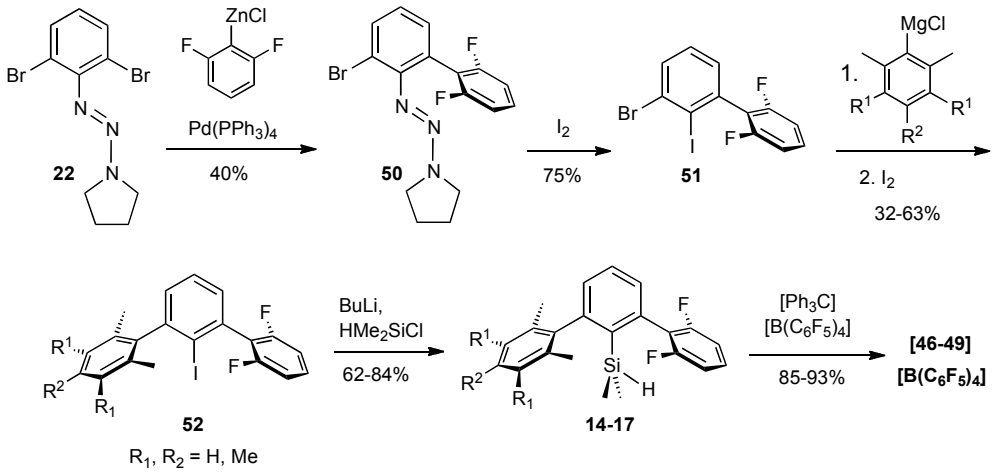

Scheme 3.8 Synthesis of silylium ions **46**–**49**.

NMR spectroscopy revealed a significant buildup of positive charge at silicon on going from silanes **14**–**17** to cations **46**–**49** ($\Delta\delta$ (^{29}Si ≈ 80–120 ppm)) with **46** and **47** being significantly more deshielded than **48** and **49** (Figure 3.21). In particular, the ^{29}Si NMR shifts of **46** and **47** fall in the region of the fully fluorinated cation **18**, while the resonances of **48** and **49** resemble those of a terphenyl with pentamethylphenyls as flanking rings. Furthermore, the signal multiplicity of the

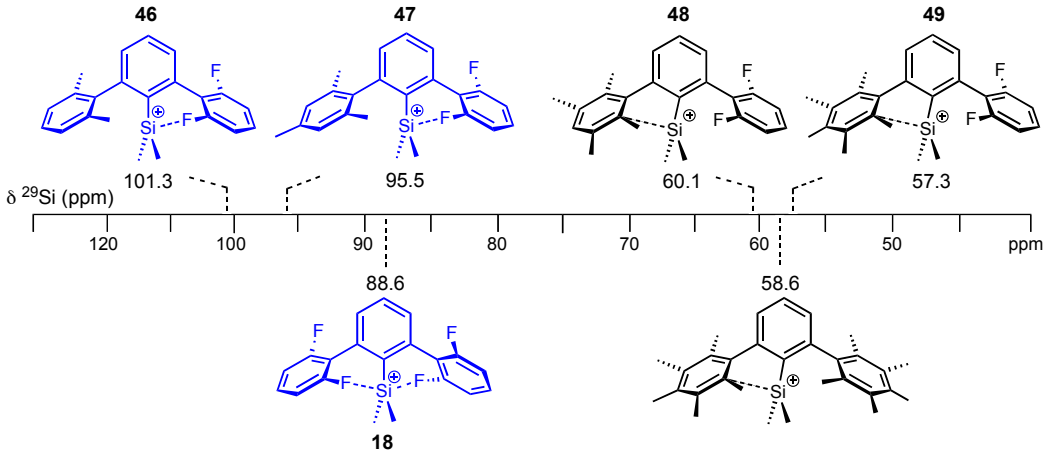

Figure 3.21 ^{29}Si NMR shift of cations **46-49** (top) compared with cation **18** and a fully methylated analog (bottom). In black, molecules with preferential π(arene)→Si interaction; in blue, molecules with preferential F→Si interaction. Solvent: C_6D_6; counterion: $B(C_6F_5)_4^-$.

resonances for the Me_2Si fragment (^{1}H, ^{13}C, ^{29}Si) indicates Si–F coupling in **46** and **49** (

Figure ***3.22***). These signals, except for the broad ^{29}Si resonance of **46**, appear as

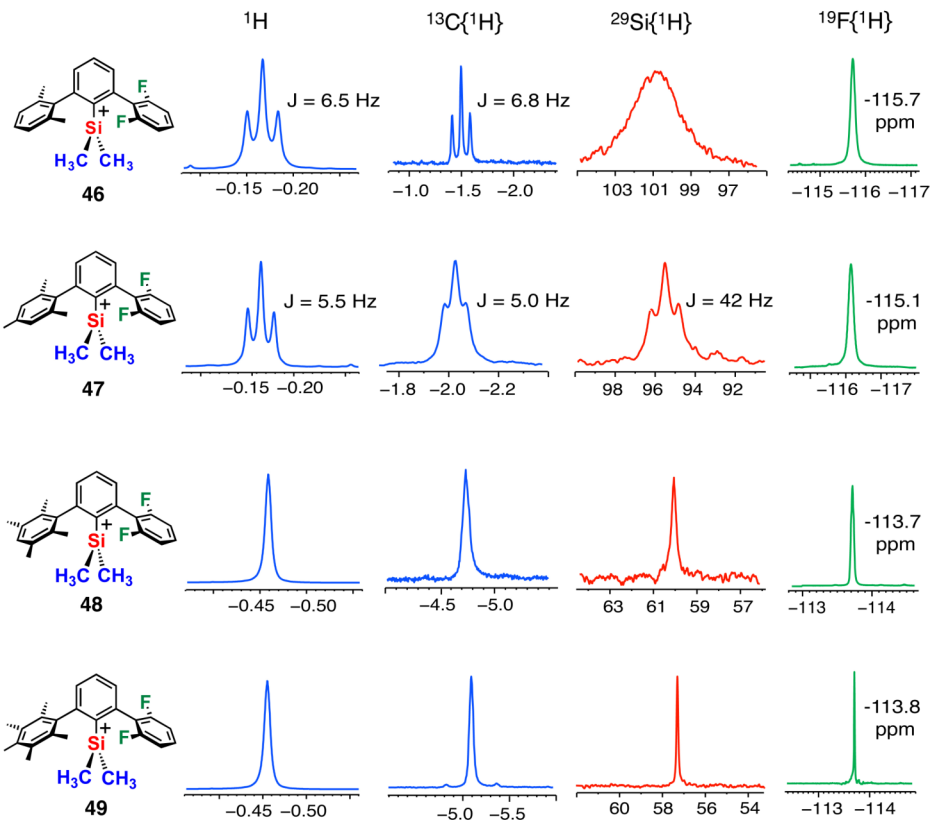

Figure 3.22 NMR analysis of **46-49**. Blue – ^{1}H and ^{13}C NMR signals for methyl groups at silicon; red – ^{29}Si NMR; green – ^{19}F NMR. Solvent: C_6D_6. Anion: $B(C_6F_5)_4^-$.

a triplet. Instead, the singlet signals for cations **48** and **49** suggest a preferential interaction of silicon with the methylated flanking ring. An analysis of the ^{13}C NMR shifts of the flanking rings nuclei is a powerful tool to detect the coordination mode that takes places and to which extent it occurs. Cations **46** and **47** show a similar behavior: the fluorinated flanking rings reveal a resonance pattern typical of the halogenated lateral rings in cations **18** and **28**; also, the methylated flanking rings present a perturbation of their electron density upon hydride abstraction, and more specifically, in the form typical of a Wheland intermediate (Figure 3.24). These data suggest that both π(arene)→Si and F→Si coordinations are taking place. However, when we compare these $\Delta\,\delta^{13}C$ NMR shifts with those for cations **48** and **49** (Figure 3.25), it clearly appears that the perturbation experienced by the duryl and pentamethylphenyl flanking rings is significantly larger than those for the xylyl and mesityl rings in cations **46** and **47**, and lead us to the conclusion that, in the case of electron-rich methylated flanking rings, *i.e.* with basicity higher than xylene, the π(arene)→Si interaction is favorable.

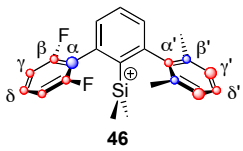

Δ (δ^{13}C) [ppm]	
C atom	$R_3Si^+ - R_3SiH$
α	– 7.3
β	+ 0.8
γ	+ 2.9
δ	+ 1.9
α'	+ 1.8
β'	– 1.3
γ'	+ 6.5
δ'	+ 4.1

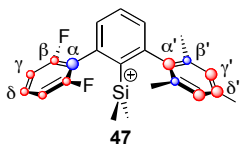

Δ (δ^{13}C) [ppm]	
C atom	$R_3Si^+ - R_3SiH$
α	– 7.3
β	+ 0.1
γ	+ 2.4
δ	+ 1.7
α'	+ 6.0
β'	– 3.2
γ'	+ 9.2
δ'	+ 6.3

δ ^{13}C ($C_{silylium\ ion} - C_{silane}$) > 0
δ ^{13}C ($C_{silylium\ ion} - C_{silane}$) < 0
= Δ (δ ^{13}C) > 5 ppm
= Δ (δ ^{13}C) < 5 ppm

Figure 3.24 ^{13}C NMR analysis of the chemical shift of the lateral ring nuclei in silylium ions **46** and **47** compared to the respective silane precursors. Anion: $B(C_6F_5)_4^-$. Solvent: C_6D_6.

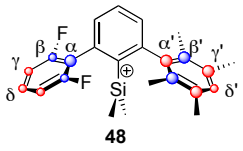

Δ (δ^{13}C) [ppm]	
C atom	$R_3Si^+ - R_3SiH$
α	– 5.4
β	– 1.2
γ	+ 1.1
δ	+ 2.0
α'	+ 26.8
β'	– 13.9
γ'	+ 34.2
δ'	+ 4.3

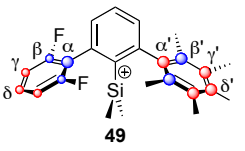

Δ (δ^{13}C) [ppm]	
C atom	$R_3Si^+ - R_3SiH$
α	– 5.4
β	– 1.1
γ	+ 1.0
δ	+ 2.0
α'	+ 26.9
β'	– 14.6
γ'	+ 34.8
δ'	+ 8.3

δ ^{13}C ($C_{silylium\ ion} - C_{silane}$) > 0
δ ^{13}C ($C_{silylium\ ion} - C_{silane}$) < 0
= Δ (δ ^{13}C) > 5 ppm
= Δ (δ ^{13}C) < 5 ppm

Figure 3.25 ^{13}C NMR analysis of the chemical shift of the lateral ring nuclei in silylium ions **48** and **49** compared to the respective silane precursors. Anion: $B(C_6F_5)_4^-$. Solvent: C_6D_6.

A series of calculations at the density functional theory level was performed on cations **46**–**48** and afforded results congruent to the experimental data. The relative energies between conformers displaying π_{arene}→Si and F→Si coordination are listed in Table 3.9. For compounds **46** and **47,** both coordination structures are considered, with a strong preference for F→Si interaction in cation **46**, whereas for compounds **48** and **49** only the π_{arene}→Si coordination mode results from the calculations. The calculated ^{29}Si NMR shifts for **48** and **49** are very close to the experimental values ($\Delta\ \delta^{29}Si \approx 6$ ppm). The discrepancy between the calculated and experimental values for **46** and **47** reflects instead the competitions between π_{arene}→Si and F→Si coordination modes and suggests that the experimental values for these cations are the results of the silicon center experiencing both π and lone pair coordination.

Table 3.9 Calculated relative energies and ^{29}Si NMR for $\pi_{arene}\rightarrow$Si and F→Si coordination in compounds **46**–**48**.

Cmpd	Symmetry	Rel E + ZPE[a]	Calcd ^{29}Si NMR[b]
46	$\pi_{arene}\rightarrow$Si	13.40	83.5
	F→Si	0.00	121.9
47	$\pi_{arene}\rightarrow$Si	0.00	81.1
	F→Si	2.64	118.9
48	$\pi_{arene}\rightarrow$Si	0.00	66.8
	F→Si	-	-
49	$\pi_{arene}\rightarrow$Si	0.00	61.4
	F→Si	-	-

[a] B98/DZ(2df,pd), units = kcal mol^{-1}. [b] SOGGA/DZ+(2df,pd)//B98/DZ(2df,pd) CSGT Si NMR, anisotropic values referenced against Me_4Si.

The results from NMR and computational studies fully match the solid state structures of **46** and **49**, which were obtained as solvent-free salts with the carborane anion $CB_{11}H_6Cl_6^-$ (Figure 3.26). Compound **46** exhibits fluorine coordination with a Si1–F1 distance of 1.8658(8) Å, 17% longer than a covalent bond (Table 3.10).[16] X-ray analysis of **49** reveals π-coordination *via* C_{ortho} with a Si2–C38 distance of 2.0890(17) Å, 11% longer than a covalent bond.[16] In both cations, the dihedral angle between the coordinating ring and the central ring deviates significantly from 90°, whereas the non-interacting ring adopts almost a perpendicular conformation relative to the central ring. Consequences of the coordination to the silicon center are also the significant elongation of the C10–F1 bond, compared to the counterpart C14–F2 in cation **46**, and the pyramidalization occurring at carbon C38 in cation **49**.

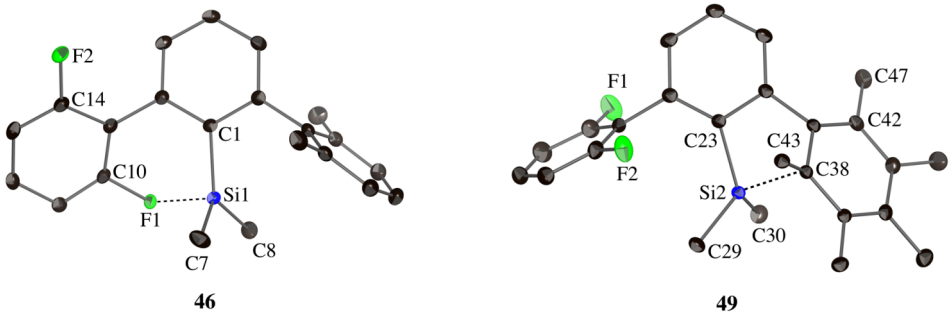

Figure 3.26 X-ray structures of [**46**][$CB_{11}H_6Cl_6$] (left) and [**49**][$CB_{11}H_6Cl_6$] (right) with 35% probability ellipsoids. Anion and hydrogen atoms omitted for clarity. Dashed lines show the interactions F→Si and π(arene)→Si.

Table 3.10 Selected distances [Å] and dihedral angles [deg] for the X-ray structure of [**46**][$CB_{11}H_6Cl_6$] and [**49**][$CB_{11}H_6Cl_6$].

Cation 46		**Cation 49**	
Parameter	**Expt.**	**Parameter**	**Expt.**
F1–Si1	1.8658(8)	C38–Si2	2.0890(17)
C10–F1	1.4484(14)	C38–C43	1.546(2)
C14–F2	1.3459(15)	C42–C47	1.508(3)
Σ C-Si-C[a]	356.81(13)	Σ C-Si-C[a]	345.49(18)
dihedral angle[b]	29.36(6)[c]	dihedral angle[b]	72.05(12)[c]
	74.63(6)[d]		45.27(10)[d]
dfp-Si[e]	0.1897(3)	dfp-Si[e]	0.4131(5)

[a] Sum of the C–Si–C angles around silicon. [b] Angles between least square planes of the flanking rings and central ring. [c] Between fluorinated ring and central ring. [d] Between the central ring and methylated ring. [e] Deviation from planarity: distance between the Si atom and the plane defined by the three C atom bound to Si.

The sum of the C-C38-C angles is 351.13(26)° and the distance of C38 from the plane defined by the carbon atoms covalently bound to it is 0.2573(16) Å (ideal values for an sp^2 carbon atom would be: Σ C-C38-C angles = 360° and dfp-C38 = 0 Å).

These results led us to the conclusion that both electron rich arenes and aromatic halogens are non-quenching donors for silylium ions. Even though the ^{29}Si shifts for these coordinated species are in the range of 60–100 ppm (far from the shift of the free trimesitylsilylium ion), they indicate that a consistent amount of positive charge remains on the silicon center. For the first time, the delicate balance of arene *vs* lone pair coordination in terphenylsilylium ions featuring both a methylated and a fluorinated flanking ring has been studied. The coordination by the π(arene) electron density is definitely predominant in the case of flanking rings of basicity higher than mesitylene; in the case of methylated rings of basicity equal or lower than mesitylene, a competitive mechanism takes place with a favorable halogen→Si interaction occurring in the presence of a xylene lateral ring.

3.4 Fluorinated Naphthyl Flanking Rings in Enshrouded Silylium Ions

The delicate balance between π(arene) *vs* lone pair-halogen stabilization of silicon cation could be further examined in systems with fluoronaphthyl lateral rings. More specifically, we envisioned compounds **54** and **55** as appropriate candidates for this study. Both cations, with fluorine substituents at positions 8 and 2 of the naphthyl

groups respectively, can be coordinated by the arene itself or by the halogen lone pair. Two different competitive mechanism of coordination can take place on the same flanking ring. It is also very intriguing to study the geometry of coordination of these compounds: they could in fact assume *syn* or *anti* arrangements with respect to the orientation of the flanking rings and, in case the *anti* configuration is dominant, we would selectively form chiral siylium ions (Figure 3.27).

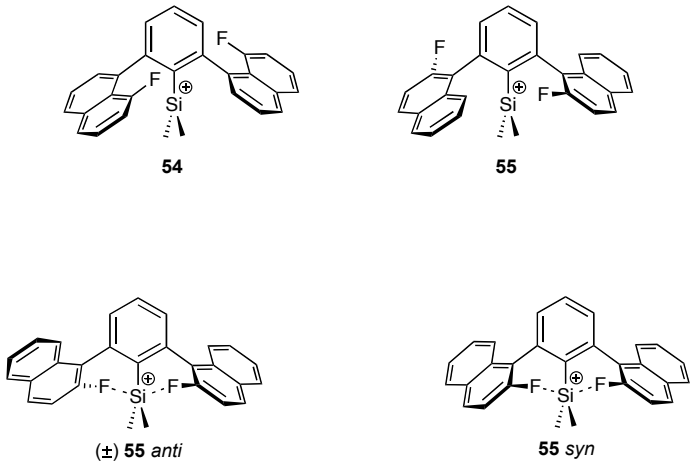

Figure 3.27 Possible configurations of cation **55** when coordinated by two fluorine atoms.

The synthesis of compound **54** commenced from commercially available 1,8-diaminonaphthalene (Scheme 3.9). Triazene **57** was isolated and purified before undergoing fluorination–deazotation *via* treatment with the HF·pyridine complex.[32,33] The resulting 8-(fluoroamino)naphthalene **58** underwent a Sandmeyer reaction to afford 1-bromo-8-fluoronaphthalene **59**. Hart couplings of the Grignard derivative of **59** with 1,3-dibromo-2-iodobenzene led to a 1: 3.6 mixture of diastereoisomer of iodoterphenyl **60** (*syn* and *anti* diastereoisomers were not assigned, their ratio was calculated via ^{19}F NMR). After heating to 380 K, the mixture reaches a thermodynamic equilibrium of 1:1 that is maintained upon cooling back to 300 K (see 5.2.38). Lithiation and silylation of **60** afforded silane **61** in a 4:1 ratio of the two diastereoisomers. Hydride abstraction on **61** was performed with $[Ph_3C][B(C_6F_5)_4]$, but decomposition occurred. Similar to cation **31**, no separation between the cationic and the neutral phases was detected in the reaction mixture.

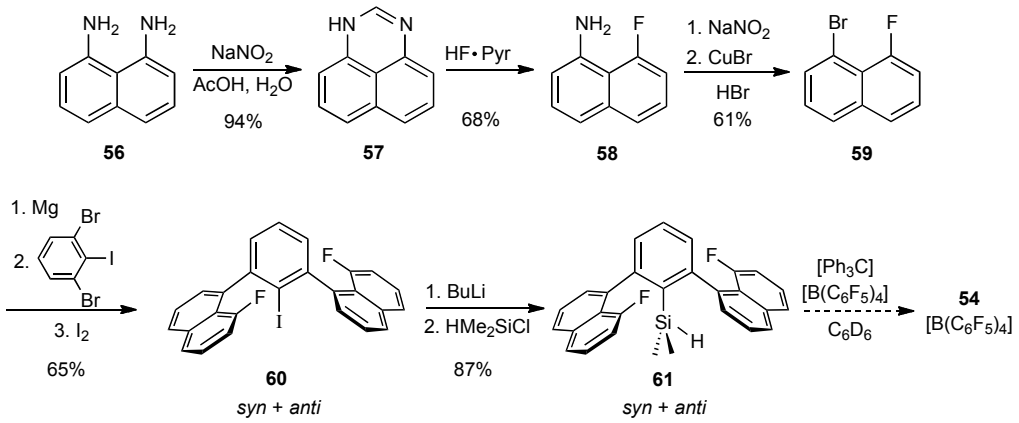

Scheme 3.9 Attempted synthesis of silylium ion **54**.

Aware of the fact that the formation of acidic species under these reaction conditions could lead to decomposition of the counterion, a proton sponge, such as the bulky tri(*o*-tolyl)phosphine, was employed in a second attempt of hydride abstraction (Scheme 3.10). Unexpectedly, compound **62**, the product of a sila-Friedel–Crafts reaction, was isolated in 42% yield. This result testifies that the hydride abstraction effectively occurs but, as soon as the silylium ion is formed, the naphthyl ring performes a nucleophilic attack on the silicon center. Subsequent proton elimination and rearomatization of the naphthyl ring afforded the neutral silane **62**. In the absence of an adequate base, the proton abstraction on intermediate **63** leads to decomposition products.

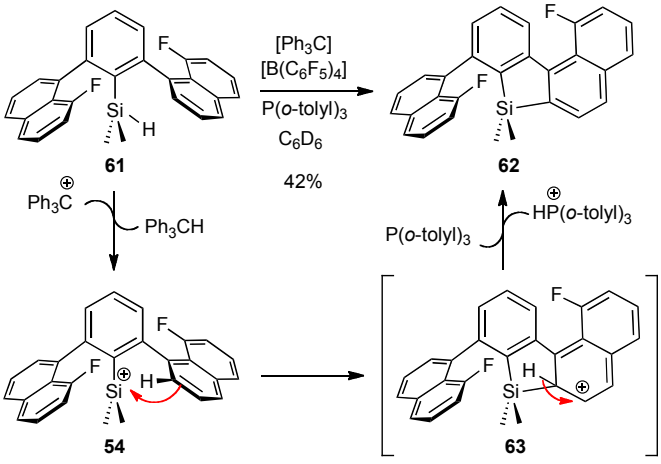

Scheme 3.10 Mechanism of sila-Friedel–Crafts on silylium ion **54**.

Crystals suitable for X-ray analysis were obtained from a saturated solution of **62** in acetonitrile (the mixture was first warmed to 70° to allow complete dissolution of the powder, then slowly cooled to room temperature). X-ray analysis confirmed the

structure postulated for **62** (Figure 3.28). The new Si1–C26 bond, formed by a sila-Friedel–Crafts reaction, has a length of 1.8725(15) Å, comparable to the one of Si1–C1, 1.8681(15) Å. The distance of Si1 from the plane defined by C1, C27, and C28 is 0.4889(4) Å, a value in the range of a tetracoordinated silicon center. The dihedral angle between the least square planes of the F1-containing lateral ring and of the central ring is 73.47(6)°, indication of little perturbation from the ideal perpendicular geometry; the angle between the plane of the naphthyl moiety that undergoes Friedel–Crafts and the central ring is instead 28.73(6) Å.

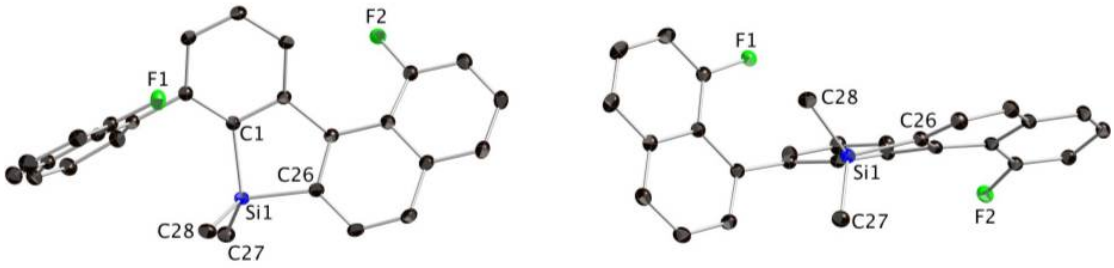

Figure 3.28 X-ray structure of **62**. Front view: left; view through Si–C_{aryl} bond: left. Hydrogen atoms omitted for clarity.

Usually, Friedel–Crafts-type silylation involving silyl cations as intermediates occurs only with electron rich aromatic rings, such as ferrocene and pyrrole.[34, 35] In the case of non-activated aromatic rings such as benzene, the conversion of the reaction markedly decreases.[36] Kawashima and coworkers reported in 2009 the use of this sila-Friedel–Crafts reaction for the construction of dibenzosilone frameworks in the synthesis of trisilasumanene **65**, a silicon analog of sumanene (Scheme 3.11).[37] Compound **62** represents even a more extreme case of sila-Friedel–Crafts on a deactivated aromatic ring such as fluoronaphthalene, and testifies that the reactivity of silyilum ions, when wisely directed, can greatly expand the synthetic chemists' toolbox.

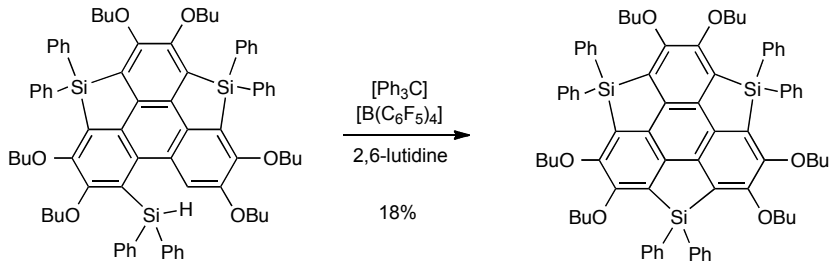

64 65

Scheme 3.11 Synthesis of trisilasumanene **65** *via* a Sila-Friedel–Crafts reaction.

The experience gained studying the unexpected reactivity of cation **54** taught us that the presence of an aromatic proton in the *ortho* position of the flanking ring leads to decomposition: the initial C_{ortho}→Si coordination evolves in a sila-Friedel–Crafts reaction. Furthermore, this kind of reactivity in cation **54** speaks to the preferential coordination of the π(aryl) system rather than of the fluorine atoms to silicon. The next step in the investigation of π(arene) *vs* halogen coordination to silylium ions involves compound **55**, which contains a fluorine atom in position 2 of the naphthalene unit. The *ortho* positions of flanking rings in **55** are both deactivated towards sila-Friedel–Crafts reactions, on one side by the fluorine substitutent, on the other by the presence of a quaternary carbon center. Our goal is, once again, to study the preferential coordination sites and conformation of cation **55**. In the direction of the synthesis of enantiomerically enriched silylium ions, the existence of a marked conformational preference is a fundamental result to obtain.

Calculations predict that the positive silicon center in **55** is coordinated by the π(aryl) system, and not by the fluorine atoms (Figure 3.29). More specifically, interactions occur between silicon and the carbon atoms in position 8 of the naphthalene unit (Si1–C4 in the *anti* conformation and Si2–C8 in the s*yn* conformation). The Si1–C4 distance is calculated to be 2.105 Å, Si2–C8 2.104 Å; these values, 12% longer than a Si–C bond,[16] are comparable to the silicon–carbon distance in compound **49** (Table 3.10), previous example of C_{ortho}–Si coordination. The pyramidalization at the silicon center is best described by the sum of angles around silicon, 348.5° for **55** *anti* and 348.2° for **55** *syn*, and by the distance of silicon from the plane defined by the carbon atoms attached to it, that is 0.370 Å in **55** *anti* and 0.375 Å in **55** *syn*. The planes of the flanking rings interacting with the silicon are

calculated to form a dihedral angle with the plane of the central ring of 41.95° for **55** *anti* and 42.06° for **55** *syn*.

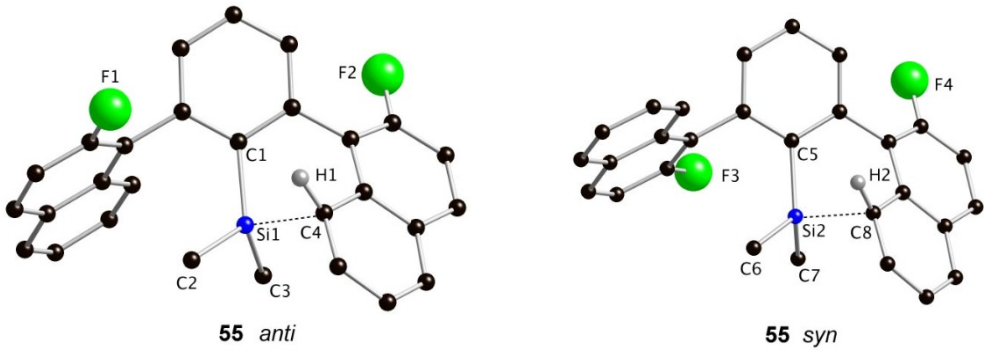

Figure 3.29 Ball and stick representation of calculated structures of *anti* and *syn* **55**. Selected distances (Å): Si1–C4 = 2.105; Si2–C8 = 2.104.

The HOMO (Highest Occupied Molecular Orbital) for *syn* and *anti* **55** were also calculated and are depicted in Figure 3.30 and Figure 3.32. It can be observed that the lobes of the HOMO are confined on the side of the non-interacting naphthyl ring for both *syn* and *anti* **55**. Electrostatic potential maps illustrate the charge distribution of *anti* and *syn* **55** three dimensionally (Figure 3.30, Figure 3.32). Areas of low electrostatic potential, red, are characterized by an abundance of electrons; areas of high potential, blue, are characterized by a relative absence of electrons. In cation **55** the charge distribution is consistent with the mechanism of coordination: the coordinating ring is more electron poor (blue colored) since it is partially donating electron density to the positively charged silicon center and the negative charge concentrates on the non-interacting naphtyl ring (red).

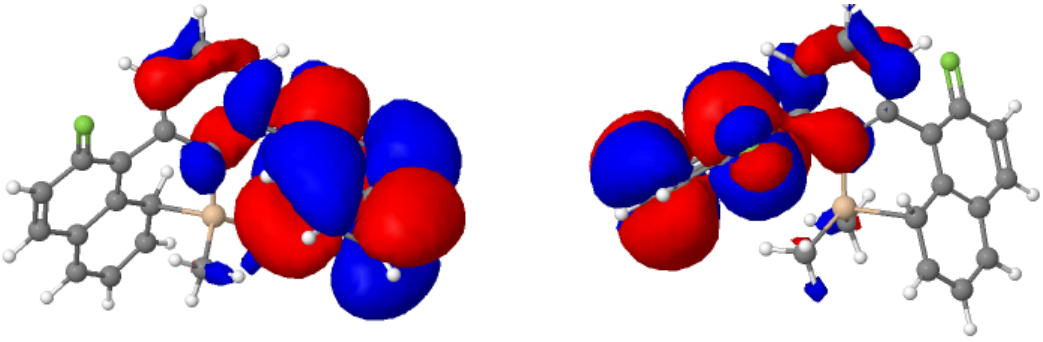

Figure 3.30 HOMO of anti **55**. View from front (left) and from back (right).

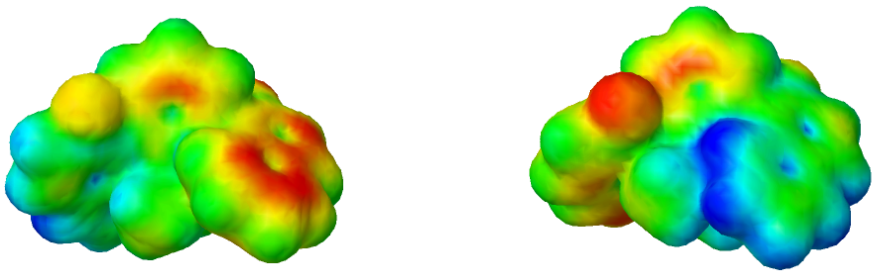

Figure 3.30 Map of electrostatic potential for *anti* **55**. View from front (left) and from back (right).

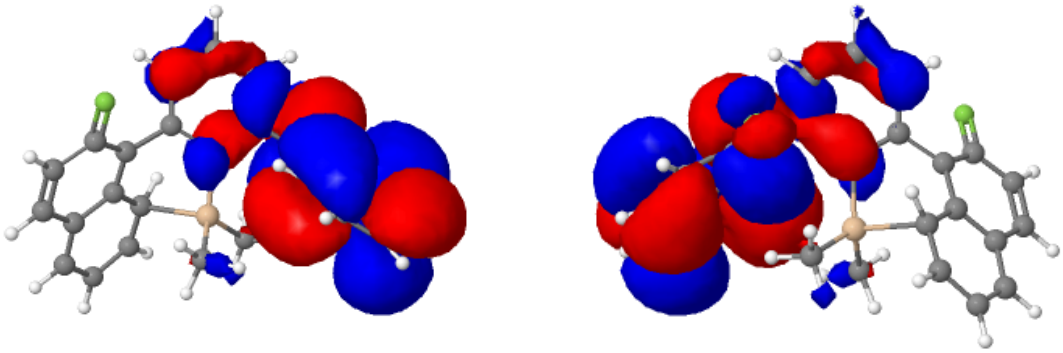

Figure 3.32 HOMO of *syn* **55**. View from front (left) and from back (right).

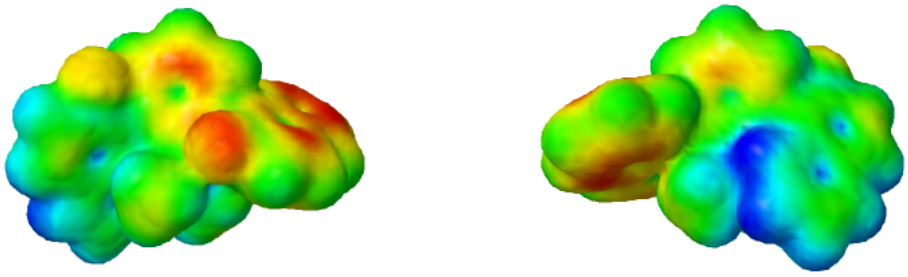

Figure 3.32 Map of electrostatic potential for *syn* **55**. View from front (left) and from back (right).

Encouraged by the calculations performed on cation **55**, we then embarked in its synthesis. An outline of our strategy for the synthesis of cation **55** is shown retrosynthetically in Scheme 3.12. It was envisioned that the final steps of the synthesis will involve lithiation and silylation of iodoterphenyl **67**, followed by hydride abstraction on silane **66**. Iodoterphenyl **67** should be accessible *via* Negishi coupling on triazene **22** with 2-fluoro-1-iodonaphthalene (**68**).[38] The preparation of the second partner for the Negishi coupling, 2-fluoro-1-iodonaphthalene **68**, or of an analog derivative such as 2-fluoro-1-bromonaphthlaene, represented for us a synthetic

challenge. There are, in fact, only few reports in the literature regarding the preparation of such compounds,[39-41] and most of them involve the use of 2-aminonaphthalene, which is no longer commercially available due to its potent bladder carcinogenicity.[42] As an alternative, we considered synthesizing **68** starting from the commercially available 2-fluoronaphthalene: directed *ortho* lithiation followed by quenching with iodine could afford the desired product. However, two big limitations appeared in this approach: the high cost of 2-fluoroaminonaphtalene (216 euro/g) and the difficulty to achieve regioselective functionalization of position 1 over position 3 in 2-fluoronaphthalene.[41]

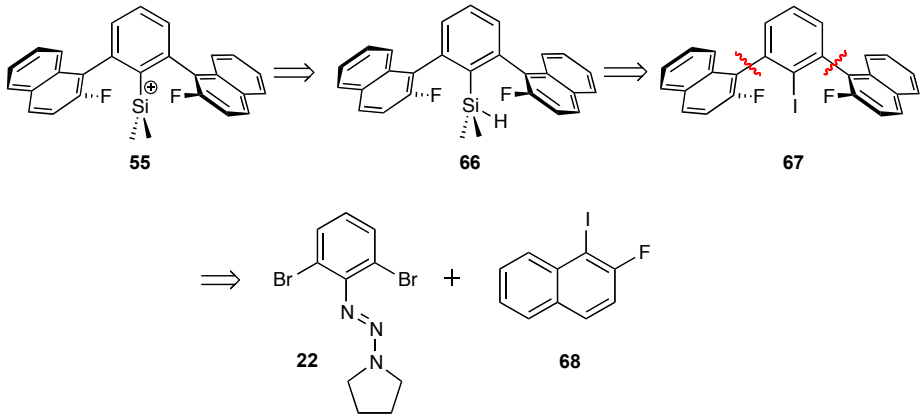

Scheme 3.12 Overall synthetic approach to cation **55**.

Because of the lack of synthetic strategies to obtain functionalized 2-fluoronaphthalenes and because of the growing importance of fluorinated molecules in the pharmaceutical industry, we decided to design a new route towards compound **68** and analogs of it. Our synthesis commenced from commercially available 1,3-difluorobenzene, which was protected at the most acidic position *via* lithiation and silylation to afford (2,6-difluorophenyl)triethylsilane **69** (Scheme 3.13).[43] Silane **69** was subjected to a sequence of lithiation and bromination and thus converted into (3-bromo-2,6-difluorophenyl)triethylsilane (**70**).[43] In the next sequence of lithiation, bromine underwent metal-halogen exchange and upon warming up to room temperature formed the corresponding aryne, which immediately reacted with furane to furnish the Diels–Alder product **71**.[44] Reduction of 1,4-epoxide **71** was carried out with a mixture of $TiCl_4$ and $LiAlH_4$ and afforded naphthalene derivative **72**.[45] Electrophilic aromatic substitution by *ipso* attack on the silylated position of naphthalene furnished the desired product **68**.[46] Alternatively, electrophilic aromatic

substitution using *N*-bromo-succinimide on silane **72** would lead to 1-bromo-2-fluoronaphthalene.[47] Future efforts are going to be directed to complete the synthesis of silylium ion **55** by performing a C(aryl)–C(aryl) coupling followed by insertion of the silane moiety and hydride abstraction, as depicted in Scheme 3.12.

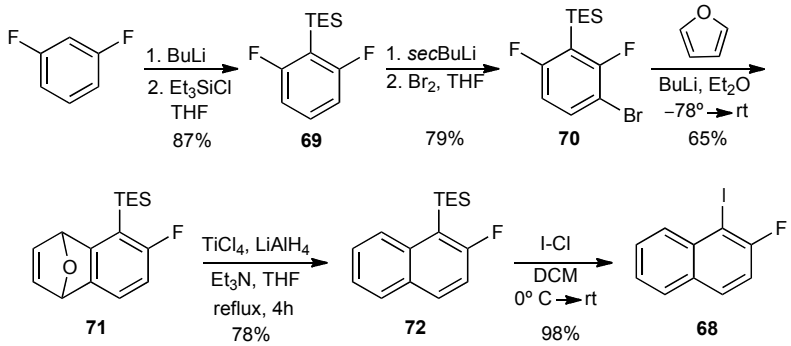

Scheme 3.13 Synthesis of 1-iodo-2-fluronaphthalene (**68**).

Our investigations of π(arene) *vs* halogen stabilization of silylium ions from the same fluoronaphthalene proximal ring allowed the discovery of sila-Friedel–Crafts reactions in cation **54**. Even though the cation was not preserved, this type of reactivity suggest that the fluorine lone pairs are not sufficient to pacify the avidity of Si^+ for electron density, and the π(arene) is rather the preferred site of interaction. We will be hopefully able to prove this concept in silyilum ion **55**, whose structure has been predicted to exhibit Si–C_{aryl} interactions as well.

3.5 References

1. Lambert, J. B.; Zhang, S. Z.; Ciro, S. M. *Organometallics* **1994**, *13*, 2430.
2. Duttwyler, S.; Do, Q. Q.; Linden, A.; Baldridge, K. K.; Siegel, J. S. *Ang. Chem. Int. Ed.* **2008**, *47*, 1719.
3. Reed, C. A.; Fackler, N. L. P.; Kim, K. C.; Stasko, D.; Evans, D. R.; Boyd, P. D. W.; Rickard, C. E. F. *J. Am. Chem. Soc.* **1999**, *121*, 6314.
4. Doering, W. V.; Saunders, M.; Boyton, H. G.; Earhart, H. W.; Wadley, E. F.; Edwards, W. R.; Laber, G. *Tetrahedron* **1958**, *4* (1-2), 178.
5. Kim, K. C.; Reed, C. A.; Elliott, D. W.; Mueller, L. J.; Tham, F.; Lin, L. J.; Lambert, J. B. *Science* **2002**, *297*, 825.
6. Liu, C. Y.; Knochel, P. *Org. Lett.* **2005**, *7*, 2543.

7. Moore, J. S. *Tetrahedron Lett.* **1994**, *35*, 5539.
8. Kost, D.; Kalikhman, I. *Acc. Chem. Res.* **2009**, *42*, 303.
9. Chauhan, M.; Chuit, C.; Corriu, R. J. P.; Mehdi, A.; Reye, C. *Organometallics* **1996**, *15*, 4326.
10. Belzner, J.; Schar, D.; Kneisel, B. O.; Herbstirmer, R., *Organometallics* **1995**, *14*, 1840.
11. Berlekamp, U. H.; Jutzi, P.; Mix, A.; Neumam, B.; Stammler, H. G.; Schoeller, W. W. *Angew. Chem. Int. Ed.* **1999**, *38*, 2048.
12. Ebata, K.; Inada, T.; Kabuto, C.; Sakurai, H. *J. Am. Chem. Soc.* **1994**, *116*, 3595.
13. Olah, G. A.; Mo, Y. K., *J. Am. Chem. Soc.* **1971**, *93*, 4942.
14. Mislow, K. *Chemtracts: Org. Chem.* **1989**, *2*, 151.
15. Reed, C. A. *Acc. Chem. Res.* **1998**, *31* (3), 133-139.
16. Rempfer, B.; Oberhammer, H.; Auner, N. *J. Am. Chem. Soc.* **1986**, *108*, 3893.
17. Saednya, A.; Hart, H. *Synthesis* **1996**, 1455.
18. Prakash, G. K. S.; Keyaniyan, S.; Aniszfeld, R.; Heiliger, L.; Olah, G. A.; Stevens, R. C.; Choi, H. K.; Bau, R., *J. Am. Chem. Soc.* **1987**, *109*, 5123.
19. Akitt, J. W., *Multinuclear NMR*. Plenum Press: New York, 1987.
20. Lehmann, M.; Schulz, A.; Villinger, A. *Angew. Chem. Int. Ed.* **2009**, *48*, 7444.
21. Zysman-Colman, E.; Arias, K.; Siegel, J. S. *Canadian Journal of Chemistry* **2009**, *87*, 440.
22. Garel, L.; Saint-Jalmes, L. *Tetrahedron Lett.* **2006**, *47*, 5705.
23. Bahr, S. R.; Boudjouk, P. *J. Am. Chem. Soc.* **1993**, *115*, 4514.
24. Kira, M.; Hino, T.; Sakurai, H. *Chem. Lett.* **1993**, 153.
25. Reed, C. A.; Kim, K. C.; Stoyanov, E. S.; Stasko, D.; Tham, F. S.; Mueller, L. J.; Boyd, P. D. W. *J. Am. Chem. Soc.* **2003**, *125*, 1796.
26. Duttwyler, S. D., C.; Fackler, N. L. P.; Tham, F. S.; Reed, C. A.; Baldridge, K. K.; Siegel, J. S. *Angew. Chem. Int. Ed.* **2010**, *49*, 7519.
27. Lambert, J. B.; Zhao, Y. *Angew. Chem. Int. Ed.* **1997**, *36*, 400.
28. Walsh, R. *Acc. Chem. Res.* **1981**, *14*, 246.
29. Becerra, R. W., R., *The Chemistry of Organic Silicon Compounds, Vol. 2*. Wiley: Chichester, 1998.
30. Xie, Z. W.; Manning, J.; Reed, R. W.; Mathur, R.; Boyd, P. D. W.; Benesi, A.; Reed, C. A. *J. Am. Chem. Soc.* **1996**, *118*, 2922.

31. Hoffmann, S. P.; Kato, T.; Tham, F. S.; Reed, C. A. *Chem. Commun.* **2006**, 767.
32. Al-Awadi, H.; Ibrahim, M. R.; Dib, H. H.; Al-Awadi, N. A.; Ibrahim, Y. A. *Tetrahedron* **2005**, *61*, 10507.
33. Zhu, Z., 2007, *Method of making 8-fluoro-naphthalen-1-ylamine and related compounds*, WO 2007/049124 A1.
34. Sollott, G. P.; Peterson, W. R. *J. Am. Chem. Soc.* **1967**, *89*, 5054.
35. Frick, U.; Simchen, G. *Synthesis* **1984**, 929.
36. Olah, G. A.; Bach, T.; Prakash, G. K. S. *J. Org. Chem.* **1989**, *54*, 3770.
37. Furukawa, S.; Kobayashi, J.; Kawashima, T. *J. Am. Chem. Soc.* **2009**, *131*, 14192.
38. Romanato, P.; Duttwyler, S.; Linden, A.; Baldridge, K. K.; Siegel, J. S. *J. Am. Chem. Soc.* **2010**, *132*, 7828.
39. Gribble, G. W. L. C. S. A., R. W.; Gilbertson J. J. *Org. Prep. Proced. Int.* **1981**, *13*, 349.
40. Repine, J. T.; Johnson, D. S.; White, A. D.; Favor, D. A.; Stier, M. A.; Yip, J.; Rankin, T.; Ding, Q. Z.; Maiti, S. N. *Tetrahedron Lett.* **2007**, *48*, 5539.
41. Kinstle, T. H.; Bechner, J. P. *J. Organomet. Chem.* **1970**, *22*, 497.
42. Searle, C. E., *Chemical Carcinogens*. American Chemical Society: Washington, D.C., 1974; Chapter 8 and 9.
43. Schlosser, M.; Heiss, C. *Eur. J. Org. Chem.* **2003**, (23), 4618.
44. Coe, P. L.; Waring, A. J.; Yarwood, T. D., *J. Chem. Soc. Perkin Trans. 1* **1995**, (21), 2729.
45. Chen, Y. L.; Hau, C. K.; Wang, H.; He, H.; Wong, M. S.; Lee, A. W. M. *J. Org. Chem.* **2006**, *71*, 3512.
46. Kotha, S.; Brahmachary, E. *J. Organomet. Chem.* **2004**, *689*, 158.
47. Widhalm, M.; Aichinger, C.; Mereiter, K. *Tetrahedron Lett.* **2009**, *50*, 2425.

4 Towards a "Free and Naked" Silylium Ion

4.1 Introduction

Silylium ions R_3Si^+ are much more reactive than their analogous carbenium ions:[1-3] their isolation has been one of the biggest challenges that chemists have faced over the past five decades and represents one more example of the "first row anomaly",[4] meaning the large gap in chemical behavior between carbon and the other elements of group 14. The kinetic instability of silylium ions originates from the high electrophilicity of the positively charged, tricoordinated silicon center, which in solution and in the solid state interacts with a variety of π- and σ-electron donors, forming tetra- or higher valent silicon species. The most successful approach to overcome this extreme kinetic lability has been the use of bulky substituents at silicon to block incoming nucleophiles. This consideration has brought about the synthesis of the long sought free silylium ion, the trimesitylsilyium ion **I** (Figure 4.1).[5] After this great achievement, many efforts have been made to develop analogous cations where the silicon center is sterically more accessible, in order to explore its reactivity when involved in chemical reactions. Most of these cations present a sensibly reduced Lewis acidity character[6-10] and the synthesis of a "free and naked" silylium ion remains an open problem.

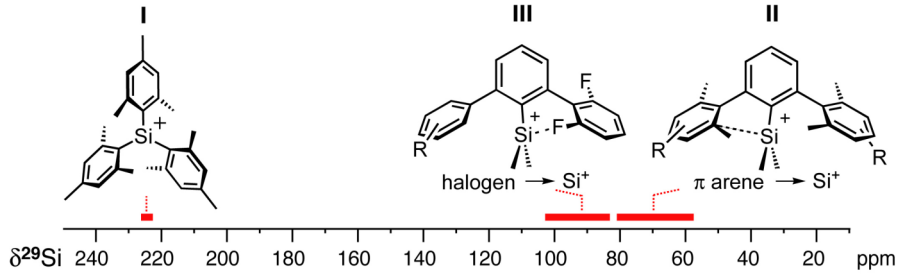

Figure 4.1 ^{29}Si NMR shift of trimesitylsilylium ion **I**, and terphenyl substituted silylium ions **II** and **III**.

A less hindered silylium ion is susceptible to interactions with solvent or an anion; in order to avoid these interactions, the positively charged silicon center can be moderately pacified by intramolecular interactions with its substituents. Our investigation in this field started with terphenyl-substituted cations: their steric shroud shields the silyl core from the ambient environment and donation of electron density from the lateral rings into the empty 3p(Si) orbital provides a vehicle to control the

reactivity of the cationic center. Varying the number of electron-donating methyl groups on the flanking rings allows a tuning of the silicon Lewis acidity as showed by the ^{29}Si NMR shifts of **II** in the region between 60 and 80 ppm.[9] A comparison with the ^{29}Si NMR resonance of trimesityl silylium ion **I** (225 ppm), indicates a consistent shielding of the positive charge in **II**. Only a slight enhancement in the ^{29}Si shift derives from the substitution of electron-donating methyl groups with electron-withdrawing halogen atoms (**III**): the π(aryl)→Si interaction is effectively quenched in favor of lone pair(halogen)→Si donation (Figure 4.1).[11] Indeed, our aspiration to obtain a new generation of free silylium ions leads us to a new strategy: the substitution of the aromatic flanking rings in the terphenyl skeleton with alkyl groups that cannot give rise to π(aryl) or lone pair coordination.

Phenylsilylium ions bearing alkyl groups near the silicon center might experience C–H→Si complexation. Such interactions can be considered as hyperconjugation effects, agostic interactions or three-center, two-electron bonds. More specifically, the term "agostic" interaction is not synonymous with all "3-center-2-electron bonds", but it refers specifically to a 3-center-2-electrons interaction involving a C–H bond. In organometallic chemistry, soon after the discovery of transition metal alkyl compounds, it became clear that the presence of the transition metal imparted properties to the alkyl group that were unprecedented in organic chemistry. For instance, the ability to extract hydride from the *β*-carbon of a transition metal–ethyl compound is an example of the impact of a transition metal on an alkyl group.[12] From variable temperature NMR studies on the dynamic equilibria in the metal complex Cp*Co(η^2-C_2H_4), it was identified that the agostic structure is thermodynamically more stable than the corresponding olefin hydride or the normal alkyl complex (Figure 4.2).[13] The agostic M–H–C interactions are characterized by relatively short M–H distances (≈ 1.8–2.3 Å) and small M–H–C bond angles (≈ 90–140º).[14-16] With respect to ^{1}H NMR spectroscopy, a signature of an agostic interaction

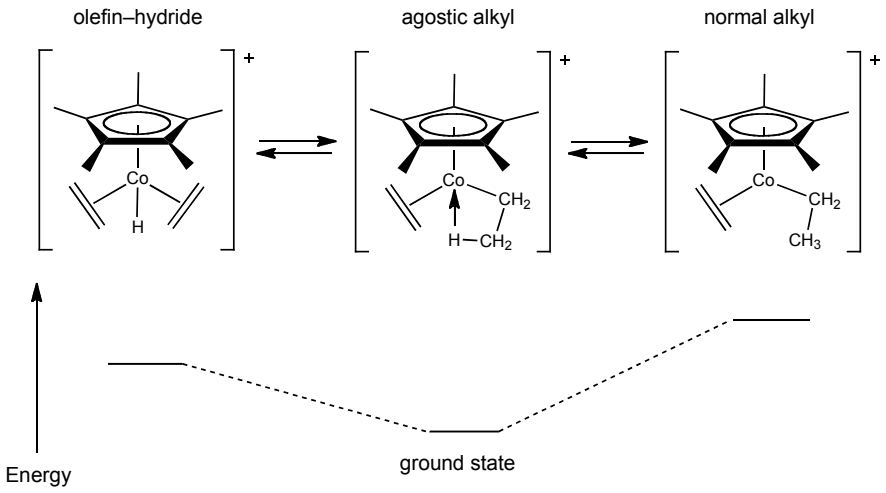

Figure 4.2 Dynamic equilibria present in Cp*Co(η^2-C_2H_4)(β–agostic-C_2H_5).

is an unusually low $^1J_{CH}$ value, which can range from 50–100 Hz, and an upfield shift of the agostic hydrogen atom. In general, agostic structures are favored for first and second row metals, especially cationic species or species possessing ligands that enhance the Lewis acidity of the metal center.

In organic chemistry, C–H bonds have been reported to coordinate carbocation centers to form a 3-center-2-electrons C–H–C bond.[17, 18] Unlike normal two-center covalent bonds, three-center bonds are flexible and can, in principle, exhibit a continuum of geometries ranging from "open" and linear to "closed" and acutely triangular (Figure 4.3). The open, linear system has no interaction between the terminal atoms, while the closed system has fully developed bonding between all

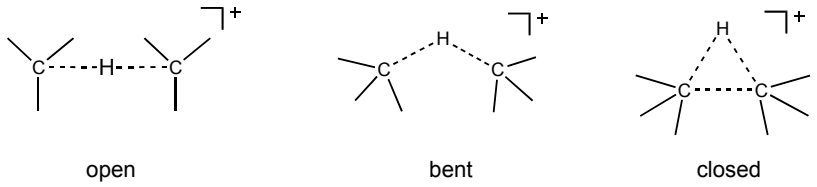

Figure 4.3 Geometries of a three-center, two-electron C–H–C bond.

three centers.[19] In between the two extremes lies a continuum of bent structures exhibiting varying degrees of bonding between the terminal atoms. As the three-center bond is bent, the chemical shift of the central hydrogen moves strongly upfield while the chemical shift of the bridgehead carbons moves proportionally downfield.

C–H hyperconjugation to low valent silicon centers was first observed by Reed and coworkers in their studies on the effect of alkyl substituents R on

$[R_3Si][CHB_{11}H_5Br_6]$ silyl cations.[20] For example, in the case of $[iPr_3Si][CHB_{11}H_5Br_6]$, the X-ray analysis shows a difference in the three isopropyl groups with respect to Si–C bond length and with respect to bond angles around their central carbon atoms. In particular, one of the Si–C bonds is shorter that the others and this carbon atom has the largest Si–C–C angle of ca. 120º. This value far exceeds the sp^3 ideal, and indeed, the carbon involved in the shortest Si–C bond is nearly planar. These data strongly suggest a C–H bond hyperconjugation between the σ_{C-H} donor orbital and the empty 3p orbital at silicon (Figure 4.4).

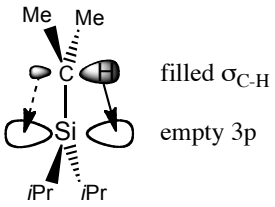

Figure 4.4 Molecular orbital description of a C–H bond hyperconjugative stabilization of triisopropylsilylium ion.

Ottosson and Cremer calculated the energetics and the ^{29}Si NMR shift of a series of silylium ions that could be stabilized by intramolecular C–H solvation (Figure 4.5).[21] The new feature of these molecules is that the C–H–Si agostic interaction is established between a carbon and a silicon atom that is not covalently bounded. The calculations suggest, in fact, that the C–H bonds are elongated and a slight shielding at the silicon occurs.

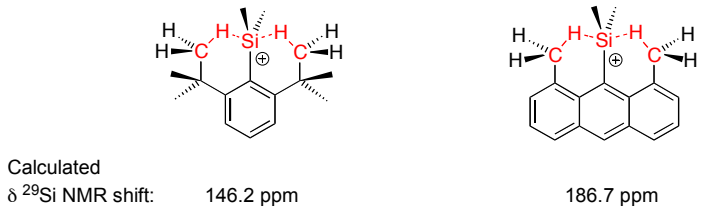

Figure 4.5 Calculated ^{29}Si NMR chemical shift of silylium ions stabilized by agostic interactions.

More suitable than C–H bonds for such interactions, Si–H bonds of silanes were envisioned as alternative ligands for low valent silicon species, such as silylium ions. Due to the higher lying σ-bonding orbital, the interaction with the empty 3p(Si) orbital is more favorable. Recently, many disilyl cations with symmetric Si–H–Si

bridges were synthesized.[22-25] The cations by Müller[8] and Nikonov,[26] shown in Figure 4.6, are representative examples of this class of compounds that features a high field-shifted resonaces in the ^{29}Si NMR, an indication that the Si–H→Si^{+} stabilization is too strong to lead to a free silylium ion. Agostic interactions between C–H bonds and a silyl cation could have a reduced stabilizing effect, therefore preserving the positive charge at the silicon center to a larger extent.

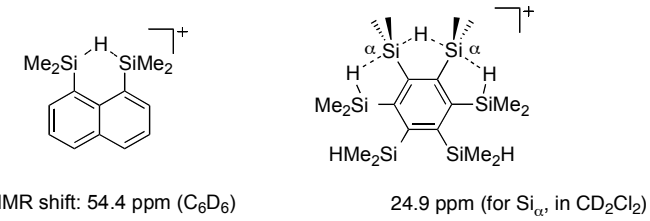

δ ^{29}Si NMR shift: 54.4 ppm (C_6D_6) 24.9 ppm (for Si_α, in CD_2Cl_2)

Figure 4.6 Silylium ions stabilized by Si–H agostic interactions.

4.2 Synthesis of Silylium Ions Bearing an Alkylated Phenyl Ring and Preliminary Interpretation of the Results

Cyclohexyl rings replacing the phenyl flanking rings were seen as good candidates to maintain steric shielding at silicon but exclude intramolecular interactions that reduce the Lewis acidity of the cation. The first synthetic target was identified in (2,4,6-tricyclohexylphenyl)silylium ion (**72**); this compound was synthetically more accessible than the analogous (2,6-tricyclohexylphenyl)silylium ion and the presence of an additional cyclohexyl ring at the *para* position of the arene was not expected to significantly influence the behavior of the silyl cation. The literature procedure for the Friedel–Crafts alkylation of benzene to obtain 1,3,5-tricyclohexylbenzene required an optimization of the isolation procedure. When the Friedel–Crafts reaction between benzene and cyclohexene was attepted,[27] a mixture of mono-, di-, tri- and tetra-alkylated products was obtained and the isolation of the desired compound was very challenging. The neat reaction between benzene and chlorocyclohexane, promoted by 0.5 equivalents of $AlCl_3$, afforded a mixture of mono-, tri- and tetra-substituted benzene that could be separated (Scheme 4.1).[28] A first bulb-to-bulb distillation allowed the removal of monocyclohexylbenzene, then treatment of the remaining mixture with acetone led to precipitation of 1,2,3,5-tetracyclohexyl-benzene. The

crude tricyclohexylbenzene **73** was finally purified by recrystallization from acetone. Monobromination of **73** afforded 2,4,6-tricyclohexylbromobenzene (**74**), which underwent lithiation and silylation to furnish silane **75**. Hydride abstraction using $[Ph_3C][B(C_6F_5)_4]$ provided a cationic species with a resonance of 163 ppm in ^{29}Si NMR spectroscopy. The resonance assignment of cation **72** in 1D and 2D NMR analyses proved to be particularly difficult: the ^{13}C NMR spectrum presents many signals that account for more than one species present in solution.

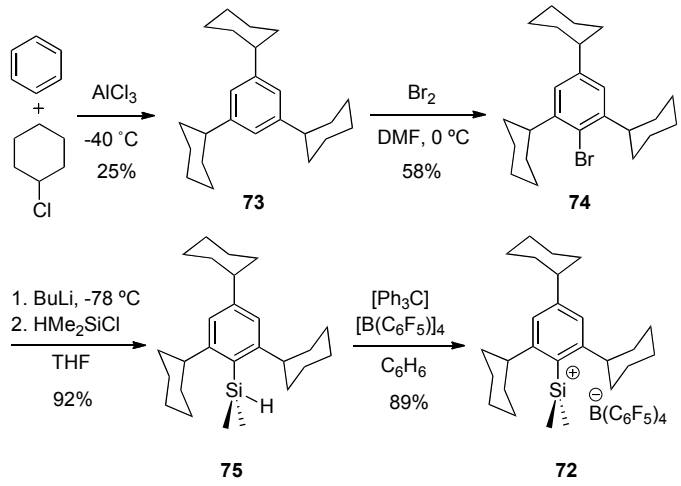

Scheme 4.1 Synthesis of (2,4,6-tricyclohexylphenyl)silylium ion.

Encouraged by the promising results obtained with cation **72**, we envisioned the possibility of substituting the cyclohexyl rings with isopropyl groups. The isopropyl groups were expected to ensure a similar steric bulk in proximity of the silicon center but could greatly simplify the NMR studies. The (2,4,6-triisopropylphenyl)silylium ion (**76**) was readily synthesized from the commercially available bromo–precursor **77** (Scheme 4.2).

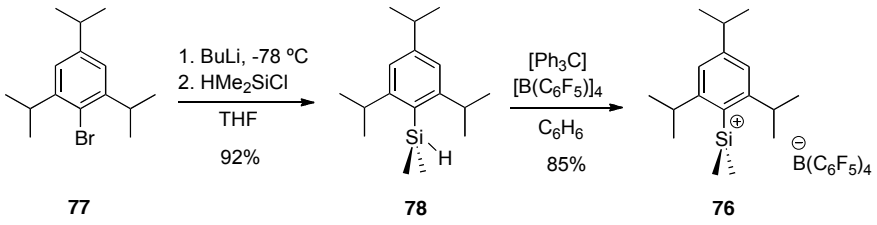

Scheme 4.2 Synthesis of (2,4,6-triisopropylphenyl)silylium ion.

Cation **76** showed an even more deshielded ^{29}Si NMR resonance at 221.2 ppm in addition to a signal at 97.0 ppm (in C_6D_6). The latter value could be compared to

the chemical shifts obtained for $[R_3Si–solvent]^+$ species;[29] therefore, it was attributed to the solvent complex of cation **76**. Comparison of the nuclei chemical shift in ^1H and ^{13}C NMR spectroscopy, between **78** and **76**, was used as indication of the electron density redistribution that takes place upon formation of the silyl cation. In cation **76** the electron density accumulates in the *ipso* position of the aromatic ring, as demonstrated by the shielding of C_b (Figure 4.7), and in the benzylic protons at the *ortho* substitutents (H_f), that in ^1H NMR are high field-shifted of 1.2 ppm with respect to the silane precursor. C_f experiences a significant buildup of positive charge (9.2 ppm low field–shifted compared to the silane), demonstrating that the *ortho* isopropyl groups are strongly perturbed by the formation of the cation.

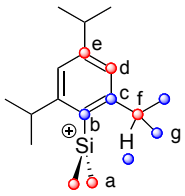

76

	Δ ^1H	Δ ^{13}C
a		+ 1.3
b		– 3.6
c		– 0.6
d		+ 2.4
e		+ 9.6
f	– 1.2	+ 9.2
g		– 0.9

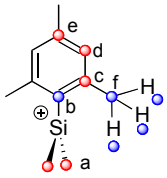

79

	Δ ^1H	Δ ^{13}C
a		+ 1.9
b		– 0.8
c		+ 0.6
d		+ 1.5
e		+ 11.3
f	– 0.4	– 0.4

● = δ (R_3Si^+ – R_3SiH) > 0
● = δ (R_3Si^+ – R_3SiH) < 0

Figure 4.7 ^1H and ^{13}C chemical shift comparison of significant nuclei of **76** (left) and **79** (right) with respect to the neutral silane precursors. Red dot, nuclei displaying buildup of positive charge; blue dot, nuclei displaying buildup of negative charge.

Analogous to cation **76**, (2,4,6-trimethylphenyl)silylium ion **79** was readily synthesized starting from the commercially available 2,4,6-trimethyl bromobenzene (Scheme 4.3). Cation **79** showed a clean resonance in the ^{29}Si NMR spectrum at 225.4

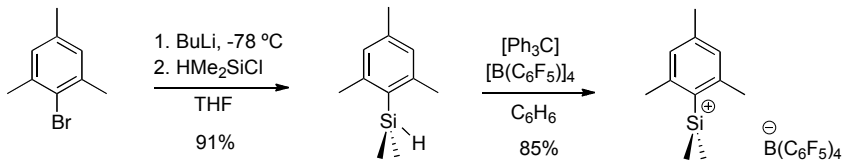

80 **79**

Scheme 4.3 Synthesis of (2,4,6-trimethylphenyl)silylium ion.

ppm. The striking feature of this molecule rested in the fact that almost no solvent coordination was observed, while, in the case of the more hindered cation **76**, one of the two species detected in solution was considered to be a silylium ion–solvent

complex. Looking at the ^{1}H and ^{13}C chemical shift comparison between silylium ion **79** and silane **80**, a similar charge redistribution as in cation **76** could be observed for the benzene ring, while the resonances of the *ortho* methyl groups were only slightly upfield shifted after the formation of the cation (Figure 4.7).

Puzzled by the different behavior of the isopropyl *ortho* substituents in cation **76** compared to the methyl *ortho* substituents in **79**, we investigated whether these groups were effectively participating in the stabilization of the positively charged silicon *via* an agostic interaction, or whether the electron density redistribution measured by NMR spectroscopy was dictated only by inductive effects. Features that are observed in presence of a C–H→metal agostic interaction and that can be taken as reference for the study of C–H→Si interactions include the presence of a $^{1}J_{Si–H}$ coupling constant with magnitude higher than 20 Hz, chemical shift of agostic hydrogen atoms upfield of the uncoordinated groups, and low $^{1}J_{C–H}$ coupling constant, from 70 to 100 Hz.[14, 30] The benzylic proton at the *ortho* position of **76** are upfield shifted compared to the silane; furthermore, the $^{1}J_{C–H}$ coupling constant of the benzylic proton at the *ortho* position is 116 Hz, while the one of the benzylic proton in *para* is 128 Hz.[2] The measurement of an eventual $^{1}J_{Si–H}$ coupling was performed *via* ^{29}Si NMR with ^{1}H single frequency decoupling from the methyl groups on silicon, at temperature as low as –60ºC: the silicon peak at 221.2 ppm appeared slightly broad but no splitting was detected. Compound **79** presents only a slight upfield shift of the benzylic protons in *ortho*, and no difference in $^{1}J_{C–H}$ coupling constant for the *ortho* and the *para* methyl groups.

Calculations at the density functional theory level predict an interaction between one of the *ortho* benzylic protons and the silicon nucleus in cation **76**. As depicted in Figure 4.8, the cation assumes a C_s symmetric geometry with Si1 distorted toward H1 and an elongated C1–H1 bond of 1.166 Å, 0.06Å longer than C2–H2. The steric hindrance of the isopropyl substituents forces the methyl groups at silicon into a perpendicular geometry with respect to the phenyl ring; this conformation suppresses the overlap between the aromatic π-orbitals and the empty 3p(Si) orbital and directs the empty silicon orbital toward the benzylic protons, which behave as ligands by virtue of the formation of a 3-center-2-electron covalent bond. The most stable structure calculated for cation **79** does not account for any specific C–H→Si

[2] $^{1}J_{C–H}$ coupling constants were measured by a proton coupled ^{13}C NMR experiment.

interaction; furthermore, the empty silicon orbital is almost parallel to the aromatic ring and can participate to π-conjugation (Figure 4.8).

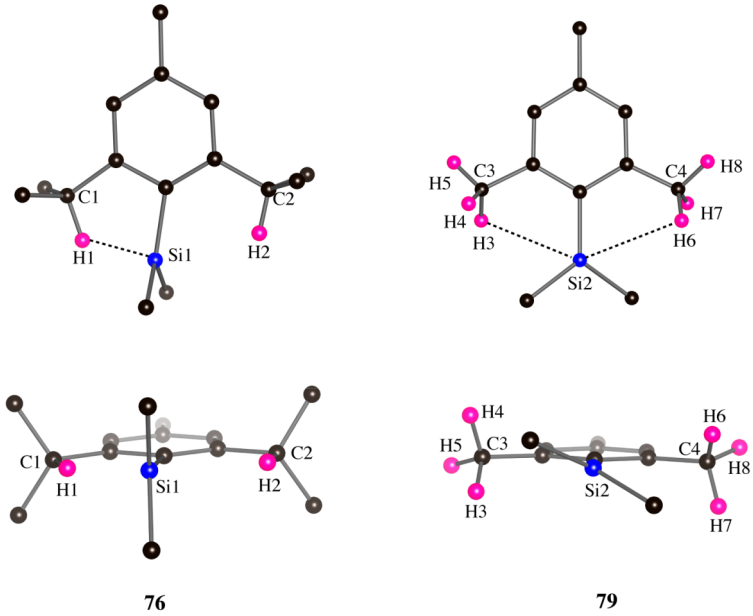

Figure 4.8 Calculated structures of silylium ions **76** (left) and **79** (right). View from the front (top), view through Si–C(aryl) bond (bottom). Selected distances (Å): Si1–H1 1.883, C1–H1 1.166, Si–H2 2.677, C2–H2 1.107, Si2–H3 2.957, C3–H3 1.093, Si2–H6 2.958, C4–H6 1.093.

Compounds **76** and **79** possess a few significant, different features. In cation **76**, both NMR and computational studies suggest the presence of a C–H–Si agostic interaction; furthermore, the free silylium ion is formed along with another species, probably the corresponding cation–solvent complex. Cation **79**, though offering less steric protection in the proximity of silicon, is formed cleanly as a single species and does not present signals for solvent or anion complexes. Moreover, the methyl groups in the *ortho* positions are not interacting with the positive silicon center. These differences in the behavior of compounds with a very similar skeleton cannot be easily explained. Undoubtedly, compounds **76** and **79** represent a challenging but promising field of investigation because they can be readily synthesized and afford very dishielded cations, with ^{29}Si NMR resonances in the region of truly tricordinated silylium ions.

4.3 NMR Studies and Revisited Structures of Cations 76 and 79

Independently, the group of Prof. Thomas Müller in Oldenburg, Germany, investigated the reactivity of cations **76** and **79** and suggested the possibility of a rearrangement of these silylium ions into more stable structures. The observation that **79** is a fairly stable silylium ion (it can be stored for several days in solution at room temperature, under inert atmosphere), does not experience solvent effects (δ^{29}Si in C_6D_6: 225.5 ppm; in toluene-d_8: 225.9 ppm), and shows almost no coordination to the solvent in the region of 80–100 ppm of the ^{29}Si NMR spectrum is, in fact, incongruent with its naked skeleton. Müller and coworkers propose that ligand redistribution takes place at silylium ion **79** to afford trimesitylsilylium ion **81** (Scheme 4.4).

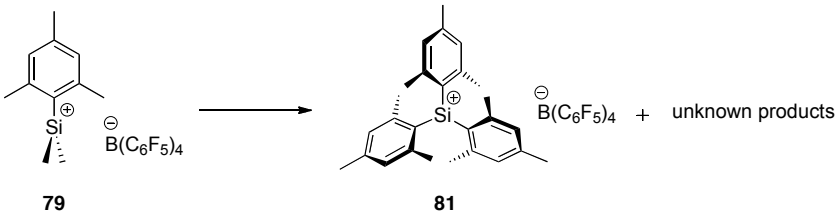

79 **81**

Scheme 4.4 Proposed decomposition pathway of silylium ion **79**.

We decided to further investigate our preliminary results reported in 4.2, performing NMR analyses aimed to identify the skeleton of cation **76** and **79**. Henceforth, **76** and **79** will be considered as reactive intermediates, because many contradictions regarding their prolonged existence in solution have appeared, both from our analysis and from the considerations in the Müller group. At first, we focused on cation **79**, whose ^{29}Si NMR spectrum accounts for one main species in solution (Figure 4.9). In order to obtain quantitative information from the integration of the silicon peaks, an inverse gated ^{29}Si NMR measurement was performed.[31] A normal broadband-decoupled ^{29}Si spectrum is not susceptible of quantitative analysis because the Nuclear Overhauser Enhancement (NOE) varies among the ^{29}Si nuclei, and the signal intensities vary accordingly. In the case of an inverse gated experiment, the ^{1}H broadband decoupling is "gated" (switched) on only during the ^{29}Si pulse and the acquisition period; it is gated off during the pulse delay period (*d*1). The NOE, a slow process, builds up only slightly during the pulse and acquisition period.

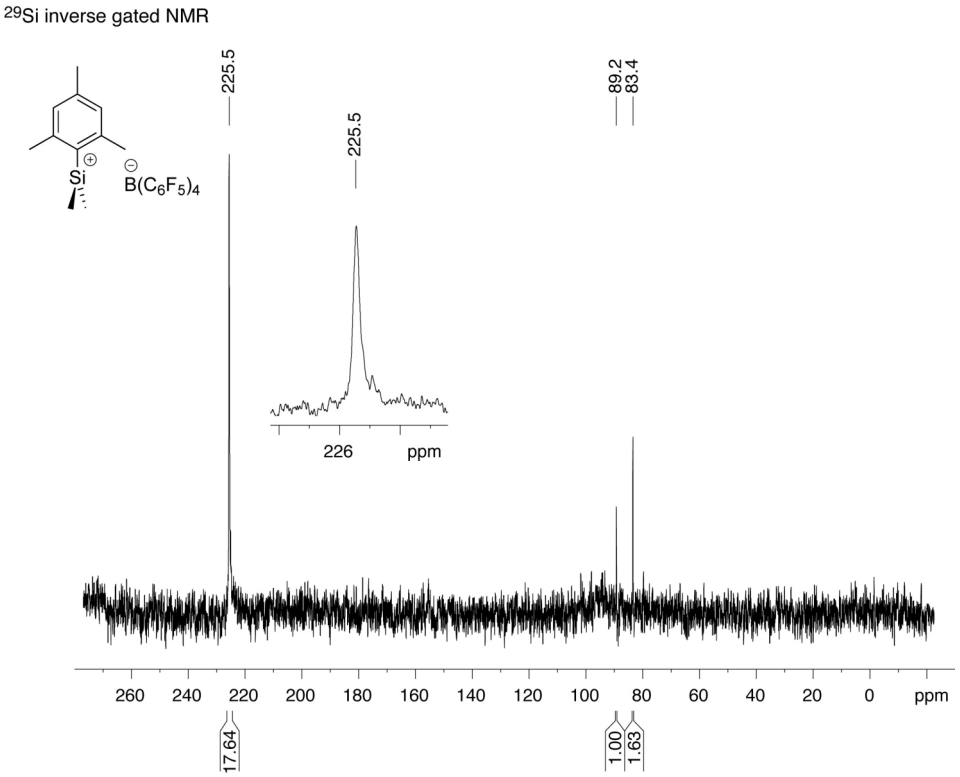

Figure 4.9 ^{29}Si inverse gated NMR spectroscopy of putative cation **79**. Solvent: C_6D_6; counterion: $B(C_6F_5)_4^-$.

Decoupling, a fast process, is established almost immediately upon irradiating with the ^{1}H broadband decoupler, so that the end result is a number of singlets whose intensities are proportional to the number of silicon atoms they represent. Of course, loss of part of the NOE means many repetitions to build up the signal intensity. A second factor that affects a quantitative analysis is the achievement of the full amplitude of the silicon signals. The ^{29}Si nucleus has a long longitudinal relaxation time (T_1); in order to obtain quantitative data, it is necessary to allow for the full longitudinal relaxation of the nuclei in the sample.[32] Failure to do so results in a saturation of the excited state population and may alter the signal. To avoid this, the interpulse delay in standard inverse-gated NMR methods is set to a value > 5•T_1.[33] In the case of the ^{29}Si nucleus, T_1 can be as long as 70 s in liquid samples. The relaxation delay ($d1$) must be set according to the T_1 of the signal of interest and, for the ^{29}Si inverse gated measurement reported here it was set to 10 sec.[34] The species that resonates at 225.5 ppm accounts for 87 mol % of the silicon-containing products (it is assumed that multi silyl species are not formed). The ^{1}H NMR spectrum of the putative cation **79** shows a methyl signal at –0.16 ppm that, at first, was attributed to the methyl substituents (a) at silicon (Figure 4.10).

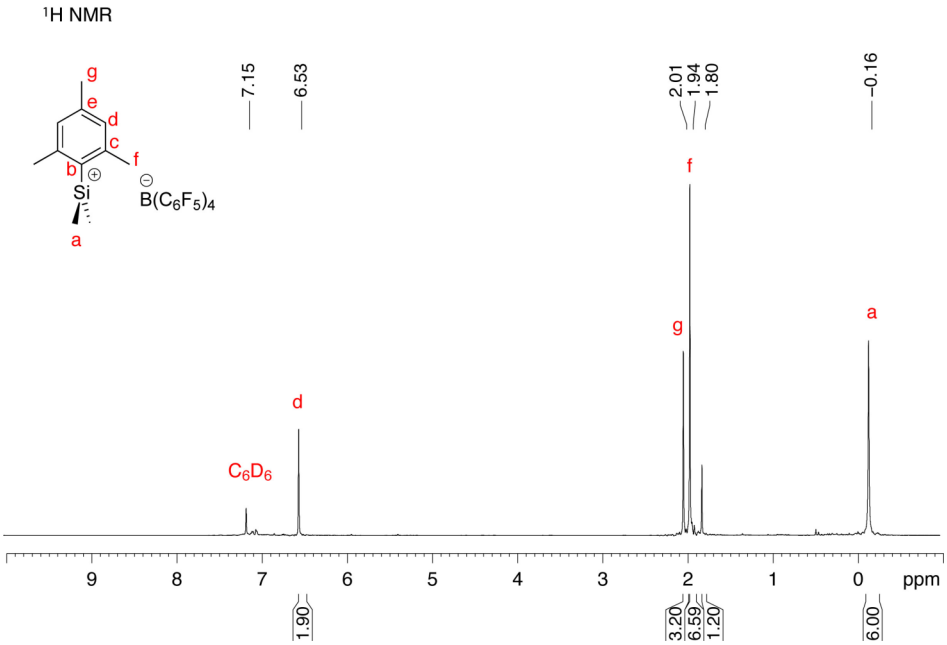

Figure 4.10 ^{1}H NMR spectroscopy of putative cation **79**. Solvent: C_6D_6; counterion: $B(C_6F_5)_4^-$.

Measurement of ^{1}H, ^{29}Si–HMBC NMR was performed in order to detect whether the methyl groups at –0.16 ppm were effectively bounded to the main silicon species (Figure 4.11). The HMBC (Heteronuclear Multple Bond Coherence) experiment suppresses correlations via $^{1}J_{Si,H}$ but preserves the correlations via $^{2}J_{Si,H}$ and $^{3}J_{Si,H}$.[31, 34] Interpretations of HMBCs requires a degree of flexibility because, whereas two-bond correlations ($^{2}J_{Si,H}$) are almost always found, the three-bond ($^{3}J_{Si,H}$) are occasionally absent. The variation in correlations that we find results from the variations in the magnitude of $^{2}J_{Si,H}$ and $^{3}J_{Si,H}$ coupling constants. The result of this analysis on the putative compound **79** shows that the silicon signals at 83.4 and 89.2 ppm are correlated to minor signals in the ^{1}H NMR; the proton signal for the methyl groups at –0.16 ppm is correlated to a silicon signal in the region of 160 ppm, that was not detected in the ^{29}Si inverse gated experiment. The silicon peak of major interest, at 225.5 ppm, is correlated to the aromatic protons and to the methyl groups identified as the *ortho* protons (f) in **79** (Figure 4.12).

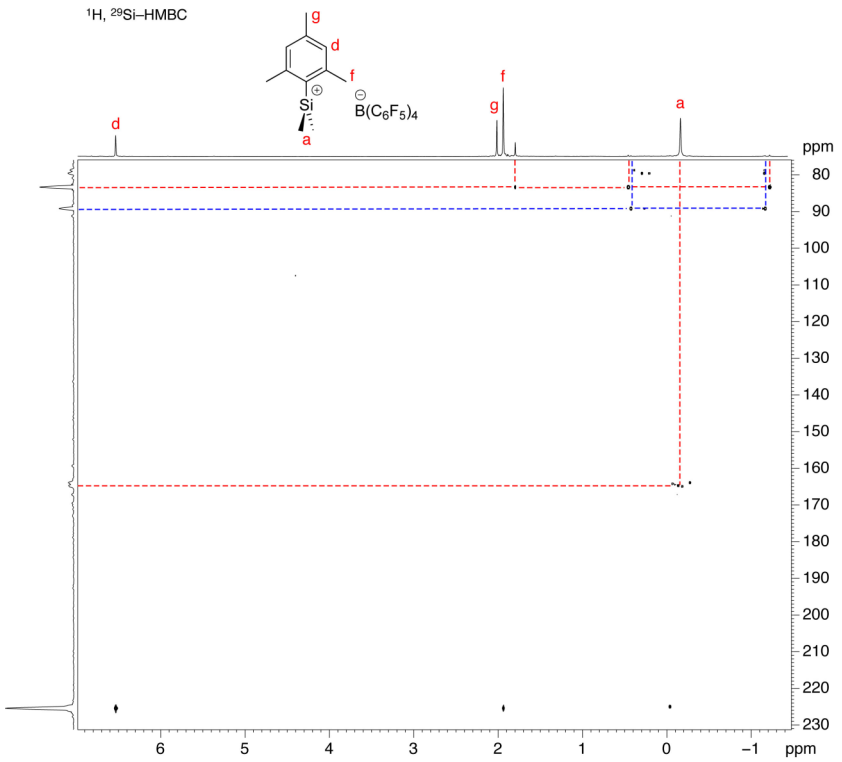

Figure 4.11 ^{1}H, ^{29}Si-HMBC spectroscopy of **79**. Solvent: C_6D_6; counterion: $B(C_6F_5)_4^-$.

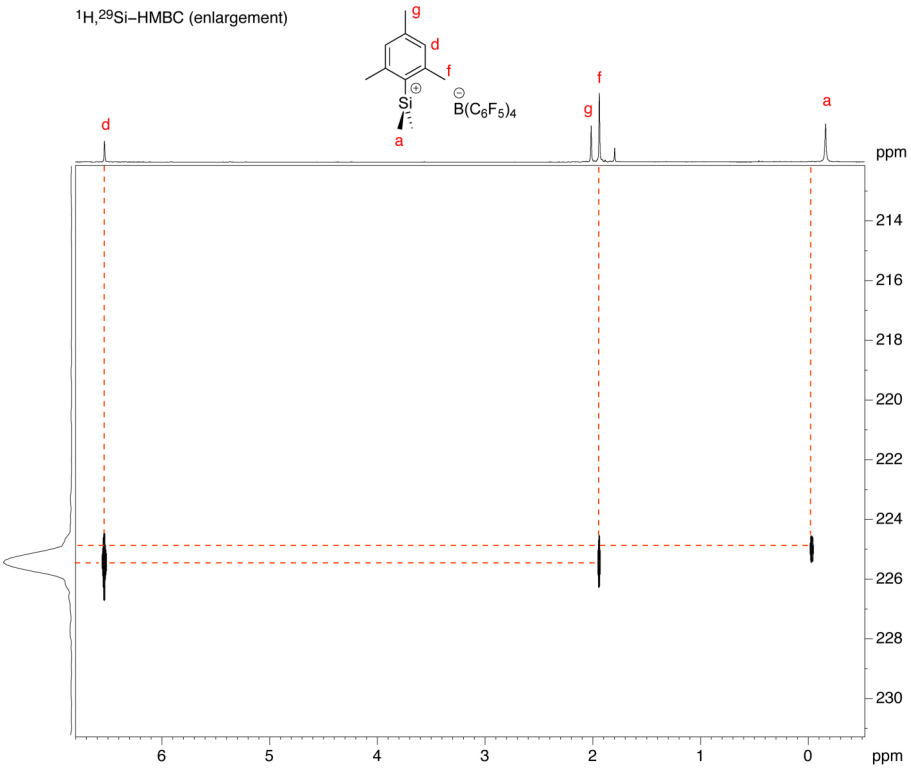

Figure 4.12 Enlargement of ^{1}H, ^{29}Si-HMBC spectroscopy of **79**. Solvent: C_6D_6; counterion: $B(C_6F_5)_4^-$.

The presence of these cross peaks indicates that, in this molecule, the ^{1}H–^{29}Si correlation can be detected up to a distance of 4 covalent bonds. Therefore, if the methyl groups (a) are covalently bond to silicon, a cross peak should be observed. The information gained with the ^{1}H, ^{29}Si–HMBC NMR experiments could be further supported by the analysis of the ^{1}H, ^{13}C–HMBC heterocorrelation. Silylium ion **42** was compared to **79** (Figure 4.13); in the case of cation **42**, the methyl groups at silicon (a) give rise to a cross peak with the aromatic carbon atom (C_b), while in the case of cation **79**, no cross peak with any aromatic carbon atom is detected.

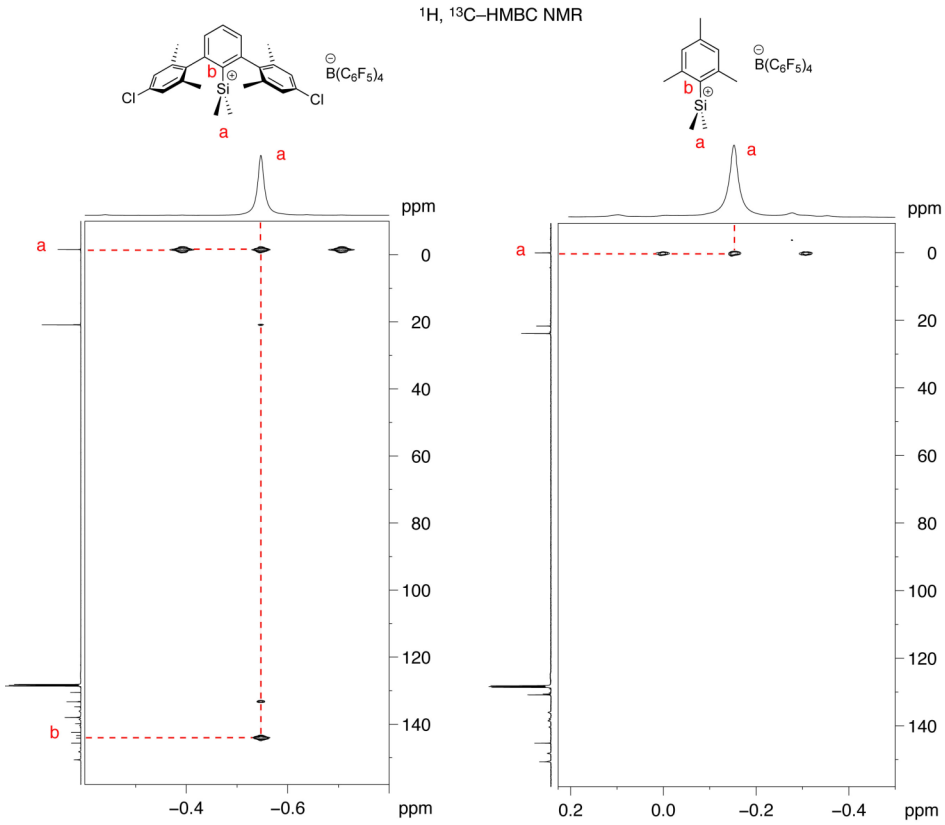

Figure 4.13 ^{1}H, ^{13}C–HMBC NMR spectra of compound **42** (left) and putative cation **79** (right). Measurements performed in C_6D_6.

In light of these NMR results, we agree with the theory proposed by the Müller group. The formation of the unstable cation **79** is determined by the detection of one of the metathesis product, *i.e.*, triphenylmethane, and of a low field-shifted silicon species. Once silylium ion **79** is formed, it readily decomposes because of its extreme lability. Surprisingly, none of the known mechanisms of decomposition, *i.e.* hydride and fluoride abstraction, takes place, neither solvent coordination can pacify this species.

We also investigated the behavior of cation **76** *via* NMR spectroscopy studies to gain information about its reactivity and eventual decomposition pathways. ^{1}H NMR shows the presence of a typical resonance for methyl groups (a) bound to a silicon nucleus (Figure 4.14). The ^{29}Si inverse gated NMR spectrum shows the presence of two main species in solution in an approximate 1: 1 ratio, with resonances of 97.0 and 221.2 ppm (Figure 4.15). The ^{29}Si chemical shift of the signal at 97.0 ppm could account for a trialkylsilyl cation coordinated by the solvent or the counterion, such as $Me_3Si–C_6D_6$ or $Me_3Si–B(C_6F_5)_4$.[29, 35] The very low field-shifted ^{29}Si resonance at 221.2 ppm is indicative of a species with free silylium ion character, analogous to trimesitylsilylium ion **81**.

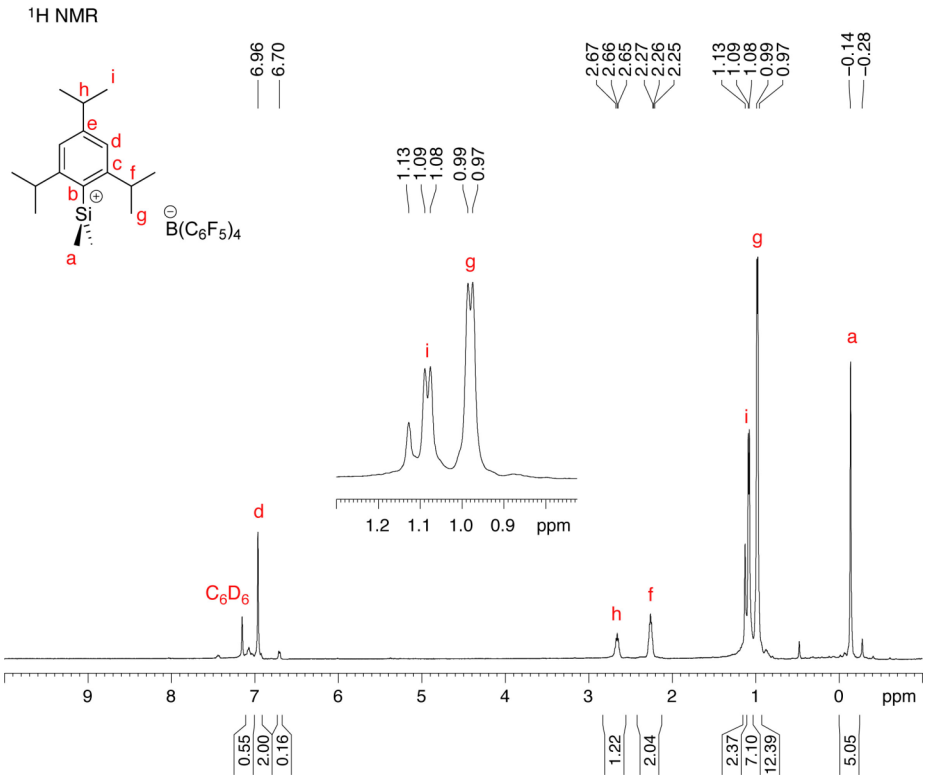

Figure 4.14 ^{1}H NMR spectroscopy of putative cation **76**. Solvent: C_6D_6; counterion: $B(C_6F_5)_4^-$.

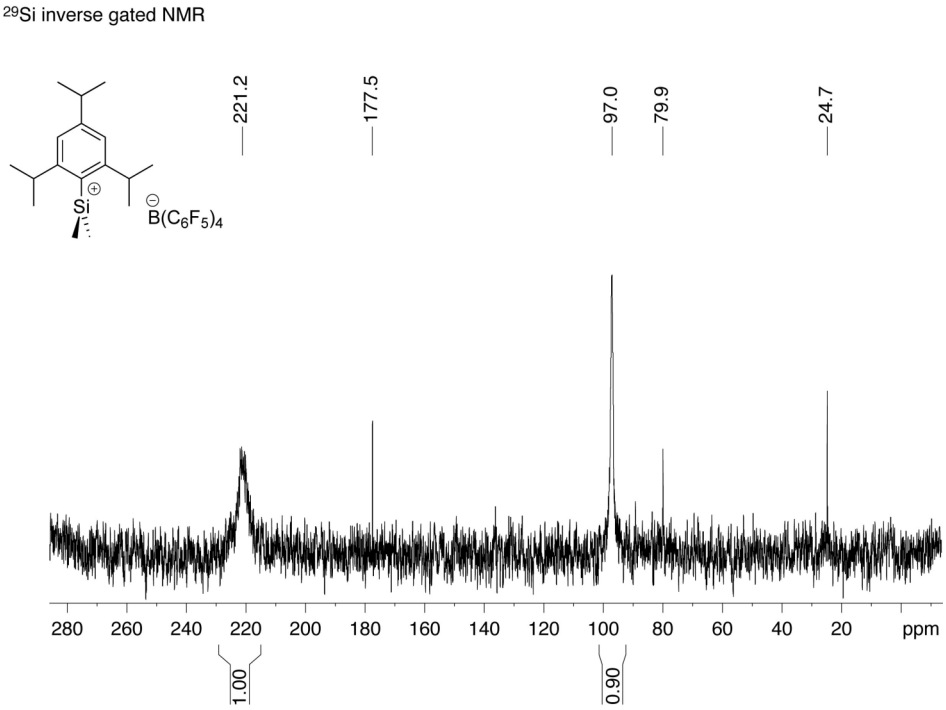

Figure 4.15 ^{29}Si inverse gated NMR spectroscopy of **76**. Solvent: C_6D_6; counterion: $B(C_6F_5)_4^-$

^{1}H, ^{29}Si–HMBC NMR spectroscopy revealed that the methyl groups (a) in **76** are correlated to the ^{29}Si signal at 97.0 ppm (Figure 4.16); on the contrary, no correlation between any proton and the low field-shifted ^{29}Si signal was observed. The latter result cannot exclude that the low field shifted silicon is part of the aromatic skeleton of the molecule; a ^{1}H,^{29}Si–HMBC experiment uses the polarization transfer from protons to silicon and, in the case of a long range transfer, the signal for this heterocorrelation might not appear. Nevertheless, the integrity of the aromatic skeleton of the putative cation **76** could be confirmed by a ^{1}H NOE NMR experiment.[31, 36] ^{1}H–^{1}H proximity within a molecule can be detected by means of the trough-space nuclear Overhauser effect, over a distance of up to about 4 Å (for example, the distance between 1,3-diaxial protons in the chair conformation of cyclohexane is ≈ 2.6 Å). The experiment involves a weak irradiation of one nucleus with a frequency ν_1 and the detection of the effect on a different nucleus with a ν_2 pulse. Polarization — that is, a change in population of the energy levels — by the weak ν_1 irradiation results, through space, in an increase in the population of the energy level in the nearby non-irradiated protons. This excess population undergoes T_1 relaxation to a lower level, thereby increasing the signal intensity of the nearby proton(s).

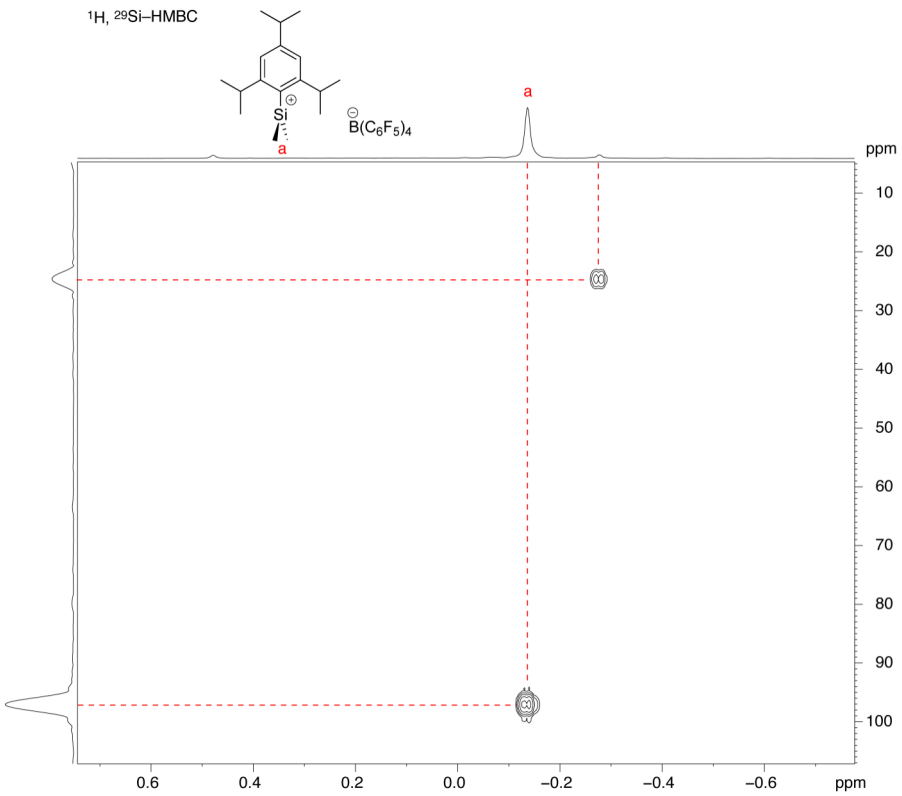

Figure 4.16 ^{1}H, ^{29}Si-HMBC spectroscopy of **76**. Solvent: C_6D_6; counterion: $B(C_6F_5)_4^-$.

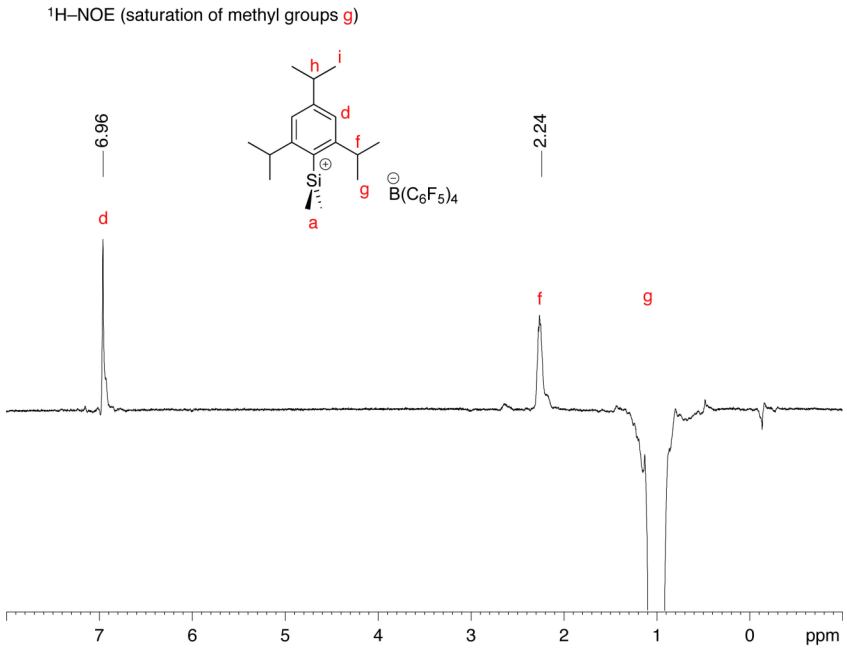

Figure 4.17 ^{1}H NOE NMR spectroscopy of putative cation **76**. Solvent: C_6D_6; counterion: $B(C_6F_5)_4^-$. Saturation of the *ortho* methyl groups (g).

In the case of cation **76**, upon irradiation of the *ortho* methyl groups (g), both H_f and H_d were enhanced (Figure 4.17); in a second experiment, H_a was irradiated, but no enhancement of any protons in the aromatic core could be observed.

Based on these data we can hypothesize that cation **76** undergoes ligand redistribution to afford tris(triisopropylphenyl)silylium ion **82** and trimethyl silyl cation **83** (Scheme 4.5). In agreement with this hypothesis, the Müller group obtained crystals displaying the structure of $[Me_3Si–toluene][B(C_6F_5)_4]$ silyl arenium ions from the reaction mixture of tri(isopropylphenyl)silane **78** and $[Ph_3C][B(C_6F_5)_4]$ in toluene.[3]

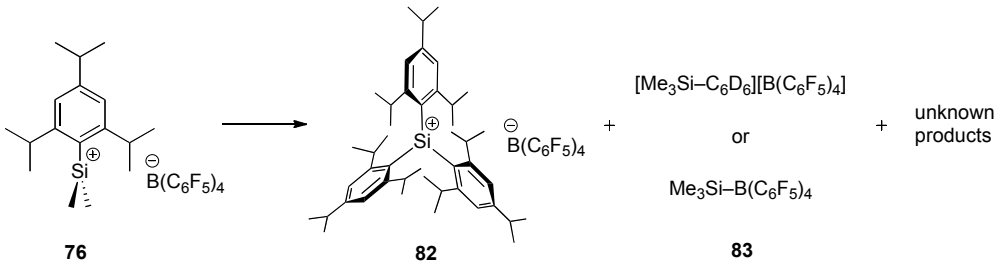

Scheme 4.5 Proposed decomposition pathway of silylium ion **76**.

The mechanism for the transformation of the transient cations **79** and **76** into silylium ions **81** and **82** is still unknown; further investigations are required to better understand this new type of reactivity. While silylium ion **82** is formed in concomitance with another cationic species, the formation of trimesitylsilylium ion **81** occurs quite cleanly. When compared to the synthesis of **81** reported by Lambert and Zhao,[37] the rearrangement just disclosed by the Müller and the Siegel groups definitely represents an appealing synthetic alternative. The initial goal of obtaining a "free and naked" silylium ion was not successful because of the extremely high reactivity of the transient cations **76** and **79**. These results reinforce the idea that a free silylium ion requires a delicate balance of steric and electronic stabilization to avoid anion or solvent coordination, or decomposition pathways. While π(arene)– and halogen–coordination to silylium ions are effective intramolecular mechanisms of stabilization, C–H–Si agostic interactions, instead, are not sufficient to eliminate intermolecular complexation or even decomposition processes. To date, the best

[3] Unpublished results from the Müller group.

example of a purely tricoordinate silyl cation still remains the trimesitylsilylium ion first synthesized by Lambert in Zhao in 1997.[37]

4.4 References

1. Kato, T.; Reed, C. A., *Angew. Chem. Int. Ed.* **2004**, *43*, 2908.
2. Reed, C. A., *Acc. Chem. Res.* **1998**, *31*, 325.
3. Kochina, T. A.; Vrazhnov, D. V.; Sinotova, E. V.; Vorokov, M. G., *Usp. Khim.* **2006**, *75*, 107.
4. Kutzelnigg, W., *Angew. Chem. Int. Ed.* **1984**, *23*, 272.
5. Kim, K. C.; Reed, C. A.; Elliott, D. W.; Mueller, L. J.; Tham, F.; Lin, L. J.; Lambert, J. B., *Science* **2002**, *297*, 825.
6. Lambert, J. B.; Zhang, S. H.; Stern, C. L.; Huffman, J. C., *Science* **1993,** *260*, 1917.
7. Müller, T.; Bauch, C.; Ostermeier, M.; Bolte, M.; Auner, N., *J. Am. Chem. Soc.* **2003**, *125*, 2158.
8. Panisch, R.; Bolte, M.; Muller, T., *J. Am. Chem. Soc.* **2006**, *128*, 9676.
9. Duttwyler, S.; Do, Q. Q.; Linden, A.; Baldridge, K. K.; Siegel, J. S., *Angew. Chem. Int. Ed.* **2008**, *47*, 1719.
10. Klare, H. F. T.; Bergander, K.; Oestreich, M., *Angew. Chem. Int. Ed.* **2009**, *48*, 9077.
11. Romanato, P.; Duttwyler, S.; Linden, A.; Baldridge, K. K.; Siegel, J. S., *J. Am. Chem. Soc.* **2010**, *132*, 7828.
12. Parkin, G.; Bunel, E.; Burger, B. J.; Trimmer, M. S.; Vanasselt, A.; Bercaw, J. E., *J. Mol. Catal.* **1987**, *41* (1-2), 21.
13. Brookhart, M.; Green, M. L. H.; Pardy, R. B. A., *J. Chem. Soc. Chem. Commun.* **1983**, 691.
14. Brookhart, M.; Green, M. L. H.; Parkin, G., *Proc. Natl. Acad. Sci. U. S. A.* **2007**, *104*, 6908.
15. Brookhart, M.; Green, M. L. H., *J. Organomet. Chem.* **1983**, *250*, 395.
16. Brookhart, M.; Green, M. L. H.; Wong, L. L., *Prog. Inorg. Chem.* **1988**, *36*, 1.
17. McMurry, J. E.; Lectka, T., *J. Am. Chem. Soc.* **1993**, *115*, 10167.

18. Sorensen, T. S.; Whitworth, S. M., *J. Am. Chem. Soc.* **1990**, *112*, 8135.
19. Bau, R.; Teller, R. G.; Kirtley, S. W.; Koetzle, T. F., *Acc. Chem. Res.* **1979**, *12*, 176.
20. Xie, Z. W.; Bau, R.; Benesi, A.; Reed, C. A., *Organometallics* **1995**, *14*, 3933.
21. Ottosson, C. H.; Cremer, D., *Organometallics* **1996**, *15*, 5309.
22. Müller, T., *Angew. Chem. Int. Ed.* **2001**, *40*, 3033.
23. Sekiguchi, A.; Murakami, Y.; Fukaya, N.; Kabe, Y., *Chem. Lett.* **2004**, *33*, 530.
24. Lickiss, P. D.; Masangane, P. C.; Sohal, W.; Veneziani, G. L., *Organosilicon Chemistry V*. Wiley-VCH: New York, 2003.
25. Hoffmann, S. P.; Kato, T.; Tham, F. S.; Reed, C. A., *Chem. Commun.* **2006**, 767.
26. Khalimon, A. Y.; Lin, Z. H.; Simionescu, R.; Vyboishchikov, S. F.; Nikonov, G. I., *Angew. Chem. Int. Ed.* **2007**, *46*, 4530.
27. Corson, B. B.; Ipatieff, V. N., *J. Am. Chem. Soc.* **1937**, *59*, 645-647.
28. Mague, J. T.; Linhardt, L.; Medina, I.; Sattler, D. J.; Fink, M. J., *Acta Crystallogr., Sect. E: Struct. Rep. Online* **2008**, *64*, 375.
29. Lambert, J. B.; Zhang, S. Z.; Ciro, S. M., *Organometallics* **1994,** *13* (6), 2430.
30. Dubberley, S. R.; Ignatov, S. K.; Rees, N. H.; Razuvaev, A. G.; Mountford, P.; Nikonov, G. I., *J. Am. Chem. Soc.* **2003**, *125*, 642.
31. Silverstein, R. M.; Webster, F., X., *Spectrometric Identification of Organic Compounds*. Wiley: New York, 1997.
32. Delak, K. M.; Farrar, T. C.; Sahai, N., *J. Non-Cryst. Solids* **2005**, *351* (27-29), 2244.
33. Claridge, T. D. W., *High Resolution NMR Techniques in Organic Chemistry*. Pergamon: Amsterdam, 1999.
34. Braun, S.; Kalinowski, H.-O.; Berger, S., *150 and More Basic NMR Experiments*. Wiley-VCH: New York, 1996.
35. Küppers, T.; Bernhardt, E.; Eujen, R.; Willner, H.; Lehmann, C. W., *Angew. Chem. Int. Ed.* **2007**, *46*, 6346.
36. Bovey, F. A.; Jelinski, L.; Mirau, P. A., *Nuclear Magnetic Resoanance Spectoscopy, Second Edition*. Academic Press: 1988.
37. Lambert, J. B.; Zhao, Y., *Angew. Chem. Int. Ed.* **1997**, *36*, 400.

5 Experimental Section

5.1 General Data

5.1.1 Nomenclature

The terphenyl compounds containing triazene or iodo subsituents at the central ring were named according to the IUPAC nomenclature recommendations for terphenyls. The general atom numbering is shown in Figure 5.1.

The neutral silicon–containing compounds were named as silanes. This is not in accord with the IUPAC nomenclature for organic molecules, which would classify them as silylterphenyls due to the usual role of $–SiR_3$ as auxiliary groups in synthetic organic chemistry. The decision to name the neutral silicon–containing compounds as silanes can be justify by the central part that the $–SiR_3$ groups played in this project. The atom numbering used in the NMR characterization is shown in Figure 5.1.

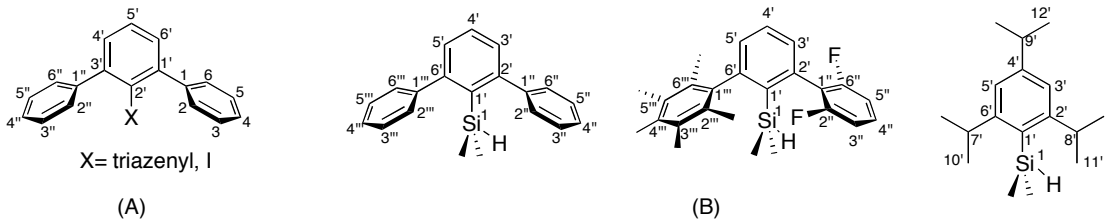

Figure 5.1 Atom numbering of triazenylterphenyls/ iodoterphenyls (A) and silanes/silylium ions (B).

5.1.2 Reaction Conditions and Reagents

Reactions in which inert atmosphere was required, were carried out under N_2. A dry N_2 atmosphere was used for the silylium ions syntesis in the glovebox (O_2 < 1 ppm, H_2O < 1 ppm). Glassware for moisture-sensitive reactions was dried at 150˚C for at least 2 hrs and allowed to cool in vacuum or under N_2 stream.

Tetrahydrofuran, toluene, Et_2O, CH_2Cl_2 used for reactions were purified by being passed through aluminium oxide in a MBraun solvent purification system. Acetonitrile was purified by distillation on CaH_2. For work-up and purification, distilled solvents of technical grade were used. Table 1 lists grades and suppliers of the chemicals used for reactions.

For glove box use, all the solvents were purified and degassed. THF, toluene, Et_2O, CH_2Cl_2 were purified by the MBraun solvent purification system. Acetonitrile was distilled from CaH_2, $CDCl_3$ from P_2O_5, C_6D_6 and toluene-d_8 from CaH_2; hexane, pentane, benzene, toluene, chlorobenzene were first washed with conc. H_2SO_4, then with H_2O and $NaHCO_3$ and finally distilled from Na/acetophenone or CaH_2; other deuterated solvents were dried over activated 3Å molecular sieves.

Table 5.1 Quality and suppliers of chemicals/solvents used for synthesis and analysis.

Compound	*Quality*	*Supplier*
Acetonitrile-d_3	99.5	Armar
Benzene-d_6	99.5	Armar
Boron trichloride in hexane	1.0	Aldrich
Bromopentafluorobenzene	99.0	Alfa Aesar
n-Butyllithium in hexane	1.6 M	Aldrich
sec-Butyllithium in cyclohexane	1.4 M	Aldrich
Chlorobenzene-d_5	99%	Armar
Chlorodimethylsilane	96%	Acros
2,6-Dibromoaniline	96%	ChemPacific
m-Difluorobenzene	99.0	Fluorochem
Hydrogen fluoride-pyridine	65-70%	Acros
Iodine monochloride in DCM	1.0 M	Acros
Toluene-d_8	99.5	Armar

5.1.3 Characterization

Melting Points were determined using a heating microscope from Christoffel Labor and Betriebstechnik and are uncorrected.

Infrared Spectra were recorded on a Perkin-Elmer Spectrum One FT-IR spectrophotometer. Compounds were measured as KBr pellets (solids) or as film between NaCl plates (oils). Absorption bands are given in wave numbers (cm^{-1}), and the intensities are characterized as follows: *s* = strong (0–33% transmission), *m* = medium (34–66% transmission), *w* = weak (67–100% transmission).

NMR Spectra were recorded on Bruker AV-300, Bruker AV-400, Bruker AV-500, Bruker ARX-500 instruments. The signals were referenced against solvent peaks (^{1}H: residual $CHCl_3$ 7.25 ppm, residual C_6HD_5 7.16 ppm; ^{13}C: $CDCl_3$ 77.0 ppm, C_6D_6 128.0 ppm) or external standards (^{29}Si: $SiMe_4$ 0 ppm; ^{19}F: CCl_3F 0 ppm). Data are reported as follows: chemical shift in ppm, multiplicity (*s* = singulet, *d* = doublet, *t* = triplet, *q* = quadruplet, *m* = multiplet, *dd* = doublet of doublet, *dt* = doublet of triplet, etc.), coupling constant ^{n}J in Hz, integration and interpretation.

Mass Spectra were recorded on a HP 5809 GC-MS instrument (EI, 70 eV). Data are reported as follows: *m*/*z*, % relative intensity and possible fragments.

X-Ray structure analyses were carried out by the Laboratorium für Computerchemie und Roentgenstrukturanalyse of the Organisch-chemisches Institut of the University of Zurich. A Nonius KappaCCD diffractometer with Mo*K*α radiation (λ = 0.71037 Å) was used.

5.2 Syntheses

5.2.1 2'-azopyrrolidine-2,6,2'',6''-tetrafluoro-1,1':3'1''-terphenyl (23)

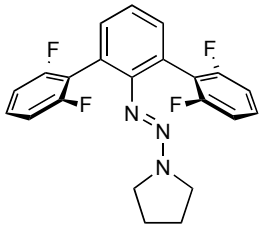

Chemical Formula: $C_{22}H_{17}F_4N_3$
Molecular Weight: 399.384

Under an inert atmosphere of N_2, *m*-difluorobenzene (9.0 mmol, 3 equiv.) was dissolved in THF (120 ml) and the mixture was cooled to – 78 ˚C. *n*-Butyllithium (1.6 M in hexane, 9.3 mmol, 3.1 equiv.) was added dropwise and the mixture was stirred at the same temperature for 1 h. Zinc chloride (10.5 mmol, 3.5 equiv.) in 20 ml THF was added to the reaction mixture. The mixture was stirred for 1 h at –78 ˚C and for 1 h at room temperature. A solution of $Pd(PPh_3)_4$ (0.3 mmol, 0.1 equiv.) and 1-(2,6-dibromophenylazo)pyrrolidine (3.0 mmol, 1 equiv.) in 20 ml THF was added to the reaction mixture. The mixture was refluxed for 72 h.

After addition of H_2O (100 ml), the THF was evaporated and the residue was extracted with Et_2O (3×300 ml). The organic layers were washed with saturated solution of EDTA (2×150 ml), then with saturated solution of NaCl (150 ml). The organic layer was dried over $MgSO_4$, filtered and evaporated. The crude was purified by column chromatography on SiO_2 (eluent hexane/EtOAc 9:1). The product (2.3 mmol, 76%), was obtained as an orange oil.

IR (KBr): 3422*w*, 3061*m*, 2981*m*, 2945*m*, 2866*m*, 2266*w*, 1930*w*, 1623*s*, 1590*s*, 1464*s*, 1409*s*, 1339*s*, 1316*s*, 1270*s*, 1232*s*, 1210*s*, 1189*m*, 1108*m*, 1075*m*, 997*s*, 850*w*, 830*w*, 799*m*, 784*s*, 761*s*, 724*m*, 599*m*, 560*m*, 547*m*, 513*m*. ^{1}HNMR (300 MHz, $CDCl_3$): δ 7.37 (m, 2 H), 7.26 (t, 1 H), 7.24 (m, 2 H), 6.88 (m, 4 H), 3.11 (s, 4 H), 1.65 (s, 4 H). $^{13}C\{^1H\}$ NMR (75 MHz, $CDCl_3$): δ 160.2 (dd, $^1J_{C-F}$ = 247 Hz, $^3J_{C-F}$ = 7.5 Hz), 148.6 (s), 132.0 (s), 128.2 (t, $^3J_{C-F}$ = 10 Hz), 123,9 (s), 122.5 (s), 118.1 (t, $^2J_{C-F}$ = 21Hz), 110.7 (dd, $^2J_{C-F}$ = 25 Hz, $^4J_{C-F}$ = 8 Hz), 45.9 (broad), 23.6 (s). $^{19}F\{^1H\}$ NMR (282 MHz, $CDCl_3$): δ –112.46. MS (EI): 399 (7, M^+), 329 (18, $[M-(CH_2)_4N]^+$), 301 (100, $[M-(CH_2)_4N_3]^+$), 281 (73), 261 (12). HRMS (EI) *m/z*: calcd for $C_{22}H_{17}N_3F_4$: 399.1359; found: 399.1352.

5.2.2 2,6,2'',6''-tetrafluoro-2'-iodo-1,1':3'1''-terphenyl (24)

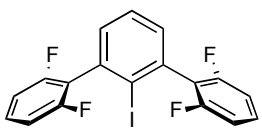

Chemical Formula: $C_{18}H_9F_4I$
Molecular Weight: 428.162

Under an inert atmosphere of N_2, 2'-azopyrrolidine-2,6,2'',6''-tetrafluoro-1,1':3'1''-terphenyl (1.16 mmol, 1 equiv.) and iodine (2.32 mmol, 2 equiv.) were dissolved in 30 ml of dichloroethane. The solution was degassed, then refluxed overnight. The reaction mixture was washed with H_2O, then with saturated Na_2SO_3 solution and again with H_2O. The organic phase was dried over $MgSO_4$, filtered and evaporated. The crude was purified via column chromatography on SiO_2 (eluent hexane/EtOAc 9:1). The product (0.96 mmol, 83%) was obtained as a slightly yellow powder.

M.p.: 142-144 ˚C. IR(KBr): 3442*w*, 3075*w*, 2262*w*, 1923*w*, 1886*w*, 1841*w*, 1755*w*, 1711*w*, 1625*s*, 1588*s*, 1566*s*, 1464*s*, 1442*s*, 1393*s*, 1265s, 1232*s*, 1055*m*, 1021*s*, 999*s*, 973*s*, 785*s*, 728*s*, 689*s*, 547*s*, 505*s*. ^{1}H NMR (300 MHz, $CDCl_3$): δ 7.51 (dd, 1H, H-C (5')), 7.38 (m, 2H, H-C (4, 4'')), 7.30 (d, 2H, H-C(4', 6'), 7.00 (m, 4H, H-C(3, 5,3'', 5'')). ^{13}C{^{1}H} (75 MHz, $CDCl_3$): δ 159.9 (dd, $^1J_{C\text{-}F}$= 249 Hz, $^3J_{C\text{-}F}$= 7 Hz, C(2, 6, 2'', 6'')), 136.9, 130.8, 130.0 (t, $^3J_{C\text{-}F}$= 10Hz, C(4, 4'')), 128.0, 122.0 (t, $^2J_{C\text{-}F}$= 23 Hz, C(1, 1'')), 111.5 (dd, $^2J_{C\text{-}F}$= 25 Hz, $^4J_{C\text{-}F}$= 7.5 Hz, C(3, 5, 3'', 5'')), 106.2. ^{19}F{^{1}H} NMR (282 MHz, $CDCl_3$): δ –111.95. MS (EI): 428 (100, M^+), 302 (29, [M-I]$^+$), 280 (49), 261 (11), 214 (8), 140 (18). HRMS (EI) *m/z*: calcd for $C_{18}H_9F_4I_1$: 427.9685; found: 427.9685.

5.2.3 [2,6-Bis(2,6-difluorophenyl)phenyl]dimethylsilane (11)

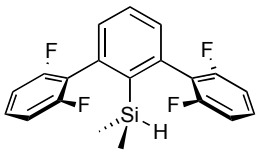

Chemical Formula: $C_{20}H_{16}F_4Si$
Molecular Weight: 360.420

Under an inert atmosphere of N_2, 2'-iodo-2,6,2'',6''-tetrafluoro-1,1':3'1''-terphenyl (1.03 mmol, 1 equiv.) was dissolved in 25 ml of dry THF. The solution was cooled to – 78˚C, then *n*-BuLi (1.6 M in hexane, 2.26 mmol, 2.2 equiv.) was added over 3 min. The reaction mixture was stirred for 1 h, then chlorodimethylsilane (2.67 mmol, 2.6 equiv.) was added. The mixture was stirred for 30 min at –78˚C and for 1 h at ambient temperature. H_2O (10 ml) was added, followed by NaOH (1M) till pH 7 was reached, then THF was evaporated. The mixture was extracted with CH_2Cl_2 (3× 20 ml), the

collected organic layers were washed with H_2O (1 × 40 ml), then dried on $MgSO_4$, filtered and evaporated. The crude product was purified via column chromatography on Al_2O_3 (deactivated with 5% H_2O) using hexane as eluent. The product (0.72 mmol, 70%) was obtained as white powder. Crystals suitable for X-ray analysis were grown from hexane at +4 ˚C.

The Si-H resonance for **2a** (see ^{1}H-NMR) has a complex multiplicity, that reveals a coupling with fluorine atoms already in the neutral species. A more detailed discussion of the NMR and the X-ray crystal structure of **2a** are included in a paper that has been submitted for publication.

M.p.: 72 - 73 ˚C. IR (KBr): 3451*w*, 3063*w*, 2960*w*, 2904*w*, 2148*s,* 1926*w*, 1624*s*, 1585*s*, 1464*s*, 1434*s*, 1402*m*, 1269*s*, 1232*s*, 1123*m*, 1056*m*, 997*s*, 886*s*, 845*s*, 805*s*, 782*s*, 724*s*, 657*m*, 546*s*. ^{1}H NMR (400 MHz, C_6D_6): δ 7.10 (m, 3 H, H-C(3', 4', 5')), 6.67 (m, 2 H, H-C(4'', 4''')), 6.56 (m, 4 H, H-C(3'', 5'', 3''', 5''')), 4.23 (triplet of septuplet, 1 H, $^3J_{H-H}$ = 4.0 Hz, J_{H-F} = 1.0 Hz, H-Si), 0.041 (d, $^3J_{H-H}$ = 4Hz, 6 H, H_3C-Si)). $^{13}C\{^1H\}$ NMR (101 MHz, C_6D_6): δ 161.2 (dd, $^1J_{C-F}$ = 247 Hz, $^3J_{C-F}$ = 7 Hz, C(2'', 6'', 2''', 6''')), 138.8 (C 1'), 137.0 (C (2', 6')), 131.4 (C (4', 6')), 130.0 (t, $^3J_{C-F}$ = 10 Hz, C(4'', 4''')), 129.7 (C4'), 121.1 (t, $^2J_{C-F}$=22Hz, C(1'', 1''')), 111.5 (dd, $^2J_{C-F}$= 19Hz, $^4J_{C-F}$=7Hz, C(3'', 5'', 3''', 5''')), -2.9 (CH_3-Si). $^{19}F\{^1H\}$ NMR (282 MHz, C_6D_6): δ –110.40. ^{29}Si NMR (60 MHz, C_6D_6): δ –19.8. MS (EI): 360 (32, M^+), 345 (36, $[M\text{-}CH_3]^+$), 325 (14), 302 (9), 262 (53), 244 (100). HRMS (EI) *m/z*: calcd for $C_{20}H_{16}F_4Si_1$: 360.0957; found: 360.0949.

5.2.4 [2,6-Bis(2,6-difluorophenyl)phenyl]dimethylsilylium tetrakis(pentafluorophenyl)borate [18][$B(C_6F_5)_4$]

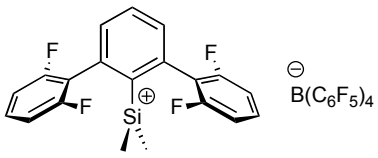

Chemical Formula: $C_{44}H_{15}BF_{24}Si^+$
Molecular Weight: 1038.44753

In a glovebox, a suspension of $[Ph_3C][B(C_6F_5)_4]$ (0.26 mmol) and the silane (0.29 mmol) in dry C_6D_6 (1 ml) was prepared. The oily brown mixture was stirred for 16 hrs

at rt. Two layers formed, a dark brown oil at the bottom and a clear yellow upper layer. The upper layer was removed and the oily phase was washed with C_6D_6 (2 × 0.5 ml). The brown oil, containing mainly the ionic product, was examined by NMR spectroscopy. After evaporation of the solvent a reddish powder was obtained in 92% yield.

^{1}H NMR (500 MHz, C_6D_6): δ 7.54 (*d*, 2H, ^{3}J = 8.0 Hz, H-C(4', 6')), 7.35 (*t*, 1H, ^{3}J = 8.0 Hz, H-C(5')), 6.91 (*q*, 2H, J = 8.0 Hz, H-C(4, 4'')), 6.70 (*dd*, 4H, ^{3}J = 8.5, $^3J_{H-F}$ = 11.0 Hz, H-C(3, 5, 3'', 5''), 0.11 (q, 6H, $^3J_{H-F}$ = 6.0 Hz, H_3C-Si). ^{13}C NMR (126 MHz, C_6D_6): δ 160.52 (*dd*, $^1J_{C-F}$ = 239 Hz, $^3J_{C-F}$ = 13 Hz, C(2, 6, 2'', 6'')), 150.3-148.3 (*m*, C-F counterion), 140.1-138.2 (m, C-F counternion), 138.1-136.2 (m, C-F counterion), 134.3 (*s*, C(5')), 132.4 (*t*, $^3J_{C-F}$ = 13 Hz, C(4, 4'')), 132.2 (*s*, C(4', 6')), 128.5 (*s*, C(1', 3')), 126.6 (*s*, C(2')), 125.1 (*m*, C-F counterion), 114.7 (*t*, $^2J_{C-F}$ = 14 Hz, C(1, 1'')), 114.0 (d, $^2J_{C-F}$ = 28 Hz, C(3,5, 3'', 5'')), -2.87 (*q*, J_{C-F} = 5.4 Hz, CH_3-Si). ^{19}F{^{1}H} NMR (282 MHz, C_6D_6): δ -112.9 (*s*, F-C(2, 6, 2'', 6'')), -132.0 (*m*, counterion), -162.6 (*t*, J = 19 Hz, counterion), 166.6 (*m*, counterion). ^{29}Si NMR (99 MHz, C_6D_6): δ 88.6 (broad resonance).

5.2.5 [2,6-Bis(2,6-difluorophenyl)phenyl]dimethylsilylium hexaclorocarborane [18][$CB_{11}H_6Cl_6$]

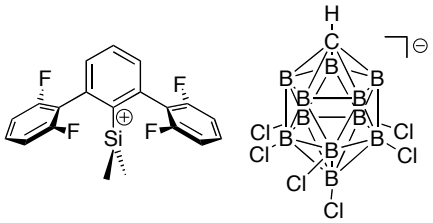

Chemical Formula: $C_{21}H_{21}B_{11}Cl_6F_4Si$
Molecular Weight: 709.118

In a glovebox, a suspension of [Ph_3C][$CB_{11}H_6Cl_6$] (0.03 mmol) and silane **2a** (0.03 mmol) in chlorobenzene (1.5 ml) was prepared. The yellow suspension was stirred for 16 hrs. A clear solution with a bit of precipitate was obtained. ^{1}H NMR of the supernatant confirmed the formation of the product. 0.5 ml of the supernatant were placed in a 5 mm NMR tube and layered with 1 ml of hexane. Within one day slightly yellow crystals, suitable for X-Ray analysis, were obtained.

5.2.6 [2,6-Bis(2,6-difluorophenyl)phenyl]diisopropylsilane (12)

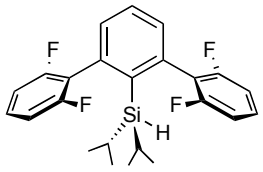

Chemical Formula: $C_{24}H_{24}F_4Si$
Molecular Weight: 416.526

The same procedure described in 5.2.3 was followed, using chlorodiisopropylsilane instead of chlorodimethylsilane. The product was obtained in 71% yield as white powder. Crystals suitable for X-ray analysis were grown from hexane at +4 ˚C.

M.p.: 127 - 127.5 ˚C. IR (neat): 2942*w*, 2864*w*, 2361*w*, 2184*w*, 2131*w*, 1623*m*, 1585*w*, 1462*s*, 1434*w*, 1271*m*, 1232*m*, 1001*s*, 880*w*, 841*w*, 808*w*, 788*m*. ^{1}H NMR (300 MHz, C_6D_6): δ 7.08 (m, 3 H, H-C(3', 4' 5')), 6.71(m, 2 H, H-C(4'', 4''')), 6.60 (m, 4 H, H-C(3'', 5'', 3''', 5''')), 3.65 (triplet of triplet, $^{3}J_{H-H}$ = 5.2 Hz, J_{H-F} = 1.5 Hz, 1 H, H-Si), 1.15 (d, 3 H, H_3C iPr), 0.95 (m, 2 H, HC *i*Pr), 0.89 (d, 3 H, H_3C *i*Pr). ^{13}C{^{1}H} NMR (75 MHz, C_6D_6): δ 161.2 (dd, $^{1}J_{C-F}$ = 246 Hz, $^{3}J_{C-F}$ = 7 Hz, C(2'', 6'', 2''', 6''')), 138.5 (C1'), 137.5 (C2'), 131.4 (C (3', 5')), 129.8 (t, $^{3}J_{C-F}$ = 10 Hz, C(4'', 4''')), 129.3 (C4'), 121.6 (t, $^{2}J_{C-F}$ = 30 Hz, C(1'', 1''')), 111.1 (dd, $^{2}J_{C-F}$ = 26 Hz, $^{4}J_{C-F}$ = 7 Hz, C(3'', 5'', 3''', 5''')), 20.7 (quintuplet, J_{C-F} = 1Hz, CH_3 *i*Pr), 20.1 (CH_3 *i*Pr), 12.5 (CH *i*Pr). ^{19}F{^{1}H} NMR (282 MHz, C_6D_6): δ –109.02. ^{29}Si NMR (59.6 MHz, C_6D_6): δ 6.4. MS (EI): 416 (30, M^+), 373 (100, $[M - CH(CH_3)_2]^+$), 331 (19), 263 (50), 244 (60), 226 (28). HRMS (EI) *m/z*: calcd for $C_{24}H_{24}F_4Si$: 416.15833; found: 416.15787.

5.2.7 [2,6-Bis(2,6-dichlorophenyl)phenyl]dimethylsilane (30)

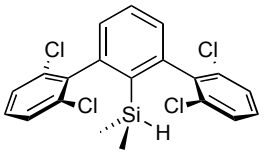

Chemical Formula: $C_{20}H_{16}Cl_4Si$
Molecular Weight: 426.238

The same procedure described in 5.2.3 was followed. The product was obtained in 52% yield as white powder. Crystals suitable for X-ray analysis were grown from hexane at +4˚C.

M.p.: 91 – 93 ˚C. IR (KBr): 3445*w*, 3053*w*, 2957*m*, 2900*w*, 2161*s*, 1934*w*, 1862*w*, 1791*w*, 1672*w*, 1583*m*, 1557*s*, 1427*s*, 1246*s*, 1190*s*, 1152*w*, 1125*s*, 1083*m*, 1051*m*, 969*w*, 899*s*, 839*s*, 781*s*, 731*s*, 650*m*. ^{1}H NMR (300 MHz, C_6D_6): δ 7.26 (t, ^{3}J = 7.6 Hz, 1 H, H-C(4')), 7.04 (d, ^{3}J = 8Hz, 4 H, H-C (3'', 5'', 3''', 5''')), 6.98 (d, ^{3}J = 7.6 Hz, 2 H, H-C(3', 5')), 6.60 (t, ^{3}J= 8Hz, 2H, H-C(4'', 4''')), 4.14 (septuplet, ^{3}J = 4.0 Hz, 1H, H-Si), 0.11 (d, ^{3}J = 4Hz, 6 H, H_3C-Si). ^{13}C{^{1}H} NMR (101 MHz, C_6D_6): δ 145.3 (C(2', 6')), 141.9 (C(1'', 1''')), 136.4 (C(2'', 6'', 2''', 6''')), 135.7 (C 1'), 130.5 (C 4'), 129.9 (C(4'', 4''')), 129.7 (C(3', 5')), 128.0 (C(3'', 5'', 3''', 5''')), -2.3 (CH_3-Si). ^{29}Si NMR (60 MHz, C_6D_6): δ –20.8. MS (EI): 425 (19, M^+), 391 (100). HRMS (EI) *m/z*: calcd for $C_{20}H_{15}Si_1Cl_4$: 422.9697; found: 422.9702.

5.2.8 [2,6-Bis(2,6-dichlorophenyl)phenyl]dimethylsilylium tetrakis(pentafluuorophenyl)borate [28][$B(C_6F_5)_4$]

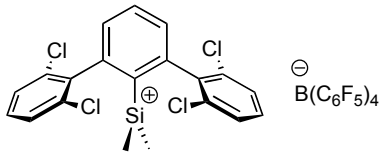

Chemical Formula: $C_{44}H_{15}BCl_4F_{20}Si^-$
Molecular Weight: 1104.26701

The same procedure described in 5.2.4 was followed and the product was obtained in 95 % yield.

^{1}H NMR (400 MHz, C_6D_6): δ 7.27 (*m*, 1H, H-C(5')), 7.20 (m, 2H, H-C(4', 6')), 7.00 (*d*, 4H, ^{3}J = 8.0 Hz, H-C(3, 5, 3'', 5'')), 6.80 (*t*, 2H, H-C(4, 4'')), -0.03 (*s*, 6H, H_3C-Si). ^{13}C{^{1}H} NMR (101 MHz, C_6D_6): δ 150.5-148.1 (*m*, C-F counterion), 140.3-138.0 (*m*, C-F counterion), 139.5 (s, C(1', 3')), 139.5 (C(1', 3')), 138.5-135.2 (*m*, C-F counterion), 135.3 (C(1, 1'')), 133.6 (C(2, 6, 2'', 6'')), 133.5 (C(5')), 133.1 (C(4', 6')), 132.1 (C(4, 4'')), 130.5 (C(3, 5, 3'', 5'')), 128.8 (C(2')). ^{29}Si NMR (79.5 MHz, C_6D_6): δ 90.5 (*s*).

5.2.9 Triphenylcarbenium tetrakis(pentafluorophenyl)borate: $[Ph_3C][B(C_6F_5)_4]$

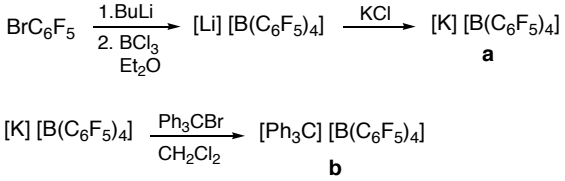

A solution of C_6F_5Br (22 mmol) in Et_2O (100 ml) was cooled to -78 ˚C. ^nBuLi (1.6 M solution in hexane, 22.5 mmol) was added dropwise and the reaction mixture was stirred for 70 min at -78 ˚C. BCl3 (1.0 M solution in hexane, 5.24 mmol) was added over 5 min and the mixture was stirred for 50 min at -78 ˚C. The cooling bath was removed and the mixture was stirred at rt for 20 h. A white suspension was obtained: KCl (41.9 mmol) was added in one portion, then H_2O (100 ml) was added and the mixture was stirred for 1h. The organic phase was washed with H_2O (3 × 50 ml) and the solvent evaporated at reduced pressure. The product **a** was dried in high vacuum at 170˚C for 16h. A brownish powder was obtained in 76% yield.

$^{19}F\{^1H\}$NMR (376 MHz, acetone-d_6): –133.2 (*m*, 8F, o-C_6F_5), –164.6 (*t*, 4F, $^3J_{F\text{-}F}$ = 18.8 Hz, *p*-C_6F_5), –168.6 (*t*, 8F, $^3J_{F\text{-}F}$ = 18.8 Hz, *m*-C_6F_5).

$K[B(C_6F_5)_4]$ (2.85 mmol) and Ph_3CBr (3.25 mmol) were dissolved in CH_2Cl_2 (40 ml). The mixture was stirred at rt for 3h. A yellow precipitate formed after stopping the stirring. The orange-brown supernatant was filtered through celite and concentrated to a volume of 5 ml. Upon addition of pentane (20 ml) a precipitate formed. The yellow powder was filtered and washed with cyclohexanone (4 × 5 ml) to remove the remaining Ph_3CBr. The product was let dry in the filter for 30 min and then out of the glove box was dried in high vacuum at 140 ˚C for 2-3h. During this process a little amount of white powder might sublime. The product **b**, as a slightly dark yellow powder, was obtained in 94% yield.

NMR measurements of $[Ph_3C][B(C_6F_5)_4]$ in C_6D_6 require ca. 200 of compound. The trityl cation in benzene is an oil that forms a layer at the bottom of the NMR tube. It gives instead an orange solution in chloroform.

^{1}H NMR (400 MHz, C_6D_6): δ 7.47 (*t*, ^{3}J = 7.8 Hz, 3H, *p*-Ph), 7.10 (*t*, ^{3}J = 8.1 Hz, 6H, *m*-Ph), 6.73 (dd, ^{3}J = 8.4 Hz, ^{4}J = 1.2 Hz, 6H, *o*-Ph). ^{13}C{^{1}H} NMR (75 MHz, C_6D_6): δ 210.2 (Ph_3C^+), 149.0 (*d*, $^{1}J_{C\text{-}F}$ = 242 Hz, $B(C_6F_5)_4^-$), 143.0, 142.1, 139.5, 138.8 (*d*, $^{1}J_{C\text{-}F}$ = 245, $B(C_6F_5)_4^-$), 136.9 (*d*, $^{1}J_{C\text{-}F}$ = 247, $B(C_6F_5)_4$), 130.1, 127-123 (broad signal, $B(C_6F_5)_4^-$). ^{19}F{^{1}H} NMR (282 MHz, benzene-d_6): δ -132.3 (*d*, 8F,$^{3}J_{F\text{-}F}$ = 10.5 Hz, *o*-C_6F_5), -162.9 (*t*, 4F, $^{3}J_{F\text{-}F}$ = 19.7 Hz), -166.9 (*t*, 8F, $^{3}J_{F\text{-}F}$ = 18.6 Hz, *m*-C_6F_5).

5.2.10 $[Ph_3C][CHB_{11}H_5Cl_6]$

$$[Ag][CHB_{11}H_5Cl_6] \xrightarrow[CH_3CN,\ PhMe]{Ph_3CBr} [Ph_3C][CHB_{11}H_5Cl_6]$$

In a glovebox $[Ag][CHB_{11}H_5Cl_6]$ (4.34 g, 9.48 mmol) was suspended in acetonitrile (50 ml) and toluene (50 ml). Ph_3CBr (3.38 g, 10.47 mmol) was added in one portion. Within seconds the mixture turned from brownish to red and an almost colorless precipitate (AgBr) formed. The mixture was stirred for 80 minutes and then filtered through a medium porosity glass frit directly into a 250 ml round bottom flask. The precipitate (AgBr) was washed with small aliquots of toluene/acetonitrile (4:1). The filtrate was concentrated under reduced pressure. When only ca. 30 ml of solvent were left, a yellow-orange precipitate (product) formed. The solid was collected in a glass frit; then it was washed with 20 ml of toluene and 20 ml of hexane. The filtrate was treated with ca. 50 ml of hexane. A second portion of the product precipitated and was collected and washed similarly to the first portion. The product $[Ph_3C][CHB_{11}H_5Cl_6]$ was obtained as a yellow powder in 89 % yield.

^{1}H NMR (400 MHz, CD_3CN): δ 8.28 (*t*, ^{3}J = 8.0 Hz, 3H, *p*-Ph), 7.88 (*t*, ^{3}J = 8.0 Hz, 6H, *m*-Ph), 7.53 (dd, ^{3}J = 8.0 Hz, ^{4}J = 1.2 Hz, 6H, *o*-Ph)

5.2.11 2-Bromo-5-fluoro-1,3-dimethylbenzene (35)

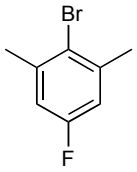

Chemical Formula: C_8H_8BrF
Molecular Weight: 203.051

In a two necked-flask with condenser, 4-bromo-3,5-dimethylbenzylamine (88 mmol, 1 eq.) was dissolved in toluene (100 ml) and the solution was degassed. Degassed $BF_3 \cdot Et_2O$ (132 mmol, 1.5 equiv.) was added and a precipitate was formed. The stirring was no longer effective. The reaction mixture was heated till 110˚C and *tert*-butyl nitrite (105 mmol, 1.2 equiv.) was slowly added over a period of 45 min. At the end of the addition the mixture turned to a brown solution. The reflux was continued for 2 h. The reaction mixture was let to cool to ambient temperature for 2 h, then H_2O (50 ml) was added. The aqueous phase was extracted with Et_2O (2× 50 ml). The collected organic layers were dried over $MgSO_4$ and filtered. The solvents (Et_2O and toluene) were distilled at ambient pressure and at a maximum temperature of 140˚C of the oil bath. The crude was purified via column chromatography on SiO_2 (eluent: hexane). The residual toluene was eliminated drying the product carefully (high volatility) under reduced pressure. The product (38 mmol) was obtained in 43% yield as colorless oil.

^{1}H NMR (300 MHz, $CDCl_3$): δ 6.83 (*dd*, $^3J_{H\text{-}F}$ = 9.0 Hz, $^4J_{H\text{-}H}$ = 0.4 Hz, 2H) 2.42 (*s*, 6H). $^{13}C\{^1H\}$ NMR (75 MHz, $CDCl_3$): δ 161.4 (*d*, $^1J_{C\text{-}F}$ = 245 Hz), 140.3 (*d*, $^3J_{C\text{-}F}$ = 7.5 Hz), 121.8 (*d*, $^4J_{C\text{-}F}$ = 2.3 Hz), 115.2 (*d*, $^2J_{C\text{-}F}$ = 21.8 Hz), 24.2 (*d*, $^4J_{C\text{-}F}$ = 1.5 Hz). $^{19}F\{^1H\}$ NMR (282 MHz, $CDCl_3$): δ -118.4.

5.2.12 4,4''-difluoro-2'-iodo-2,6,2'',6''-tetramethyl-1,1':3'1''-terphenyl (36)

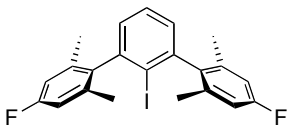

Chemical Formula: $C_{22}H_{19}F_2I$
Molecular Weight: 448.28754

Under an inert atmosphere of N_2, Mg turnings (4 mmol, 4 equiv.) and 3 ml of dry THF were charged in the reaction flask. A small crystal of I_2 was added to activate the Mg. A solution of
2-Bromo-5-fluoro-1,3-dimethylbenzene (4 mmol, 4 equiv.) in 20 ml of dry THF was added dropwise over 20 min. After the addition of the first drops the mixture was warmed and the Grignard formation started. The mixture was refluxed for 2.5 h. A solution of 1,3-dibromo-2-iodobenzene (1 mmol, 1 equiv.) in 20 ml of dry THF was added dropwise over 20 min. The mixture was refluxed for 18 h. It was allowed to cool to rt, then cooled to 0˚C in an ice bath. I_2 (4 mmol, 4 equiv.) was added in one portion. After 30 min the ice bath was removed and the brown mixture was stirred at rt for 8 h. After addition of H_2O (20 ml), Na_2SO_3 was added until the I_2 color no longer persisted. The THF was evaporated and the mixture was extracted with CH_2Cl_2 (3 × 25 ml); the organic layers were washed with H_2O (40 ml), dried on $MgSO_4$, filtered and evaporated. The crude was purified via column chromatography on SiO_2 (eluent: hexane/EtOAc 98:2). The product (0.74 mmol) was obtained as a white powder in 74% yield.

M.p.: 215-216 ˚C. IR (KBr): 3469*w*, 3420*w*, 3051*w*, 2974*m*, 2945*m*, 2916*m*, 2854*m*, 1711*w*, 1607*s*, 1484*s*, 1449*s*, 1377*s*, 1303*s*, 1281*m*, 1263*m*, 1176*w*, 1129*s*, 1096*w*, 1014*s*, 1002*m*, 963*m*, 857*s*, 843*m*, 803*s*, 739*s*, 700*m*, 592*w*, 572*m*, 546*m*. ^{1}H NMR (400 MHz, $CDCl_3$): δ 7.50 (t, ^{3}J = 7.6 Hz, 1 H), 7.10 (d, ^{3}J = 7.6 Hz, 2 H), 6.86 (d, ^{3}J = 9.2 Hz, 4 H), 2.01 (s, 6 H). ^{13}C{^{1}H} NMR (400 MHz, $CDCl_3$): δ 161.9 (d, $^1J_{CF}$ = 244Hz), 146.5, 140.5, 137.9, 137.8, 129.1, 128.2, 114.0, 20.4. ^{19}F{^{1}H} NMR (300 MHz, $CDCl_3$): δ –116.72. MS (EI): 448 (100, M^+), 320 (9, $[M-I]^+$), 306 (39). HRMS (EI) *m/z*: calcd for $C_{22}H_{19}F_2I_1$: 448.0500; found: 448.0502.

5.2.13 [2,6-Bis(4-fluoro-2,6-dimethylphenyl)phenyl]dimethylsilane (37)

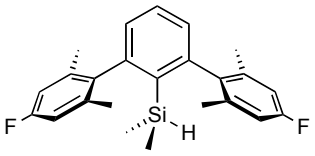

Chemical Formula: $C_{24}H_{26}F_2Si$
Molecular Weight: 380.545

The same procedure described in 5.2.3 was followed. The product was obtained in 85% yield as white powder. Crystals suitable for X-Ray analysis were grown from acetonitrile at -20˚C.

M.p.: 121-122 ˚C. IR (neat): 3031*w*, 2958*m*, 2916*m*, 2855*m*, 2150*s*, 1955*w*, 1699*m*, 1606*s*, 1553*m*, 1479*s*, 1438*s*, 1376*m*, 1300*s*, 1276*m*, 1246*s*, 1171*m*, 1129*s*, 1044*m*, 1018*s*, 965*m*, 897*s*, 879*s*, 855*s*, 837*s*, 813*s*, 786*s*, 735*s*. ^{1}H NMR (500 MHz, C_6D_6): δ 7.16 (m, 1 H, H-C(4')), 6.72 (*m*, 6 H, H-C(3', 5', 3'', 5'', 3''', 5''')), 3.84 (septuplet, ^{3}J = 4 Hz, 1 H, H-Si), 1.84 (*s*, 12 H, CH_3-C_{ring}), - 0.27 (d, ^{3}J = 4 Hz, 6 H, CH_3-Si). $^{13}C\{^{1}H\}$ NMR (400 MHz, C_6D_6): δ 162.4 (d, $^{1}J_{C\text{-}F}$ = 243 Hz, C(4'', 4''')), 148.5 (C(2', 6')), 139.1 (d, $^{4}J_{C\text{-}F}$ = 3Hz, C(1'', 1'''), 138.6 (d, $^{3}J_{C\text{-}F}$ = 8 Hz, C(2'', 6'', 2''', 6''')), 134.8 (C 1'), 130.4 (C 4'), 128.6 (C 3', 5'), 114.1 (d, $^{2}J_{C\text{-}F}$ = 21 Hz, C(3'', 5'', 3''', 5''')), 21.1 (d, $^{1}J_{C\text{-}F}$ = 1 Hz, CH_3-C_{ring}), -2.58 (CH_3-Si). $^{19}F\{^{1}H\}$ NMR (300 MHz, C_6D_6): δ –116.19. ^{29}Si NMR (300 MHz, C_6D_6): δ –23.1. MS (EI): 380 (11, M^+), 365 (100, $[M\text{- }CH_3]^+$). HRMS (EI) *m/z*: calcd for $C_{24}H_{26}F_2Si_1$: 380.1772; found: 380.1767.

5.2.14 [2,6-Bis(4-fluoro-2,6-dimethylphenyl)phenyl]diisopropylsilane (40)

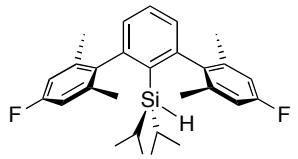

Chemical Formula: $C_{28}H_{34}F_2Si$
Molecular Weight:: 436.65187

The same procedure described in 5.2.3 was followed, using chlorodiisopropylsilane instead of chlorodimethylsilane. The product was obtained in 82% yield as white powder.

M.p.: 96-98 ˚C. IR (neat): 2952 *w*, 2926 *w*, 2865 *w*, 2140 *w*, 1606 *m*, 1473 *w*, 1447 *w*, 1380 *w*, 1304 *s*, 1133 *m*, 1022 *m*, 856 *s*, 811 *m*, 747 *m*. ^{1}H NMR (400 MHz, $CDCl_3$): δ 7.43 (*t*, ^{3}J = 7.2 Hz, 1H), 6.99 (*d*, ^{3}J = 7.6 Hz, 2H), 6.80 (*d*, $^{3}J_{H-F}$ = 9.6 Hz, 4H), 3.03 (*t*, ^{3}J = 3.6 Hz, 1H), 2.04 (*s*, 12H), 0.79 (*d*, ^{3}J = 6.8 Hz, 6H), 0.73 - 0.70 (*m*, 2H), 0.60 (*d*, ^{3}J = 6.8 Hz, 6H). $^{13}C\{^{1}H\}$ NMR (75 MHz, $CDCl_3$): δ 161.8 (*d*, $^{1}J_{C-F}$ = 244.5 Hz), 148.3, 139.7 (*d*, $^{4}J_{C-F}$ = 3.0 Hz), 138.6 (*d*, $^{3}J_{C-F}$ = 7.5 Hz), 136.7, 129.5, 129.0, 113.8 (*d*, $^{2}J_{C-F}$ = 21.1 Hz), 22.4, 21.5 (*d*, $^{4}J_{C-F}$ = 2.2 Hz), 18.6, 11.4. ^{19}F NMR (376 MHz, C_6D_6): δ –116.3 (*t*, $^{3}J_{F-H}$ = 7.5 Hz). ^{29}Si NMR (79.5 MHz, C_6D_6): δ 3.7. MS (EI): 393 (100, [M- *i*Pr]$^{+}$), 365 (15), 351 (27), 322 (10). HRMS (EI) *m/z*: calcd for $C_{28}H_{34}F_2Si_1$: 436.2398; found: 436.2385.

5.2.15 [2,6-Bis(4-fluoro-2,6-dimethylphenyl)phenyl]dimethylsilylium tetrakis(pentafluorophenyl)borate-CD_3CN complex (38)

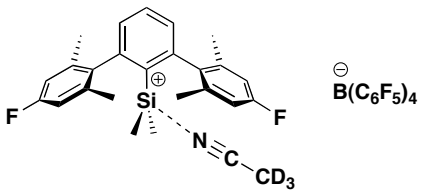

Chemical Formula: $C_{50}H_{25}D_3BF_{22}NSi$
Molecular Weight: 1102.64388

In a glovebox, $[Ph_3C][B(C_6F_5)_4]$ (0.24 mmol) and the silane (0.26 mmol) were dissolved in dry C_6D_6 (1 ml) and few drops of CD_3CN. The reaction mixture was a red-brown solution and it was stirred for 16 hrs at rt. The solvents were evaporated under vacuum and the crude orange-yellow powder was washed with hexane (3 × 1 ml) to remove the excess of silane and the triphenylmethane formed in the reaction. The product was obtained in 83 % yield as a bright yellow powder (7% of unreacted $[Ph_3C][B(C_6F_5)_4]$ was recovered along with the product).

^{1}H NMR (400 MHz, C_6D_6 + few drops CD_3CN): δ 7.25 (*t*, ^{3}J = 7.6 Hz, 1H), 6.67 (*t*, $^{3}J_{H\text{-}F}$ = 9.2 Hz, 4H), 6.65 (*d*, $^{3}J_{H\text{-}F}$ = 8.0 Hz, 2H), 1.75 (*s*, 12H), -0.01 (*s*, 6H). $^{13}C\{^{1}H\}$ NMR (100.6 MHz, C_6D_6 + few drops CD_3CN): δ 163.3 (*d*, $^{1}J_{C\text{-}F}$ = 248 Hz), 148.2, 140.2 (*d*, $^{3}J_{C\text{-}F}$ = 8 Hz), 137.0 (*d*, $^{4}J_{C\text{-}F}$ = 3 Hz), 134.0, 130.5, 125.2, 117.7, 115.1 (*d*, $^{2}J_{C\text{-}F}$ = 21 Hz), 21.1 (*d*, $^{4}J_{C\text{-}F}$ = 1.5 Hz), 1.09, 0.44 (*m*, -CD_3). ^{19}F NMR (376 MHz, C_6D_6 + few drops CD_3CN): δ –113.7 (2F), –132.5 (8F), –163.2 (4F), –167.2 (8F). ^{29}Si NMR (79.5 MHz, C_6D_6 + few drops CD_3CN): δ 17.0.

5.2.16 4,4''-dichloro-2'-iodo-2,6,2'',6''-tetramethyl-1,1':3'1''-terphenyl (44)

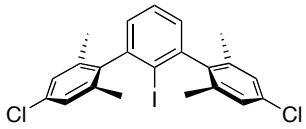

Chemical Formula: $C_{22}H_{19}Cl_2I$
Molecular Weight: 481.19673

In a 100 ml 2 necked flask, equipped with condenser, under N_2 atmosphere, Mg turnings (7.46 mmol) and THF (20 ml) were charged. 1,2-dibromoethane (7.46 mmol) was added dropwise. After addition of the first few drops of 1,2-dibromoethane, the Grignard formation was initiated with a gentle heating, but afterwards the reaction mixture was cooled with an ice bath. The Mg was completely consumed after ca. 1 hour and a grey solution of $MgBr_2$ was formed. In the meanwhile, in a 50 ml 2 necked flask, 2-bromo-5-chloro-1,3-dimethylbenzene (7.29 mmol) was dissolved in THF (30 ml) and the solution was cooled to -78˚C (acetone-dry ice bath). *n*-BuLi (1.6 M in hexane, 7.46 mmol) was added dropwise to this solution and the reaction mixture was stirred at -78˚C for 1 h. The lithiated species was canulated into the $MgBr_2$ solution, that was in the meanwhile cooled as well to -78˚C. The reaction mixture was allowed to warm to rt and stir for an additional hour; during this time the reaction mixture turned deep yellow and then colorless. A solution of 1,3-dichloro-2-iodobenzene (1.82 mmol) in THF (5 ml) was canulated into the reaction mixture, that was then refluxed for 18 hrs at 75 ˚C. The reaction mixture was cooled to 0˚C with an ice bath, and I_2 (1.82 mmol) was added in one portion. The brown mixture was stirred for 20 hrs and allowed to warm to rt in the meanwhile. H_2O (20 ml) and Na_2SO_3 (to reduce the excess of I_2) were added and the mixture turned light yellow. THF was evaporated

and the residual was extracted with EtOAc (3 × 30 ml), dried on $MgSO_4$ and the solvent evaporated. The crude was purified via column chromatography on SiO_2 (eluent: hexane). The product was obtained as a white powder in 68% yield.

M.p.: 228-230 ˚C. IR (neat): 3049 *w*, 2921 *m*, 2850 *w*, 1729 *w*, 1587 *m*, 1573 *m*, 1476 *w*, 1442 *m*, 1409 *w*, 1383 *m*, 1253 *m*, 1120 *m*, 1013 *m*, 876 *m*, 857 *s*, 801 *m*, 737 *s*, 696 *w*, 577 *m*. ^{1}H NMR (400 MHz, $CDCl_3$): δ 7.50 (*t*, ^{3}J = 7.6 Hz, 1H), 7.14 (*s*, 4H), 7.07 (*t*, ^{3}J = 7.2 Hz, 2H), 1.99 (*s*, 12H). ^{13}C{^{1}H} NMR (100.6 MHz, $CDCl_3$): δ 146.5, 143.1, 137.7, 133.3, 129.4, 128.2, 127.5, 106.6, 20.4. MS (EI): 480 (98, $[M]^+$), 354 (5, $[M - I]^+$), 318 (41, $[M - I - Cl]^+$), 283 (22, $[M - I - 2Cl]^+$), 267 (17), 253 (11), 240 (8). HRMS (EI) *m/z*: calcd for $C_{22}H_{19}Cl_2I_1$: 479.9909; found: 479.9909.

5.2.17 [2,6-Bis(4-chloro-2,6-dimethylphenyl)phenyl]dimethylsilane (45)

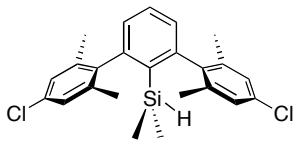

Chemical Formula: $C_{24}H_{26}Cl_2Si$
Molecular Weight: 413.455

The same procedure described in 5.2.3 was followed. The product was obtained in 77% yield as white powder.

M.p.: 90-92 ˚C. IR (neat): 3049 *w*, 2954 *m*, 2920 *m*, 2855 *w*, 2152 *m*, 1585 *m*, 1472 *m*, 1443 *m*, 1378 *w*, 1248 *m*, 1172 *w*, 1120 *m*, 1084 *w*, 1049 *w*, 1031 *w*, 996 *w*, 896 *s*, 877 *s*, 858 *s*, 837 *s*, 810 *m*, 774 *m*, 740 *m*. ^{1}H NMR (400 MHz, C_6D_6): δ 7.16 (*t*, ^{3}J = 7.6 Hz, 1 H, H–C(4')), 7.01 (*s*, 4 H, H–C(3'',5'', 3''', 5''')), 6.70 (*d*, ^{3}J = 7.6 Hz, 2 H, H–C(3', 5')), 3.80 (*eptuplet*, ^{3}J = 4.4 Hz, 1 H, H–Si), 1.82 (*s*, 12 H, H_3C–C(2'', 6'', 2''', 6''')), -0.31 (*d*, ^{3}J = 4.0 Hz, 6 H, H_3C–Si). ^{13}C{^{1}H} NMR (100.6 MHz, C_6D_6): δ 148.6 (C(2', 6')), 142.0 (C(1'', 1''')), 138.6 (C(2'', 6'', 2''', 6''')), 134.5 (C(1')), 133.5 (C(4'', 4''')), 130.8 (C(4')), 128.7 (C(3', 5')), 127.9 (C(3'', 5'', 3''', 5''')), 21.2 (Me–C), -2.2 (Me–Si). ^{29}Si NMR (79.5 MHz, C_6D_6): δ -22.9. MS (EI): 412 (14, $[M]^+$), 397 (100, $[M - CH_3]^+$), 354 (37). HRMS (EI) *m/z*: calcd for $C_{24}H_{26}Si_1Cl_2$: 412.1181; found: 412.1182.

5.2.18 [2,6-Bis(4-chloro-2,6-dimethylphenyl)phenyl]dimethylsilylium tetrakis(pentafluorophenyl)borate [42][B(C_6F_5)$_4$]

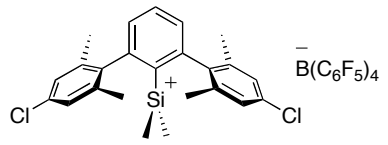

Chemical Formula: $C_{48}H_{25}BCl_2F_{20}Si$
Molecular Weight: 1091.483

The same procedure described in 5.2.4 was followed and the product was obtained in 80% yield, as yellow powder. The conversion of the reaction was 82% after 30 hrs of stirring; 12% of residual [Ph_3C][B(C_6F_5)$_4$] was recovered with the product.

^{1}H NMR (400 MHz, C_6D_6): δ 7.35 (*t*, ^{3}J = 7.6 Hz, 1 H, H–C(4')), 7.02 (*s*, 4 H, H–C (3'', 5'', 3''', 5''')), 6.96 (*d*, ^{3}J = 7.6 Hz, 2 H, H–C(3', 5')), 1.59 (*s*, 12 H, Me–C), -0.56 (*s*, 6 H, Me–Si). ^{13}C{^{1}H} NMR (100.6 MHz, C_6D_6): δ 150.6 (C(1'', 1''')), 145.6 (C(2', 6')), 144.1 (C(1')), 137.9 (C(3'', 5'', 3''', 5''')), 137.8 (C(4'', 4''')), 134.8 (C(4')), 133.3 (C(2'', 6'', 2''', 6''')), 128.8 (C(3', 5')), 20.9 (Me–C), -1.5 (Me-Si). ^{29}Si NMR (79.5 MHz, C_6D_6): δ 95.4.

5.2.19 [2,6-Bis(4-chloro-2,6-dimethylphenyl)phenyl]dimethylsilylium hexachlorocarborane [42][$CHB_{11}H_5Cl_6$]

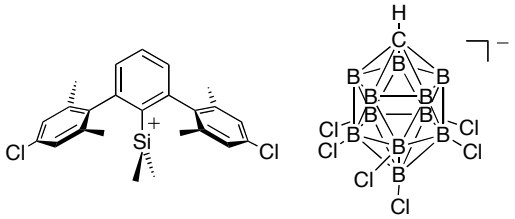

Chemical Formula: $C_{25}H_{26}B_{11}Cl_8Si$
Molecular Weight: 757.10389

The same procedure described for the synthesis and crystallization in 5.2.5 was followed. Crystals suitable for X-ray analysis were obtained at rt after 2 weeks.

5.2.20 2'-azopyrrolidine-3'-bromo-2,6-difluoro-1:1'-diphenyl (50)

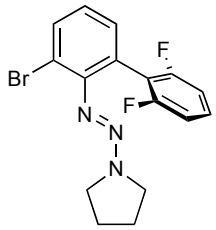

Chemical Formula: $C_{16}H_{14}BrF_2N_3$
Molecular Weight: 366.203

The same procedure described in 5.2.1 was followed. The product was obtained in 40% yield as yellow oil.

IR (solution in CH_2Cl_2): 3069*w*, 2980*m*, 2877*m*, 1921*w,* 1626*m*, 1588*m*, 1553*w*, 1466*s*, 1443*m*, 1416*s*, 1341*s*, 1317*s*, 1221*m*, 1233*m*, 1073*m*, 1001*s*, 970*w*, 906*w*, 849*w*, 788*s*, 765*s*, 698*m*, 598*w*, 543*w*. ^{1}H NMR (400 MHz, $CDCl_3$): δ 7.65 (*dd*, ^{3}J = 8 Hz, J_{H-F} = 1.2 Hz, 1 H), 7.50 (*t*, ^{3}J = 7.6 Hz, 1 H), 7.21 (*m*, 2 H), 6.85 (*m*, 2 H), 3.46 (*t*, ^{3}J = 6.8 Hz, 4 H), 1.86 (*s* broad, 4 H). ^{13}C{^{1}H} NMR (100.6 MHz, $CDCl_3$): δ 160.2 (dd, $^1J_{C-F}$ = 248 Hz, $^3J_{C-F}$ = 8.1Hz), 148.3, 133.5, 130.9, 128.5 (t, ^{3}J=10.6 Hz), 125.2, 122.9, 118.7, 117.6 (t, ^{2}J= 20Hz), 110.6 (dd, ^{2}J= 26 Hz, ^{4}J= 7.0 Hz), 50.8, 46.0, 23.7. ^{19}F{^{1}H} NMR (282 MHz, $CDCl_3$): δ –111.82. MS (EI): 365 (35, M^+), 357 (5), 323 (8), 295 (9), 268 (6), 188 (100). HRMS (EI) *m/z*: calcd for $C_{16}H_{14}N_3F_2Br_1$: 365.0339; found: 365.0335.

5.2.21 3'-bromo-2'-iodo-2,6-difluoro-1:1'-diphenyl (51)

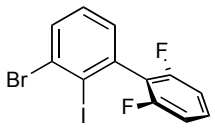

Chemical Formula: $C_{12}H_6BrF_2I$
Molecular Weight: 394.981

The same procedure described in 5.2.2 was followed. The product was obtained in 73 % yield as white powder.

M.p.: 104-104.5 ˚C. IR (neat): 3070*w*, 1626*m*, 1585*m*, 1548*m*, 1463*s*, 1434*m*, 1389*m*, 1274*m*, 1234*m*, 1185*w*, 1138*w*, 1066*w*, 1035*w*, 998*s*, 781*s*, 730*m*, 709*m*, 688*m*, 550*m*, 513*m*. ^{1}H NMR (300 MHz, $CDCl_3$): δ 7.70 (*dd*, ^{3}J = 7.6 Hz, $^{4}J_{C\text{-}F}$ = 1.5Hz, 1 H), 7.40 (*m*, 1 H), 7.31 (*m*, 1 H), 7.19 (*dd*, ^{3}J = 7.6 Hz, $^{4}J_{C\text{-}F}$ = 1.5Hz, 1 H), 7.01 (*m*, 2 H). $^{13}C\{^{1}H\}$ NMR (75 MHz, $CDCl_3$): δ 159.8 (dd, $^{1}J_{C\text{-}F}$ = 249 Hz, $^{3}J_{C\text{-}F}$ = 6.8 Hz), 138.7, 132.7, 131.1, 130.2 (t, $^{3}J_{C\text{-}F}$ = 10Hz), 129.4, 129.3, 122.6 (t, $^{2}J_{C\text{-}F}$= 20 Hz), 111.7 (dd, $^{2}J_{C\text{-}F}$ = 25 Hz, $^{4}J_{C\text{-}F}$ = 7.5Hz), 107.9. $^{19}F\{^{1}H\}$ NMR (282 MHz, $CDCl_3$): δ –112.00. MS (EI): (68, M^{+}), 188 (100). HRMS (EI) *m/z*: calcd for $C_{12}H_6BrF_2I$: 393.866567; found: 393.86636.

5.2.22 2,6-difluoro-2'-iodo-2'',3'',4'',5'',6''-pentamethyl-1,1':3'1''-terphenyl

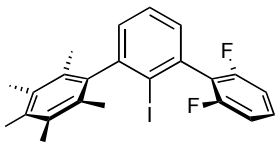

Chemical Formula: $C_{23}H_{21}F_2I$
Molecular Weight: 462.314

The same procedure described in 5.2.12 was followed. The product was obtained in 42% yield as white powder.

M.p.: 127-128 ˚C. IR (neat): 2923*m*, 1625*m*, 1581*w*, 1465*s*, 1386*w*, 1274*m*, 1234*m*, 1053*w*, 1003*s*, 834*w*, 785*m*, 729*m*, 699*w*. ^{1}H NMR (300 MHz, $CDCl_3$): δ 7.45 (*m*, 1 H), 7.34 (*m*, 1 H), 7.16 (*m*, 2 H), 6.96 (*m*, 2 H), 2.30 (*s*, 3 H), 2.25 (*s*, 6 H), 1.92 (*s*, 6 H). $^{13}C\{^{1}H\}$ NMR (75 MHz, $CDCl_3$): δ 159.9 (dd, $^{1}J_{C\text{-}F}$ = 247 Hz, $^{3}J_{C\text{-}F}$ = 6.8Hz), 149.3, 142.6, 136.4, 134.5, 132.3, 131.0, 129.7 (t, $^{3}J_{C\text{-}F}$ = 12 Hz), 129.6, 128.7, 128.2, 122.4 (t, $^{2}J_{C\text{-}F}$ = 20 Hz), 111.3 (dd, $^{2}J_{C\text{-}F}$ = 25Hz, $^{4}J_{C\text{-}F}$ = 7.5 Hz), 107.6, 17.7, 16.9, 16.6. $^{19}F\{^{1}H\}$ NMR (282 MHz, $CDCl_3$): δ –120.51. MS (EI): (462, M^{+}), 447 (14), 336 (15), 320 (47), 305 (41). HRMS (EI) *m/z*: calcd for $C_{23}H_{21}F_2I$: 462.0656; found: 462.0652.

5.2.23 [2-(2,6-difluorophenyl)-6-(2,3,4,5,6-pentamethylphenyl)phenyl] dimethylsilane (17)

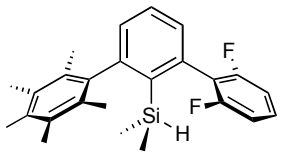

Chemical Formula: $C_{25}H_{28}F_2Si$
Molecular Weight: 394.572

The same procedure described in 5.2.3 was followed. The product was obtained in 77% yield as white powder.

M.p.: 58-59˚C. IR (neat): 2920*m*, 2158*m*, 1624*m*, 1606*m*, 1582*m*, 1464*s*, 1442*m*, 1378*w*, 1304*m*, 1273*m*, 1247*m*, 1232*m*, 1133*m*, 1052*m*, 999*s*, 890*s*, 837*m*, 786*m*, 731*m*. ^{1}H NMR (500 MHz, C_6D_6): δ 7.20 (*t*, ^{3}J = 7.5 Hz, 1 H, H-C(4')), 7.08 (*dd*, ^{3}J = 7.5 Hz, ^{4}J = 1Hz, 1 H, H-C(3')), 7.00 (*dd*, ^{3}J = 7.5 Hz, ^{4}J = 1Hz, 1 H, H-C(5')), 6.69 (*m*, 1 H, H-C(4'')), 6.58 (*m*, 2 H, H-C (3'', 5'')), 4.26 (*triplet of septuplet*, ^{3}J = 4.1 Hz, J_{H-F} = 1.4 Hz 1 H, H-Si), 2.07 (*s*, 3 H, H_3C-C(4''')), 2.06 (*s*, 6 H, H_3C-C(3''', 5''')), 1.97 (*s*, 6 H, H_3C-C (2''',6''')), 0.11 (*d*, ^{3}J= 4.5 Hz, 6 H, H-C2). ^{13}C{^{1}H} NMR (75 MHz, C_6D_6): δ 161.0 (dd, $^1J_{C-F}$ = 246 Hz, $^3J_{C-F}$ = 7.5 Hz, C(2'', 6'')), 151.4 (C6'), 140.7 (C1'''), 136.9 (C2'), 136.8 (C1'), 134.0 (C4'''), 132.2 (C(2''', 6''')), 131.9 (C(3''', 5''')), 130.2 (C5'), 129.7 (C4'), 129.4 (t, $^3J_{C-F}$ = 10Hz, C4''), 129.3 (C3'), 121.5 (t, $^2J_{C-F}$ = 22Hz, C1''), 111.2 (dd, $^2J_{C-F}$ = 26Hz, $^4J_{C-F}$ = 6Hz, C(3'', 5'')), 19.1 (CH_3-C(2''', 6''')), 16.8 (CH_3-C(4''')), 16.6 (CH_3-C(3''', 5''')), -2.8 (CH_3-Si). ^{19}F{^{1}H} NMR (282 MHz, C_6D_6): δ –111.17. ^{29}Si (59.6 MHz, C_6D_6): δ –21.6. MS (EI): 394 (25, M^+), 379 (100), 349 (6), 336 (44), 321 (23). HRMS (EI) *m/z*: calcd for $C_{25}H_{28}F_2Si$: 394.1928; found: 394.1931.

5.2.24 [2-(2,6-difluorophenyl)-6-(2,3,4,5,6-pentamethylphenyl)phenyl] dimethylsilylium tetrakis(pentafluorophenyl)borate [49][B(C$_6$F$_5$)$_4$]

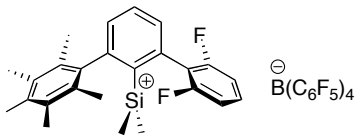

Chemical Formula: $C_{49}H_{27}BF_{22}Si$
Molecular Weight.: 1072.600

The same procedure described in 5.2.4 was followed and the product was obtained in 90 % yield, as a yellow powder.

^{1}H NMR (500 MHz, C_6D_6): δ 7.32 (*t*, ^{3}J = 7.5 Hz, 1 H, H-C(4')), 7.24 (*d*, ^{3}J = 7.5 Hz, 1 H, H-C(3')), 7.23 (*d*, ^{3}J = 7.5 Hz, 1 H, H-C(5')), 6.92 (*m*, 1 H, H-C(4'')), 6.69 (*m*, 2 H, H-C(3'', 5'')), 1.79 (*s*, 6 H, Me–C(3''', 5''')), 1.76 (*s*, 3 H, Me–C(4''')), 1.50 (*s*, 6 H, Me–C(2''', 6''')), -0.46 (*s*, 6 H, Me–Si). ^{13}C{^{1}H} NMR (125.8 MHz, C_6D_6): δ 167.6 (C(1''')), 166.8 (C(3''', 5''')), 159.8 (*dd*, $^1J_{C\text{-}F}$ = 248 Hz, $^3J_{C\text{-}F}$ = 6 Hz, C(2'', 6'')), 146.8 (C(1')), 145.7 (C(6')), 142.3 (C(4''')), 135.3 (C(2')), 132.3 (C(4')), 131.4 (*t*, $^3J_{C\text{-}F}$ = 10 Hz, C(4'')), 131.3 (C(3')), 127.5 (C(5')), 117.6 (C(2''', 6''')), 116.1 (*t*, $^2J_{C\text{-}F}$ = 18 Hz, C(1'')), 112.2 (*dd*, $^2J_{C\text{-}F}$ = 20 Hz, $^4J_{C\text{-}F}$ = 5 Hz, C(3'', 5'')), 19.2 (Me–C(2''', 6''')), 19.1 (Me–C(3''', 5''')), 15.6 (Me–C(4''')), -5.1 (Me–Si). ^{19}F{^{1}H} NMR (282 Hz, C_6D_6): δ –113.8 (*s*, 2 F), -132.1 (*m*, 8 F), -162.8 (*t*, J = 20 Hz, 4 F), -166.7 (*m*, 8 F). ^{29}Si (99.4 Hz, C_6D_6): δ 57.3.

5.2.25 [2-(2,6-difluorophenyl)-6-(2,3,4,5,6-pentamethylphenyl)phenyl]dimethyl silylium hexaclorocarborane [49][CHB$_{11}$H$_5$Cl$_6$]

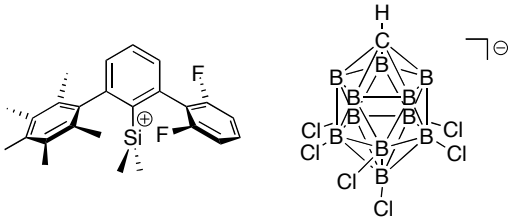

Chemical Formula: $C_{26}H_{28}B_{11}Cl_6F_2Si^+$
Molecular Weight: 738.22128

The same procedure used for the synthesis and crystallization in 5.2.5 was followed; colorless crystals suitable for X-ray analysis were obtained.

5.2.26 2,6-difluoro-2'-iodo-2'',3'',5'',6''-tetramethyl-1,1':3'1''-terphenyl

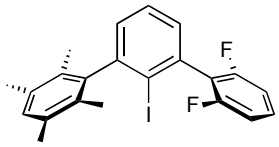

Chemical Formula: $C_{22}H_{19}F_2I$
Molecular Weight: 448.287

The same procedure described in 5.2.12 was followed. The product was obtained in 32% yield as white powder.

M.p.: 130-131 ˚C. IR (neat): 2919 *w*, 1626 *m*, 1588 *m*, 1465 *s*, 1448 *m*, 1386 *m*, 1275 *m*, 1234 *m*, 999 *s*, 871 *w*, 785 *s*, 729 *m*, 550 *w*. ^{1}H NMR (300 Hz, $CDCl_3$): δ 7.48 (*t*, ^{3}J = 7.5Hz, 1 H), 7.37 (*m*, 1 H), 7.21 (*m*, 1H), 7.13 (*m*, 1 H), 7.00 (*m*, 2 H), 2.27 (*s*, 6 H), 1.87 (*s*, 6 H). ^{13}C{^{1}H}NMR (75 Hz, $CDCl_3$): δ 159.9 (*dd*, $^{1}J_{C\text{-}F}$ = 248 Hz, $^{3}J_{C\text{-}F}$ = 7.5 Hz), 148.6, 144.8, 136.5, 133.6, 131.5, 130.9, 129.7 (*t*, $^{3}J_{C\text{-}F}$ = 9.8 Hz), 129.4, 128.9, 128.3, 122.3 (*t*, $^{2}J_{C\text{-}F}$ = 21 Hz), 111.4 (*dd*, $^{2}J_{C\text{-}F}$ = 26 Hz, $^{4}J_{C\text{-}F}$ = 7.5 Hz), 107.1, 20.1, 16.6. ^{19}F{^{1}H} NMR (282 Hz, $CDCl_3$): δ -112.50. MS (EI): 448 (35, M^+), 322 (100), 307 (62), 291 (25), 277 (19). HRMS (EI) *m/z*: calcd for $C_{22}H_{19}F_2I$: 448.04995; found: 448.04976.

5.2.27 [2-(2,6-difluorophenyl)-6-(2,3,5,6-tetramethylphenyl)phenyl]dimethyl silane (16)

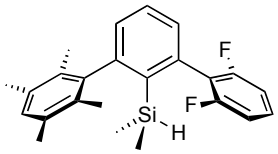

Chemical Formula: $C_{24}H_{26}F_2Si$
Molecular Weight: 380.545

The same procedure described in 5.2.3 was followed. The product was obtained in 81% yield as white powder.

M.p.: 78-79 ˚C. IR (neat): 2918 *m*, 2152 *m*, 1625 *m*, 1580 *m*, 1464 *s*, 1441 *m*, 1273 *m*, 1248 *w*, 1233 *m*, 1121 *w*, 1053 *w*, 998 *s*, 890 *s*, 840 *m*, 786 *m*, 731 *m*. ^{1}H NMR (500 MHz, C_6D_6): δ 7.23 (*t*, ^{3}J = 7.5 Hz, 1 H, H-C4'), 7.11 (*d*, ^{3}J = 7.5Hz, 1 H, H-C3'), 6.99 (*d*, ^{3}J = 7.5Hz, 1 H, H-C5'), 6.73 (*m*, 1 H, H-C4''), 6.62 (*m*, 2 H, H-C(3'', 5'')), 4.12 (*triplet of septuplet*, ^{3}J = 4.0 Hz, J_{H-F}= 1.5 Hz, 1 H, H-Si), 2.12 (*s*, 6 H, H_3C-C(3''', 5''')), 1.94 (*s*, 6 H, H_3C-C(2''', 6''')), -0.09 (*d*, ^{3}J = 4Hz, 6 H, H_3C-Si). ^{13}C{^{1}H} NMR (125.8 MHz, C_6D_6): δ 161.4 (*dd*, $^{1}J_{C-F}$ = 246 Hz, $^{3}J_{C-F}$ = 7.5 Hz, C(2'', 6'')), 150.9 (C6'), 143.3 (C1'''), 137.3 (C2'), 137.1 (C1'), 133.9 (C(3''', 5''')), 132.8 (C(2''', 6''')), 131.5 (C4'''), 130.3 (C5'), 130.1 (C4'), 129.8 (*t*, $^{3}J_{C-F}$ = 6 Hz, C4''), 129.8 (C3'), 121.8 (*t*, $^{2}J_{C-F}$ = 21 Hz, C(1'')), 111.6 (*dd*, $^{2}J_{C-F}$ = 26Hz, $^{4}J_{C-F}$ = 6Hz, C(3'', 5'')), 20.6 (C-C(3''', 5''')), 18.2 (C-C(2''', 6''')), -2.5 (CH_3-Si). ^{19}F{^{1}H} NMR (282 MHz, C_6D_6): δ –111.17. ^{29}Si NMR (79.5 MHz, C_6D_6): δ –21.5. MS (EI): 380 (13, M^+), 365 (50), 322 (100), 307 (61). HRMS (EI) *m/z*: calcd for $C_{24}H_{26}F_2Si$: 380.1772; found: 380.1772.

5.2.28 [2-(2,6-difluorophenyl)-6-(2,3,5,6-tetramethylphenyl)phenyl] dimethylsilylium tetrakis(pentafluorophenyl)borate [48][$B(C_6F_5)_4$]

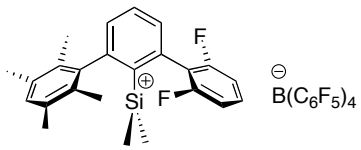

Chemical Formula: $C_{48}H_{25}BF_{22}Si$
Molecular Weight: 1058.57347

The same procedure described in 5.2.4 was followed and the product was obtained in 90% yield, as yellow powder (10% of unreacted [Ph_3C][$B(C_6F_5)_4$] was recovered along with the product).

^{1}H NMR (300 MHz, C_6D_6): δ 7.32 (*t*, ^{3}J = 7.5 Hz, 1 H, H–C(4')), 7.29 (*s*, 1 H, H–C(4''')), 7.24 (*d*, 1 H, H–C(3')), 7.20 (*d*, 1 H, H–C(5')), 6.92 (*m*, 1 H, H–C(4'')), 6.69 (*m*, 2 H, H–C(3'', 5'')), 1.84 (*s*, 6 H, CH_3–C(3''', 5''')), 1.44 (*s*, 6 H, CH_3–

C(2’’’, 6’’’), -0.44 (*s*, 6 H, CH_3–Si). $^{13}C\{^1H\}$ NMR (75 MHz, C_6D_6): δ 170.1 (C1’’’), 168.1 (C3’’’, C5’’’)), 160.2 (*dd*, $^1J_{C\text{-}F}$ = 247 Hz, $^3J_{C\text{-}F}$ = 7 Hz, C(2’’, 6’’)), 149. 5 (*d*, $^1J_{C\text{-}F}$ = 239 Hz, anion), 146.6 (C1’), 145.6 (C6’), 139.2 (*dt*, $^1J_{C\text{-}F}$ = 245Hz, anion), 137.4 (*d*, $^1J_{C\text{-}F}$ = 247 Hz, anion), 135.8 (C2’, C4’’’), 132.7 (C4’), 131.8 (C3’), 131.8 (*t*, $^3J_{C\text{-}F}$ = 11 Hz, C4’’) 127.9 (C5’), 125.5 (*m*, broad signal, anion), 118.9 (C2’’’, C6’’’), 116.4 (*t*, $^2J_{C\text{-}F}$ = 18 Hz, C1’’), 112.7 (*dd*, $^2J_{C\text{-}F}$ = 25 Hz, $^4J_{C\text{-}F}$ = 8Hz, C(3’’, 5’’)), 22.1 (Me–C(2’’’, 6’’’)), 18.8 (Me–C(3’’’, 5’’’)), -4.7 (Me–Si). $^{19}F\{^1H\}$ NMR (376.5 MHz, C_6D_6): δ –113.7 (2 F), -132.0 (8 F, anion), -162.7 (4 F, anion), -166.6 (8 F, anion). ^{29}Si NMR (59.6 MHz, C_6D_6): δ 60.1.

5.2.29 2,6-difluoro-2’-iodo-2’’,4’’,6’’-trimethyl-1,1’:3’1’’-terphenyl

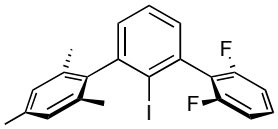

Chemical Formula: $C_{21}H_{17}F_2I$
Molecular Weight: 434.261

The same procedure described in 5.2.12 was followed. The product was obtained in 35% yield as white powder.

M.p.: 115-116 ˚C. IR (neat): 2917 *w*, 1626 *m*, 1589 *m*, 1465 *s*, 1389 *m*, 1275 *m*, 1233 *m*, 1002 *s*, 851*m*, 798 *m*, 784 *m*,732 *m*, 693 *w*. ^1H NMR (300 MHz, $CDCl_3$): δ 7.47 (*t*, ^3J = 7.5 Hz, 1 H), 7.35 (*m*, 1 H), 7.18 (*m*, 2 H), 6.97 (*m*, 4 H), 2.34 (*s*, 3 H), 1.98 (*s*, 6 H). ^{13}C NMR (75 MHz, $CDCl_3$): δ 159.9 (*dd*, $^1J_{C\text{-}F}$ = 248 Hz, $^3J_{C\text{-}F}$ = 6.8 Hz), 147.4, 141.8, 137.3, 136.6, 135.5, 129.8 (*t*, $^3J_{C\text{-}F}$ = 10 Hz), 129.4, 129.1, 128.4, 128.1, 122.3 (*t*, $^2J_{C\text{-}F}$= 21 Hz), 111.4 (*dd*, $^2J_{C\text{-}F}$ = 26 Hz, $^4J_{C\text{-}F}$ = 7.5 Hz), 106.9, 21.2, 20.2. $^{19}F\{^1H\}$ NMR (282 MHz, $CDCl_3$): δ –112.49. MS (EI): 434 (100, M^+), 307 (26), 292 (41), 277 (27). HRMS (EI) *m/z*: calcd for $C_{21}H_{17}F_2I$: 434.03430; found: 434.03405.

5.2.30 [2-(2,6-difluorophenyl)-6-(2,4,6-trimethylphenyl)phenyl]dimethylsilane (15)

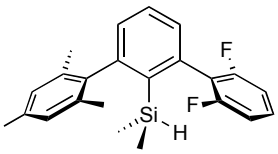

Chemical Formula: $C_{23}H_{24}F_2Si$
Molecular Weight: 366.519

The same procedure described in 5.2.3 was followed. The product was obtained in 62% yield as white powder.

M.p.: 65-65.5 ˚C. IR (neat): 2955 *w*, 2918 *w*, 2153 *m*, 1624 *m*, 1583 *m*, 1464 *s*, 1442 *m*, 1273 *m*, 1248 *w*, 1233 *m*, 1121 *w*, 1051 *w*, 998 *s*, 890 *s*, 850 *m*, 807 *m*, 786 *m*, 727 *m*, 657 *w*, 550 *w*. ^{1}H NMR (400 MHz, C_6D_6): δ 7.21 (*t*, ^{3}J= 7.6 Hz, 1 H, H-C4'), 7.09 (*dd*, ^{3}J = 7.6 Hz, ^{4}J = 1.2 Hz, 1 H, H-C3'), 6.95 (*dd*, ^{3}J = 7.6 Hz, ^{4}J = 1.2 Hz, 1 H, H-C5'), 6.82 (*s*, 2 H, H-C(3''', 5''')), 6.71 (*m*, 1 H, H-C(4'')), 6.60 (*m*, 2 H, H-C(3'', 5'')), 4.13 (*triplet of septuplet*, ^{3}J = 4.0 Hz, J_{H-F} = 1.2 Hz, 1 H, H-Si), 2.16 (*s*, 3 H, H_3C-C(4''')), 2.02 (*s*, 6 H, H_3C-C(2''', 6''')), -0.05 (*d*, ^{3}J = 4 Hz, 6 H, H_3C-Si). ^{13}C NMR (100.6 MHz, C_6D_6): δ 161.1 (*dd*, $^1J_{C-F}$ = 246Hz, $^3J_{C-F}$ = 7 Hz, C(2'', 6'')), 149.3 (C6'), 140.3 (C1'''), 137.0 (C(2', 4''')), 136.8 (C1'), 136.4 (C(2''', 6''')), 129.9 (C(4', 5')), 129.6 (C4''), 129.5 (C3'), 128.6 (C(3''',5''')), 121.4 (*t*, $^2J_{C-F}$ = 22 Hz, C(1'')), 111.31 (*dd*, $^2J_{C-F}$ = 26 Hz, $^4J_{C-F}$ = 7 Hz, C(3'',5'')), 21.24 (C(2''', 4''', 6''')), -2.72 (H_3C-Si). ^{19}F{^{1}H} NMR (282 MHz, C_6D_6): δ –111.07. ^{29}Si NMR (59.6 MHz, C_6D_6): δ –21.5. MS (EI): 366 (12, M^+), 351 (38), 308 (100). HRMS (EI) *m/z*: calcd for $C_{23}H_{24}F_2Si$: 366.1615; found: 366.1613.

5.2.31 [2-(2,6-difluorophenyl)-6-(2,4,6-trimethylphenyl)phenyl] dimethylsilylium tetrakis(pentafluorophenyl)borate [47][$B(C_6F_5)_4$]

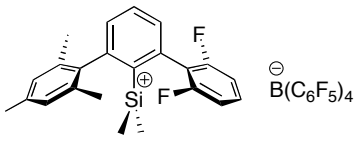

Chemical Formula: $C_{47}H_{23}BF_{22}Si$
Molecular Weight: 1044.54744

The same procedure used in 5.2.4 was followed and the product was obtained in 85% conversion (15% of residual $[Ph_3C][B(C_6F_5)_4]$ was detected in the ^1H NMR) after 22 hrs of stirring. In the ^1H NMR the protons in the *meta* positions of the methylated flanking ring (H–C(3''', 5''')) are not detectable, probably because of an H–D exchange.

^1H NMR (500 MHz, C_6D_6): δ 7.63 (*d*, ^3J = 7.5 Hz, 1 H, H–C(3')), 7.32 (*t*, ^3J = 8.0 Hz, 1 H, H–C(4'), 6.95 (*d*, ^3J = 7.5 Hz, 1 H, H–C(5')), 6.86 (*m*, 1 H, H–C(4'')), 6.68 (*m*, 2 H, H–C(3'', 5'')), 2.07 (*s*, 3 H, Me–C(4''')), 1.61 (*s*, 6 H, Me–C(2''', 6''')), -0.18 (*t*, J_{H-F} = 5.5 Hz, 6 H, Me–Si). ^{13}C NMR (125.8 MHz, C_6D_6): δ 161.2 (*dd*, $^1J_{C-F}$ = 241 Hz, $^3J_{C-F}$ = 8 Hz, C(2'', 6'')), 149.9 (*d*, $^1J_{C-F}$ = 241 Hz, anion), 146.3 (C1'''), 145.8 (C6'), 143.3 (C4'''), 138.8 (*m*, $^1J_{C-F}$ = 230 Hz, anion), 137.8 (C(3''', 5''')), 136.9 (*m*, $^1J_{C-F}$ = 236 Hz, anion), 134.8 (*t*, $^4J_{C-F}$ = 5 Hz, C1'), 133.8 (C4'), 133.2 (C(2''', 6''')), 132.7 (C2'), 131.3 (*t*, $^3J_{C-F}$ = 14 Hz, C(4'')), 130.0 (*t*, $^4J_{C-F}$ = 5 Hz, C3'), 129.1 (C5'), 125.5 (*m*, broad signal, anion), 114.1 (*t*, $^2J_{C-F}$ = 14 Hz, C(1'')), 113.7 (*m*, $^2J_{C-F}$ = 38 Hz, C(3'', 5'')), 20.3 (Me–C(2''', 6''')), 20.2 (Me–C(4''')), -2.0 (*t*, J_{C-F} = 5 Hz, Me–Si). $^{19}F\{^1H\}$ NMR (282 MHz, C_6D_6): δ -115.1 (2 F), -132.1 (8 F, anion), -162.8 (4 F, anion), -166.7 (8 F, anion). ^{29}Si $\{^1H\}$ NMR (59.6 MHz, C_6D_6): δ 95.5 (*t*, J_{Si-F} = 42 Hz).

5.2.32 2,6-difluoro-2'-iodo-2'',6''-dimethyl-1,1':3'1''-terphenyl

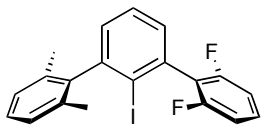

Chemical Formula: $C_{20}H_{15}F_2I$
Molecular Weight: 420.234

The same procedure described in 5.2.12 was followed. The product was obtained in 63% yield as white powder.

M.p.: 117-118˚C. IR (neat): 3065 *w*, 2917 *w*, 1626 *m*, 1587 *m*, 1464 *s*, 1388 *m*, 1276 *m*, 1234 *m*, 999 *s*, 797 *m*, 784 *s*, 770 *s*, 728 *s*, 686 *m*, 565 *w*, 548 *m*. ^1H NMR (400 MHz, $CDCl_3$): δ 7.47 (*t*, ^3J= 7.6, 1 H), 7.30 (*m*, 1 H), 7.17-7.22 (*m*, 2 H), 7.10-7.16

(*m*, 3 H), 6.96 (*m*, 2 H), 2.01 (*s*, 6 H). $^{13}C\{^{1}H\}$ NMR (75 MHz, $CDCl_3$): δ 159.8 (*dd*, $^{1}J_{C\text{-}F}$ = 248 Hz, $^{3}J_{C\text{-}F}$ = 6.8 Hz), 147.2, 144.5, 136.7, 135.6, 129.8 (*t*, $^{3}J_{C\text{-}F}$ = 10Hz), 129.2, 129.1, 128.4, 127.7, 127.3, 122.2 (*t*, $^{2}J_{C\text{-}F}$ = 20 Hz), 111.3 (*dd*, $^{2}J_{C\text{-}F}$ = 25 Hz, $^{4}J_{C\text{-}F}$ = 6.8 Hz), 106.4, 20.3. $^{19}F\{^{1}H\}$ NMR (376 MHz, $CDCl_3$): δ –112.46. MS (EI): 420 (100, M^+), 293 (42), 277 (44), 257 (15). HRMS (EI) *m/z*: calcd for $C_{20}H_{15}F_2I$: 420.01865; found: 420.01811.

5.2.33 [2-(2,6-difluorophenyl)-6-(2,6-dimethylphenyl)phenyl]dimethylsilane (14)

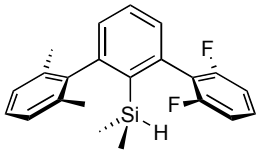

Chemical Formula: $C_{22}H_{22}F_2Si$
Molecular Weight: 352.492

The same procedure described in 5.2.3 was followed. The product was obtained in 84% yield as colorless oil.

IR (neat): 3058 *w*, 2957 *w*, 2916 *w*, 2150 *m*, 1624 *m*, 1583 *m*, 1464 *s*, 1442 *m*, 1378 *w*, 1273 *m*, 1249 *m*, 1233 *m*, 1123 *w*, 1052 *w*, 998 *s*, 889 *s*, 838 *m*, 807 *m*, 787 *m*, 769 *m*, 731 *m*, 655 *w*, 549 *w*. ^{1}H NMR (500 MHz, C_6D_6): δ 7.18 (*t*, ^{3}J= 7.5 Hz, 1 H, H-C(4')), 7.07 (*m*, 2 H, H-C(3',4''')), 6.98 (*d*, ^{3}J= 7.5 Hz, 2 H, H-C(3''',5''')), 6.88 (*dd*, ^{3}J = 8Hz, ^{4}J = 1.5Hz, 1 H, H-C(5')), 6.71 (*m*, 1 H, H-C(4'')), 6.59 (*m*, 2 H, H-C(3'',5'')), 4.08 (*triplet of septuplet*, $^{3}J_{H\text{-}H}$ = 4.1 Hz, $J_{H\text{-}F}$ = 1.1 Hz, 1 H, H-Si), 2.00 (*s*, 6 H, H_3C-C(2''', 6''')), -0.09 (*dd*, ^{3}J= 4 Hz, $J_{H\text{-}F}$ = 1Hz, 6 H, H_3C-Si). $^{13}C\{^{1}H\}$ NMR (125.8 MHz, C_6D_6): δ 161.35 (dd, $^{1}J_{C\text{-}F}$ = 246 Hz, $^{3}J_{C\text{-}F}$ = 7.3 Hz, C(2'',6'')), 149.4 (C6'), 143.4 (C1'''), 137.4 (C2'), 136.9 (C(2''',6''')), 136.8 (C1'), 130.2 (C4'), 130.0 (C3'), 129.9 (s+t, $^{3}J_{C\text{-}F}$ = 11Hz, C(4'',5')), 128.1 (C4'''), 127.9 (C(3''',5''')), 121.6 (t, $^{2}J_{C\text{-}F}$ = 22Hz, (C1'')), 111.6 (dd, $^{2}J_{C\text{-}F}$ = 26Hz, $^{4}J_{C\text{-}F}$ = 6Hz, C(3'',5'')), 21.6 (H_3C-C(2''',6''')), -2.5 (H_3C-Si). $^{19}F\{^{1}H\}$ NMR (282 MHz, C_6D_6): δ –111.08. ^{29}Si NMR (59.6 MHz, C_6D_6): δ –21.4. MS (EI): 352 (12, M^+), 337 (46), 275 (76), 255 (48), 241 (100). HRMS (EI) *m/z*: calcd for $C_{22}H_{22}F_2Si$: 352.1459; found: 352.1454.

5.2.34 [2-(2,6-difluorophenyl)-6-(2,6-dimethylphenyl)phenyl] dimethylsilylium tetrakis(pentafluorophenyl)borate [46][$B(C_6F_5)_4$]

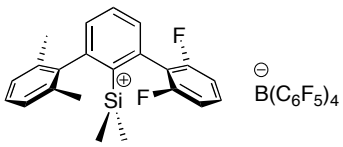

Chemical Formula: $C_{46}H_{21}BF_{22}Si$
Molecular Weight: 1030.52031

The same procedure described in 5.2.4 was followed and the product was obtained with 93% conversion (7% of residual $[Ph_3C][B(C_6F_5)_4]$ was detected in the ^1H NMR) after 21 hrs of stirring. In the ^1H NMR the protons in the *meta* and *para* positions of the methylated flanking ring (H–C(3’’’, 4’’’, 5’’’)) are not detectable, because of an H–D exchange. Also the carbon atoms of these positions are not clearly detectable when the ^{13}C NMR is recorded in C_6D_6. When the measurements were performed in C_6H_6 (with DMSO capillary in the tube for locking and shimming) the proton and carbon signals for the *meta* and *para* positions were identified.

^1H NMR (400 MHz, $CDCl_3$): δ 7.69 (*d*, ^3J= 8.1 Hz, 1 H, H-C(3’)), 7.31 (*t*, ^3J= 8.1 Hz, 1 H, H-C(4’)), 6.82 (*m*, 2 H, H–C(4’’) + H–C(5’)), 6.69 (*m*, 2 H, H-C(3’’, 5’’)), 1.61 (*s*, 6 H, Me-C(2’’’, 6’’’)), -0.17 (*s*, 6 H, Me-Si). $^{13}C\{^1H\}$ NMR (75 MHz, C_6D_6): δ 162.2 (*dd*, $^1J_{C\text{-}F}$ = 239 Hz, $^3J_{C\text{-}F}$ = 9 Hz, C(2’’, 6’’)), 149.5 (*d*, $^1J_{C\text{-}F}$ = 240 Hz, anion), 146.9 (C6’), 145.2 (C1’’’), 139.2 (*d*, $^1J_{C\text{-}F}$ = 246 Hz, anion), 137.4 (*d*, $^1J_{C\text{-}F}$ = 241 Hz, anion), 135.6 (C(2’’’, 6’’’)), 134.6 (C4’), 134.4 (C3’’’, 5’’’), 132.5 (C2’), 132.2 (C4’’’), 132.0 (*t*, $^4J_{C\text{-}F}$ = 7 Hz, C1’), 131.8 (*t*, $^3J_{C\text{-}F}$ = 14 Hz, C4’’), 130.1 (*t*, $^4J_{C\text{-}F}$ = 7 Hz, C3’), 130.1 (C5’), 125.5 (broad signal, anion), 114.5 (*m*, $^2J_{C\text{-}F}$ = 28 Hz, C(3’’, 5’’)), 114.3 (*t*, $^2J_{C\text{-}F}$ = 16 Hz, C1’’), 20.6 (*s*, Me–C(2’’’, 6’’’)), -1.5 (*t*, $J_{C\text{-}F}$ = 7 Hz, Me–Si). $^{19}F\{^1H\}$ NMR (282 MHz, C_6D_6): δ –115.7 (2 F), -132.0 (8 F, anion), -116.7 (4 F, anion), -166.6 (8 F, anion). ^{29}Si $\{^1H\}$ NMR (79.5 MHz, C_6D_6): δ 101.0 (broad signal).

5.2.35 [2-(2,6-difluorophenyl)-6-(2,6-dimethylphenyl)phenyl] dimethylsilylium hexaclorocarborane [46][$CHB_{11}H_5Cl_6$]

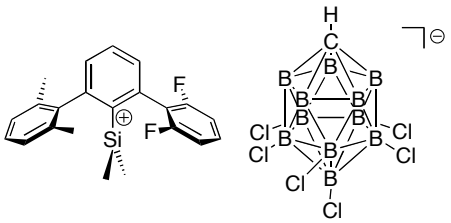

Chemical Formula: $C_{23}H_{22}B_{11}Cl_6F_2Si^+$
Molecular Weight: 696.14154

The same procedure described for the synthesis and crystallization in 5.2.5 was followed and slightly yellow crystals suitable for X-ray analysis were obtained.

5.2.36 8-fluoronaphthalen-1-amine (58)

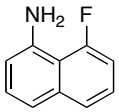

Chemical Formula: $C_{10}H_8FN$
Molecular Weight: 161.175

This molecule has been synthesized introducing little modifications to the procedure published in the Patent with international application n. PCT/IB2006/002979, international publication n. WO 2007/049124 A1, applicant Pfizer Products Inc., publication date May 3, 2007.

Hydrogen fluoride-pyridine (70% HF / 30% pyridine, 6 ml) was placed in a PET bottle and cooled with an ice bath. Naphthol[1,8-de][1,2,3]triazene (synthesized as described in *Tetrahedron* **2005**, *61*, 10507; 8.87 mmol) was added in portions. After the addition the bottle was rinsed with additional 4 ml of hydrogen fluoride-pyridine, to wash down the solid on the sidewall of the container. The bottle was sealed and connected to a N_2 line through a syringe needle; a second exit needle was connected to a washing bottle containing 1M KOH. The reaction mixture was stirred under N_2 at rt for 7 days. After this time the reaction mixture was cooled in an ice bath and KOH (60% w/w in water, 60 ml) was added slowly until pH > 11. The resulting mixture was diluted with EtOAc (100 ml) and stirred for 30 min. The organic layer was

extracted and then filtered through a pad of celite. The bi-layer filtrate was separated; the organic layer was washed with brine (2 × 50 ml), H_2O (2 × 50 ml), sat. sol. $NaHCO_3$ (2 × 50 ml), brine (2 × 50 ml). The solution was degassed with N_2 for 20 min to prevent the oxidation of the amino group. The solution was concentrated to afford a dark red oil that was purified via column chromatography on SiO_2 (eluent: hexane/EtOAc 9:1). The product was obtained in 68% yield as light pink powder.

^{1}H NMR (500 MHz, DMSO-d_6): δ 7.53 (*dd*, ^{3}J= 8 Hz, 1 H), 7.31 (*m*, 1H), 7.24 (m, 1H), 7.10-7.00 (*m*, 2 H), 6.70 (*dd*, ^{3}J= 8 Hz, 1 H), 5.70 (*s*, 2H). ^{13}C{^{1}H} NMR (100.6 MHz, DMSO-d_6): δ 159.8 (*d*, $^1J_{C\text{-}F}$ = 248 Hz), 143.7 (*d*, $J_{C\text{-}F}$ = 3 Hz), 136.9 (*d*, $J_{C\text{-}F}$ = 5 Hz), 127.9, 125.4 (*d*, $J_{C\text{-}F}$ = 10 Hz), 124.2 (*d*, $J_{C\text{-}F}$ = 4 Hz), 114.9 (*d*, $J_{C\text{-}F}$ = 4 Hz), 112.2 (*d*, $J_{C\text{-}F}$ = 10 Hz) 109.1, 108.4 (*d*, $J_{C\text{-}F}$ = 23 Hz). ^{19}F{^{1}H} NMR (376 MHz, DMSO-d_6): δ -114.7. MS (EI): 161 (100, M^+), 140 (15), 133 (22), 114 (14), 80 (9). HRMS (EI) *m/z*: calcd for $C_{10}H_8N_1F_1$: 161.0641; found: 1610642.

5.2.37 1-bromo-8-fluoronaphthalene (59)

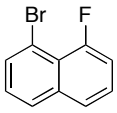

Chemical Formula: $C_{10}H_6BrF$
Molecular Weight: 225.057

In a one necked flask, 8-fluoronaphthalenamine (3.1 mmol) was suspended in HBr (48% w/w in water, 10 ml). A gentle heating was applied to favor the protonation of the amino group. The suspension was cooled to ~ 3˚C (ice bath) and a solution of $NaNO_2$ (3.3 mmol in 3 ml of H_2O) was added dropwise, controlling the temperature. The reaction mixture turned dark yellow and was stirred at 3˚C for 30 min. A solution of CuBr (2.05 mmol) in HBr (48% w/w in water, 4 ml) was cooled to 3˚C in a round bottom flask. The diazonium salt, formed in the meanwhile, was poured at once in the CuBr solution. The dark mixture was heated at 80˚C for 30 min. The crude was diluted in CH_2Cl_2, the organic phase was separated and washed with NaOH (1 M, 20 ml) and H_2O (20 ml). The purification on SiO_2 (eluent: hexane) afforded the product in 61% yield as a white powder.

^{1}H NMR (400 MHz, $CDCl_3$): δ 7.77-7.80 (*m*, 2 H), 7.64-7.62 (*m*, 1 H), 7.44-7.39 (*m*, 1 H), 7.28 (*t*, ^{3}J = 8 Hz,1 H), 7.25-7.19 (*m*, 1 H). ^{13}C{^{1}H} NMR (100.6 MHz, $CDCl_3$): δ 158.1 (*d*, $^{1}J_{C-F}$ = 257 Hz), 137.0, 132.9, 127.7 (*d*, J_{C-F} = 4 Hz), 126.9, 126.4 (*d*, J_{C-F} = 8 Hz), 124.7 (*d*, J_{C-F} = 5 Hz), 122.4 (*d*, J_{C-F} = 9 Hz), 115.0, 112.4 (*d*, J_{C-F} = 23 Hz). ^{19}F{^{1}H} NMR (376 MHz, $CDCl_3$): δ -112.7. MS (EI): 224 (100, M^+), 145 (75, [M - Br] $^{+}$), 125 (24, M – Br - F] $^{+}$), 112 (10), 99 (7), 72 (12). HRMS (EI) *m/z*: calcd for $C_{10}H_6F_1Br_1$: 223.9637; found: 223.9637.

5.2.38 2,6-Bis(8-fluoronaphthyl)iodobenzene (60)

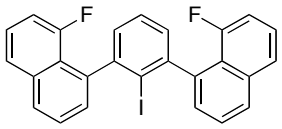

Chemical Formula: $C_{26}H_{15}F_2I$
Molecular Weight: 492.298

The same procedure described in 5.2.12 was followed. The crude was purified via column chromatography on SiO_2 (eluent: hexane/EtOAc 99:1 to 96:4). The product was obtained as a yellow powder in 65% yield as a mixture of two diastereomer in a ratio of 80:20. A variable temperature ^{1}H and ^{19}F NMR analysis was performed in DMSO-d_6. The solution was heated in the temperature range 300-380 K, and then cooled to 300 K again. During the heating process the ratio between the two diastereomers reaches the equilibrium of 1:1 that is maintained upon cooling back to 300 K. The mixture has reached in this way its thermodynamic equilibrium (Figure 5.2).

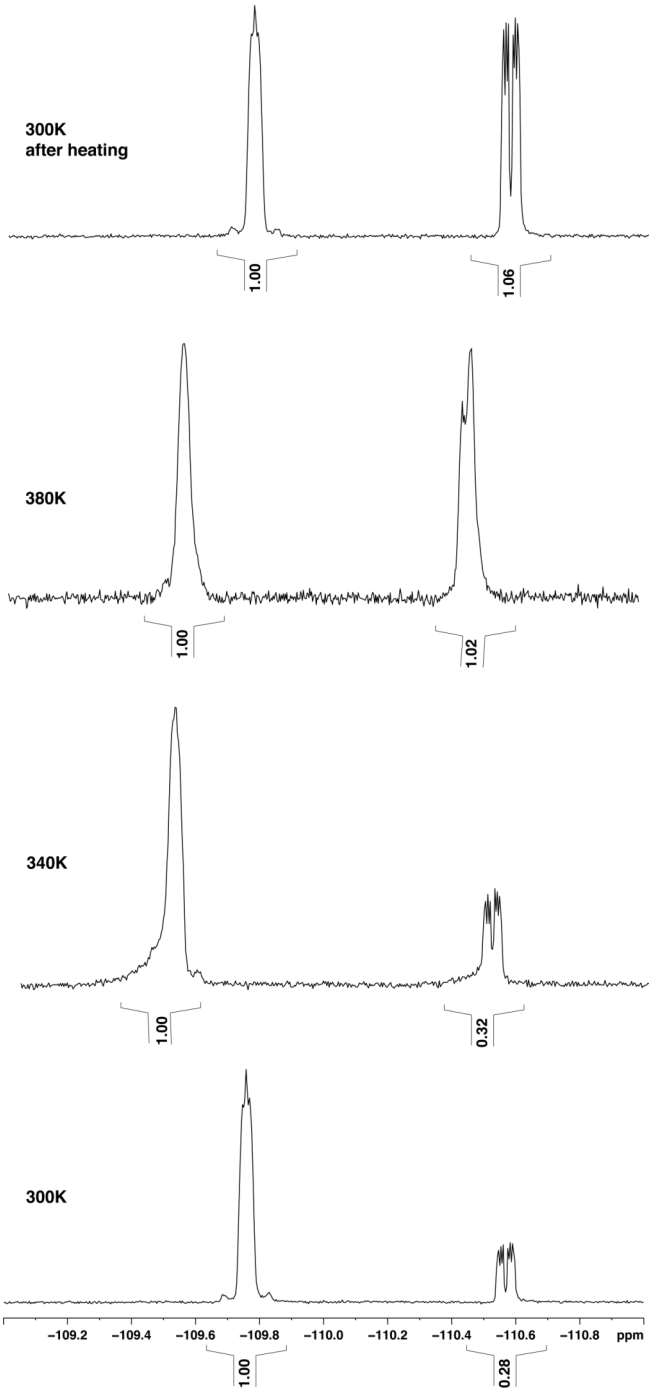

Figure 5.2 Variable temperature ^{19}F NMR analysis of **60** in DMSO-d_6.

IR (neat): 3053 *w*, 2920 *w*, 2848 *w*, 1628 *w*, 1595 *m*, 1574 *m*, 1509 *m*, 1468 *m*, 1428 *w*, 1375 *s*, 1333 *m*, 1279 *w*, 1235 *s*, 1095 *m*, 1070 *w*, 1026 *m*, 1009 *m*, 987 *m*, 821 *s*, 811 *m*, 759 *s*, 731 *s*, 677 *m*. ^1H NMR (500 MHz, $CDCl_3$): δ 7.91 (*d*, int.: 2.0), 7.70 (*m*, int.: 2.0), 7.56 (*m*, int.: 2.1), 7.45-7.40 (*m*, int.: 3.5), 7.34-7.32 (*m*, int.: 3.6), 7.16-7.12 (*m*, int.: 1.6), 7.10-7.07 (*m*, int.: 0.5). $^{13}C\{^1H\}$ NMR (100.6 MHz, $CDCl_3$): δ 159.1 (*d*, $^1J_{C\text{-}F}$ = 259 Hz), 148.1, 140.1, 135.5, 129.1, 128.7, 127.9, 127.6, 126.5,

126.0, 125.9, 124.3, 111.5, 111.3, 111.1. $^{19}F\{^{1}H\}$ NMR (282 MHz, $CDCl_3$): δ -110.0 (integral: 1.00), -110.7 (integral: 0.25). MS (EI): 492 (100, M^+), 365 (18, $[M\text{-}I]^+$), 344 (37), 324 (7), 246 (18), 220 (6), 181 (15), 172 (27). HRMS (EI) *m/z*: calcd for $C_{26}H_{15}F_2I_1$: 492.0187; found: 492.0183.

5.2.39 [2,6-Bis(8-fluoronaphtyl)phenyl]dimethylsilane (61)

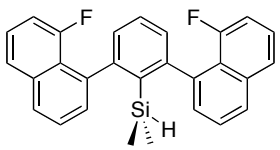

Chemical Formula: $C_{28}H_{22}F_2Si$
Molecular Weight: 424.556

The same procedure described in 5.2.3 was followed. The product was obtained in 87% yield as white powder. Starting from the iodo–precursor in 80:20 ratio of two diastereomers, the product was obtained in a ~ 50:50 ratio. During the lithiation a racemization process takes place and results in the loss of stereogenic information.

IR (neat): 3052 *w*, 2958 *w*, 2921 *w*, 2154 *w*, 1628 *w*, 1595 *w*, 1577 *w*, 1560 *w*, 1509 *w*, 1466 *w*, 1426 *w*, 1372 *m*, 1332 *w*, 1264 *m*, 1240 *m*, 1026 *w*, 986 *w*, 886 *m*, 823 *m*, 762 *m*, 735 *s*, 705 *w*. ^{1}H NMR (400 MHz, C_6D_6): δ 7.58-7.51 (*m*, int.: 2.7), 7.39-7.31 (*m*, int.: 5.6), 7.27-7.15 (*m*, int.: 9.4), 7.03-6.95 (*m*, int.: 2.7), 6.91-6.83 (*m*, int.: 2.8), 3.91-3,83 (*m*, int.: 1.0), -0.31 (*m*, int.: 5.4), -0.44 (*d*, int.: 1.6). $^{13}C\{^{1}H\}$ NMR (125.8 MHz, C_6D_6): δ 160.5 (*d*), 150.5, 139.7, 139.5, 136.4, 130.7, 130.0, 128.0, 127.7,126.6,126.4, 126.3,126.0, 125.0, 124.8, 111.9, 111.7, -0.9, -1.5, -2.0. $^{19}F\{^{1}H\}$ NMR (282 MHz, C_6D_6): δ -106.1 (int.: 1.00), -107.3 (int.: 0.78). $^{29}Si\ \{^{1}H\}$ NMR (79.5 MHz, C_6D_6): δ -21.3, -21.4. MS (EI): 424 (7, M^+), 366 (19, $[M - Me_2Si]^+$), 347 (100, $[M - Me_2Si - F]$), 327 (77, $[M - Me_2Si - 2F)]$. HRMS (EI) *m/z*: calcd for $C_{28}H_{22}F_2Si_1$: 424.1459; found: 424.1452.

5.2.40 Product of sila-Friedel–Crafts 62

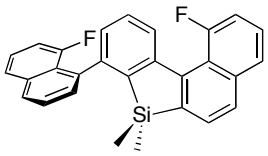

Chemical Formula: $C_{28}H_{20}F_2Si$
Molecular Weight: 422.54071

In glove box, the silane (0.18 mmol), $[Ph_3C][B(C_6F_5)_4]$ (0.18 mmol) and P(*o*-tolyl)$_3$ were charged in a vial with 1 ml of C_6D_6. The reaction mixture, formed by a brown oily phase and a transparent upper layer, was stirred at rt for 29 hrs. The upper layer was analyzed via ^{29}Si, ^{19}F NMR, and GC-MS till no more starting material was detected. The upper layer was diluted in EtOAc (5 ml), washed with H_2O, dried with $MgSO_4$, and the solvent was evaporated. The crude was purified via column chromatography on Al_2O_3 (eluent: hexane). The product was obtained as a yellow oil in 42% yield. This reaction was performed only once, but in a future attempt it is advisable to charge the crude directly in column chromatography, skipping the work up step. Crystals suitable for X-ray analysis were obtained by dissolving, at ~ 70°C, 20 mg of product in a small vial with 0.5 ml of acetonitrile; a clear solution was obtained and upon cooling to rt crystals slowly formed (after 3 days they had reached a suitable size for the analysis).

IR (neat): 3053 *w*, 2957 *w*, 2865 *w*, 1625 *w*, 1595 *w*, 1564 *m*, 1543 *m*, 1509 *w*, 1468 *m*, 1433 *w*, 1374 *m*, 1336 *m*, 1238 *s*, 1118 *m*, 1093 *w*, 1045 *w*, 1024 *w*, 989 *w*, 867 *m*, 825 *s*, 812 *s*, 765 *s*, 749 *s*. ^{1}H NMR (400 MHz, $CDCl_3$): δ 7.95-7.92 (*m*), 7.76-7.42 (*m*), 7.31-7.05 (*m*), 0.12 (*s*, 3H), -0.25 (*s*, 3H). $^{13}C\{^1H\}$ NMR (100.6 MHz, C_6D_6): δ 159.4 (*d*, $^1J_{C\text{-}F}$ = 256 Hz), 158.5 (*d*, $^1J_{C\text{-}F}$ = 253 Hz), 148.5, 148.2 (*d*, $J_{C\text{-}F}$ = 3 Hz), 143.6 (*d*, $J_{C\text{-}F}$ = 3 Hz), 142.0, 138.5, 138.0 (*d*, $J_{C\text{-}F}$ = 5 Hz), 137.8, 129.9, 129.0 (*d*, $J_{C\text{-}F}$ = 3 Hz), 128.7, 127.6, 127.3 (*d*, $J_{C\text{-}F}$ = 4 Hz), 127.2 (*d*, $J_{C\text{-}F}$ = 3 Hz), 126.6, 126.4, 126.2-126.0 (4 signals, belonging to 2C), 125.9, 125.0 (*d*, $J_{C\text{-}F}$ = 3 Hz), 124.5 (*d*, $J_{C\text{-}F}$ = 3 Hz), 122.3 (*d*, $J_{C\text{-}F}$ = 11 Hz), 119.3 (*d*, $J_{C\text{-}F}$ = 15 Hz), 111.8 (*d*, $J_{C\text{-}F}$ = 32 Hz), 111.6 (*d*, $J_{C\text{-}F}$ = 30 Hz), -2.0, -4.2. $^{19}F\{^1H\}$ NMR (376 MHz, C_6D_6): δ -98.2 (int.: 1.00), -106.1 (int.: 0.79). ^{29}Si $\{^1H\}$ NMR (79.5 MHz, C_6D_6): δ 1.7. MS (EI): 422 (94, M^+),

366 (49), 344 (22), 326 (100, [M – Me_2Si – 2F]$^+$). HRMS (EI) *m/z*: calcd for $C_{28}H_{20}F_2Si_1$: 422.1302; found: 422.1303.

5.2.41 1,4-Epoxynaphthalene, 8-triethylsilyl-7-fluoro-1,4-dihydro (70)

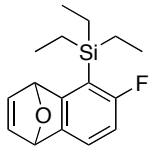

Chemical Formula: $C_{16}H_{21}FOSi$
Molecular weight: 276.42124

In a 25 ml schlenk flask under N_2 atmosphere, 1-bromo-2,4-difluoro-3-triethylsilyl benzene (5 mmol, ref.: Schlosser, M.; Heiss, C. *Eur. J. Org. Chem.* **2003**, 4618) was dissolved in dry Et_2O (7 ml). The solution was cooled to -78˚C (acetone/dry ice bath) and degassed via few vacuum/N_2 cycles. The furan (25 mmol, freshly distilled from Na/benzophenone) was added. *n*-BuLi (1.6 M in hexane, 5 mmol) was added over 5 min. The reaction mixture was stirred for 1h at -78˚C then it was allowed to warm up to rt overnight (no removal of cooling bath); during this time the colorless solution turned orange. The mixture was diluted with Et_2O and washed with H_2O (2 × 20 ml). The organic phase was dried on $MgSO_4$ and the solvent evaporated. The crude was purified via column chromatography on SiO_2 (solvent: hexane/EtOAc 95/5). The product was obtained in 65% yield as yellow oil.

IR (neat): 2954 *m*, 2912 *m*, 2875 *m*, 1610 *m*, 1575 *m*, 1458 *m*, 1425 *m*, 1392 *m*,1280 *m*, 1224 *m*, 1202 *m*, 1189 *m*, 1115 *w*, 1011 *s*, 974 *w*, 937 *w*, 884 *m*, 867 *s*, 34 *m*, 817 *s*, 795 *m*, 759 *m*, 730 *s*, 711 *s*, 697 *s*, 650 *m*, 623 *w*, 606 *w*, 585 *m*. ^{1}H NMR (400 MHz, $CDCl_3$): δ 7.16 (*m*, 1 H), 7.03 (*m*, 2 H), 6.58 (*m*, 1 H), 5.83 (*s*, 1 H), 5.67 (*s*, 1 H), 1.00-0.75 (*m*, 15 H). $^{13}C\{^1H\}$ NMR (100.6 MHz, CCl_3): δ 165.2 (*d*, $^1J_{C\text{-}F}$ = 240 Hz), 158.8 (*d*, $J_{C\text{-}F}$ = 12 Hz), 143.8,143.5 (*d*, $J_{C\text{-}F}$ = 3 Hz), 142.6, 121.9 (*d*, $J_{C\text{-}F}$ = 10 Hz), 118.5 (*d*, $J_{C\text{-}F}$ = 34 Hz), 109.8 (*d*, $J_{C\text{-}F}$ = 29 Hz), 83.1 (*d*, $J_{C\text{-}F}$ = 2 Hz), 81.8, 7.5, 4.5 (*d*, $J_{C\text{-}F}$ = 3 Hz). $^{19}F\{^1H\}$ NMR (376.5 MHz, CCl_3): δ - 104.9. MS (EI): 276 (14, M^+), 247 (65), 219 (94), 191 (100), 171 (31), 163 (58), 141 (14), 128 (33), 115 (26). HRMS (EI) *m/z*: calcd for $C_{16}H_{21}O_1F_1Si_1$: 276.1346; found: 276.1343.

5.2.42 2-fluoro-1-triethylsilylnaphthalene (71)

Chemical Formula: $C_{16}H_{21}FSi$
Molecular Weight: 260.422

In a 50 ml 2-necked flask with condenser, under N_2 atmosphere, $LiAlH_4$ (12.5 mmol) was suspended in THF (13 ml). The suspension was immediately cooled to 0°C and $TiCl_4$ (35 mmol) was added dropwise very carefully (during the addition a lot of yellow gas is formed). Dry Et_3N (45 mmol) was added; the mixture was stirred at 0°C for 30 min, then warmed up to rt. A solution of 1,4-Epoxynaphthalene, 8-triethylsilyl-7-fluoro-1,4-dihydro (1 mmol) in THF (13 ml) was added and the reaction mixture was refluxed for 3 h. The reaction mixture was poured into a mixture of ice (~ 5g) and HCl (1 M solution, 10 ml). The organic phase was extracted with EtOAc, dried on $MgSO_4$ and the solvent evaporated. The crude was purified via column chromatography on SiO_2 (eluent: hexane). The product was recovered in 78% yield as colorless oil.

IR (neat): 3062 *w*, 2954 *s*, 2929 *s*, 2874 *s*, 2358 *w*, 1619 *w*, 1590 *m*, 1572 *m*, 1509 *m*, 1456 *m*, 1426 *m*, 1374 *m*, 1314 *m*, 1304 *m*, 1260 *w*, 1209 *s*, 1126 *m*, 1006 *s*, 917 *w*, 811 *s*, 775 *m*, 745 *s*, 733 *s*, 718 *m*, 698 *m*. ^{1}H NMR (400 MHz, $CDCl_3$): δ 8.11 (*d*, ^{3}J = 8.8 Hz, 1 H), 7.82 (*m*, 2 H), 7.45 (*t*, ^{3}J = 8.4 Hz, 1 H), 7.41 (*t*, ^{3}J = 8.0 Hz, 1 H), 7.16 (*d*, ^{3}J = 8.8 Hz, 1 H), 1.12-1.04 (*m*, 6 H), 1.02-0.96 (*m*, 9 H). ^{13}C{^{1}H} NMR (100.6 MHz, CCl_3): δ 166.6 (*d*, $^1J_{C\text{-}F}$ = 241 Hz), 138.5 (*d*, $J_{C\text{-}F}$ = 13 Hz), 132.7 (*d*, $J_{C\text{-}F}$ = 11 Hz), 131.0, 129.2, 127.8 (*d*, $J_{C\text{-}F}$ = 5 Hz), 126.5, 124.5 (*d*, $J_{C\text{-}F}$ = 2 Hz), 116.6 (*d*, $J_{C\text{-}F}$ = 33 Hz), 116.4 (*d*, $J_{C\text{-}F}$ = 33 Hz), 7.9 (*d*, $J_{C\text{-}F}$ = 1 Hz), 5.7 (*d*, $J_{C\text{-}F}$ = 4 Hz). ^{19}F{^{1}H} NMR (376.5 MHz, CCl_3): δ - 96.2. MS (EI): 260 (17, M^+), 203 (73), 175 (100), 153 (4), 141 (7), 115 (4). HRMS (EI) *m/z*: calcd for $C_{16}H_{21}F_1I_1$: 260.1397; found: 260.1394.

5.2.43 2-fluoro-1-iodonaphthalene (67)

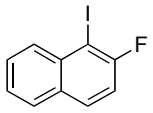

Chemical Formula: $C_{10}H_6FI$
Molecular Weight: 272.057

In a 100 ml 2-necked flask under N_2 atmosphere, 2-fluoro-1-triethylsilylnaphthalene (3.43 mmol) was dissolved in CH_2Cl_2 (50 ml). The solution was cooled to 0˚C and then I-Cl (1 M in CH_2Cl_2, 3.77 mmol) was slowly added. After 30 min the cooling bath was removed and the violet reaction mixture was stirred at rt overnight. The mixture was diluted with CH_2Cl_2; the organic phase was washed with aq. Na_2SO_3, H_2O and brine, then it was dried with $MgSO_4$ and the solvent evaporated. The crude was purified via column chromatography on SiO_2 (eluent: hexane). The product was obtained in 89% yield as a yellow powder.

M.p.: 49-50˚C. IR (neat): 3057 *w*, 2943 *w*, 1619 *m*, 1597 *m*, 1502 *m*, 1459 *m*, 1354 *m*, 1252 *m*, 1229 *s*, 983 *m*, 920 *m*, 803 *s*, 761 *s*, 742 *s*, 714 *m*, 637 *m*, 516 *m*, 507 *m*, 426 *m*. ^{1}H NMR (400 MHz, $CDCl_3$): δ 8.00 (*dd*, ^{3}J = 8.4 Hz, 1 H), 7.60 (*m*, 2 H), 7.46 (*m*, 1 H), 7.36 (*m*, 1 H), 7.08 (m, 1 H). ^{13}C{^{1}H} NMR (100.6 MHz, C_6D_6): δ 160.3 (*d*, $^1J_{C\text{-}F}$ = 244 Hz), 135.0 ($J_{C\text{-}F}$ = 3 Hz), 131.1 ($J_{C\text{-}F}$ = 6 Hz), 131.0, 130.9, 128.5, 128.4, 125.8 ($J_{C\text{-}F}$ = 3 Hz), 128.5, 128.4. ^{19}F{^{1}H} NMR (376.5 MHz, CCl_3): δ - 88.7. MS (EI): 272 (100, M^+), 145 (63, $[M - I]^+$), 125 (24), 99 (8), 75 (7). HRMS (EI) *m/z*: calcd for $C_{10}H_6F_1I_1$: 271.9498; found: 271.9497.

5.2.44 1,3,5-tricyclohexylbenzene (73)

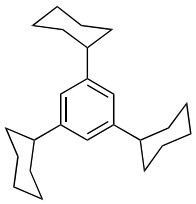

Chemical Formula: $C_{24}H_{36}$
Molecular Weight: 324.542

In a 100 ml 3 necked vessel with N_2 inlet and mechanical stirrer, benzene (4,5 ml, 50 mmol) and chlorocyclohexane (62,3 ml, 525 mmol) were charged. The mixture was cooled to -40˚C and $AlCl_3$ was added in portions over 15 min. At the end of the addition the mixture was allowed to warm to -15˚C and then the stirring was continued for 2.5 h at this temperature. The orange mixture was quenched by pouring ice in it and stirring overnight. A white precipitate, $Al(OH)_3$, was removed by filtration on filter paper. From the filtrate, the organic phase was first diluted with hexane then extracted, dried on $MgSO_4$ and the solvent was evaporated at rotavapor. The residual clorocyclohexane was removed via kugelrohr distillation (150˚C, 60 mbar). Addition of acetone to the residual oil allowed the precipitation of a pure white compound (300 mg): 1,2,4,5-tetrayclohexylbenzene. A new kugelrohr distillation (250˚C, 10^{-2} mbar) afforded an oil containing mostly the desired product. A column chromatography on SiO_2 (eluent: hexane, stainer: *p*-anisaldehyde) did not help to increase the purity of the product. The crude was then crystallized from hot acetone (5.0 g in 6 ml); upon cooling to rt overnight colorless crystals of pure 1,3,5-tricyclohexylbenzene formed (25% yield).

M.p.: 58-60˚C. IR (neat): 2922 *s*, 2849 *s*, 2143 *w*, 1600 *m*, 1447 *m*, 1417 *w*, 1382 *w*, 1361 *w*, 1349 *w*, 1249 *w*, 942 *w*, 896 *m*, 854 *m*, 742 *m*, 711 *m*, 648 *w*. ^{1}H NMR (500 MHz, $CDCl_3$): δ 6.86 (*s*, 3 H), 2.48 (*m*, 3H), 1.90-1.73 (*m*, 15 H), 1.47-1.21 (*m*, 15 H). $^{13}C\{^1H\}$ NMR (125.8 MHz, $CDCl_3$): δ 148.0, 123.1, 45.0, 34.8, 27.2, 26.5. MS (EI): 324 (100, M^+), 255 (12), 241 (41, $[M - Cy]^+$), 199 (7), 173 (21), 159 (33, $[M - 2Cy]^+$), 143 (5), 129 (10), 117 (17), 83 (35), 55 (25). HRMS (EI) *m/z*: calcd for $C_{24}H_{36}$: 324.2817; found: 324.2816.

5.2.45 1-bromo-2,4,6-tricyclohexylbenzene (74)

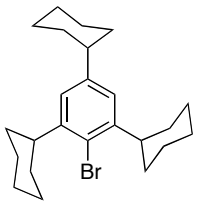

Chemical Formula: $C_{24}H_{35}Br$
Molecular Weight: 403.439

An ice-cold solution of Br_2 (3.7 mmol) in DMF (1 ml) was prepared by slowly adding Br_2 to stirred, chilled DMF. This solution was slowly added to a light-protected ice-bathed solution of 1,3,5-tricyclohexylbenzene (0.92 mmol) in DMF (4 ml). The orange reaction mixture was stirred for 30 min at 0˚C and after this time it was poured into ice/H2O/ Na_2SO_3. After a few minutes of stirring the mixture became colorless. The organic phase was extracted with EtOAc, dried on $MgSO_4$ and the solvent evaporated. ^{1}H NMR of the crude oil showed a conversion of 80%, with 20% residual starting material. A first purification was attempted via column chromatography on SiO_2 (eluent: hexane), but no separation was obtained. Crystallization from MeOH/*i*PrOH (1:2) (15 ml of solvent mixture for ~ 300 mg of crude, heating till 65 ˚C, followed by cooling to rt), afforded the desired product as white powder in 58 % yield.

M.p.: 166-168˚C. IR (neat): 2922 *s*, 2849 *s*, 1573 *w*, 1447 *m*, 1428 *w*, 1012 *m*, 860 *m*. ^{1}H NMR (500 MHz, $CDCl_3$): δ 6.94 (*s*, 2 H), 3.07 (*t*, ^{3}J = 11 Hz, 2 H), 2.45 (*m*, 1 H), 1.92-1.75 (*m*, 15 H), 1.51-1.23 (*m*, 15 H). ^{13}C{^{1}H} NMR (125.8 MHz, $CDCl_3$): δ 147.0, 146.5, 124.2, 123.6, 44.7, 44.3, 34.7, 33.7, 27.2, 27.1, 26.5, 26.3. MS (EI): 404 (100, M^+), 324 (18, $[M- Br]^+$), 255 (23), 241 (12), 159 (27), 83 (76). HRMS (EI) *m/z*: calcd for $C_{24}H_{35}Br_1$: 402.1922; found: 402.1920.

5.2.46 (2,4,6-tricyclohexylphenyl)dimethylsilane (75)

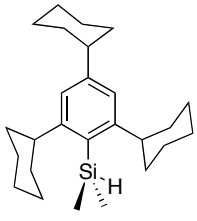

Chemical Formula: $C_{26}H_{42}Si$
Molecular Weight: 382.697

The same procedure described in 5.2.3 was followed. The product was purified via filtration on a plug of Al_2O_3 (eluent: hexane, stain: $KMnO_4$) and then recrystallized from *i*PrOH (4 ml for ~ 160 mg of compound, heating till 80˚C followed by cooling to rt). The product was obtained as white powder in 92 % yield.

M.p.: 134-136˚C. IR (neat): 2923 *s*, 2849 *s*, 2364 *w*, 2140 *m*, 1602 *m*, 1548 *m*, 1447 *m*, 1419 *w*, 1248 *m*, 1070 *w*, 951 *w*, 908 *m*, 888 *m*, 860 *w*, 834 *m*, 740 *m*, 691 *w*. ^{1}H NMR (500 MHz, C_6D_6): δ 7.16 (*s*, 2H), 5.09 (*eptuplet*, ^{3}J = 4.5 Hz, 1 H), 3.11 (*tt*, ^{3}J = 12.0 Hz, ^{3}J = 3.0 Hz, 2 H), 2.51 (*tt*, ^{3}J = 12.0 Hz, ^{3}J = 3.5 Hz, 1 H), 1.95 (*m*, 6 H), 1.79-1.20 (*m*, 24 H), 0.48 (*d*, ^{3}J = 4.0 Hz, 6 H). ^{13}C{^{1}H} NMR (125.8 MHz, C_6D_6): δ 155.1, 149.8, 131.2, 122.8, 45.8, 45.0, 36.0, 35.2, 27.7, 26.9, -0.7. ^{29}Si{^{1}H} NMR (79.5 MHz, C_6D_6): δ -28.7. MS (EI): 382 (82, M^+), 323 (100, M – $[Me_2SiH]^+$), 299 (46), 255 (32), 241 (38), 217 (12), 173 (17), 159 (51), 83 (54). HRMS (EI) *m/z*: calcd for $C_{26}H_{42}Si_1$: 382.3056; found: 382.3055.

5.2.47 (2,4,6-triisopropylphenyl)dimethylsilane (78)

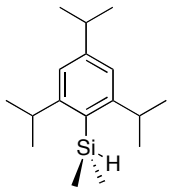

Chemical Formula: $C_{17}H_{30}Si$
Molecular Weight.: 262.506

The same procedure described in 5.2.3 was followed. The crude was purified via column chromatography on Al_2O_3 (eluent: hexane, stain: $KMnO_4$). The product was obtained as a white powder in 92% yield.

M.p.: 58-60˚C. IR (neat): 2959 *s*, 2932 *w*, 2869 *w*, 2151 *m*, 1601 *m*, 1551 *m*, 1459 *m*, 1418 *m*, 1360 *m*, 1249 *m*, 1042 *w*, 939 *m*, 896 *s*, 877 *m*, 829 *m*, 763 *m*, 741 *s*. ^{1}H NMR (500 MHz, C_6D_6): δ 7.13 (*s*, 2 H, H-C(3', 5')), 5.04 (*eptuplet*, ^{3}J = 4.1 Hz, 1 H, H-Si), 3.45 (*eptuplet*, ^{3}J = 6.8 Hz, 2 H, H-C(7',8'), 2.79 (*eptuplet*, ^{3}J = 6.9 Hz, 1 H, H-C9'), 1.27 (*d*, ^{3}J = 6.8 Hz, 12 H, H-C(10', 11')), 1.23 (*d*, ^{3}J = 7.0 Hz, 6 H, H-C12'), 0.42 (*d*, ^{3}J = 4.1 Hz, 6 H, Me-Si). ^{13}C{^{1}H} NMR (100.6 MHz, C_6D_6): δ 156.1 (C(2', 6')), 150.9 (C4'), 130.7 (C1'), 121.5 (C(3', 5')), 35.2 (C9'), 34.1 (C(7' 8')), 25.4 (C(10', 11')), 24.5 (C12'), -0.7 (Me-Si). ^{29}Si{^{1}H} NMR (79.5 MHz, C_6D_6): δ -28.7 MS (EI): 262 (28, M^+), 245 (100), 229 (6), 217 (13), 203 (50), 187 (11), 161 (12), 145 (6), 73 (12). HRMS (EI) *m/z*: calcd for $C_{17}H_{30}Si_1$: 262.2117; found: 262.2114.

5.2.48 (2,4,6-triisopropylphenyl)dimethylsilylium tetrakis(pentafluorophenyl) borate–CD_3CN complex [76-CD_3CN][$B(C_6F_5)_4$]

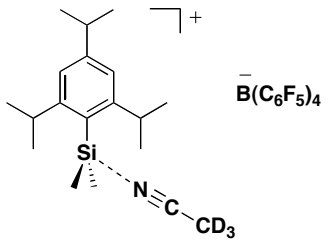

Chemical Formula: $C_{43}H_{29}D_3BF_{20}NSi$
Molecular Weight: 984.604

The same procedure used described in 5.2.15 was used. The product was obtained as light brown powder in 94% yield.

^{1}H NMR (400 MHz, C_6D_6 + 3 drops CD_3CN): δ 7.03 (*s*, 2 H, H-C(3', 5')), 2.87 (*eptuplet*, ^{3}J = 6.4 Hz, 2 H, H-C(7', 8')), 2.71 (*eptuplet*, ^{3}J = 6.8 Hz, 1 H, H-C9'), 1.11 (*d*, ^{3}J = 6.8 Hz, 6 H, H-C12'), 0.98 (*broad* , 12 H, H-C(10', 11')), 0.22 (*s*, 6 H, Me-Si). ^{13}C{^{1}H} NMR (100.6 MHz, C_6D_6 + 3 drops CD_3CN): δ 154.4 (C(2', 6')), 154.0 (C4'), 148.7 (*d*, $^1J_{C\text{-}F}$ = 242 Hz, anion), 138.6 (*d*, $^1J_{C\text{-}F}$ = 247 Hz, anion), 136.6 (*d*, $^1J_{C\text{-}F}$ = 248 Hz, anion), 126-123 (*broad*, anion), 124.2 (C1'), 122.8 (C(3', 5')), 116.7(C-N), 34.8 (C(7', 8')), 34.3 (C9'), 24.2 (C(10', 11')), 23.2 (C12'), 23.2 (C(10', 11')), -0.2 (-CD3), -2.1 (Me-Si). ^{29}Si {^{1}H} NMR (79.5 MHz, C_6D_6 + 3 drops CD_3CN): δ 32.4.

5.2.49 (2,4,6-triisopropylphenyl)dimethylsilylium tetrakis(pentafluorophenyl)borate [76][$B(C_6F_5)_4$]

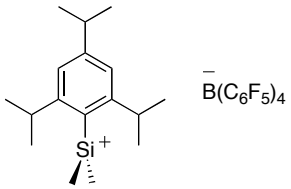

Chemical Formula: $C_{41}H_{29}BF_{20}Si$
Molecular Weight: 940.533

The same procedure described in 5.2.4 was followed. The product was obtained in 85% yield as yellow powder.

^{1}H NMR (400 MHz, C_6D_6): δ 6.97 (*s*, 2H, H-C(3', 5')), 2.67 (*eptuplet*, ^{3}J = 6.8 Hz, 1 H, H-C9'), 2.26 (*eptuplet*, ^{3}J = 6.4 Hz, 2 H, H-C(7', 8')), 1.09 (*d*, ^{3}J = 7.2 Hz, 6 H, H-C12'), 1.00 (*d*, ^{3}J = 6.0 Hz, 12 H, H-C(10', 11')), -0.21 (*s*, 6 H, Me-Si). ^{13}C{^{1}H} NMR (100.6 MHz, C_6D_6): δ 160.5 (C4'), 155.5 (C(2', 6')), 149.3 (*d*, $^{1}J_{C\text{-}F}$ = 242 Hz, anion), 139.1 (*d*, $^{1}J_{C\text{-}F}$ = 246 Hz, anion), 137.3 (*d*, $^{1}J_{C\text{-}F}$ = 246 Hz, anion), 127.1 (C1'), 127-124 (*broad*, anion), 123.9 (C(3', 5')), 43.3 (C(7', 8')), 35.3 (C9'), 24.5 (C(10', 11')), 23.4 (C12'), 0.6 (Me-Si). ^{29}Si{^{1}H} NMR (79.5 MHz, C_6D_6): δ 231.2 (88% molar fraction), 209.2, 178.3, 92.7 (8% molar fraction).

5.2.50 (2,4,6-trimethylphenyl)dimethylsilane (80)

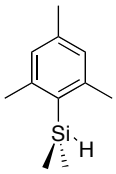

Chemical Formula: $C_{11}H_{18}Si$
Molecular Weight: 178.346

The same procedure described in 5.2.3 was followed. The crude was purified via column chromatography on Al_2O_3 (eluent: hexane, stain: $KMnO_4$). The product was obtained as colorless oil in 91% yield.

IR (neat): 3026 *w*, 2957 *m*, 2923 *m*, 2868 *w*, 2362 *w*, 2145 *m*, 1605 *m*, 1549 *w*, 1447 *w*, 1414 *w*, 1377 *w*, 1352 *w*, 1249 *m*, 1166 *w*, 1071 *m*, 1029 *w*, 932 *m*, 888 *s*, 847 *m*, 835 *m*, 768 *m*, 712 *m*, 700 *w*, 663 *m*.

^{1}H NMR (400 MHz, C_6D_6): δ 6.74 (*s*, 2 H, H-C(3', 5')), 4.93 (*eptuplet*, ^{3}J = 4.0 Hz, 1H, H-Si), 2.38 (*s*, 6 H, H-C(7', 8')), 2.13 (*s*, 3 H, H-C9'), 0.32 (*s*, 6 H, Me-Si). ^{13}C{^{1}H} NMR (100.6 MHz, C_6D_6): δ 144.6 (C(2', 6')), 139.3 (C4'), 131.4 (C1'), 129.4 (C(3', 5')), 24.4 (C(7', 8')), 21.5 (C9'), -1.8 (Me-Si). ^{29}Si{^{1}H} NMR (79.5 MHz, C_6D_6): δ -26.0. MS (EI): 178 (54, M^+), 163 (100, $[M - Me]^+$), 147 (10), 135 (11), 119 (13), 105 (7). HRMS (EI) *m/z*: calcd for $C_{11}H_{18}Si_1$: 178.1178; found: 178.1176

5.2.51 (2,4,6-trimethylphenyl)dimethylsilylium tetrakis(pentafluorophenyl)borate [79][$B(C_6F_5)_4$]

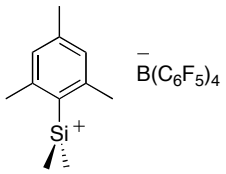

Chemical Formula: $C_{35}H_{17}BF_{20}Si$
Molecular Weight: 856.374

The same procedure described in 5.2.4 was followed. The product was obtained in 85% yield as yellow powder.

^{1}H NMR (400 MHz, C_6D_6): δ 6.54 (*s*, 2 H, H-C(3', 5')), 2.02 (*s*, 3 H, H-C9'), 1.94 (*s*, 3 H, H-C(7', 8')), -0.15 (*s*, 6 H, Me-Si). $^{13}C\{^1H\}$ NMR (100.6 MHz, C_6D_6): δ 150.6 (C4'), 149.4 (*d*, $^1J_{C\text{-}F}$ = 249 Hz, anion), 145.2 (C(2', 6')), 139.2 (*d*, $^1J_{C\text{-}F}$ = 245 Hz, anion), 137.3 (*d*, $^1J_{C\text{-}F}$ = 249 Hz, anion), 130.9 (C(3', 5')), 130.6 (C1'), 127-124 (*broad*, anion), 24.0 (C(7' 8')), 21.7 (C9'), 0.1 (Me-Si). $^{29}Si\{^1H\}$ NMR (79.5 MHz, C_6D_6): δ 225.4 (96% molar fraction), 83.5 (4% molar fraction).

5.2.52 (2,6-dimethyphenyl)dimethylsilane

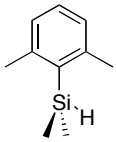

Chemical Formula: $C_{10}H_{16}Si$
Molecular Weight: 164.319

The same procedure described in 5.2.3 was followed. The crude was purified via column chromatography on Al_2O_3 (eluent: hexane, stain: $KMnO_4$). The product was obtained as colorless oil in 80% yield.

IR (neat): 3052 *w*, 2957 *m*, 2927 *w*, 2873 *w*, 2144 *m*, 1587 *w*, 1563 *w*, 1447 *m*, 1402 *w*, 1378 *w*, 1249 *m*, 1165 *w*, 1127 *m*, 1063 *w*, 1028 *w*, 921 *m*, 882 *s*, 835 *m*, 766 *s*, 715 *m*, 659 *m*, 636 *w*. ^{1}H NMR (500 MHz, C_6D_6): δ 7.07 (*t*, ^{3}J = 8.0 Hz, 1 H, H-C4'), 6.90 (*d*, ^{3}J = 7.5 Hz, 2 H, H-C(3', 5')), 4.90 (*eptuplet*, ^{3}J = 4.0 Hz, 1 H, H-Si), 2.36 (*s*,

6 H, Me-C(7', 8')), 0.29 (*d*, ^{3}J = 4.5 Hz 6 H, Me-Si). $^{13}C\{^{1}H\}$ NMR (125.8 MHz, C_6D_6): δ 144.5 (C(2', 6')), 135.0 (C1'), 130.0 (C4'), 128.4 (C3', 5'), 24.4 (C(7', 8')), -2.0 (Me-Si). $^{29}Si\{^{1}H\}$ NMR (79.5 MHz, C_6D_6): δ -25.9. MS (EI): 164 (46, M^+), 149 (100, $[M - Me]^+$). HRMS (EI) *m/z*: calcd for $C_{10}H_{16}Si_1$: 164.1021; found: 164.101

5.3 NMR Spectra

5.3.1 ^{1}H, ^{13}C, variable temperature ^{19}F NMR spectra of [18][$B(C_6F_5)_4$]

^{1}H in C6D6,ext. ref.: Me_4Si, 300K, SF = 500.30 MHz

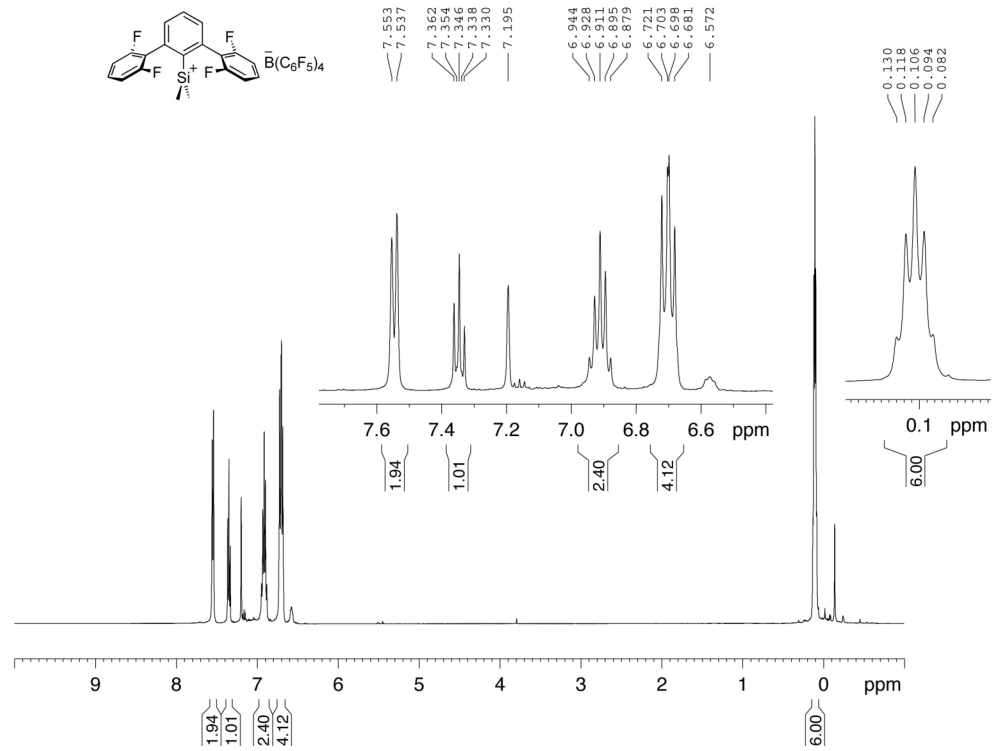

^{13}C in C_6D_6, 300K, SF = 125.80 MHz

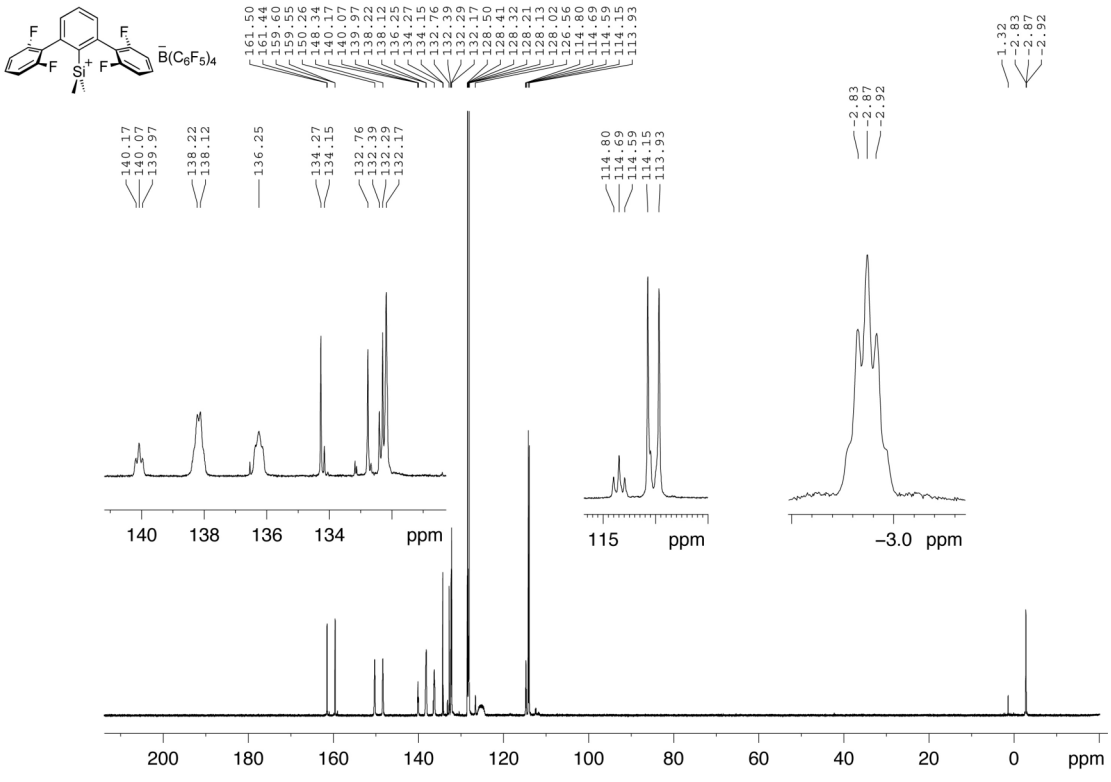

$^{19}F\{^{1}H\}$-NMR: in tol-d_8/chlorobenzene (1:1)

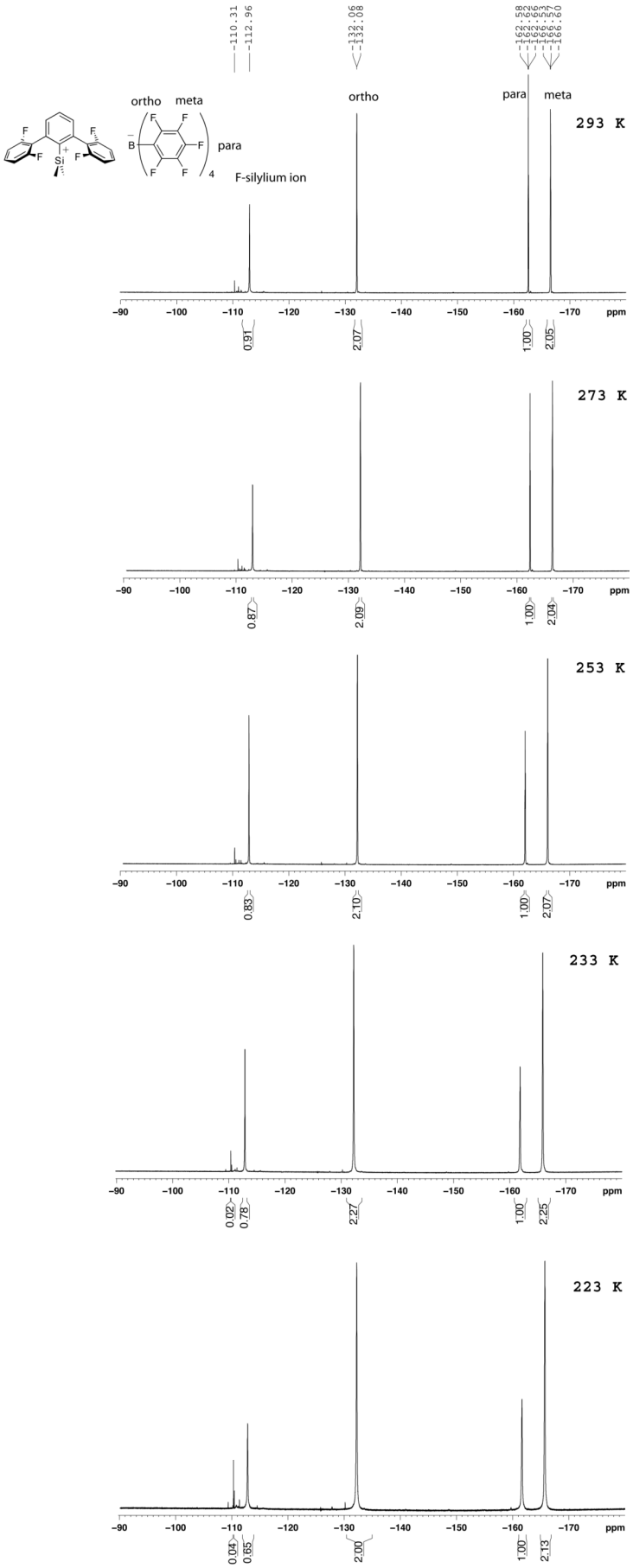

5.3.2 ^{1}H, ^{13}C, ^{29}Si NMR spectra of [28][$B(C_6F_5)_4$]

^{1}H in C_6D_6, ext.ref.: Me_4Si, 300K, SF = 400.23

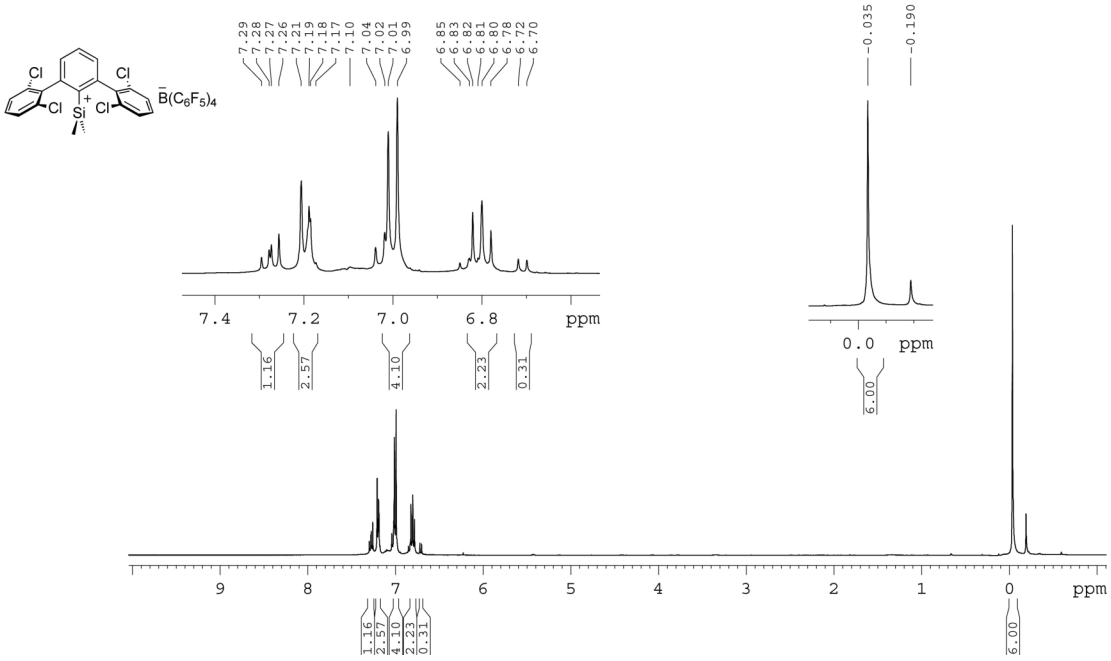

^{13}C in C_6D_6, 300K, SF = 100.638 MHz

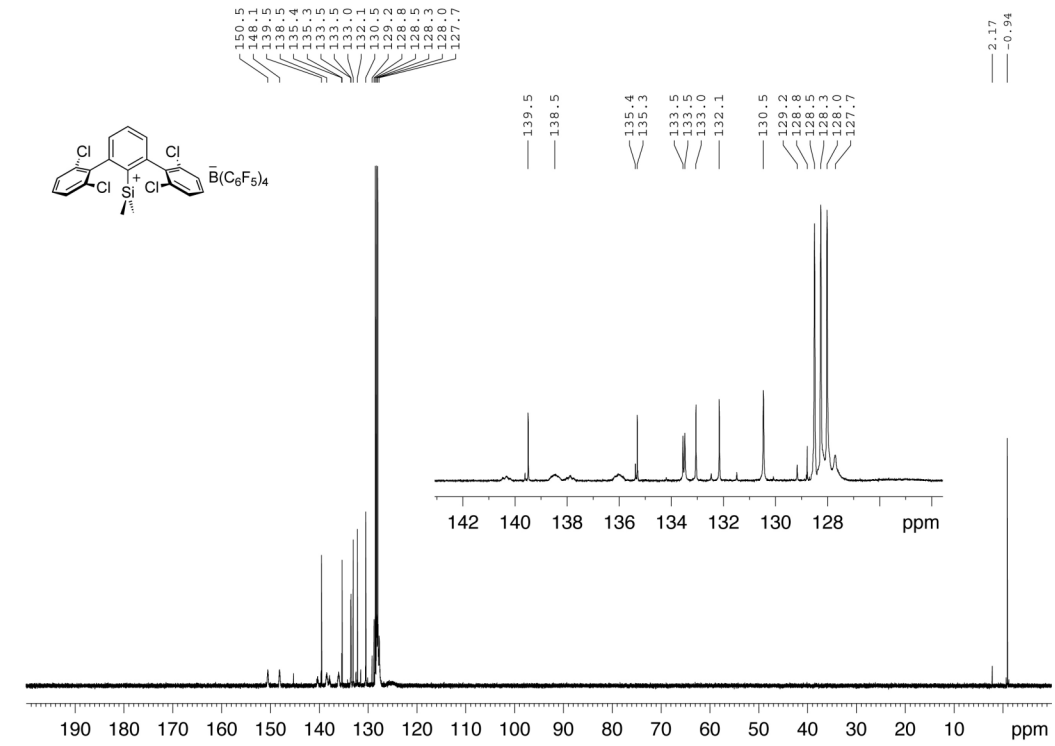

^{29}Si in C_6D_6,ext. ref.: Me_4Si, 300K, SF = 99.38 MHz

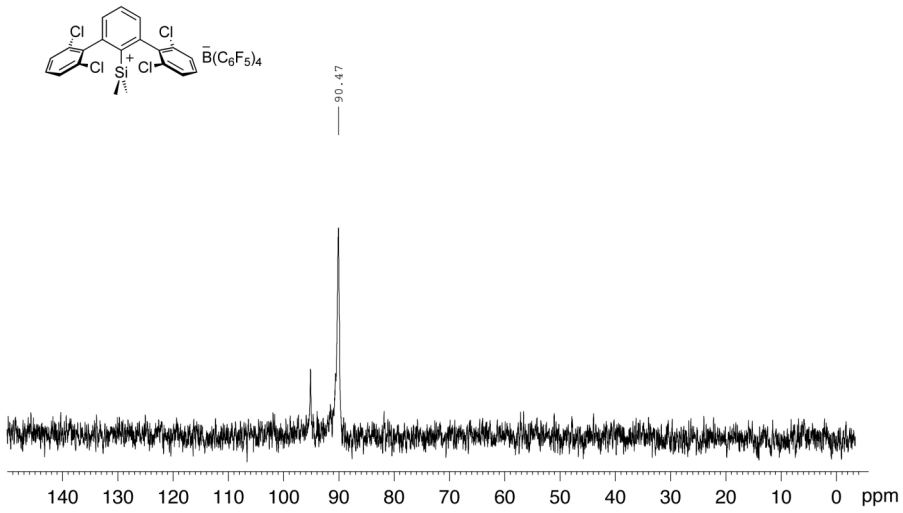

5.3.3 ^{1}H, NMR spectra of $[Ph_3C][CHB_{11}H_5Cl_6]$

^{1}H NMR of $[Ph_3C][CB_{11}H_6Cl_6]$, in CD_3CN, 300 K. SF = 400.2 MHz.

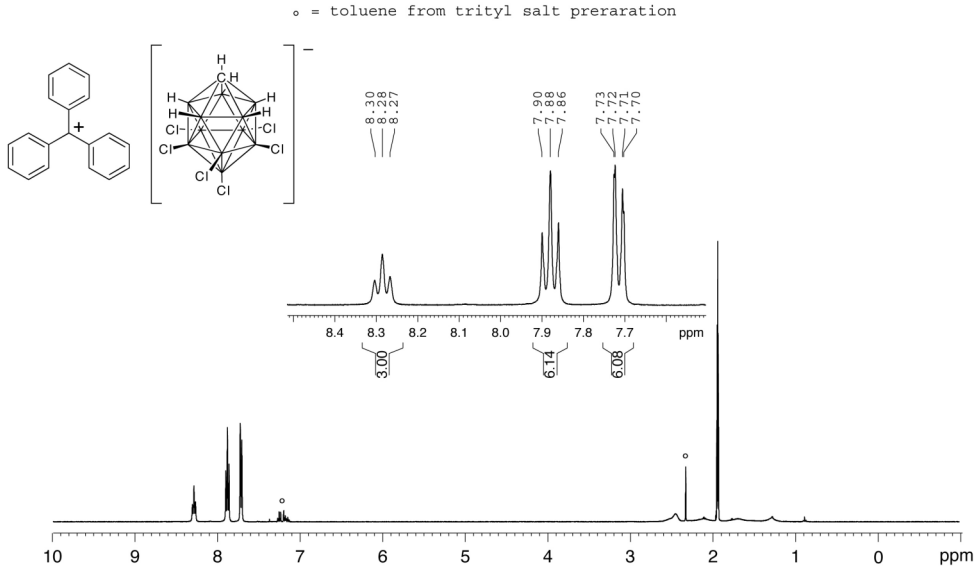

5.3.4 ^{1}H, ^{13}C, ^{29}Si NMR spectra of [42][$B(C_6F_5)_4$]

^{1}H NMR in C_6D_6, ext. ref.: Me_4Si, 300K. SF = 400.2 MHz

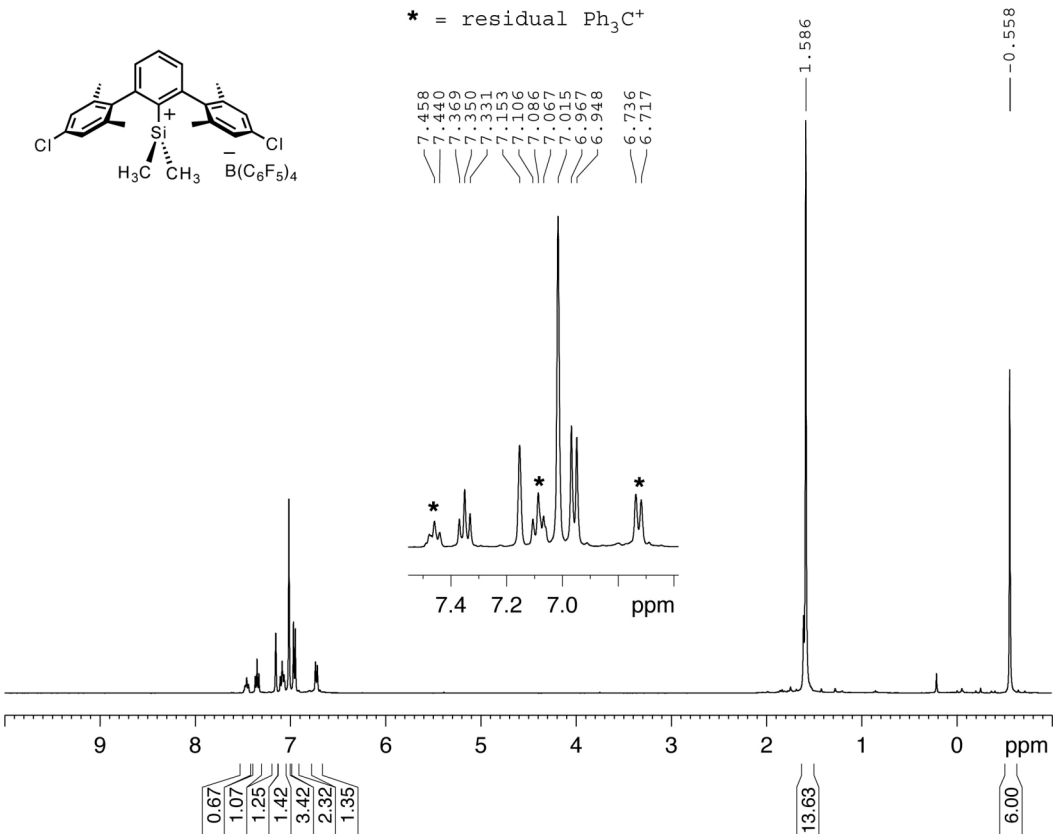

^{13}C NMR in C_6D_6, 300K. SF = 100.6 MHz

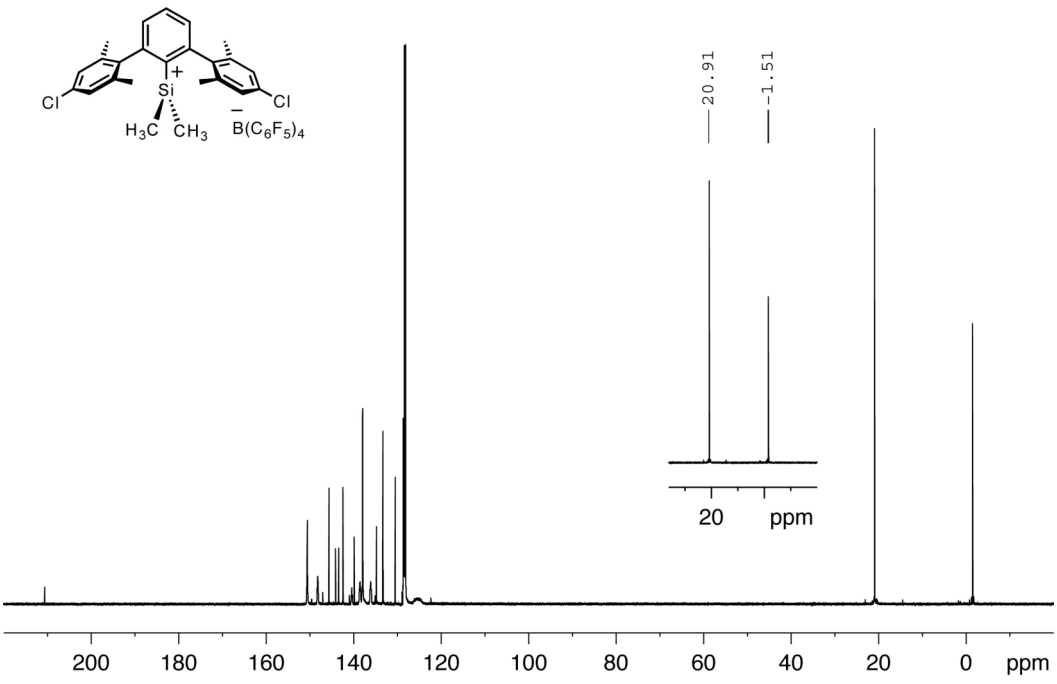

^{13}C NMR(enlargement)in C_6D_6, 300K. SF = 100.6 MHz

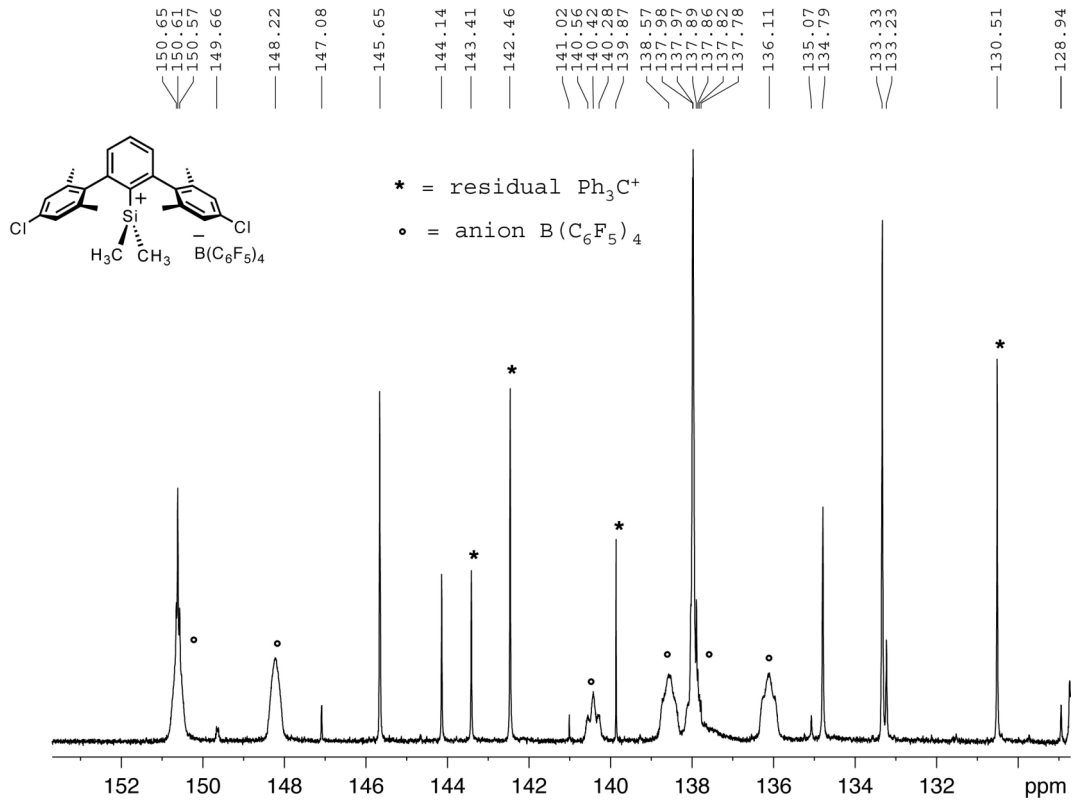

^{29}Si NMR in C_6D_6, ext. ref.: Me_4Si 300K. SF = 79.5 MHz

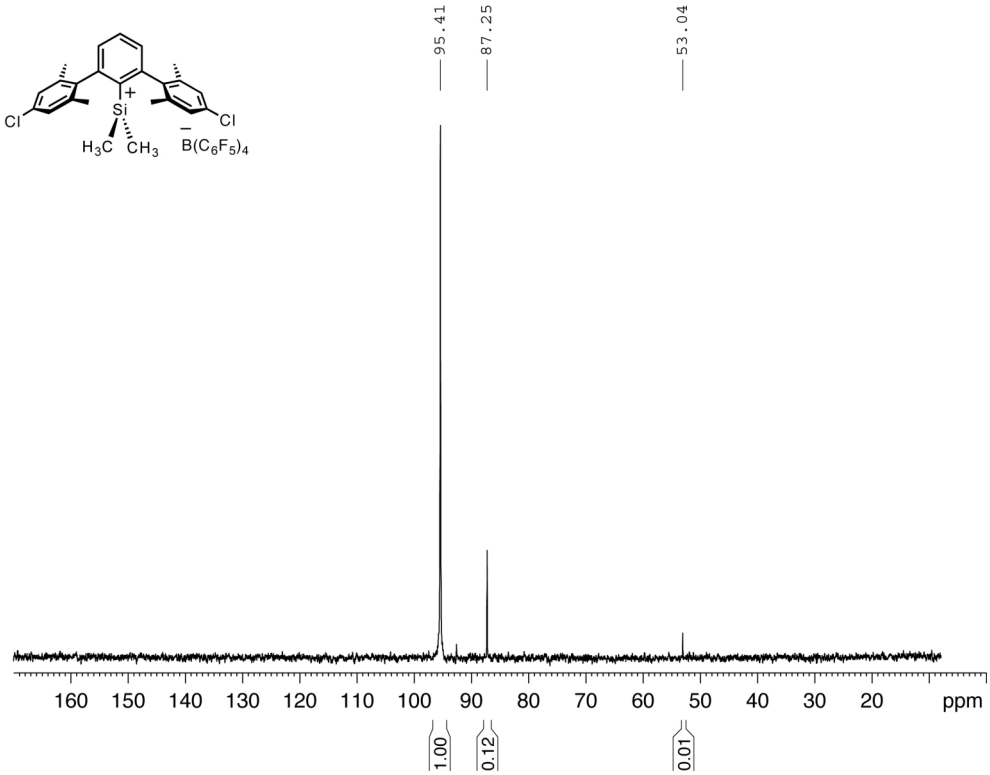

5.3.5 ^{1}H, ^{13}C, ^{19}F, ^{29}Si NMR spectra of [46][$B(C_6F_5)_4$]

^{1}H NMR in C_6D_6, ext. ref.: Me_4Si 300K. SF = 400.2 MHz

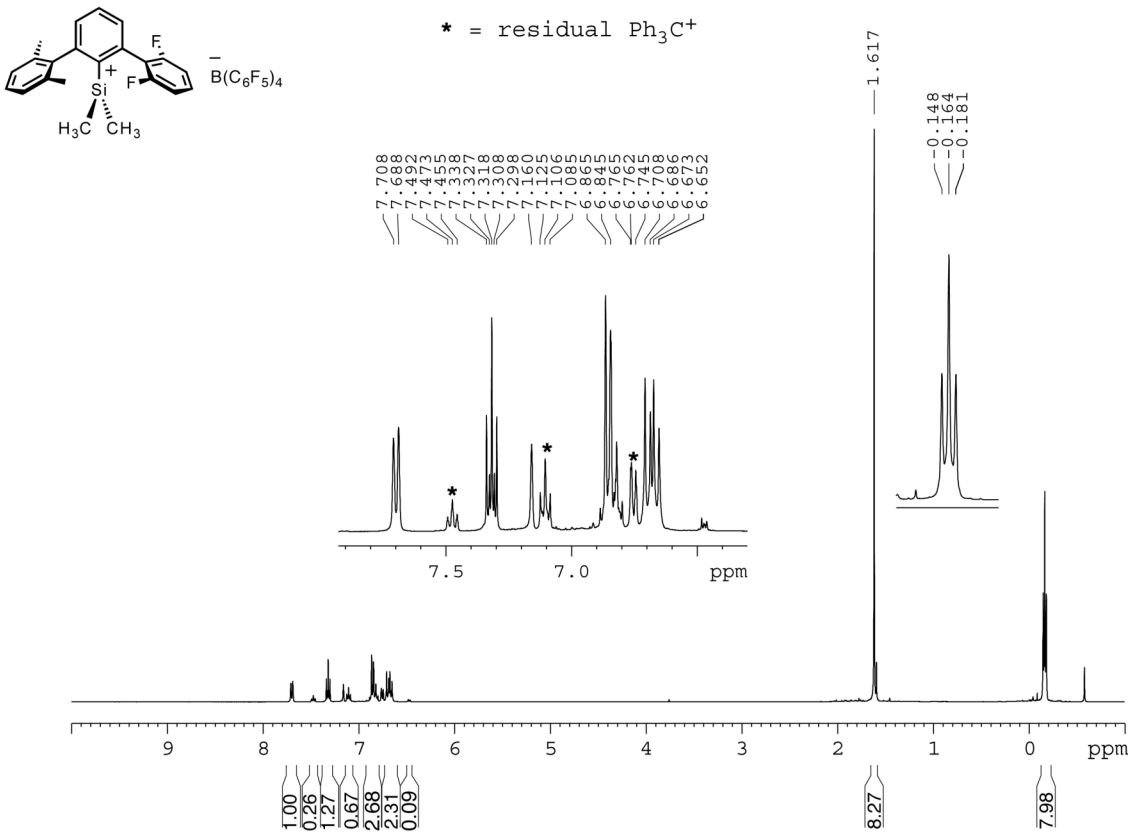

^{13}C NMR in C_6D_6, 300K. SF = 100.6 MHz

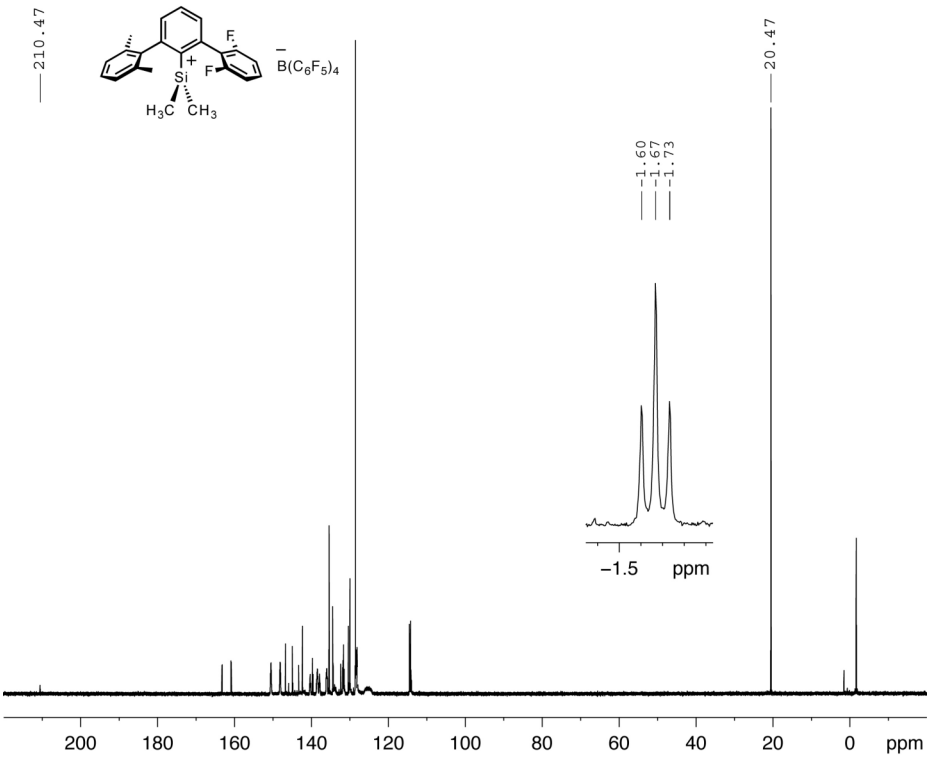

^{13}C NMR(enlargement) in C_6D_6, 300K. SF = 100.6 MHz

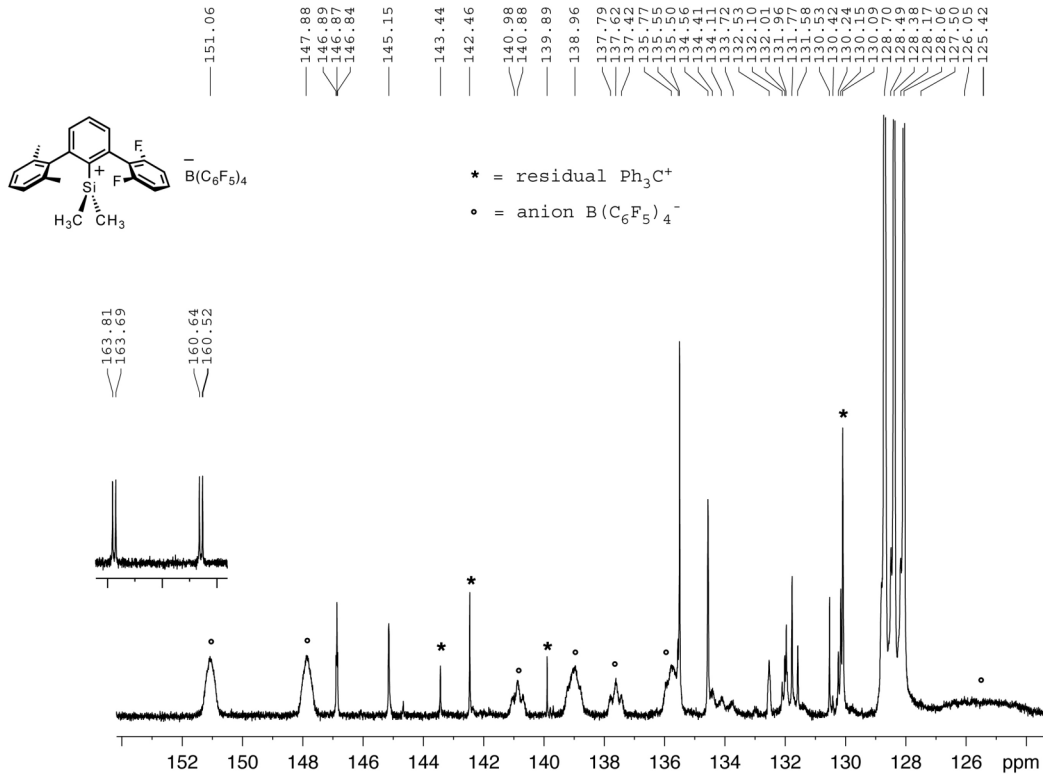

^{19}F NMR in C_6D_6, 300K. SF = 376.5 MHz

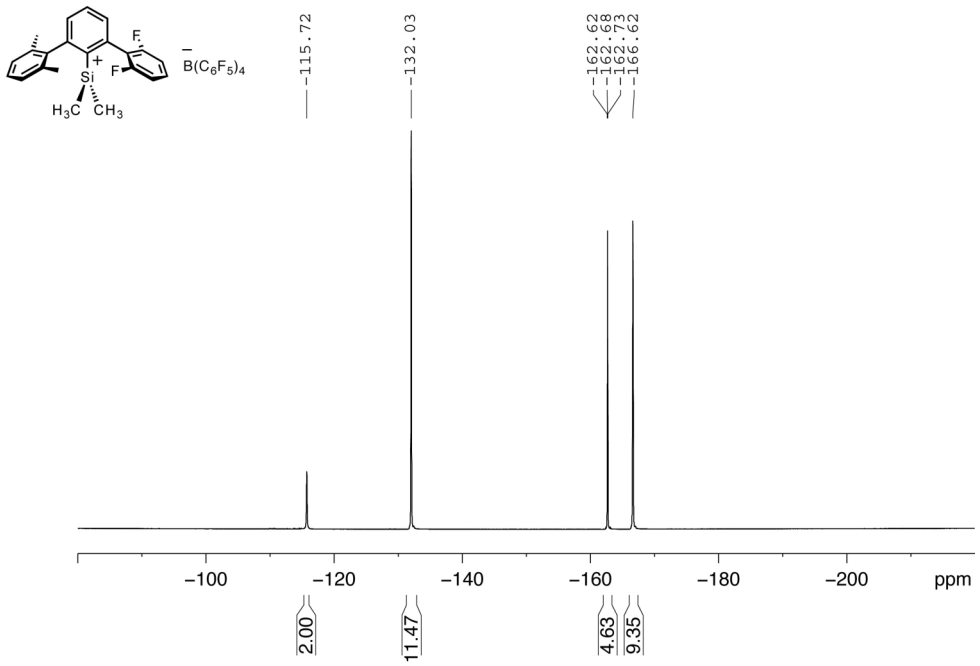

$^{29}Si\{^{1}H\}$ NMR in C_6D_6 , ext. ref.: Me_4Si, 300K. SF = 79.5 MHz

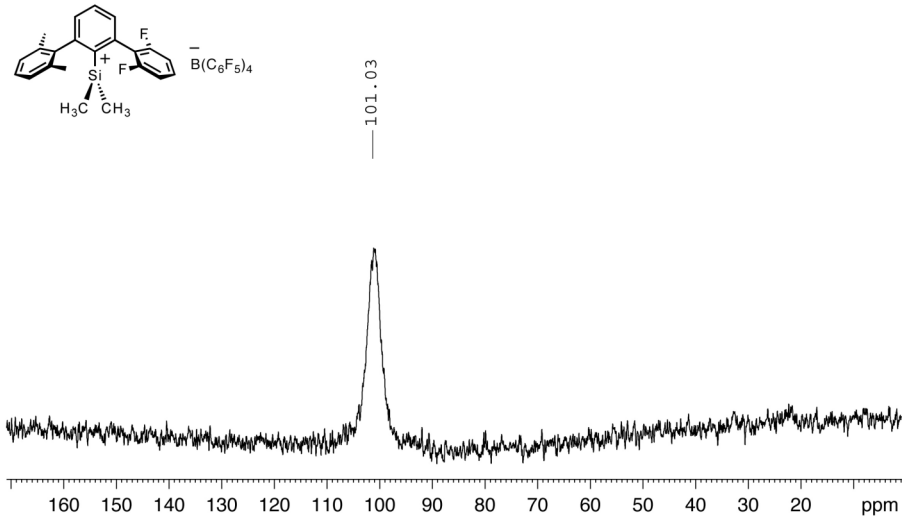

5.3.6 ^{1}H, ^{13}C, ^{19}F, ^{29}Si NMR spectra of [47][$B(C_6F_5)_4$]

^{1}H NMR in C_6D_6, ext. ref.: Me_4Si, 300K. SF = 400.2 MHz

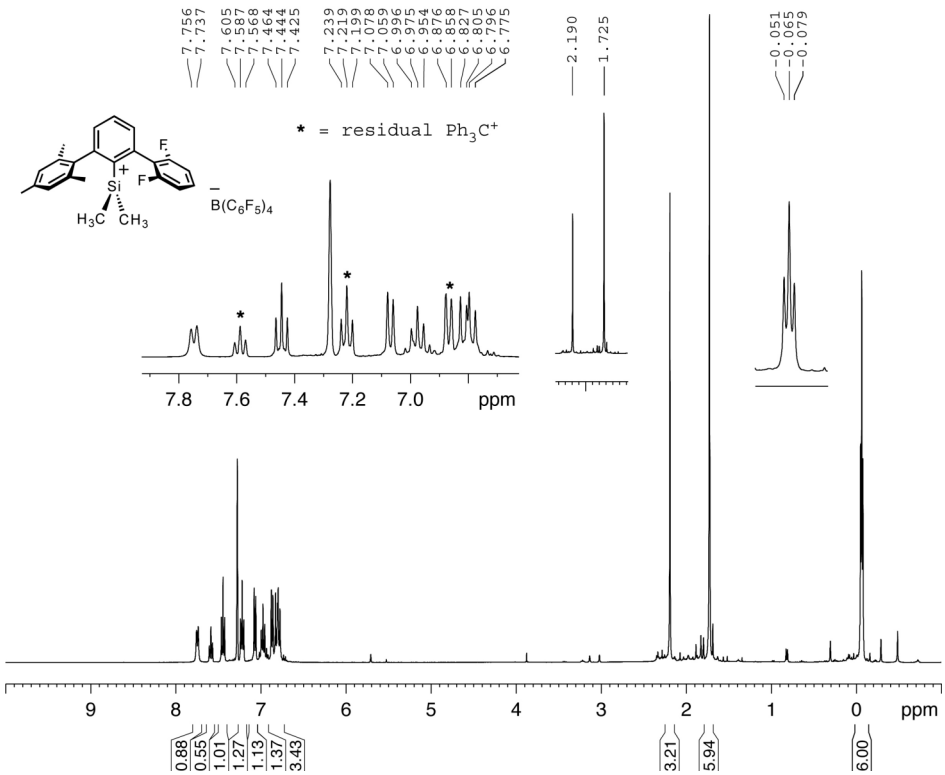

^{13}C NMR of in C_6D_6, 300 K. SF = 125.8 MHz

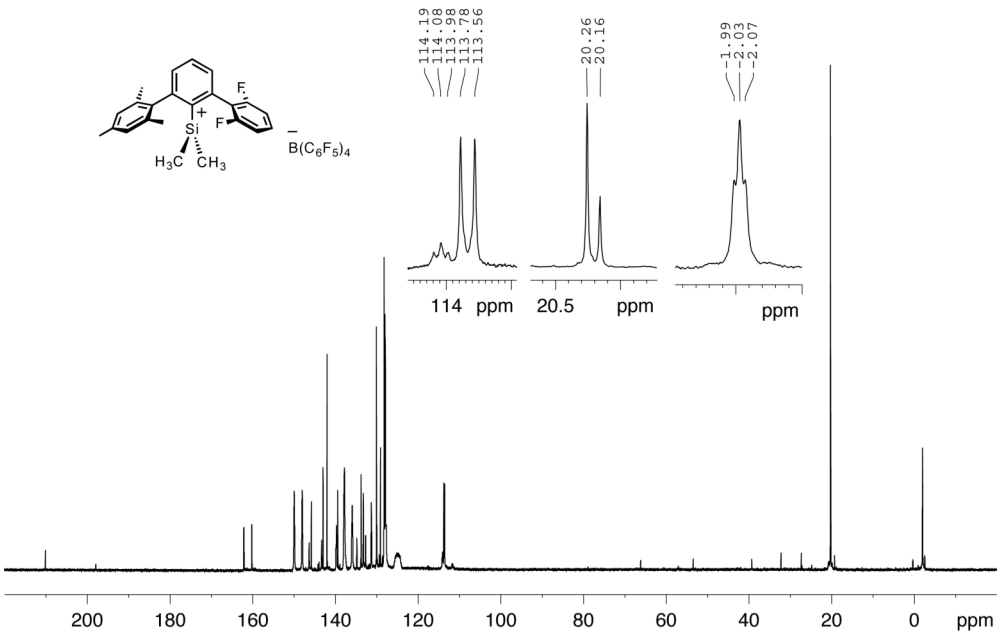

^{13}C NMR(enlargement) in C_6D_6, 300 K. SF = 125.8 MHz

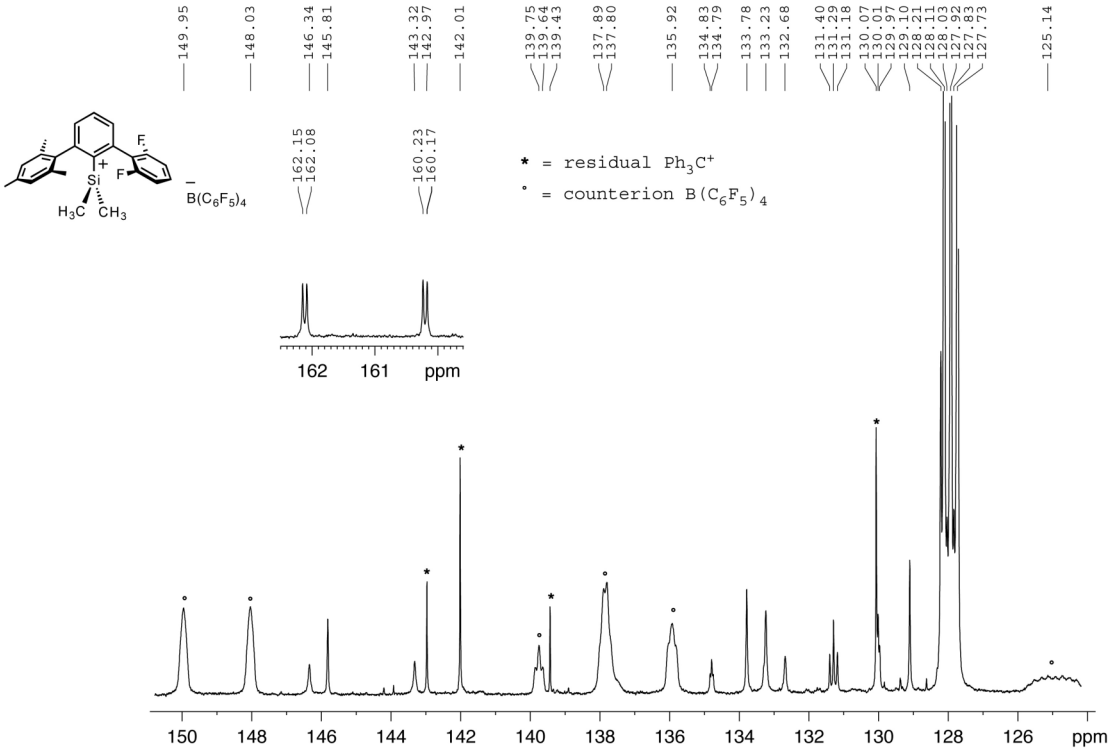

^{19}F NMR in C_6D_6, 300 K. SF = 282.4 MHz

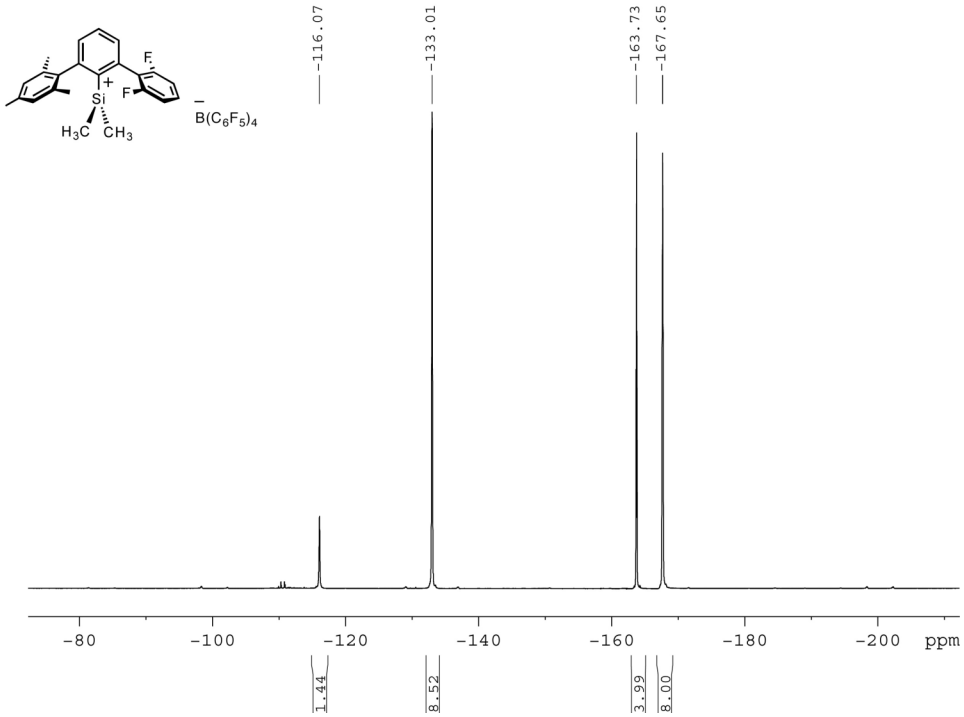

$^{29}Si\{^{1}H\}$ NMR in C_6D_6,ext. ref.: Me_4Si, 300K. SF = 59.6 MHz

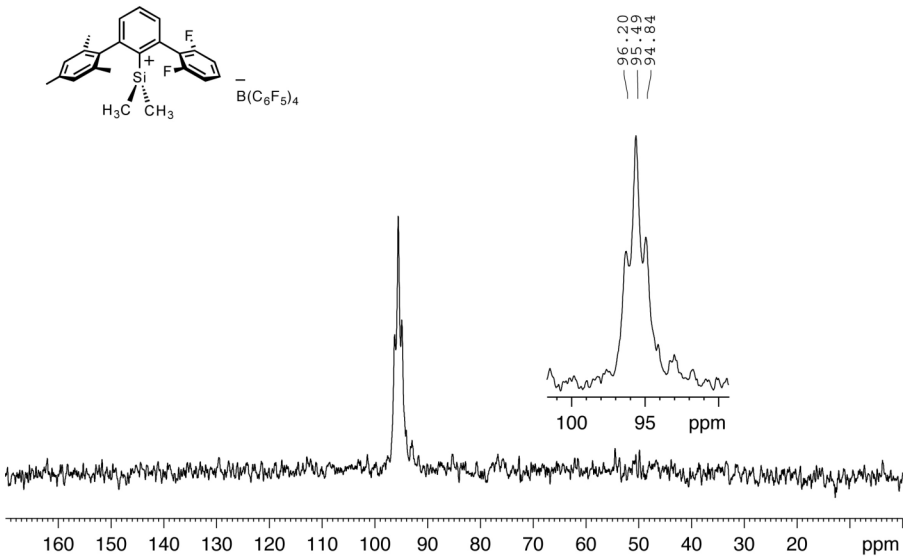

5.3.7 ^{1}H, ^{13}C, ^{19}F, ^{29}Si NMR spectra of [48][$B(C_6F_5)_4$]

^{1}H NMR in C_6D_6,ext. ref.: Me_4Si, 300K. SF = 300.1 MHz

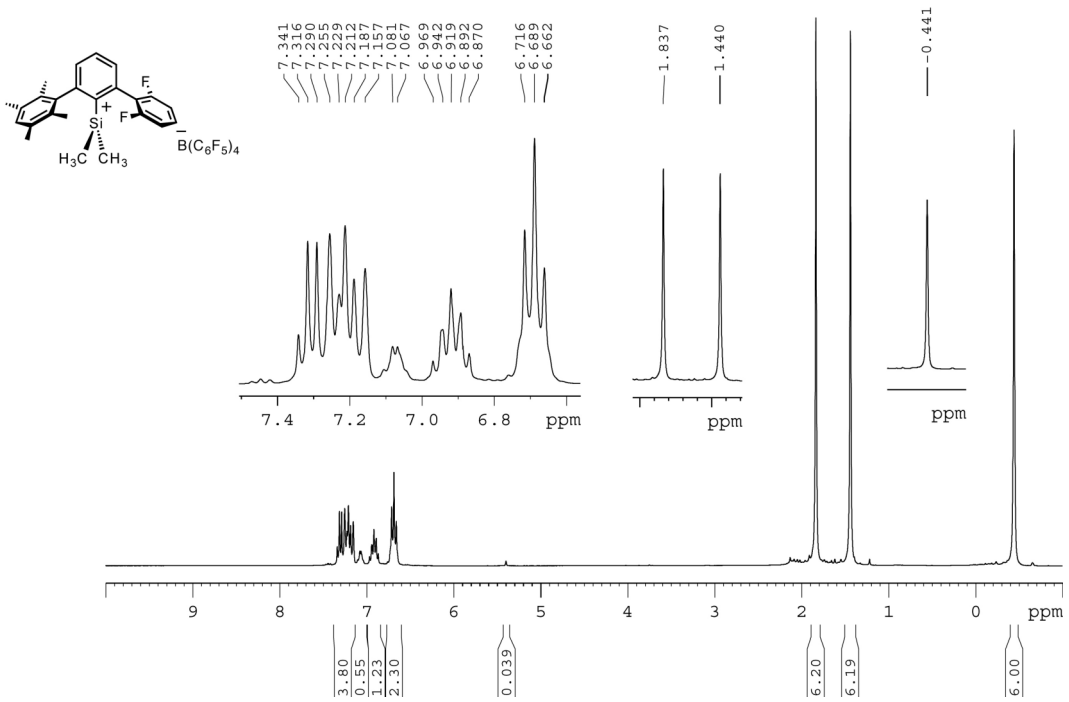

^{13}C NMR in C_6D_6, 300K. SF = 75.5 MHz

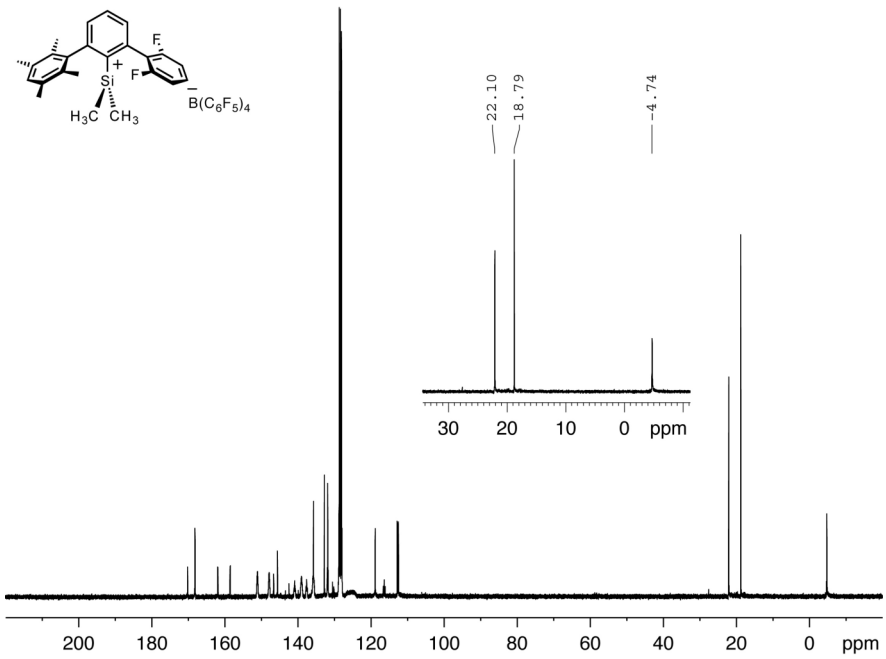

^{13}C NMR (enlargement) in C_6D_6, 300K. SF = 75.5 MHz

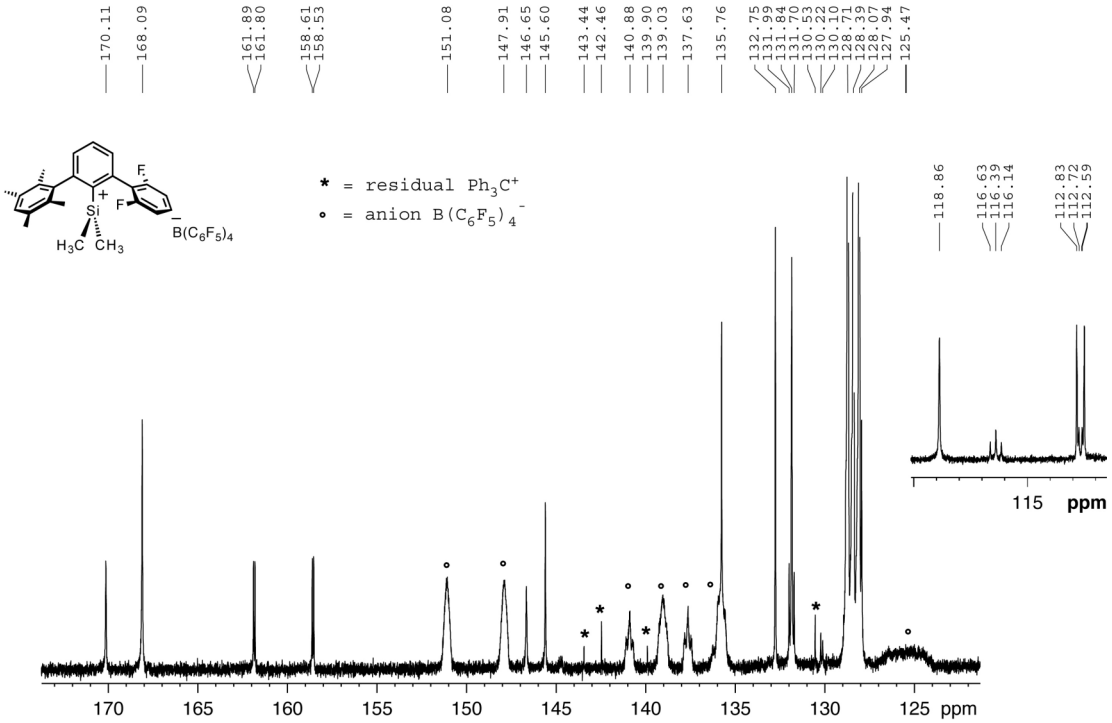

^{19}F NMR in C_6D_6, 300K. SF = 376.5 MHz

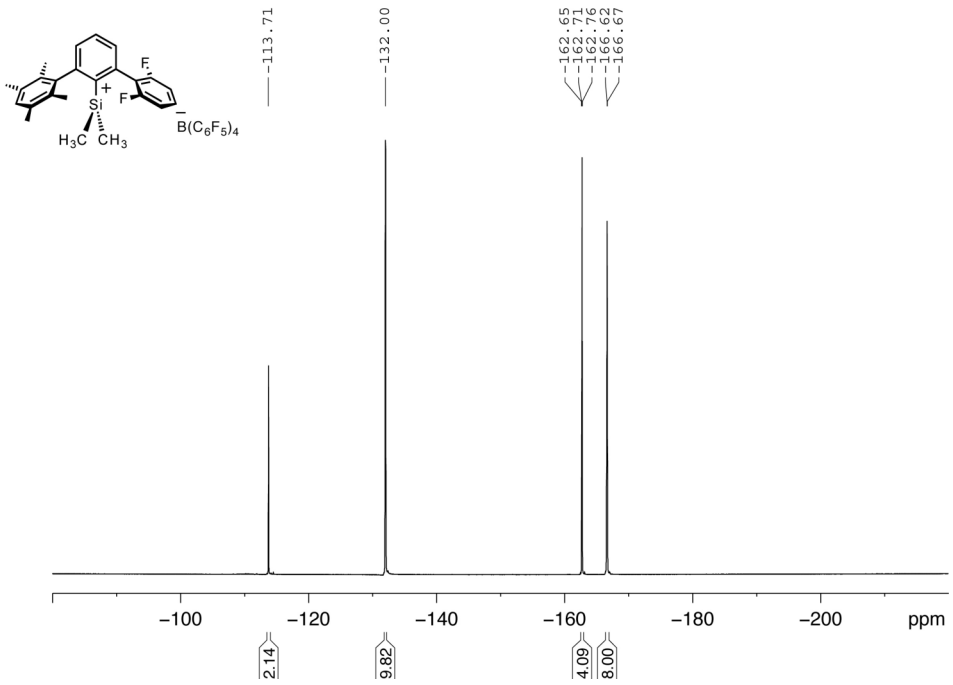

$^{29}Si\{^{1}H\}$ NMR in C_6D_6, ext. ref.: Me_4Si, 300K. SF = 59.6 MHz

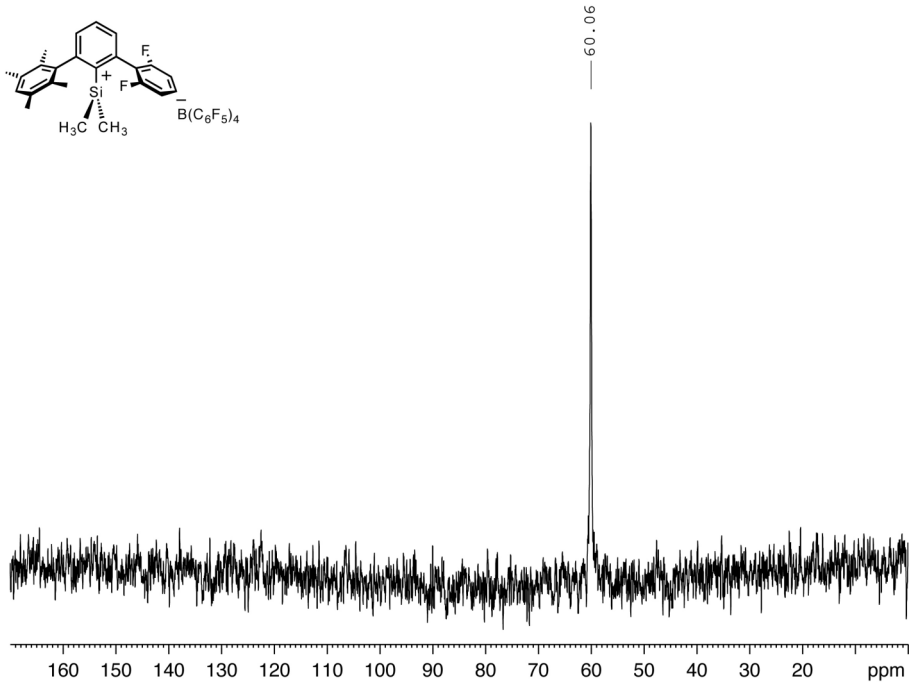

5.3.8 ^{1}H, ^{13}C, ^{19}F, ^{29}Si NMR spectra of [49][$B(C_6F_5)_4$]

^{1}H NMR in C_6D_6, ext. ref.:Me_4Si, 300K. SF = 500.1 MHz

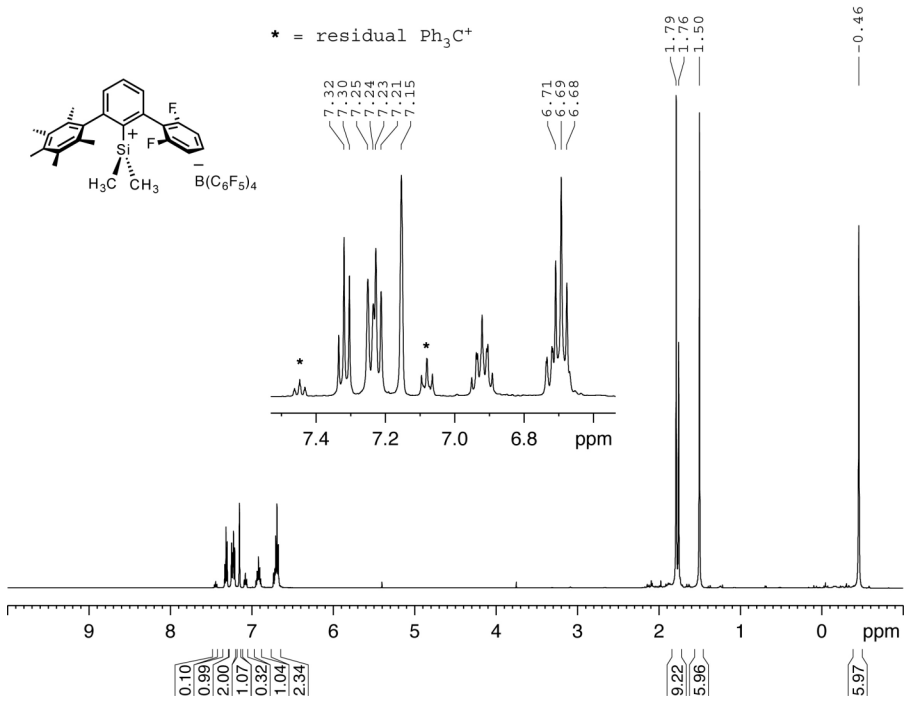

^{13}C NMR, in C_6D_6, 300K. SF = 125.8 MHz.

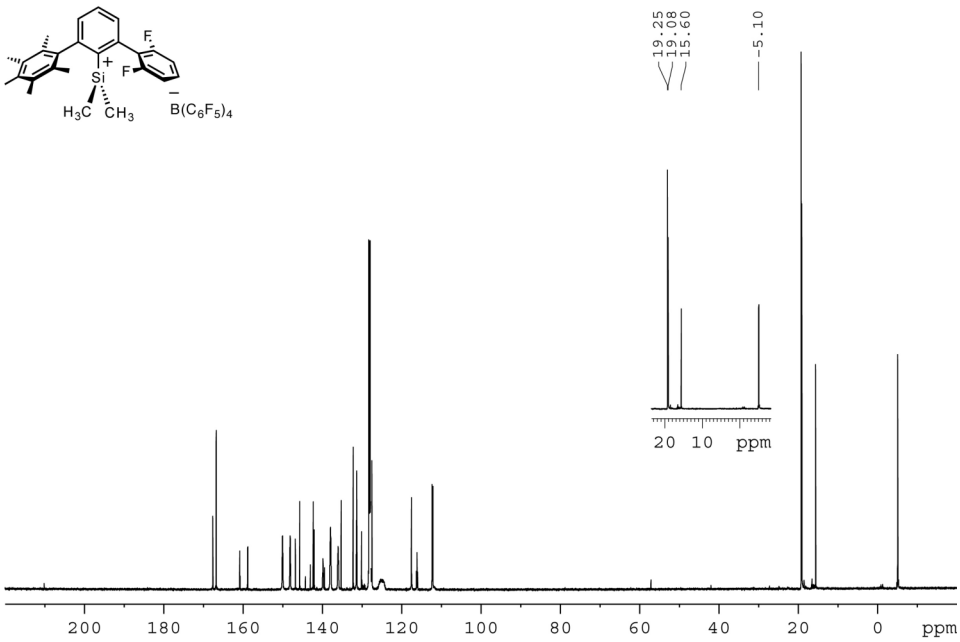

^{13}C NMR(enlargement) in C_6D_6, 300K. SF = 125.8 MHz

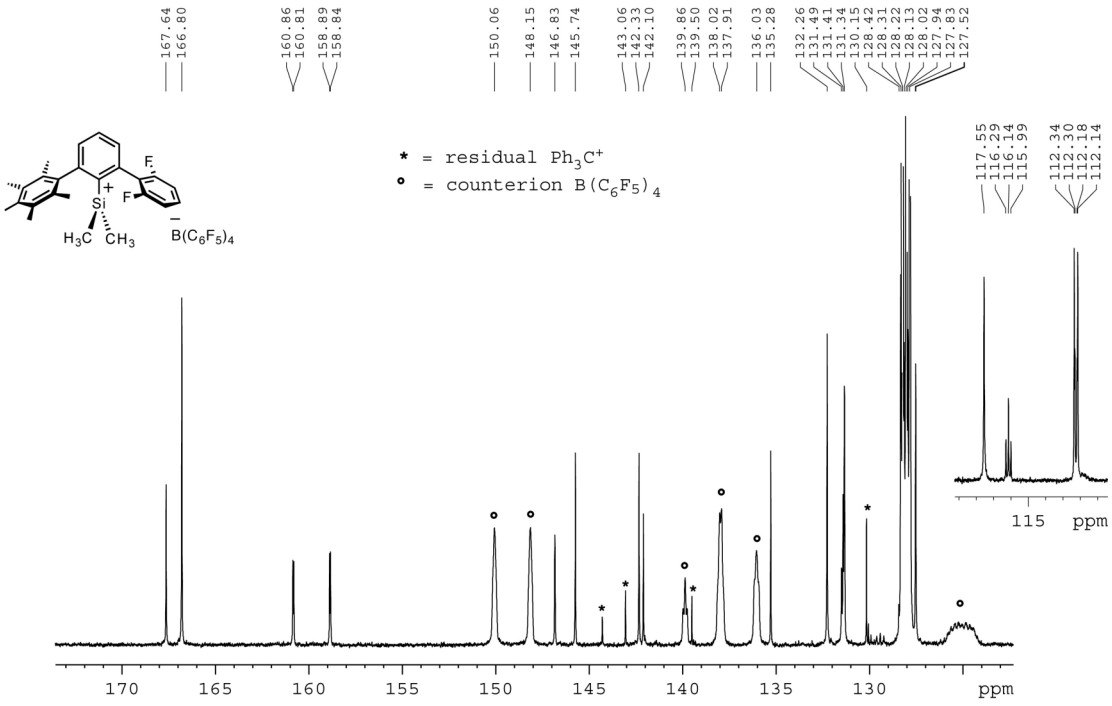

^{19}F NMR in C_6D_6, 300K. SF = 282.4 MHz

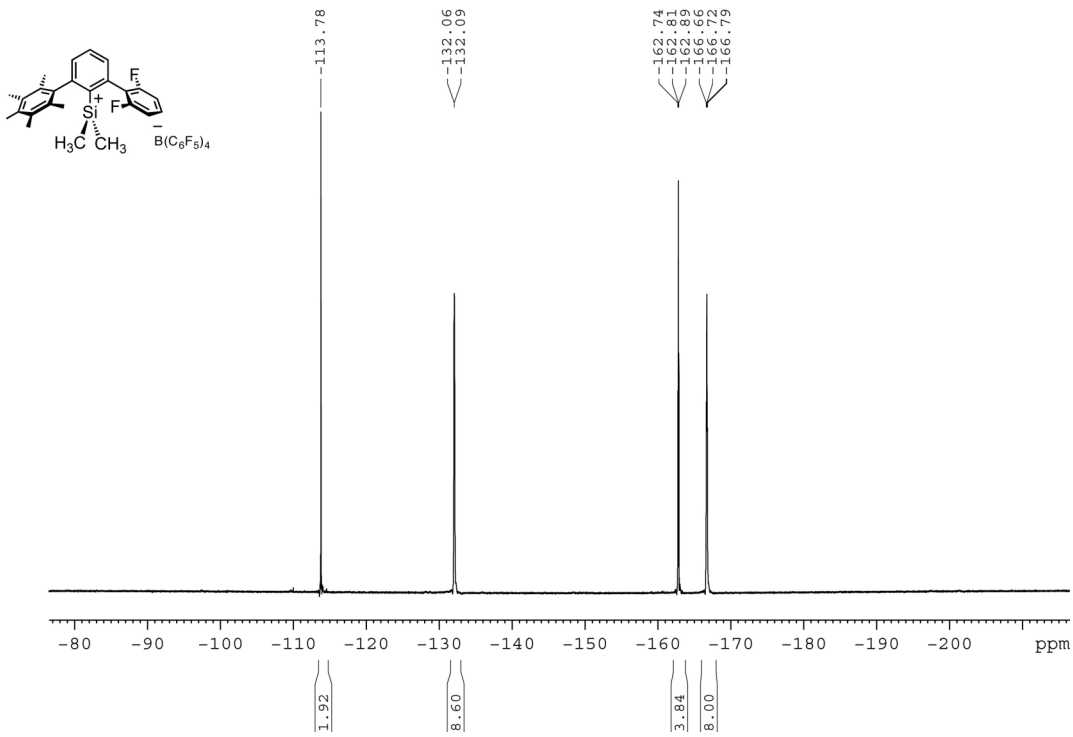

$^{29}Si\{^1H\}$ NMR in C_6D_6, ext. ref.: Me_4Si, 300K. SF = 99.4 MHz

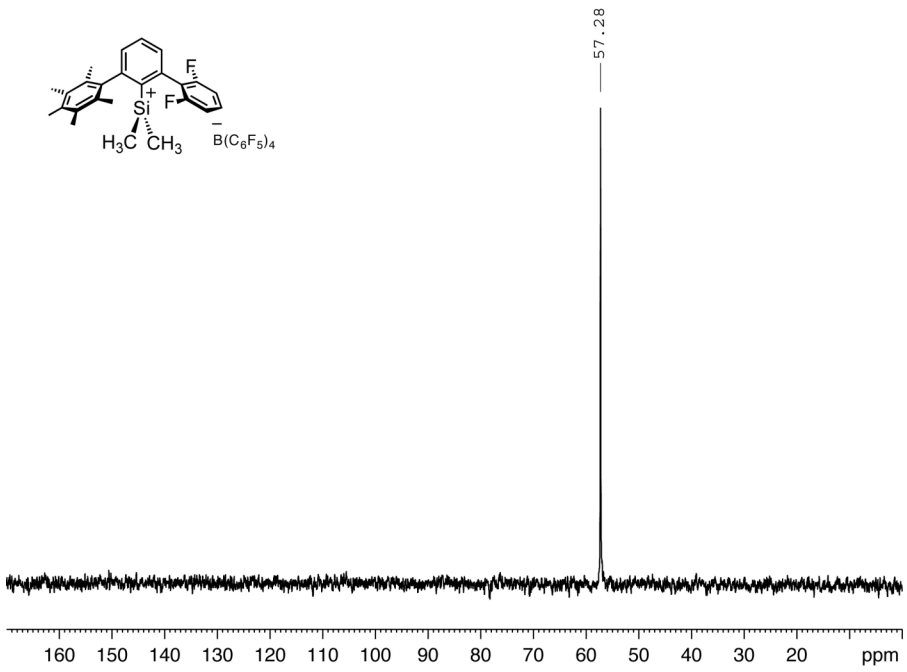

5.4 Crystallographic Data

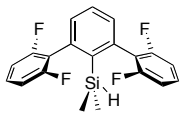

Table 5.2 Crystallographic data for **11**

Crystallized from	hexane
Empirical formula	$C_{20}H_{16}F_4Si$
Formula weight [g mol^{-1}]	360.42
Crystal color, habit	colorless, prism
Crystal dimensions [mm]	0.15 × 0.22 × 0.28
Temperature [K]	160(1)
Crystal system	monoclinic
Space group	$P2_1/c$ (#14)
Z	12
Reflections for cell determination	85764
2θ range for cell determination [°]	4 – 50
Unit cell parameters a [Å]	27.2182(5)
b [Å]	15.3523(3)
c [Å]	13.0983(2)
α [°]	90
β [°]	100.942(1)
γ [°]	90
V [Å^3]	5373.8(2)
$F(000)$	2232
D_x [g cm^{-3}]	1.336
μ(Mo $K\alpha$) [mm^{-1}]	0.169
Scan type	ϕ and ω
2θ(max) [°]	50
Transmission factors (min; max)	0.824; 0.991
Total reflections measured	85515
Symmetry independent reflections	9440
R_{int}	0.095
Reflections with $I > 2\sigma(I)$	6405
Reflections used in refinement	9440
Parameters refined	683
Final $R(F)$ [$I > 2\sigma(I)$ reflections]	0.0515
$wR(F^2)$ (all data)	0.1321
Weights: $w = [\sigma^2(F_o^2) + (0.0631P)^2 + 2.3975P]^{-1}$ where $P = (F_o^2 + 2F_c^2)/3$	
Goodness of fit	1.034
Secondary extinction coefficient	0.0074(4)
Final Δ_{max}/σ	0.001
$\Delta\rho$ (max; min) [e Å^{-3}]	0.35; -0.31
$\sigma(d_{(C-C)})$ [Å] 0.003 – 0.007	

Table 5.3 Crystallographic data for **30**

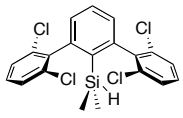

Crystallized from	hexane
Empirical formula	$C_{20}H_{16}Cl_4Si$
Formula weight [g mol^{-1}]	426.24
Crystal color, habit	colorless, prism
Crystal dimensions [mm]	0.17 × 0.25 × 0.28
Temperature [K]	160(1)
Crystal system	monoclinic
Space group	$P2_1/c$ (#14)
Z	4
Reflections for cell determination	89238
2θ range for cell determination [°]	4 – 60
Unit cell parameters a [Å]	15.9849(3)
b [Å]	8.6106(2)
c [Å]	15.3889(3)
α [°]	90
β [°]	107.460(1)
γ [°]	90
V [Å^3]	2020.54(7)
$F(000)$	872
D_x [g cm^{-3}]	1.401
μ(Mo $K\alpha$) [mm^{-1}]	0.645
Scan type	ω
$2\theta_{(max)}$ [°]	60
Transmission factors (min; max)	0.714; 0.899
Total reflections measured	54996
Symmetry independent reflections	5849
R_{int}	0.071
Reflections with $I > 2\sigma(I)$	4930
Reflections used in refinement	5847
Parameters refined	228
Final $R(F)$ [$I > 2\sigma(I)$ reflections]	0.0574
$wR(F^2)$ (all data)	0.1563
Weights: $w = [\sigma^2(F_o^2) + (0.0817P)^2 + 2.44P]^{-1}$ where $P = (F_o^2 + 2F_c^2)/3$	
Goodness of fit	1.058
Final Δ_{max}/σ	0.001
$\Delta\rho$ (max; min) [e Å^{-3}]	0.68; -0.45
$\sigma(d_{(C-C)})$ [Å]	0.003 – 0.005

Table 5.4 Crystallographic data for **12**

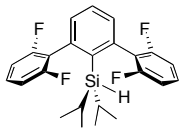

Crystallized from	hexane
Empirical formula	$C_{24}H_{24}F_4Si$
Formula weight [g mol^{-1}]	416.53
Crystal color, habit	colorless, plate
Crystal dimensions [mm]	0.08 × 0.22 × 0.25
Temperature [K]	160(1)
Crystal system	monoclinic
Space group	$P2_1/n$ (#14)
Z	4
Reflections for cell determination	3891
2θ range for cell determination [°]	4 – 50
Unit cell parameters a [Å]	9.1615(3)
b [Å]	14.8113(5)
c [Å]	15.8961(5)
α [°]	90
β [°]	99.103(2)
γ [°]	90
V [Å^3]	2129.8(1)
F(000)	872
D_x [g cm^{-3}]	1.299
μ(Mo $K\alpha$) [mm^{-1}]	0.151
Scan type	ω
$2\theta_{(max)}$ [°]	50
Total reflections measured	29302
Symmetry independent reflections	3741
R_{int}	0.048
Reflections with $I > 2\sigma(I)$	3026
Reflections used in refinement	3741
Parameters refined; restraints	282; 46
Final $R(F)$ [$I > 2\sigma(I)$ reflections]	0.0511
$wR(F^2)$ (all data)	0.1382
Weights: $w = [\sigma^2(F_o^2) + (0.0616P)^2 + 1.5707P]^{-1}$ where $P = (F_o^2 + 2F_c^2)/3$	
Goodness of fit	1.051
Secondary extinction coefficient	0.007(2)
Final Δ_{max}/σ	0.001
$\Delta\rho$ (max; min) [e Å^{-3}]	0.43; -0.42
$\sigma(d_{(C-C)})$ [Å]	0.003 – 0.004

Table 5.5 Crystallographic data for **13**

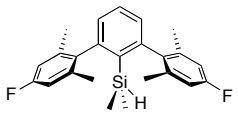

Crystallized from	MeCN
Empirical formula	$C_{24}H_{26}F_2Si$
Formula weight [g mol^{-1}]	380.55
Crystal color, habit	colorless, needle
Crystal dimensions [mm]	0.05 × 0.12 × 0.22
Temperature [K]	160(1)
Crystal system	monoclinic
Space group	$P2_1/n$ (#14)
Z	8
Reflections for cell determination	68777
2θ range for cell determination [°]	4 – 50
Unit cell parameters a [Å]	13.4207(4)
b [Å]	22.7003(7)
c [Å]	14.3655(5)
α [°]	90
β [°]	107.952(2)
γ [°]	90
V [Å^3]	4163.4(2)
F(000)	1616
D_x [g cm^{-3}]	1.214
μ(Mo $K\alpha$) [mm^{-1}]	0.135
Scan type	ϕ and ω
$2\theta_{(max)}$ [°]	50
Transmission factors (min; max)	0.907; 0.999
Total reflections measured	72813
Symmetry independent reflections	7329
R_{int}	0.154
Reflections with $I > 2\sigma(I)$	4178
Reflections used in refinement	7329
Parameters refined	508
Final $R(F)$ [$I > 2\sigma(I)$ reflections]	0.0579
$wR(F^2)$ (all data)	0.1384
Weights: $w = [\sigma^2(F_o^2) + (0.0489P)^2 + 2.669P]^{-1}$ where $P = (F_o^2 + 2F_c^2)/3$	
Goodness of fit	1.010
Secondary extinction coefficient	0.0007(2)
Final Δ_{max}/σ	0.007
$\Delta\rho$ (max; min) [e Å^{-3}]	0.27; -0.30
$\sigma(d_{(C-C)})$ [Å]	0.004

Table 5.6 Crystallographic data for **62**

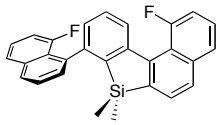

Crystallized from	MeCN
Empirical formula	$C_{28}H_{20}F_2Si$
Formula weight [g mol^{-1}]	422.54
Crystal color, habit	colorless, prism
Crystal dimensions [mm]	0.20 × 0.25 × 0.40
Temperature [K]	160(1)
Crystal system	monoclinic
Space group	$P2_1$ (#4)
Z	2
Reflections for cell determination	28019
2θ range for cell determination [°]	4 – 60
Unit cell parameters a [Å]	10.3234(1)
b [Å]	8.8141(1)
c [Å]	12.6603(2)
α [°]	90
β [°]	111.3897(8)
γ [°]	90
V [Å^3]	1072.63(2)
F(000)	440
D_x [g cm^{-3}]	1.308
μ(Mo $K\alpha$) [mm^{-1}]	0.139
Scan type	ϕ and ω
$2\theta_{(max)}$ [°]	60
Transmission factors (min; max)	0.885; 0.975
Total reflections measured	30684
Symmetry independent reflections	6183
R_{int}	0.043
Reflections with $I > 2\sigma(I)$	5708
Reflections used in refinement	6180
Parameters refined; restraints	284; 1
Final $R(F)$ [$I > 2\sigma(I)$ reflections]	0.0348
$wR(F^2)$ (all data)	0.0842
Weights: $w = [\sigma^2(F_o^2) + (0.0397P)^2 + 0.2254P]^{-1}$ where $P = (F_o^2 + 2F_c^2)/3$	
Goodness of fit	1.028
Secondary extinction coefficient	0.013(3)
Final Δ_{max}/σ	0.001
$\Delta\rho$ (max; min) [e Å^{-3}]	0.18; -0.20
$\sigma(d_{(C-C)})$ [Å]	0.002 – 0.003

Table 5.7 Crystallographic data for [**25**][$B(C_6F_5)_4$] and [**26**][$B(C_6F_5)_4$]

Crystallized from	fluorobenzene
Empirical formula	$C_{102}H_{62.71}B_2F_{48}O_2Si_2$
Formula weight [g mol^{-1}]	2310.03
Crystal color, habit	colorless, prism
Crystal dimensions [mm]	0.20 × 0.25 × 0.32
Temperature [K]	160(1)
Crystal system	triclinic
Space group	$P\bar{1}$ (#2)
Z	2
Reflections for cell determination	50720
2θ range for cell determination [°]	4 – 50
Unit cell parameters a [Å]	15.9428(4)
b [Å]	17.3376(3)
c [Å]	19.1253(3)
α [°]	76.719(1)
β [°]	76.937(1)
γ [°]	79.564(1)
V [Å^3]	4965.1(2)
F(000)	2321.42
D_x [g cm^{-3}]	1.545
μ(Mo $K\alpha$) [mm^{-1}]	0.176
Scan type	ω
$2\theta_{(max)}$ [°]	50
Transmission factors (min; max)	0.911; 0.968
Total reflections measured	69174
Symmetry independent reflections	17369
R_{int}	0.044
Reflections with $I > 2\sigma(I)$	12924
Reflections used in refinement	17366
Parameters refined; restraints	1425; 84
Final $R(F)$ [$I > 2\sigma(I)$ reflections]	0.0441
$wR(F^2)$ (all data)	0.1235
Weights: $w = [\sigma^2(F_o^2) + (0.0661P)^2 + 1.1489P]^{-1}$ where $P = (F_o^2 + 2F_c^2)/3$	
Goodness of fit	1.046
Secondary extinction coefficient	0.0037(3)
Final Δ_{max}/σ	0.002
$\Delta\rho$ (max; min) [e Å^{-3}]	0.67; -0.41
$\sigma(d_{(C-C)})$ [Å]	0.003 – 0.02

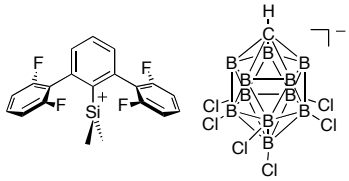

Table 5.8 Crystallographic data for [**18**][$CHB_{11}H_5Cl_6$]

Crystallized from	chlorobenzene / hexane
Empirical formula	$C_{21}H_{21}B_{11}Cl_6F_4Si$
Formula weight [g mol^{-1}]	709.10
Crystal color, habit	colorless, prism
Crystal dimensions [mm]	0.17 × 0.20 × 0.20
Temperature [K]	160(1)
Crystal system	orthorhombic
Space group	*Pnma* (#62)
Z	8
Reflections for cell determination	60946
2θ range for cell determination [°]	4 – 50
Unit cell parameters a [Å]	17.7592(3)
b [Å]	19.4726(2)
c [Å]	18.2732(2)
α [°]	90
β [°]	90
γ [°]	90
V [Å^3]	6319.2(1)
F(000)	2832
D_x [g cm^{-3}]	1.491
μ(Mo $K\alpha$) [mm^{-1}]	0.621
Scan type	ω
$2\theta_{(max)}$ [°]	50
Transmission factors (min; max)	0.858; 0.899
Total reflections measured	69387
Symmetry independent reflections	5753
R_{int}	0.075
Reflections with $I > 2\sigma(I)$	4443
Reflections used in refinement	5752
Parameters refined	408
Final $R(F)$ [$I > 2\sigma(I)$ reflections]	0.0357
$wR(F^2)$ (all data)	0.0913
Weights: $w = [\sigma^2(F_o^2) + (0.0390P)^2 + 4.7879P]^{-1}$ where $P = (F_o^2 + 2F_c^2)/3$	
Goodness of fit	1.038
Final Δ_{max}/σ	0.002
$\Delta\rho$ (max; min) [e Å^{-3}]	0.74; -0.27
$\sigma(d_{(C-C)})$ [Å]	0.003 – 0.004

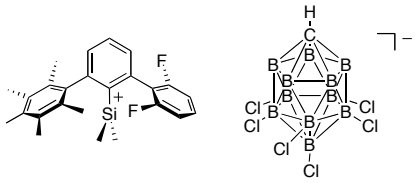

Table 5.9 Crystallographic data for [**49**][$CHB_{11}H_5Cl_6$]

Crystallized from	chlorobenxene / hexane
Empirical formula	$C_{26}H_{33}B_{11}Cl_6F_2Si$
Formula weight [g mol^{-1}]	743.25
Crystal color, habit	pale-yellow, prism
Crystal dimensions [mm]	0.30 × 0.35 × 0.40
Temperature [K]	160(1)
Crystal system	orthorhombic
Space group	$Pna2_1$ (#33)
Z	4
Reflections for cell determination	49656
2θ range for cell determination [°]	4 – 60
Unit cell parameters a [Å]	27.1144(3)
b [Å]	15.1513(2)
c [Å]	8.5484(1)
α [°]	90
β [°]	90
γ [°]	90
V [Å^3]	3511.8(2)
F(000)	1512
D_x [g cm^{-3}]	1.406
μ(Mo $K\alpha$) [mm^{-1}]	0.554
Scan type	ϕ and ω
$2\theta_{(max)}$ [°]	60
Transmission factors (min; max)	0.774; 0.851
Total reflections measured	52378
Symmetry independent reflections	10039
R_{int}	0.064
Reflections with $I > 2\sigma(I)$	8628
Reflections used in refinement	10038
Parameters refined; restraints	422; 1
Final $R(F)$ [$I > 2\sigma(I)$ reflections]	0.0373
$wR(F^2)$ (all data)	0.0912
Weights: $w = [\sigma^2(F_o^2) + (0.0458P)^2 + 0.7658P]^{-1}$ where $P = (F_o^2 + 2F_c^2)/3$	
Goodness of fit	1.029
Final Δ_{max}/σ	0.002
$\Delta\rho$ (max; min) [e Å^{-3}]	0.62; -0.24
$\sigma(d_{(C-C)})$ [Å]	0.003 – 0.004

Table 5.10 Crystallographic data for [**46**][$CHB_{11}H_5Cl_6$]

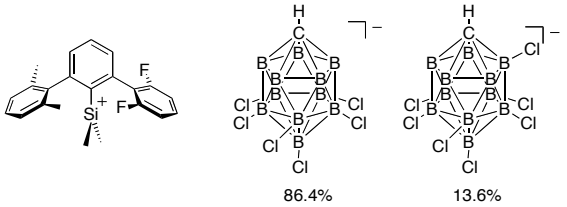

Crystallized from	chlorobenzene / hexane
Empirical formula	$C_{23}H_{26.86}B_{11}Cl_{6.14}F_2Si$
Formula weight [g mol^{-1}]	705.86
Crystal color, habit	pale yellow, prism
Crystal dimensions [mm]	0.20 × 0.20 × 0.30
Temperature [K]	160(1)
Crystal system	monoclinic
Space group	$P2_1/c$ (#14)
Z	4
Reflections for cell determination	20178
2θ range for cell determination [°]	6−61
Unit cell parameters a [Å]	11.5421(1)
b [Å]	14.6978(2)
c [Å]	19.3449(2)
α [°]	90
β [°]	94.908(1)
γ [°]	90
V [Å^3]	3269.71(6)
F(000)	1424.96
D_x [g cm^{-3}]	1.434
μ(Mo $K\alpha$) [mm^{-1}]	0.602
Scan type	ω
$2\theta_{(max)}$ [°]	61
Total reflections measured	33301
Symmetry independent reflections	8954
R_{int}	0.020
Reflections with $I > 2\sigma(I)$	7244
Reflections used in refinement	8954
Parameters refined	402
Final $R(F)$ [$I > 2\sigma(I)$ reflections]	0.0279
$wR(F^2)$ (all data)	0.0822
Weights: $w = [\sigma^2(F_o^2) + (0.0464P)^2 + 0.3950P]^{-1}$ where $P = (F_o^2 + 2F_c^2)/3$	
Goodness of fit	1.060
Final Δ_{max}/σ	0.001
$\Delta\rho$ (max; min) [e Å^{-3}]	0.39; -0.27
$\sigma(d_{(C-C)})$ [Å]	0.002

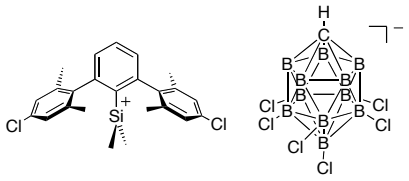

Table 5.11 Crystallographic data for [**42**][$CHB_{11}H_5Cl_6$]

Crystallized from	chlorobenzene / hexane
Empirical formula	$C_{25}H_{31}B_{11}Cl_8Si$
Formula weight [g mol^{-1}]	762.13
Crystal color, habit	pale-yellow, prism
Crystal dimensions [mm]	0.15 × 0.20 × 0.25
Temperature [K]	160(1)
Crystal system	orthorhombic
Space group	$P2_12_12_1$ (#19)
Z	4
Reflections for cell determination	29443
2θ range for cell determination [°]	6.4 – 60.8
Unit cell parameters a [Å]	9.4761(1)
b [Å]	18.8805(1)
c [Å]	20.5176(2)
α [°]	90
β [°]	90
γ [°]	90
V [Å^3]	3670.87(5)
F(000)	1544
D_x [g cm^{-3}]	1.379
μ(Mo $K\alpha$) [mm^{-1}]	0.665
Scan type	ω
$2\theta_{(max)}$ [°]	61
Total reflections measured	47283
Symmetry independent reflections	10117
R_{int}	0.027
Reflections with $I > 2\sigma(I)$	8916
Reflections used in refinement	10116
Parameters refined	412
Final $R(F)$ [$I > 2\sigma(I)$ reflections]	0.0280
$wR(F^2)$ (all data)	0.0702
Weights: $w = [\sigma^2(F_o^2) + (0.0446P)^2]^{-1}$ where $P = (F_o^2 + 2F_c^2)/3$	
Goodness of fit	1.026
Final Δ_{max}/σ	0.11
$\Delta\rho$ (max; min) [e Å^{-3}]	0.61; -0.33
$\sigma(d_{(C-C)})$ [Å]	0.002 – 0.003

6 Curriculum Vitae

Education

January 2007–present	**University of Zurich, Switzerland** PhD thesis on synthesis and study of intramolecularly stabilized silicon cations
October 2006–October 2001	**University of Milan, Italy** Master in Industrial Chemistry and Management Bachelor in Industrial Chemistry
July 2001–September 1996	**Liceo Scientifico E. Majorana, Milan, Italy** Scientific Lyceum (High School)

Work Experience

	University of Zurich, Switzerland
January 2007–present	Doctoral research in the group of Prof. Jay S. Siegel (Organic Chemistry Institute) on development of intramolecularly stabilized silicon cations. Teaching assistant in practical courses of General Chemistry and Advanced Organic Chemistry.
	University of Milan, Italy
November 2006–December 2006	Research associate; work on functionalization of silicon surfaces via hydrosilylation of alkynes.
October 2005–Octtober 2006	Undergraduate research in the group pf Prof, Franco Cozzi; thesis: "*Synthesis of sterically hindered binaphthyldiamines for asymmetric catalysis*".
April 2004–August 2004	Undergraduate research in the group of Prof. Elisabetta Ranucci; work on development of biodegradable copolymers derived from condensation of L-(+)-tartaric acid and α,ω-dihydroxy polycaprolactone.
June 2002–December 2006	**Bookmaking Agency, Milan, Italy** Bookmaker cashier (part time job)

Awards	Poster prize at the Dorothy Crowfoot Hodgkin Symposium in Zurich, November 2010 and November 2009

Publications

Intramolecular Halogen Stabilization of Silylium Ions Directs Gearing Dynamics, P. Romanato, S. Duttwyler, A. Linden, K. K. Baldridge, J. S. Siegel *J.Am. Chem. Soc.* **2010**, *132*, 7828.

Through-Space Interactions in Enshrouded meta-Terphenylsilanes, P. Romanato, S. Duttwyler, A. Linden, K. K. Baldridge, J. S. Siegel, *manuscript submitted.*

Competition between π-Aryl and Halogen-Lone Pair Stabilization in Silylium Ions, P. Romanato, S. Duttwyler, A. Linden, K. K. Baldridge, J. S. Siegel, *manuscript in preparation.*

Oral Presentations and Posters

Presentations

Presentation at the EuCheMS Chemistry Congress, Nürnberg, August 2010
Presentation at the Fall Meeting of the Swiss Chemical Society, Lausanne, September 2009

Posters

Posters presented at the following events:
Stereochemistry Gordon Conference, Newport (RI, USA), August 2010
Dorothy Crowfoot Hodgkin Symposium, Zurich, November 2010, November 2009 and September 2007
Meeting of the Swiss Chemical Society, Zurich, September 2010 and September 2008
EuCheMS Chemistry Congress, Turin, September 2008